Study of biological effects induced in *Arabidopsis thaliana* following uranium exposure, including mixed exposure to cadmium or external gamma radiation: applying a multi-biomarkers approach

Nathalie Vanhoudt

SCK-mentor: Dr. H. Vandenhove
Promotor: Prof. dr. A. Cuypers
Co-promotor: Prof. dr. J. Vangronsveld

Chapter 1

Introduction

1.1 Uranium

1.1.1 Physical, chemical and radiological properties

Uranium, a member of the actinide series with atomic number 92, is a silvery-white, ductile and slightly paramagnetic heavy metal that is pyrophoric when finely divided. It is a bit softer than steel and reacts with cold water when present in a finely divided state. In air, uranium easily oxidizes and becomes coated with a layer of oxide (Burkart et al., 2005). It is able to adopt four valences resulting in the ions U^{3+} (III), U^{4+} (IV), UO_2^{+} (V) and UO_2^{2+} (VI), which is the uranyl ion (Ribera et al., 1996). Some important physical and chemical properties are summarized in table 1.1.

Table 1.1 - Physical and chemical properties of uranium.

Properties	**Uranium**
Chemical symbol	U
Atomic number	92
Atomic weight	238.03 g mol^{-1}
Boiling point	4203 K
Melting point	1405.2 K
Density	19.05 g cm^{-3}

Uranium is a primordial radionuclide with ^{238}U (99.3%), ^{235}U (0.72%) and ^{234}U (0.006%) as its three naturally occurring isotopes (Bleise et al., 2003). All uranium isotopes have the same chemical properties, but different radiological properties. The activities of the different uranium isotopes depend on their physical half-life. ^{238}U for example, the most abundant uranium isotope, has a physical half-life of 4.5×10^9 y, giving it a low specific activity of 1.24×10^4 Bq g^{-1} (Sheppard et al., 2005). Table 1.2 presents an overview of the characteristics of the three natural uranium isotopes.

Table 1.2 - Properties of the three natural occurring uranium isotopes (Bleise et al., 2003).

Isotope	**Half-life [y]**	**Relative mass [%]**	**Specific activity [Bq g^{-1}]**
^{238}U	4.47×10^9	99.3	12455
^{235}U	7.04×10^8	0.72	80011
^{234}U	2.46×10^5	0.006	231×10^6

^{238}U and ^{235}U are the heads of two radioactive decay chains, respectively uranium and actinium chain. By successive decay, with the emission of alpha or beta particles, a stable lead isotope is formed at the end of each chain.

All natural uranium isotopes emit alpha particles, consisting of two protons and two neutrons, which is the configuration of a helium core. This heavy, charged particle will lose its energy fast by colliding with other molecules as it passes through matter or tissue and consequently, has limited penetrating power. Because of its high LET-value (Linear Energy Transfer) alpha particles will cause a high number of ionizations over a short pathway covered in the matter or tissue. As uranium isotopes decay to other radionuclides, beta and gamma radiation will also be emitted in the decay process. Beta particles have greater ability to penetrate matter or tissue, and will, in contrast with alpha particles and due to their smaller mass, charge and energy, cause less ionizations over a longer pathway. Gamma radiation consists of high energy photons and is extremely penetrating but has, similar with beta particles, less ionizing capacity than alpha particles (Bleise et al., 2003).

1.1.2 Natural occurrence in the environment

Uranium is a naturally occurring radionuclide and heavy metal with an average concentration in the continental crust of 1.7 ppm (Wedepohl, 1995). The main natural sources of uranium are hydrothermal veins, sedimentary rocks and pyritic conglomerate beds. Uranium is an important constituent of several minerals such as uranite and autunite. It is also found in phosphate rock, lignite and monazite sand. There are several main geographical locations of minerals containing uranium such as Australia, Canada, Germany and South Africa (Ribera et al., 1996).

Although uranium occurs in the valences +3 to +6, the two most important oxidation states for the conditions of soils are U^{4+} and U^{6+}. The uranyl ion, UO_2^{2+}, is the most stable uranium species in an oxidizing solution and the most prevalent form in the environment. The uranyl ion forms complexes with carbonate, phosphate and sulfate ions in which forms uranium is soluble and readily transported. In contrast, under reducing conditions, uranium occurs as

U^{4+}, which has a strong tendency to bind to organic material and to precipitate and is therefore immobile (Sheppard et al., 2005).

The speciation of uranium in soil and aqueous systems is strongly dependent on the pH. Under acidic conditions and in the absence of fluoride, the uranyl ion is the predominant uranium form in the soil. Hydroxide complexes such as UO_2OH^+ and $(UO_2)_2(OH)_2^{2+}$ and phosphate complexes such as $UO_2(HPO_4)_2^{2+}$ are formed under near neutral conditions while carbonate complexes such as $UO_2(CO_3)_2^{2-}$ and $UO_2(CO_3)_3^{4-}$ predominate under alkaline conditions. The stability of these complexes varies but $UO_2(HPO_4)_2^{2-}$ is the most stable complex from pH 4.0 to 7.5 and in the absence of dissolved inorganic ligands (carbonate, fluoride, sulfate and phosphate) (Ebbs et al., 1998; Shahandeh & Hossner, 2002; Vandenhove, 2004). Figure 1.1 illustrates the pH dependence of uranium speciation.

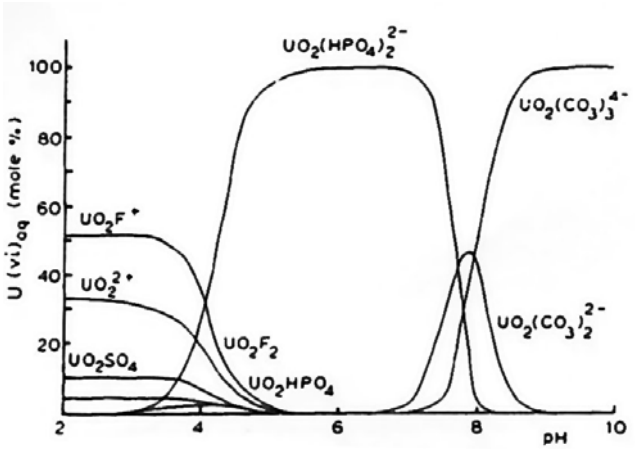

Figure 1.1 - Distribution of some uranyl complexes versus pH for a typical ligand concentration in groundwaters of the Wind River Formation at 25°C. $P_{CO2}=10^{-}15$ atm, F=0.3 mg l^{-1}, Cl=10 g l^{-1}, SO_4=100 mg l^{-1}, SiO_2=30 mg l^{-1} (Langmuir, 1978).

In geographic areas that contain high levels of uranium in rocks and soil, additional uranium can be introduced into the atmosphere by natural processes of erosion and wind activity. Other natural processes such as volcanic eruptions can also cause enhanced levels of uranium in the atmosphere (ATSDR, 1999).

Redistribution of uranium and its decay products to surface water and ground water occurs primarily from the natural erosion of rocks and soil (ATSDR, 1999).

Table 1.3 gives an overview of typical uranium concentrations in several environmental matrices.

Table 1.3 - Uranium concentrations in several environmental matrices (Bleise et al., 2003).

Matrix	Typical concentration range
Soil	0.3-11.7 mg kg^{-1}
Air	2.5×10^{-8}-10^{-7} mg m^{-3}
Surface water	3×10^{-2}-2.1 µg l^{-1}
Ground water	3×10^{-3}-2.0 µg l^{-1}

1.1.3 Industrial applications and transfer to the environment

An important industrial application for uranium is its usage as fuel in nuclear power plants. As only ^{235}U can be used directly as nuclear fuel, natural uranium needs to be enriched, increasing the fraction of ^{235}U. ^{238}U can also be converted into ^{239}Pu in fast-breeder reactors which in turn can be used as reactor fuel. Depleted uranium is for example also used as counterweights for rudders and elevators in commercial aircrafts and fork lifts and in the keels of sailing yachts (Bleise et al., 2003). Uranium is often considered a waste product in several industrial applications as it is naturally present in several ores and minerals.

In general, anthropogenic activities as uranium mining, milling and processing, phosphate mining, heavy metal mining, coal use and inappropriate waste disposal can contribute to the redistribution of uranium in the environment (ATSDR, 1999; Vandenhove, 2002). All these industrial activities may result in soil deposition while uranium will be mostly released into the atmosphere from mining and milling activities, by uranium processing facilities or burning coal. During mining operations and radioactive waste disposal, uranium can also be discharged to surface water and/or ground water.

1.1.4 Exposure pathways and toxicity effects in man and animal species

As uranium is naturally present in food, air, soil and water in limited concentrations, man and animal species are always exposed via these compartments. Typical uranium concentrations of 0.08-70 µg kg^{-1} or 0.4-1.4 µg l^{-1} can be found in food or drinking water respectively (ATSDR, 1999). Uranium can penetrate the organism via different pathways: aerosol inhalation, ingestion

or wounds (Ribera et al., 1996). Uranium is a radiotoxic and chemotoxic element with a greater risk of chemical toxicity than radiological toxicity.

This limited radiological toxicity is primarily due to its large physical half-life. ^{238}U has a physical half-life of 4.5×10^9 y, giving it a very low specific activity of 12.4 kBq g^{-1} (Sheppard et al., 2005). Secondly, all uranium isotopes emit alpha particles which, with a penetration depth of a few cm in air and only µm in tissue, are unable to penetrate the outer skin layer. On the other hand, alpha particles have a high ionizing capacity over a short pathway when they pass through tissue. Consequently, there is a high probability for irreversible cellular damage after internal contamination by an alpha emitter. As uranium successively decays to other radionuclides, beta and gamma radiation can also be emitted, increasing the risk of radiological toxicity. When exposed to ionizing radiation, molecular and cellular effects are induced directly through energy transfers to macromolecules or indirectly through a water radiolysis reaction (Ribera et al., 1996).

The chemical toxicity is of particular importance when studying uranium induced effects and depends on the form in which uranium is present. Compounds soluble in organic fluids and water are more toxic than non-soluble compounds as oxides. The aqueous uranyl ion is the major cause of chemical toxicity. Macromolecules such as nucleic acids, proteins and lipids can be attacked, causing DNA damage, enzyme inactivation and membrane damage (Ribera et al., 1996).

When uranium is ingested, most of it (> 95 %) will leave the body within a few days in the feces and will never be transferred to the blood stream. The small portion that enters the blood will be filtered by the kidneys (50 %) and leaves the body within days. The rest will be mostly accumulated in the bones (22 %) and kidneys (21 %) causing renal dysfunction. When inhaled, uranium can enter the blood stream via the lungs but can also be retained in the longs depending on its particle size and the absorption is dependent on the solubility in body fluids ranging from 0.7 to 5 %. When retained in the lungs, uranium can decay to other radionuclides, causing a radiation hazard. Besides acute toxicity effects, stochastic effects, such as cancer, can manifest at a later stage with a probability proportional to the dose (Ribera et al., 1996; ATSDR, 1999).

1.1.5 Uptake, distribution and toxicity effects in plants

Nutrients are essential for normal plant growth and development and are readily taken up from the exchangeable and soluble fractions of the soil. Although uranium and its decay products are not essential for plant growth and can even be toxic, they will also be taken up by several plant species. Soil characteristics influence the form in which uranium is present, affecting uranium uptake and transfer in plants (Shahandeh et al., 2001). Ebbs et al. (1998) reported that the uranyl ion, which predominates at a pH of 5.0-5.5, is the form of uranium most readily taken up and transferred to the shoots. By using a computer speciation model, Ebbs et al. (1998) also indicated that in the presence of phosphate, uranium-phosphate complexes will be formed and will be stable over a pH range from 4.5 to 9.0. The formation of uranium-phosphate complexes was predicted to reduce the level of free uranyl ions and uranyl hydroxides, reducing the bioavailability of uranium to plants. Laroche et al. (2005) also showed that by increasing the phosphate concentration in the solution, a decreasing gradient of free uranyl ions was generated, but it did not affect uranium uptake by *Phaseolus vulgaris*.

In general, uranium uptake and distribution depends on the nature and age of the plant as was reported by Singh et al. (2005). Uranium accumulates mainly in the roots with limited transfer to the shoots as was reported by several authors (Sela et al., 1988; Ebbs et al., 1998; Shahandeh & Hossner, 2002; Singh et al., 2005; Vandenhove et al., 2006). Ebbs et al. (1998) also reported that the root-to-shoot transfer of uranium was dependent on the pH of the nutrient solution with the highest uranium concentration in the leaves at pH 5.0 when uranium was present as the free uranyl ion. This study also showed that the amount of uranium taken up by the roots was the highest at pH 6.0 and 8.0.

Little information on uranium toxicity effects is available for plants, especially exposure to low uranium concentrations and investigation of effects on biochemical and molecular level. For the available studies, contradictory information on uranium toxicity effects for plants exists. Sheppard et al. (2005) summarized data that showed toxicity effects in plants exposed to concentrations of 0.5-5.0 mg uranium kg^{-1} dry soil while other data reported no toxicity effects in plants after exposure to 100-1000 mg kg^{-1} dry soil. Within the

available studies on uranium toxicity effects for plants, several endpoints and toxicity effects were reported. According to Ebbs et al. (1998), 5 µM uranium was toxic to roots of *Pisum sativum* causing stunting of lateral root growth and blackening of existing root apices. Vandenhove et al. (2006) reported that after 4 days exposure to 1000 µM uranium, leaves of *Phaseolus vulgaris* started to show chlorosis and roots turned yellow. Vandenhove et al. (2006) also reported a tendency to increased growth when *Phaseolus vulgaris* was exposed to uranium concentrations between 0.1 and 10 µM. A transient hormesis response was also shown by Straczek et al. (2009) for hairy roots of carrots exposed to uranium concentrations ranging from 2.5 to 5 mg l^{-1}. In a study by Sela et al. (1988) *Azolla filiculoides* was grown on tap water contaminated with 10 ppm $UO_2(NO_3)_2$ and harvested after 4 days. At that time toxicity effects as changes in frond pigmentation and loss of rigidity became visible.

Uranium can also react with several plant nutrients, interfere with their uptake and distribution and disturb their function in the plant cell. Plant and animal cell membranes are known to be stabilized by Ca^{2+} (Nieboer et al., 1979). Since UO_2^{2+} binds more strongly than Ca^{2+} to Ca^{2+}-type binding sites, it has the potential to damage cell membranes and increase K^+ permeability as was reported by Nieboer & Richardson (1980).

1.1.6 Uranium in a mixed stressor environment

Uranium never occurs as a single pollutant in the environment, but always in combination with other stressors such as heavy metals and other radionuclides with their concomitant radiation. As previous studies showed that responses induced in plants exposed to a combination of various stressors are generally different from responses induced by each of the stressors alone (Chaoui et al., 1997; An et al., 2004; Charles et al., 2006; Mittler, 2006), the simultaneous presence of other stressors and the mixed nature of uranium contamination should be accounted for. Charles et al. (2006) for example showed that applying a combination of uranium and copper to *Lemna aequinoctialis* in their EC_{50} concentrations resulted in an antagonistic effect on growth inhibition.

In general, two models, concentration addition and independent action, are available to predict mixed effects from the toxicity of the individual components

(Altenburger et al., 2000; Backhaus et al., 2000). The model of concentration addition assumes that the stressors have the same mode of action, therefore acting through the same cellular mechanism on the same target. The effect of the mixture can then be predicted from the known toxic units, which is the concentration of a compound divided by its effect concentration (EC_x) at a given level x, of all components in the mixture. The model of independent action assumes that the toxicants have different modes of action. The effect of the mixture can then be predicted from the effects of the individual components. Both models however assume that the mixture is fully described in its chemical composition and the dose-response curves of all the compounds are known. Both models are simplifications of a complex reality and besides considering them as equally valid alternatives to which data can be compared, Jonker et al. (2005) defined some biologically relevant patterns in which deviations can occur (figure 1.2).

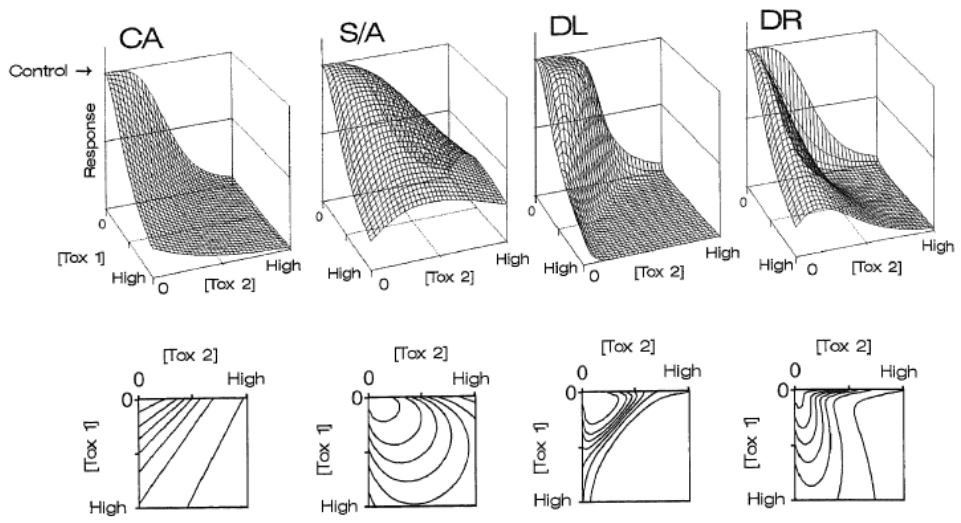

Figure 1.2 - Binary mixture dose-response relationships illustrating concentration addition (CA) and 3 deviation patterns from this reference: no deviation (CA), synergistic/antagonistic deviation (S/A), dose level-dependent deviation (DL) and dose ratio-dependent deviation (DR). Top row: 3D response surfaces. Bottom row: 2D isobolic representation of the response surfaces. The biological response is high in the control group and decreases as doses of toxicants increase (Jonker et al., 2005).

When there is "no deviation", the mixture effects are adequately described by the concentration addition or independent action model. Under "synergism or antagonism" mixture of several stressors causes effects that are more severe or less severe than calculated from either reference model. When the deviation

from either reference model at low dose levels is different from the deviation at high dose levels "dose level-dependent deviation" is used. "Dose ratio-dependent deviation" is used when the deviation from either reference model depends on the composition of the mixture (Jonker et al., 2005).

1.2 Cadmium

1.2.1 Chemical and physical properties

Cadmium, together with zinc and mercury a member of group II_b of the periodic table, is a very soft, silvery-white, ductile metal with atomic number 48. In air, cadmium is rapidly oxidized into cadmium oxide and the most common oxidation state is Cd^{2+} (II). Its physical and chemical properties are similar to those of zinc, and to a lesser degree, mercury. Several inorganic cadmium compounds such as acetate, chloride and sulfate are soluble in water whereas cadmium oxide, carbonate and sulfide are almost insoluble (WHO, 2000). Some important physical and chemical properties of cadmium are summarized in table 1.4.

Table 1.4 - Physical and chemical properties of cadmium.

Properties	**Cadmium**
Chemical symbol	Cd
Atomic number	48
Atomic weight	112.41 g mol^{-1}
Boiling point	1038 K
Melting point	594.1 K
Density	8.65 g cm^{-3}

1.2.2 Natural environmental presence

Cadmium is a relatively rare element with an average concentration of 0.2 ppm in the earths crust. Most cadmium in nature occurs in association with the sulfide ores of zinc, lead and copper. Only a few relatively pure cadmium minerals are known such as greenockite, which is cadmium sulfide. In addition, cadmium can also occur as an impurity in phosphate minerals. It therefore occurs naturally in the environment from the gradual process of erosion and abrasion of rocks and soils but also from forest fires and volcanic eruptions

though the latter makes up only a small percentage (< 10 %) of the total airborne cadmium in comparison with anthropogenic activities. Cadmium is therefore naturally present in all environmental matrices. Table 1.5 gives an overview of typical cadmium concentrations in several environmental compartments.

Table 1.5 – Natural cadmium levels in the environment.

Matrix	**Concentration range**
Atmosphere	0.1-5 ng m^{-3}
Earth's crust	0.1-0.5 µg g^{-1}
Marine sediment	~1 µg g^{-1}
Sea water	~0.1 µg l^{-1}
River sediment	~5 µg g^{-1}
River water	<0.1 µg l^{-1}

1.2.3 Industrial applications and discharge to the environment

Most cadmium used in industry is recovered from sphalerite (zinc sulfide), the principal ore of zinc where cadmium atoms replace some of the zinc atoms. The cadmium is removed when zinc metal is purified in a refinery. Cadmium is therefore an important by-product of the zinc industry. Before World War I, cadmium was almost never recovered from zinc plants resulting in an uncontrolled contamination of the environment for decades (WHO, 2000). Besides the most important use of cadmium in the production of nickel-cadmium batteries, cadmium can also be used in protective plating of steel, in pigments or stabilizers for plastics and as a component of various alloys. As cadmium is able to absorb neutrons, it can be used in nuclear reactor control rods to keep fission reactions under control.

Approximately 85-90 % of the atmospheric cadmium emissions arise from anthropogenic sources such as smelting and refining of non-ferrous metals, fossil fuel combustion and municipal waste incineration. In 1982, the total atmospheric cadmium emission was estimated at 1144 tons y^{-1} in Western Europe. By application of new technology to control emissions from non-ferrous smelters these emissions where brought back to 158 tons y^{-1} in 1990 (WHO, 2000). Most of the cadmium that occurs in air is associated with particulate matter in the respirable range. Via wet or dry deposition, elevated cadmium

levels can be found in soil and crops. Therefore, cadmium in food comes mostly from atmospheric cadmium as a result of foliar absorption or root uptake of cadmium deposited on soils. It is important to stress that excessive soil cadmium levels presently found in some industrialized areas are largely the result of emissions in the past when smelters were operating under less stringent conditions without recovering cadmium during zinc production. Another important source of soil contamination can be attributed to the use of commercial fertilizers derived from rock phosphate and sewage sludge. Non-ferrous metal mines represent an important source of cadmium release to the aquatic environment due to for example drainage water, waste water from ore processing and rain water run off from the mine area (WHO, 2000).

Certain Belgian areas such as the Meuse valley near Liège and the rural northern part of the Kempen are polluted by cadmium, mainly because of past emissions from non-ferrous industries (primarily zinc smelters and cadmium producing plants). The cadmium concentration in the soil in the Liège area ranged from 4 to 39 mg kg^{-1} measured between 1978 and 1987 whereas the cadmium concentration in the top-layer soil from kitchen-gardens ranged from 0.5 to 24 mg kg^{-1} measured between 1983 and 1984 (Lauwerys et al., 1990).

1.2.4 Exposure and toxicological effects for man and animal species

As cadmium is present in all environmental compartments, man and animal species are always exposed to certain cadmium levels via inhalation and ingestion of food and drinking water. The average cadmium level inhaled daily depends greatly on the area and ranges from 0.01 µg day^{-1} in rural regions to 0.4 µg day^{-1} in industrialized zones (WHO, 2000). Up to 50 % cadmium can be deposited in the lungs depending on the particle size and cadmium absorption in the lungs depends on the chemical nature of the particles, which is high for cadmium oxide but considerably less for insoluble salts such as cadmium sulfide. Smoking is an important source of cadmium exposure which may equal or exceed that from food and a person smoking 20 cigarettes a day will absorb up to 1 µg cadmium each day (Järup et al., 1998). In general, drinking water contains very low cadmium concentrations, usually in the range of 0.01-1 µg l^{-1}, and does not contribute much to the total cadmium intake. Food is the most important source for cadmium exposure in a nonsmoking population. While the

average amount of cadmium absorbed via food can be estimated at 1 µg day^{-1}, concentrations vary greatly between different food sources. The lowest concentrations are found in milk (1 µg l^{-1}) while the highest cadmium levels up to 1000 µg kg^{-1} are found in internal organs of mammals (kidney and liver) and in mussels, scallops and oysters (WHO, 2000).

Cadmium has an exceptionally long biological half-life of 10-30 years, resulting in an almost irreversible accumulation in the body (Staessen et al., 1990). The cadmium concentration in the blood is a good indicator of the absorption over the previous months. The liver and the kidneys are the main storage sites for cadmium in the body (Järup et al., 1998). The cadmium concentration increases with age up to about 50-60 years. Cadmium is mainly eliminated from organisms via urine. However the excreted cadmium concentration is very low and represents 0.005-0.01 % of the total body burden, the 24 hour urinary excretion is a relevant biomarker of lifetime exposure (Staessen et al., 1990; WHO, 2000). With chronic oral exposure, kidneys appear to be the most sensitive organs. Cadmium can affect the resorption function of the proximal tubules with the first symptom being an increase in the urinary excretion of low-molecular-weight proteins, called tubular proteinuria. More severe cadmium damage may also involve the glomerulus and disturbances in renal handling of phosphorous and calcium may cause resorption of minerals from bone, resulting in kidney stones and osteomalacia (WHO, 2004). Staessen et al. (1999) also reported from a population study that even at a low degree of environmental exposure, cadmium may promote skeletal demineralization which may lead to increased bone fragility and raised risk of fractures. Cadmium has also been classified as a carcinogen by the International Agency for Research on Cancer in 1993 which was based on the observation of excess lung cancer mortality of workers in cadmium processing plants (Nawrot et al., 2006).

1.2.5 Uptake, distribution and toxicity effects for plants

The cadmium uptake by plants is dependent on its concentration in the soil and its bioavailability modulated by the presence of organic matter, pH, redox potential, temperature and concentrations of other elements (Benavides et al., 2005). Although Cd^{2+} is a non-essential element for plants, it is readily taken up by the root system as it enters plant cells via uptake systems for essential

cations and can be transported to the shoots, though only in relatively small amounts. As was reviewed by Clemens et al. (2006), Cd^{2+} ions are apparently taken up into plant cells by Fe^{2+}/Zn^{2+} transporters and possibly by Ca^{2+} transporters and channels. Cadmium is able to activate the synthesis of phytochelatins that can form various complexes with cadmium to prevent it from circulating as free Cd^{2+} in the cytosol (di Toppi & Gabbrielli, 1999). Phytochelatins can therefore reduce the cytoplasmic toxicity as the metal chelate is expected to be less toxic to the cellular metabolism than the free metal ion (Hasan et al., 2009). Cadmium chelates are then transferred into the vacuole or transported to the shoots through the cells of vascular bundles (Hasan et al., 2009). Figure 1.3 gives a schematic representation of processes involved in the uptake, sequestration and translocation of cadmium in plant roots.

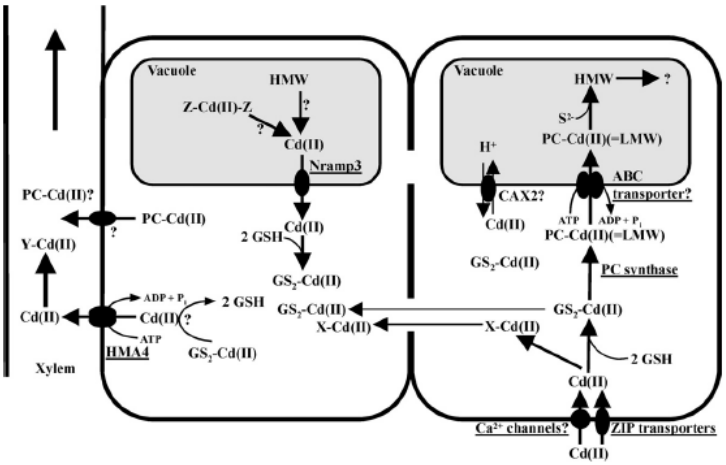

Figure 1.3 - Cd^{2+} ions are apparently taken up into plant cells by Fe^{2+}/Zn^{2+} transporters of the ZIP family and possibly by Ca^{2+} transporters/channels. In the cytosol they are chelated and most likely not present as "free" hydrated ions. Initial ligands could be GSH (bisglutathionato-Cd complexes, GS_2-Cd(II)) and potentially other unknown molecules (X-Cd(II)). GS_2-Cd(II) interacts with the constitutively expressed enzyme PCS resulting in the activation of PC synthesis. PC-Cd(II) complexes (=LMW complexes) are hypothesized to be transported into the vacuole by an (unknown) ABC-type transporter. Inside the vacuole, HMW complexes are formed that contain sulfide, but their metabolic fate is unknown. A second pathway of vacuolar sequestration could be Cd^{2+}/H^+ antiport with CAX2 a candidate protein in *A. thaliana*. Activity of metal-sequestering pathways in root cells likely plays a key role in determining the rate of translocation to the aerial parts of the plant. A second factor is the degree of accessibility and mobilization of sequestered metal. Thirdly, the efficiency of radial symplastic passage through the root and across the endodermis is important and finally, the xylem loading activity, i.e. the efflux activity from xylem parenchyma cells into the xylem. At least a fraction of the vacuolar Cd (HMW complexes or unidentified complexes (Z-Cd-(II)-Z) can apparently be mobilized back into the cytosol by proteins such as AtNramp3. Symplastic transfer requires the availability of mobile high affinity ligands (GS_2-Cd(II), X-Cd(II)). Loading of the xylem is dependent on efflux pumps (e.g. AtHMA4) residing in the plasma membrane of surrounding cells. An efflux of PC-Cd(II) complexes has also been proposed. Ligands of Cd(II) in the acidic xylem are not known but could be nitrogen or oxygen ligands (Clemens et al., 2006).

Cadmium toxicity effects on growth, photosynthesis, nutrient uptake, water balance, cation efflux, enzyme capacities, plant metabolism etc. were reviewed by several authors (Prasad, 1995; Das et al., 1997; Hasan et al., 2009). Exposure of plants to elevated cadmium concentrations can inhibit growth and cause chlorosis and the production of anthocyanins in leaves as was reported by various authors (Smeets et al., 2005; Van Belleghem et al., 2007). Cadmium is also known to interfere with the uptake and translocation of several nutrients as was demonstrated in several studies (Hernández et al., 1996; Zhang et al., 2000; Zhu et al., 2004; Smeets at al., 2008). It can also induce lipid peroxidation affecting membrane structure and function (Smeets et al., 2005; Razinger et al., 2008; Tamás et al., 2008). Several studies have also indicated that cadmium can alter plant metabolism and induce oxidative stress resulting in an enhanced production of ROS and an induction of alterations within the antioxidative defense mechanism (Lin et al., 2007; Romero-Puertas et al., 2007; Semane et al., 2007; Razinger et al., 2008; Smeets et al., 2008).

1.3 Gamma radiation

1.3.1 Properties of gamma radiation

Radioactivity describes the process in which an unstable nuclide aims to return to a stable condition by emitting particles, such as alpha and beta particles but also protons and neutrons, and/or by emitting energy as photons, called gamma radiation.

Ionizing radiation is every form of radiation capable of causing ionizations and excitations by energy transfer from the radiation field to matter or tissue. In contrast to alpha or beta radiation, which can directly cause ionization by interaction with tissue, gamma radiation is characterized as indirect ionizing radiation as it first generates secondary reactive intermediates that in turn can react with the target. Not all ionizing radiation is necessarily originating from radioactive decay processes but can also be generated by for example Röntgen tubes. In contrast with gamma radiation, that due to its short wavelength and consequently high energy can cause ionizations, other electromagnetic radiation with lower energies such as UV (ultraviolet), visible light, IR (infrared) and

micro- and radio-waves are not able to produce ionization and are examples of non-ionizing radiation.

An important ionization process by interaction of ionizing radiation with plant or animal tissue is the radiolysis of water, producing several highly reactive intermediates that can initiate cellular damage. The ionization process in water is generally written as the following equation (Ward, 1988).

H_2O + radiation $\rightarrow$ H_2O^+ + e

The ionized water molecule reacts at the first collision with another water molecule to produce the $^{\bullet}OH$ radical.

$H_2O^+ + H_2O \rightarrow {}^{\bullet}OH + H_3O^+$

The electron loses energy and becomes hydrated.

$e + nH_2O \rightarrow e_{aq}$

Immediately after their formation, the radicals begin to interact at every collision with each other, producing hydrogen molecules, hydrogen peroxide and water.

$e_{aq} + e_{aq}\ (2H_2O) \rightarrow H_2 + 2OH^-$

$^{\bullet}OH + {}^{\bullet}OH \rightarrow H_2O_2$

$e + {}^{\bullet}OH \rightarrow OH^-$

Besides immediate mutual reactions, the highly reactive intermediates can also interact with biomolecules affecting their structure and function.

1.3.2 Natural sources of ionizing radiation in the environment

The radionuclides that are naturally present in the environment can be divided into 3 groups. The first group contains radionuclides that are part of 3 naturally occurring radioactive decay chains, headed by ^{238}U, ^{235}U or ^{232}Th and referred to as the uranium, actinium and thorium series, respectively. By successive decay, emitting alpha and beta particles in combination with gamma radiation, a stable nuclide is formed. The primordial radionuclides ^{238}U, ^{235}U or ^{232}Th, have large half-lives with a magnitude of some billion years. Uranium and thorium, and hence their decay products, are for example present in igneous, sedimentary

and phosphate rocks and several ores and minerals (Cowart & Burnett, 1994; Paschoa & Godoy, 2002; Vandenhove, 2002).

A number of primordial radionuclides that are not part of the radioactive decay chains in the first group are categorized in the second group. Of these radionuclides, ^{40}K and ^{87}Rb, with half-lives of 1.28×10^9 y and 4.8×10^{10} y respectively, are of principal significance because of their relatively high abundance in crustal rock. ^{40}K emits both gamma radiation and beta particles and ^{87}Rb emits only beta particles. They are present in crustal rock, but their concentrations vary widely with rock type and location. As these radionuclides are transferred to water, plants and animals, they are also taken up by man via the food chain. Since potassium is an essential element in the body it is readily taken up with a ^{40}K concentration of 60 Bq kg^{-1} body weight. For ^{87}Rb, the average concentration in the body is 8.5 Bq kg^{-1} body weight (Van der Stricht & Kirchmann, 2001).

Finally, the last group contains radionuclides that are continuously formed in nuclear reactions with atmospheric gases initiated by cosmic radiation. High energy charged particles from outer space or the sun can react with the nuclei of atmospheric components, producing secondary particles, including cosmogenic radionuclides and neutrons, and gamma radiation. ^{3}H, ^{7}Be, ^{10}Be, ^{14}C, ^{22}Na and ^{24}Na are examples of cosmogenic radionuclides which can emit beta particles and/or gamma radiation (Van der Stricht & Kirchmann, 2001).

1.3.3 Artificial sources of ionizing radiation in the environment

There are several anthropogenic sources of ionizing radiation in the environment including production processes, normal operation releases, accidental releases and nuclear explosions. By irradiating heavy nuclides as ^{235}U and ^{239}Pu with thermal neutrons under normal operating conditions, fission products as ^{90}Sr, ^{131}I and ^{137}Cs, all emitting beta particles and/or gamma radiation, will be formed. Due to nuclear accidents, such as the Chernobyl reactor explosion, fission products can be an important source for environmental artificial radioactivity. By irradiating other nuclides with neutrons, specific radionuclides can be produced for usage in medical, industrial or scientific applications (Moller & Mousseau, 2006).

Under normal nuclear power plant operation, discharges can be made to the atmosphere and the aquatic environment but these are kept low in order to protect man and environment and the doses received under normal operating conditions are in general negligible. Atmospheric discharges consist mostly of short-lived isotopes of noble gases, but also ^{3}H, ^{14}C and ^{131}I. In liquid effluents from nuclear power plants, ^{3}H is the dominating radionuclide. Besides the nuclear energy industry, hospitals are the main users of unsealed radionuclides such as ^{99m}Tc, ^{32}P, ^{35}S and ^{131}I which consequently can be found in the effluents from hospitals (Van der Stricht & Kirchmann, 2001).

Throughout the years, accidents involving releases of radioactive material to the environment, together with an input of artificial radioactivity from nuclear weapon testing in the atmosphere has occurred. During these incidents, radionuclides such as ^{137}Cs, $^{239;240}Pu$, $^{89;90}Sr$ and ^{131}I were released into the environment (Higgy & Pimpl, 1998; Van der Stricht & Kirchmann, 2001).

1.3.4 Ionizing radiation effects on man and animal species

Radiation effects in man and animal species are caused by the interaction of ionizing radiation with cells. Via water radiolysis, producing several reactive intermediates, or via direct interaction with biomolecules such as the induction of DNA strand brakes and the inactivation of enzymes, cellular damage can be initiated resulting in cellular death in most cases. When exposed to a high radiation dose, expressed in Gray (Gy), which gives the absorbed dose kg^{-1} tissue, or expressed in Sievert (Sv), taken into account the radiation type and organ irradiated, damage will be experienced in the organ or tissue and by the man or animal itself as a large number of cells is affected or death. In contrast to this deterministic damage that occurs after exposure to an absorbed dose above a certain threshold, there is a certain possibility, even after exposure to low doses that stochastic effects such as the formation of carcinogenic cells can occur.

Radiation induced effects depend on the radiosensitivity of the various organs and the total absorbed dose. The radiosensitivity of cells is proportional to the cell division rate. Therefore, rapidly dividing blood and intestine cells are extremely sensitive while muscle and nerve cells are least sensitive in an adult

body. After an acute full body irradiation dose above 1 Gy, a decrease in leucocytes, thrombocytes and erythrocytes will occur, causing bleedings, infections and anemia while after exposure to 6 Gy, the intestines will be affected causing diarrhea, infections and resorption disturbances.

Under normal circumstances man and animal species are exposed to very low doses from natural and artificial sources (table 1.6).

Table 1.6 - Annual radiation exposure for the average world citizen (UNSCEAR, 2000).

Radiation source	**Radiation dose [mSv y^{-1}]**
Natural sources	*2.4*
Cosmic radiation	0.4
Radionuclides and radon in soil	1.7
and constructing materials	
Radionuclides in human body	0.3
Artificial sources	*0.4*
Medical applications	0.4
Nuclear applications	0.008
Total	*2.8*

1.3.5 Effects of ionizing radiation on plants

To evaluate the effect of ionizing radiation on plants, endpoints such as growth, development, DNA damage, the reproductive capacity and death are mostly studied. Similar with human and animal cells, besides the immediate induction of DNA strand breaks, or attacking other biomolecules, the water radiolytic reaction is an important pathway by which highly reactive intermediates are produced causing cellular damage. Young plants are generally more radiosensitive than mature plants as cells with high proliferation rates are more radiosensitive than resting cells. It has also been assumed that the radiosensitivity is related with the size of the genome where species with small chromosomes seem more radioresistant (Sparrow & Miksche, 1961).

Most effect studies with ionizing radiation are performed for crops, but in the aftermath of the Chernobyl accident, radiation effects on pine trees have been studied and indicated them as very radiosensitive species with acute doses of 60 Gy resulting in massive mortality and no regeneration (Arkhipov et al., 1994). Following radiation exposure, morbidity endpoints such as reduced growth,

morphological changes, alterations in productivity and abnormal shape and appearance have been reported by several authors (Daly & Thompson, 1975; Zaka et al., 2004; Marciulioniene et al., 2005). To adequately protect the environment against the effects of radioactive substances, a screening value of 70 μGy h^{-1} for plants has been derived to represent a no effect dose rate and to be able to screen out situations of no concern when dose rates are below the screening level (PROTECT, 2008).

Ionizing radiation is also known to induce DNA damage that needs to be repaired before cell division to ensure the transmission of an intact genetic code. Depending on the level of DNA damage, the cellular response can lead to the recovery of the cell, induction of mutations or the initiation of programmed cell death. Several studies have identified genes important in DNA repair following irradiation (Davies et al., 1994; Doucet-Chabeaud et al., 2001) and indicated effects of ionizing radiation on the duration of the cell cycle (Okamoto & Tatara, 1995).

Besides negative irradiation effects, exposure to low radiation doses have been shown to stimulate growth and development as was reviewed by Sax (1954). These radiation hormesis effects have not only been reported for plants, but also for mammals, insects and bacteria (Upton, 2001).

1.4 Oxidative stress

1.4.1 Dual role reactive oxygen species

A dual role has been ascribed to the presence of reactive oxygen species (ROS) in plant cells, produced under normal and stress conditions. Primarily, ROS are toxic byproducts of aerobic metabolism capable of unrestricted oxidation of various cellular components which can lead to the oxidative destruction of the cell (Mittler, 2002; Mittler et al., 2004). Secondly, ROS can also function as signaling molecules to control and regulate biological processes such as growth, development and defense pathways (Dat et al., 2000; Mittler et al., 2004).

To defend the cell against ROS induced damage but to allow ROS signaling, plants possess a well equipped antioxidative defense system comprising

enzymes and metabolites (Foyer & Noctor, 2005a). A regulated balance between ROS production and scavenging is required if metabolic efficiency and function are to be maintained in optimal and stress conditions (Foyer et al., 1994). As oxidative stress implies a negative situation to be avoided, Foyer & Noctor (2005b) proposed to describe the syndrome as oxidative signaling which implies an important and critical function associated with the mechanisms by which plant cells sense the environment and make appropriate adjustments to gene expression, metabolism and physiology.

1.4.2 Reactive oxygen species production

There are many potential sources of reactive oxygen species in plants (figure 1.4). During the stepwise reduction of molecular oxygen (O_2) to water (H_2O), several ROS intermediates are generated (Dat et al., 2000).

$$O_2 \rightarrow (H)O_2^{\bullet -} \rightarrow H_2O_2 \rightarrow {}^{\bullet}OH + H_2O \rightarrow 2H_2O$$

During the first step hydroperoxyl ($HO_2^{\bullet -}$) and mainly superoxide ($O_2^{\bullet -}$) are produced. Superoxide is a moderately reactive, short lived ROS with a half life of approximately 2-4 μs. It can not pass through biological membranes as it is readily dismutated to hydrogen peroxide (H_2O_2). Superoxide is also reactive in a hydrophobic environment, causing lipid peroxidation and thereby weakening cell membranes (Dat et al., 2000; Bhattacharjee, 2005).

In the second step hydrogen peroxide, a relatively long lived molecule (1 ms), is generated. As an uncharged, relatively long lived molecule, it can diffuse through membranes, some distance from its site of production. An important signaling role has been ascribed to hydrogen peroxide in response to various stresses (Bhattacharjee, 2005). Increased hydrogen peroxide levels can initiate signaling responses such as enzyme activation, gene expression, programmed cell death and cellular damage (Neill et al., 2002). Hydrogen peroxide can inactivate enzymes through oxidation of their thiol groups (Bhattacharjee, 2005). Superoxide and hydrogen peroxide can, in the presence of metal catalysts, form the very reactive hydroxyl radical ($^{\bullet}OH$) through Haber-Weiss and Fenton reactions (Dat et al., 2000).

$O_2^{\bullet-} + Fe^{3+} \rightarrow Fe^{2+} + O_2$

$H_2O_2 + Fe^{2+} \rightarrow Fe^{3+} + OH^- + OH^{\bullet}$ (Fenton reaction)

Overall: $H_2O_2 + O_2^{\bullet-} \rightarrow OH^- + OH^{\bullet} + O_2$ (Haber-Weiss reaction)

The hydroxyl radical is the final ROS generated during the reduction process of molecular oxygen. It is very reactive with a half life of less than 1 μs, affecting molecules at its site of production (Dat et al., 2000). They are able to cause lipid peroxidation, protein denaturation and DNA mutations (Bowler et al., 1992).

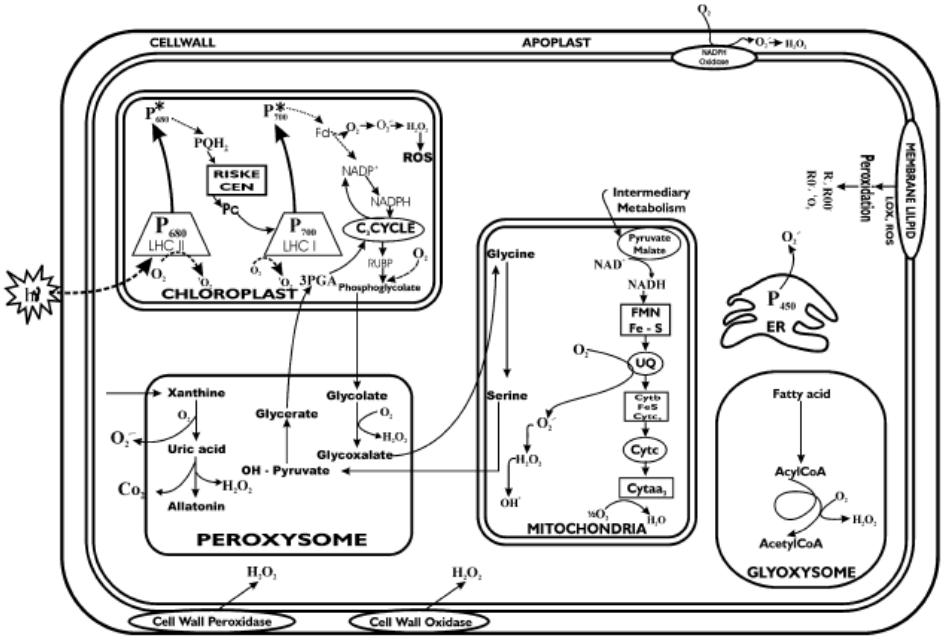

Figure 1.4 – Sources of ROS in plant cells (Bhattacharjee, 2005).

Through energy transfer to oxygen, the spin restriction can be overcome, and the highly destructing singlet oxygen ($^1O_2$) can be generated that will react with most biological molecules (Arora et al., 2002; Halliwell, 2006).

Singlet oxygen, superoxide and hydrogen peroxide are important ROS produced in the chloroplasts (Asada, 2006). Within the photosynthesis process, electrons can be transferred from the electron transport chains to oxygen, producing superoxide as a toxic byproduct which can further be detoxified by superoxide dismutase (SOD) to hydrogen peroxide. Also through energy transfer, necessary

for photosynthesis, the highly reactive singlet oxygen can be generated (Bowler et al., 1992; Arora et al., 2002). As the leakage of electrons from electron transport chains to oxygen is an important source of ROS in plants, superoxide, hydrogen peroxide and hydroxyl radicals will also be generated as byproduct during cellular respiration in the mitochondria (Bhattacharjee, 2005). Another ROS producing source includes photorespiration in the peroxisomes, producing hydrogen peroxide.

In plants, ROS are also generated at the plasma membrane level or extracellularly in the apoplast. Plasma membrane located NADPH oxidases, which catalyze the production of superoxides (Sagi & Fluhr, 2006), together with cell wall peroxidases, have been suggested to play an important role as ROS source during an oxidative burst (Dat et al., 2000; Bhattacharjee, 2005). Changes in the expression of NADPH oxidases provoked through disturbed ROS homeostasis under stress conditions, suggest that transcriptional activation of certain NADPH oxidases is an essential step in the activation of defense responses (Mittler et al., 2004).

Environmental fluctuations (e.g. metal exposure, UV irradiation, pathogen attack) can cause an oxidative burst at the plasma membrane (Low & Merida, 1996). The production of ROS is one of the earliest responses of plant cells under biotic and abiotic stresses, which suggests that the oxidative burst could function as a general alarm signal which serves to alert or notify metabolism and gene expression for possible modifications (Foyer et al., 1994). During the oxidative burst, the increase in superoxide and hydrogen peroxide production can be related with an increased plasma membrane NADPH oxidases mediated superoxide production together with apoplastic SOD for the conversion of superoxide into hydrogen peroxide (Bhattacharjee, 2005). The increase in superoxide and hydrogen peroxide occurs in the apoplastic space of the plasma membrane. In comparison with the cytoplasm, the apoplastic space and cell wall have relatively little antioxidative defense and hence the strong oxidative signal can persist much longer (Foyer et al., 2003). During an oxidative burst, hydrogen peroxide can also be generated by specific enzymes in response to various stresses (Neill et al., 2002). Hydrogen peroxide can than function as a signaling molecule that mediates plant responses to a range of biotic and abiotic stresses, leading to an enhanced expression of antioxidative enzymes or other

defense proteins or it can initiate cell death depending on the intensity of the oxidative signal (Neill et al., 2002; Foyer et al., 2003).

Reactive oxygen species can cause lipid peroxidation, affecting membrane structure and function. Peroxidation of lipids in plant cells is also a potential source of other ROS. Species such as the hydroxyl radical can extract a hydrogen atom from methylene (-CH_2-), creating the carbon radical (-$^{\bullet}$CH-). This carbon radical then attacks other methylene groups in lipid molecules, creating a chain reaction which can be terminated through the formation of fatty acid dimers or peroxide bridged dimers (Bhattacharjee, 2005; Magder, 2006). Lipid peroxidation in plant cells can also be initiated by lipoxygenases (LOXs) which are known to initiate the formation of oxylipins, which are products of fatty acid oxidation, with diverse functions in cells including signaling in wounding and other stress situations (Porta & Rocha-Sosa, 2002).

1.4.3 Antioxidative defense system

Exposure of plant cells to biotic and abiotic stress can cause a disruption of the metabolic balance of cells, resulting in an enhanced production of ROS (Mittler et al., 2004). To regulate ROS presence and to ensure control of the cellular redox state, plants possess a well equipped antioxidative defense system comprising enzymes and metabolites (figure 1.5) (Foyer et al., 1994). The antioxidants determine if ROS escape destruction and if they are being transformed into other ROS to function as signaling molecules (Foyer & Noctor, 2003; Foyer & Noctor, 2005b).

Within a cell, SODs constitute the first line of defense against ROS as they catalyze the disproportionation of superoxide into hydrogen peroxide (McCord & Fridovich, 1969). Superoxide dismutases are present in different cellular compartments, including mitochondria, chloroplasts, microsomes, glyoxysomes, peroxisomes, apoplasts and the cytosol, as superoxide can not cross membranes and must be detoxified at their sites of production (Bowler et al., 1994; Alscher et al., 2002).

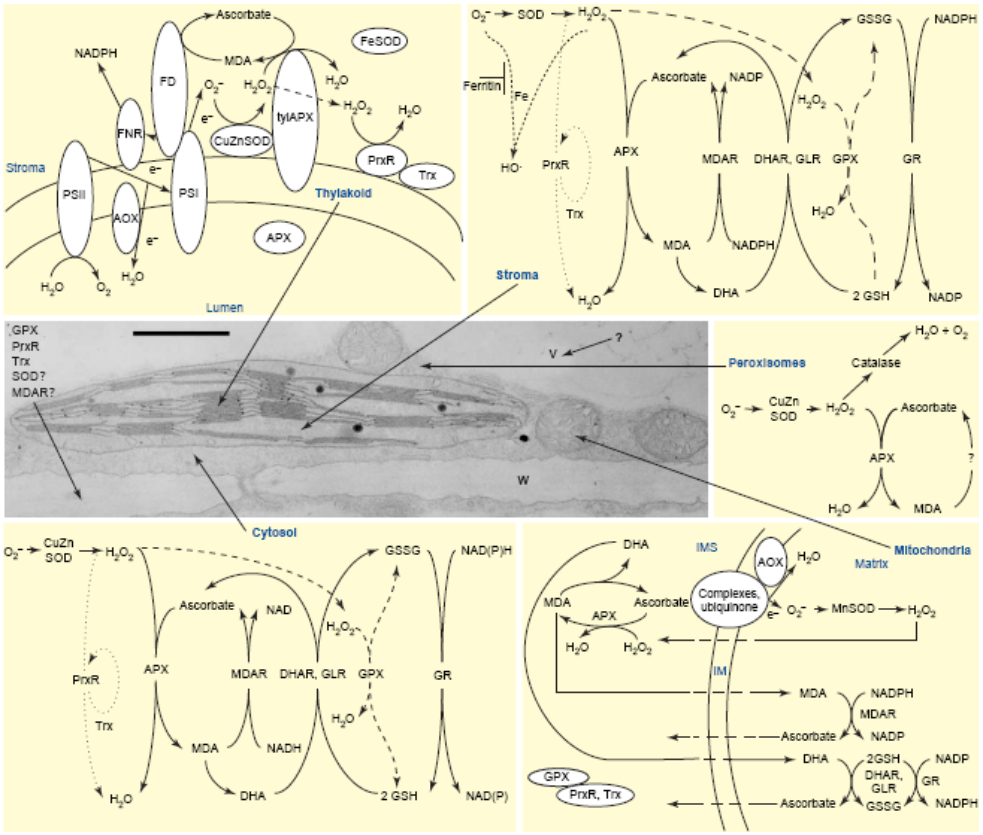

Figure 1.5 - Localization of reactive oxygen species (ROS) scavenging pathways in plant cells. A transmission electron micrograph of a portion of a plant cell is used to demonstrate the relative volumes of the different cellular compartments and their physical separation (middle left). The water-water cycle detoxifies superoxide and hydrogen peroxide and alternative oxidase (AOX) reduces the production rate of superoxide in the thylakoids (top left). ROS that escape this cycle and/or are produced in the stroma undergo detoxification by superoxide dismutase (SOD) and the stromal ascorbate-glutathione cycle. Peroxiredoxin (PrxR) and glutathione peroxidase (GPX) are also involved in hydrogen peroxide removal in the stroma (top right). ROS produced in peroxisomes during photorespiration, fatty acid oxidation or other reactions are decomposed by SOD, catalase (CAT) and ascorbate peroxidase (APOD) (middle right). SOD, components of the ascorbate-glutathione cycle and AOX are present in the mitochondria (bottom right). The cytosol contains the same set of enzymes found in the stroma (bottom left). The enzymatic components responsible for ROS detoxification in the apoplast and cell wall (W) are only partially known and the ROS scavenging pathways at the vacuole (V) are unknown. Membrane bound enzymes are depicted in white, GPX pathways are indicated by dashed lines and PrxR pathways are indicated by dotted lines in the stroma and cytosol. Abbreviations: DHA, dehydroascorbate; DHAR, DHA reductase; FD, ferredoxin; FNR, ferredoxin NADPH reductase; GLR, glutaredoxin; GR, glutathione reductase; GSH, reduced glutathione; GSSG, oxidized glutathione; IM, inner membrane; IMS, IM space; MDA, monodehydroascorbate; MDAR, MDA reductase; PSI, photosystem I; PSII, photosystem II; Trx, thioredoxin; tyl, thylakoid (Mittler et al., 2004).

Based on the metal co-factor used by the enzyme, SODs can be classified into 3 groups: (1) manganese SOD (MnSOD) is mainly present in the mitochondria and peroxisomes, (2) iron SOD (FeSOD) though predominantly present in the chloroplasts, can also be found in the cytosol, mitochondria and peroxisomes

and (3) copper/zinc SOD (CuZnSOD) is located in the cytosol, chloroplasts and mitochondria (Arora et al., 2002). There can be differences in responses to stress situations between the SOD isoforms due to their disparate subcellular locations and the site of action at which oxidative stress is generated (Bowler et al., 1992; Alscher et al., 2002).

After conversion of superoxide into hydrogen peroxide, several enzymes regulate the transformation of hydrogen peroxide into water. As important signaling functions are suggested for hydrogen peroxide, its cellular levels need to be regulated (figure 1.6). The balance between SODs and the different hydrogen peroxide scavenging enzymes in cells is crucial in determining the steady state level of superoxide and hydrogen peroxide (Mittler et al., 2004).

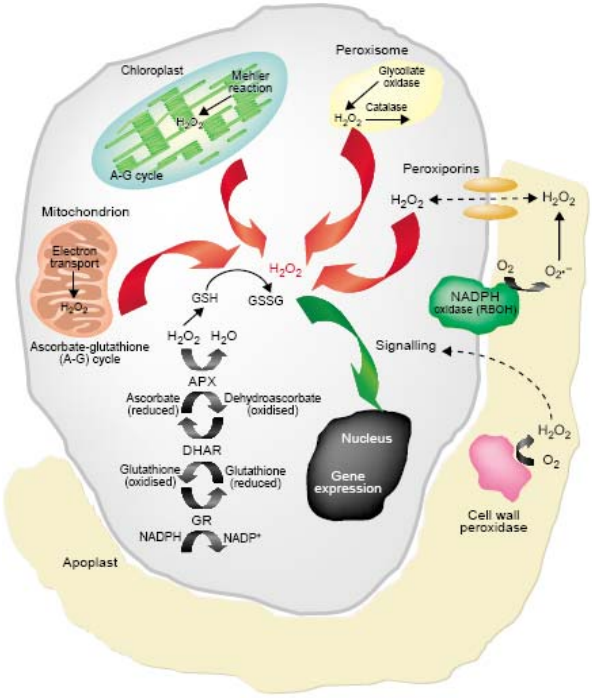

Figure 1.6 - Hydrogen peroxide turnover in the plant cell. Hydrogen peroxide is generated in normal metabolism in the chloroplasts, mitochondria and peroxisomes. Biotic and abiotic stresses enhance hydrogen peroxide generation via these routes and also via enzymatic sources such as plasma membrane localized NADPH oxidases or cell wall peroxidases. Hydrogen peroxide can diffuse freely, perhaps facilitated by movement through peroxiporin membrane channels. Cellular hydrogen peroxide levels can be determined by the rates of hydrogen peroxide production and metabolism via catalase, the ascorbate-glutathione cycle and glutathione directly (Neill et al., 2002).

Catalases catalyze the conversion of hydrogen peroxide into water and are primarily present in peroxisomes and glyoxysomes (Willekens et al., 1995). There are 3 main isoforms of catalase: CAT1, CAT2 and CAT3. In *Arabidopsis thaliana* plants, CAT1 is mainly found in vascular tissue, CAT2 is highly expressed in leaves, is light dependent and involved in the removal of hydrogen peroxide during photorespiration and CAT3 is mainly involved in the removal of hydrogen peroxide from glyoxysomes and is highly abundant in seeds and young seedlings (Dat et al., 2000). The expression of catalase genes is developmentally regulated but also sensitive to environmental stress situations and an early loss of catalase was suggested as a signal for antioxidative defense (Dat et al., 2000). Because of its discrete and specific localization in the peroxisomes, the protective action of catalase is limited and an array of other hydrogen peroxide scavenging pathways is present in plant cells (Halliwell, 2006). Catalase, the ascorbate-glutathione cycle and other peroxidases function in parallel as important hydrogen peroxide scavenging pathways. Catalase does not require reducing power and has a high reaction rate but a low substrate affinity, since the reaction requires the simultaneous access of 2 hydrogen peroxide molecules to the active site. Thereby only the bulk of hydrogen peroxide is removed. In contrast, peroxidases such as ascorbate peroxidase (APX) require reductants (e.g. ascorbate) and are found throughout the cell and have a higher affinity for hydrogen peroxide, allowing for the scavenging of small amounts of hydrogen peroxide in more specific locations (Asada, 1992; Noctor & Foyer, 1998; Dat et al., 2000).

Ascorbate, glutathione and α-tocopherol are important antioxidants for the scavenging of several ROS. The membrane associated α-tocopherol scavenges singlet oxygen and blocks the propagation step of lipid peroxidation. Ascorbate is present in chloroplasts, the cytosol, the vacuole, the apoplastic space, mitochondria and peroxisomes and plays a fundamental role in the removal of hydrogen peroxide (Foyer et al., 1994; Mittler et al., 2004). Ascorbate can react directly with hydroxyl radicals, superoxide and singlet oxygen. It is also an important secondary antioxidant, reducing the oxidized form of α-tocopherol (Noctor & Foyer, 1998). Glutathione is the predominant non protein thiol and has important roles in sulfur transport and the expression of defense genes.

Glutathione can react with singlet oxygen and hydroxyl radicals and protects the thiol groups of enzymes (Foyer et al., 1994).

The ascorbate-glutathione pathway is also an important hydrogen peroxide detoxification pathway present in the chloroplast, cytosol, peroxisomes and mitochondria (Foyer et al., 2003). Within this cycle, ascorbate (AsA) is used as a substrate to reduce hydrogen peroxide by APX, generating dehydroascorbate (DHA). Subsequently, glutathione (GSH) can than be used as reducing substrate to regenerate AsA from DHA by DHA reductase (DHAR), generating glutathione disulphide (GSSG). Glutathione is regenerated by glutathione reductase (GR) in a NADPH dependent reaction (Foyer et al., 1994; Noctor & Foyer, 1998).

As ascorbate and glutathione determine the fate and therefore signaling function of hydrogen peroxide in plant cells, the redox balance of the ascorbate and glutathione pools are important for redox signaling under various stress situations. Changes in the ratios of AsA to DHA and GSH to GSSG together with changes in absolute amounts of ascorbate and glutathione can regulate gene transcription (Mittler, 2002; Foyer et al., 2003).

Chapter 2

Scope and objectives

Anthropogenic activities such as uranium mining and milling, metal mining and smelting and the phosphate industry have caused radioactive contamination of the environment in many countries. In these areas, radioactive elements such as ^{238}U, ^{226}Ra and ^{232}Th can occur simultaneous with non-radioactive elements such as cadmium and zinc. Although toxicity effects for other heavy metals on plants are rather well studied, little information on uranium toxicity effects is available. When aiming to evaluate the uranium impact on the environment, it is important to study uranium induced biological effects on plants and to unravel the mechanisms by which they respond to uranium stress. As oxidative stress seems an important modulator under other heavy metal stresses, the role and importance of oxidative stress as a response mechanism to uranium stress should be investigated.

As uranium never occurs as a single pollutant, the multiple pollution and mixed nature of the contamination should not be neglected.

The **first part** of this research aimed to analyze morphological, physiological and oxidative stress related responses induced by bioaccumulation of uranium in *Arabidopsis thaliana* using a multi-biomarkers approach. Subtle effects (oxidative stress related enzymes on protein and transcriptional level, metabolites, DNA damage …) viewed as early responses for individual disturbances (growth, development …) were analyzed.

After optimization of the experimental setup (chapter 3), uranium induced effects on growth development and the nutrient profile of *Arabidopsis thaliana* seedlings were investigated (chapter 4). Subsequently, the importance of oxidative stress related responses were investigated for roots (chapter 5) and leaves (chapter 6) following uranium exposure. Finally the induction of DNA damage and repair related responses were studied (chapter 7).

As uranium occurs in combination with other stressors, in the **second part** of this research, the same biological effects were analyzed for *Arabidopsis thaliana* seedlings exposed to uranium in combination with cadmium or gamma radiation.

As they are both heavy metals, effects on growth, development and the nutrient profile and the importance of the antioxidative defense system were first

investigated for uranium in combination with cadmium (chapter 8). As ionizing radiation is also known to generate ROS but is very distinct from cadmium as stressor, similar effects were investigated in *Arabidopsis thaliana* seedlings after exposure to uranium in combination with gamma radiation (chapter 9).

Chapter 3

Effects of uranium and phosphate concentrations on oxidative stress related responses induced in *Arabidopsis thaliana*

Vanhoudt N., Vandenhove H., Smeets K., Remans T., Van Hees M., Wannijn J., Vangronsveld J. & Cuypers A. (2008) Effects of uranium and phosphate concentrations on oxidative stress related responses induced in *Arabidopsis thaliana*. *Plant Physiology and Biochemistry* 46, 987-996.

Abstract

The production of reactive oxygen species (ROS) and the induction of the antioxidative defense mechanism are very important in heavy metal toxicity. In this study, biological effects induced after uranium contamination were investigated for *Arabidopsis thaliana*. Three-week-old seedlings were exposed for 4 days to 100 µM U in an adjusted Hoagland solution. Uranium exposure caused a decreased growth of leaves (38 %) and roots (70 %) and a modified nutrient profile was observed. Investigation of lipid peroxidation products indicated a significant increase of membrane damage. Important ROS-producing and -scavenging enzymes were studied at transcriptional and protein level to investigate the importance of the ROS-signature in uranium toxicity. Elevated gene expression was observed for NADPH-oxidase, a ROS-producing enzyme. Changes in gene expression for different ROS-scavenging enzymes as Cu/ZnSOD, FeSOD and APX were also observed. Analysis of enzyme capacities showed little effects after uranium contamination. Higher ascorbate levels in uranium exposed leaves suggested an increase of antioxidative defense via the ascorbate-glutathione pathway after uranium exposure. Theoretical calculations indicated rapid formation of uranium-phosphate precipitates if normal phosphate concentrations are used. Precipitation tests recommend the use of 25 µM P in combination with 100 µM U to inhibit uranium precipitation. Because this combination was used for uranium toxicity investigation, the influence of this low phosphate concentration on plant growth and oxidative stress had to be evaluated. Minor differences between low phosphate (25 µM P) and high phosphate (100 µM P) treatments were observed justifying the use of the low phosphate concentration in combination with uranium.

3.1 Introduction

Uranium is a naturally occurring radionuclide and heavy metal with an average concentration in the continental crust of 1.7 ppm (Wedepohl, 1995). As a member of the actinide series, uranium has an atomic number of 92 with ^{238}U (99.27 %), ^{235}U (0.72 %) and ^{234}U (0.0055 %) as the 3 most abundant radioactive isotopes (Sheppard et al., 2005). Uranium mining and milling, metal mining and smelting and the phosphate industry have caused radioactive contamination of the environment in many countries (Vandenhove, 2002). Uranium toxicity effects are predominantly studied on man and animal species (Ribera et al., 1996), but little information is available for plants. If phytoremediation of uranium contaminated soils is considered, biological effects on the vegetation have to be investigated. Information on the contamination impact can also be used for risk assessment and derivation of clean-up standards.

Uranium is a radiotoxic and chemotoxic element with a greater risk of chemical toxicity than radiological toxicity because of the large physical half-life. ^{238}U has a physical half-life of 4.5×10^9 a, giving it a very low specific activity of 12.4 kBq g^{-1} (Sheppard et al., 2005). When exposed to ionizing radiation, molecular and cellular effects are induced directly through energy transfers to macromolecules or indirectly through a water radiolytic reaction producing ROS (Ribera et al., 1996). The chemical toxicity is of particular importance when studying uranium induced effects. Chemical effects depend on the form in which uranium is present. Compounds soluble in organic fluids and water are more toxic than non-soluble compounds as oxides. The aqueous uranyl ion (UO_2^{2+}) is the major cause of chemical toxicity (Ribera et al., 1996). Uranium can cause macroscopic effects as stunted growth and reduced biomass-production (Charles et al., 2006; Vandenhove et al., 2006). At the cellular level UO_2^{2+} can interact with macromolecules as proteins and nucleic acids and can affect enzyme capacities and membrane permeability (Nieboer et al., 1979; Nieboer & Richardson, 1980; Boileau et al., 1985). A possible underlying mechanism is the replacement of Ca^{2+} and Mg^{2+} with UO_2^{2+} or the interaction of UO_2^{2+} with phosphate and carboxylic groups.

Plants can experience oxidative stress when they are exposed to environmental stress situations (e.g. exposure to heavy metals (Arora et al., 2002)). ROS are produced in both stressed and unstressed cells. ROS have a dual role in plant biology as both toxic byproducts of aerobic metabolism and key regulators of growth, development and defense pathways (Mittler, 2002; Mittler et al., 2004). Under unstressed conditions, the formation and removal of ROS are in balance. The steady-state level of ROS in cells needs to be tightly regulated. Consequently, cells have developed an antioxidative defense system consisting of ROS-scavenging enzymes (e.g. superoxide dismutase (SOD), catalase (CAT), ascorbate peroxidase (APX) …) and antioxidants (e.g. ascorbate (AsA), glutathione (GSH) …) (Arora et al., 2002; Mittler, 2002; Mittler et al., 2004). Under stress conditions there is an imbalance between the oxidative and antioxidative capacities resulting in an increase/decrease of the capacity of the antioxidative defense system as was shown by several authors for heavy metal stress (Clijsters et al., 1999; Drazkiewicz et al., 2003; Smeets et al., 2005; Vandenhove et al., 2006).

Uranium is present in the soil primarily in the U^{6+} oxidation state as UO_2^{2+}. The uranyl ion, UO_2^{2+}, is the most stable uranium species in an oxidizing solution and the most prevalent form in the environment (Sheppard et al., 2005). Uranium in soil and water forms complexes with sulfate and phosphate as well as with carbonate and hydroxide. These complexes increase the total solubility of uranium (Shahandeh et al., 2001). Laroche et al. (2005) reported that uranium uptake by *Phaseolus vulgaris* seems to be governed by UO_2^{2+} at pH 4.9, hydroxyl complexes at pH 5.8 or carbonate complexes at pH 7. Ebbs et al. (1998) indicated, using a computer speciation model, that in the presence of phosphate, uranium-phosphate complexes will be formed and will be stable over a pH range from 4.5 to 9.0. The formation of the uranium-phosphate complexes was predicted to reduce the level of free uranyl cations and uranyl hydroxides. According to Ebbs et al. (1998), addition of phosphate to a uranium containing solution reduced the toxic effects of uranium to peas, most likely due to complexation of uranium with phosphate. Complexation may have also reduced the bioavailability of uranium to peas. Laroche et al. (2005) showed that increasing phosphate in solution generates a decreasing gradient of free UO_2^{2+}, whatever the pH, but it did not affect uranium uptake by *Phaseolus vulgaris*.

Phosphorus fertilization of uranium contaminated soils resulted in reduced uranium solubility and extractability in soil most likely due to the formation of phosphate surface complexes as shown by Rufyikiri et al. (2006). Phosphorus is an essential nutrient element and its availability is one of the major factors affecting plant growth and development. Preliminary tests have indicated that lower phosphate concentrations, compared to standard nutrient solutions, should be used in combination with uranium for minimization of uranium-phosphate precipitation. However it is important to investigate whether low phosphate concentrations have an influence on growth parameters and the antioxidative defense system of plants.

The first objective of our study was to analyze the biological effects induced in *Arabidopsis thaliana* exposed to uranium using a low phosphate concentration. We aimed to analyze early responses on growth and the antioxidative defense system of plant cells. The second objective was to investigate the influence of low phosphate concentration on the same biological effects.

3.2 Materials and methods

3.2.1 Plant material and phosphate/uranium treatment

Seeds of *Arabidopsis thaliana* (Columbia ecotype) were placed on moist filter paper at 4 °C for 3 days in order to synchronize germination. Afterwards, seeds were placed on rockwool-holding plugs from 1.5 ml polyethylene centrifuge tubes. The plugs were positioned in a PVC cover capable of holding 81 plugs. The PVC cover was placed on a container filled with 2.8 l of a modified Hoagland solution (macro-elements without phosphate: 1/10 diluted, phosphate solution: 1/20 diluted, micro-elements: 1/10 diluted and iron solution: 1/10 diluted). Plants were grown in a growth chamber (Microclima 1000E, Snijders Scientific B.V.) under a 14 h photoperiod (photosynthetic photon flux density of 200 µmol m^{-2} s^{-1} at the leaf level, supplied by Sylvania BriteGro F36WT8/2084 and F36WT8/2023), with day/night temperatures of 22 °C/18 °C and 65 % relative humidity.

Subsequently, 3-week-old plants were divided in 3 groups and treated for 4 days with respectively 100 µM P, 25 µM P (control) and 25 µM P + 100 µM ^{238}U.

Phosphate was supplied as $NH_4H_2PO_4$ and uranium was added as $UO_2(NO_3)_2.6H_2O$ (Sigma). After uranium addition, pH was adjusted to ± 5.5 with NaOH.

Uranium speciation calculations, using the geochemical computer code *The Geochemist's Workbench®* database Pro 5.04 (Bethke, 2001) using the NEA thermodynamic data review by Grenthe et al. (1992), and precipitation tests recommended the use of 25 µM P in combination with 100 µM U to prevent uranium-phosphate precipitation.

3.2.2 Plant sampling and biometric measurements

At harvest, leaf and root fresh weight was determined and samples were frozen in liquid nitrogen and stored at -80 °C. At least 20 biological replicates of ± 100 mg FW were harvested per treatment.

Samples for nutrient and uranium analyses were dried at least for 1 week at 70 °C. Leaves were rinsed with distilled water en roots were washed twice for 10 minutes with 1 mM $Pb(NO_3)_2$ at 4 °C to exchange surface-bound U. Two biological replicates of ± 300 mg FW were harvested for the leaves of each treatment and one biological replicate ± 300 mg FW was harvested for the roots of each treatment.

3.2.3 Nutrient and uranium analysis

After dry-ashing using a muffle furnace, dried plant material was digested in 0.1 M HCl for determination of ^{238}U and several nutrients. The ^{238}U concentration was determined by inductively coupled plasma mass spectrometry (ICP-MS, Perkin-Elmer, Elan 5000 utilizing a cross flow nebulizer and a ryton spray chamber). Calibration curves were obtained using uranium standard solutions (0-10 µg l^{-1}) prepared from the elemental standard SPEX solution (SPEX Industries Inc.). The instrumental detection limit of uranium was 10 ng l^{-1}. Typical precision for the samples was below 5 % (relative standard deviation, 10 replicates). A specific activity of 12436 Bq g^{-1} for ^{238}U was considered (Joint Evaluated File (JEF) version 2.2, OECD/NEA Data Bank, Paris, France). Different elements (Fe, Ca, Mn, Cu, Zn, K, Mg, Na, P) were determined by inductively coupled plasma – atomic emission spectrometry (ICP-AES).

3.2.4 Determination of lipid peroxidation

TBA reactive compounds (mainly malondialdehyde) were used as a measure of lipid peroxidation in leaves of *Arabidopsis thaliana*. Plant tissue (approximately 100 mg) was homogenized with 2 ml 0.1 % TCA buffer using a mortar and pestle. After centrifugation at 20000 × g for 10 minutes, 0.5 ml of the supernatant was added to 2 ml 0.5 % TBA. This mixture was heated at 95 °C for 30 minutes and quickly cooled in an ice bath. After centrifugation at 20000 × g for 10 minutes, the absorbance of the supernatant was measured spectrophotometrically at 532 nm corrected for unspecific absorbance at 600 nm according to Dhindsa et al. (1981).

3.2.5 Analysis of enzyme capacities

Frozen leaf or root tissue (approximately 100 mg) was homogenized in ice-cold 0.1 M Tris-HCl buffer (pH 7.8) containing 1 mM EDTA, 1 mM dithiotreitol and 4 % insoluble polyvinylpyrrolidone (2 ml buffer 100 mg^{-1} FW) using a mortar and pestle. The homogenate was squeezed through a nylon mesh and centrifuged at 20000 × g and 4 °C for 10 minutes. The enzyme capacities, i.e. potential activity measured in vitro under non-limiting reaction conditions, were measured spectrophotometrically in the supernatant at 25 °C.

Guaiacol peroxidase and syringaldazine peroxidase capacities (GPOD, SPOD, EC 1.11.1.7) were measured at 436 nm and 530 nm according to Bergmeyer et al. (1974) and Imberty et al. (1984), respectively. Ascorbate peroxidase capacity (APOD, EC 1.11.1.11) was measured at 298 nm following the method of Gerbling et al. (1984). Analysis of superoxide dismutase capacity (SOD, EC 1.15.1.1) was based on the inhibition of cytochrome c at 550 nm according to McCord and Fridovich (1969). Analysis of the capacities of glutathione reductase (GR, EC 1.6.4.2) and catalase (CAT, EC 1.11.1.6) were performed as described by Bergmeyer et al. (1974).

3.2.6 Metabolite analysis

Ascorbate in the leaves of *Arabidopsis thaliana* was determined by HPLC analysis. Therefore approximately 100 mg of tissue was ground thoroughly in liquid nitrogen using a pre-cooled mortar and pestle. When a homogenous

powder was obtained 2 ml of ice cold 6 % (w/v) meta-phosphoric acid containing 1 mM Na_2EDTA was added and the mixture was clarified by centrifugation at 20000 × g and 4 °C for 10 minutes. The resulting supernatant was kept frozen until HPLC analysis. Antioxidants were separated on a 100 mm × 4.6 mm Polaris C18-A reversed phase HPLC column (3 µm particle size, 30 °C, Varian, CA USA) with an isocratic flow of 1 ml min^{-1} of the elution buffer (25 mM K/PO_4-buffer, pH 3.0). The components were quantified using a home-made electrochemical detector with glassy carbon electrode and a Schott pt 62 reference electrode (Mainz, Germany). The purity and identity of the peaks was confirmed using a diode array detector (SPD-M10AVP, Shimadzu, Hertogenbosch, Netherlands) which was placed on line with the electrochemical detector. The concentration of oxidized DHA was measured indirectly as the difference between the total ascorbate concentration in a DTT-reduced fraction and the concentration in the sample prior to reduction. Reduction of the sample was obtained by incubation of an aliquot of the extract in 400 mM Tris and 200 mM DTT for 15 minutes in the dark. The pH of this mixture was checked to be between 6.0 and 7.0. After 15 minutes the pH was lowered again by 4-fold dilution in elution buffer prior to HPLC analysis.

3.2.7 Gene expression analysis

Frozen leaf tissue (approximately 100 mg) was ground thoroughly in liquid nitrogen using a mortar and pestle. RNA was extracted using the RNeasy Plant Mini Kit (Qiagen). The concentration of the RNA was determined spectrophotometrically at 260 nm (Nanodrop, Isogen Life Science). The RNA purity was checked spectrophotometrically by means of the 260/280-ratio. First strand cDNA synthesis was primed with an $oligo(dT)_{16}$-primer according to the manufacturer's instructions using Taqman Reverse Transcription Reagents (Applied Biosystems), and equal amounts of starting material (RNA) were used (1 µg). Quantitative PCR was performed with the ABI Prism 7000 (Applied Biosystems), Sybr® Green chemistry. Primers used for the analysis of several genes are given in table 3.1. At4g34270 and at4g26410 were used as reference genes. PCR amplifications were performed in a total volume of 25 µl, containing 2.5 µl cDNA sample, 12.50 µl Power Sybr® Green PCR Master Mix (Applied Biosystems), 0.75 µl forward primer, 0.75 µl reverse primer and 8.50 µl RNase-

free water. Gene expression data were calculated relative to the reference genes following the $2^{-\Delta\Delta Ct}$ method (Livak & Schmittgen, 2001). Gene expression was represented relative to the gene expression observed in leaves exposed to 25 µM P.

Table 3.1 - Primer sequentions used for quantitative real time PCR of several genes.

Gene	Forward primer	Reverse primer
At4g34270	GTGAAAACTGTTGGAGAGAAGCAA	TCAACTGGATACCCTTTCGCA
At4g26410	GAGCTGAAGTGGCTTCCATGAC	GGTCCGACATACCCATGATCC
Csd1	TCCATGCAGACCCTGATGAC	CCTGGAGACCAATGATGCC
Fsd1	CTCCCAATGCTGTGAATCCC	TGGTCTTCGGTTCTGGAAGTC
Msd1	ATGTTTGGGAGCACGCCTAC	AACCTCGCTTGCATATTTCCA
Cat1	AAGTGCTTCATCGGGAAGGA	CTTCAACAAAACGCTTCACGA
Apx1	TGCCACAAGGATAGGTCTGG	CCTTCCTTCTCTCCGCTCAA
RbohC	TCACCAGAGACTGGCACAATAAA	GATGCTCGACCTGAATGCTC

3.2.8 Statistical analysis

Statistical analyses were performed using an ANOVA test (Neter et al., 1996) in SAS 9.1. The ANOVA test was carried out separately for leaves and roots. Mean values of treatments were compared using Tukey's multiple comparison test. Transformations were applied when necessary to approximate the assumptions of normality and same error variance. Data presented are mean values ± standard error.

3.3 Results

3.3.1 Growth responses

A significant decrease in biomass production was observed for leaves and roots of *Arabidopsis thaliana* exposed for 4 days to 100 µM U (figure 3.1). Leaves started to show chlorosis and roots were stunted and turned yellow (figure 3.2).

Phosphate fertilization seemed to have no influence on growth as no significant effect in fresh weight for leaves or roots was observed for *Arabidopsis thaliana* seedlings exposed to 100 µM P or 25 µM P (figure 3.1).

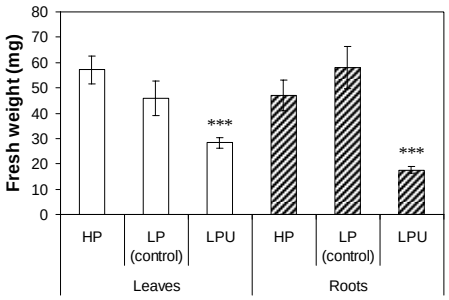

Figure 3.1 - Fresh weight (mg) of leaves and roots of 3-week-old *Arabidopsis thaliana* seedlings treated for 4 days with 100 µM P (HP), 25 µM P (LP) or 25 µM P + 100 µM U (LPU). Each point represents the mean ± S.E. of at least 20 biological replicates. Fresh weight measurements with *** are significantly different as compared to LP (p = 0.01).

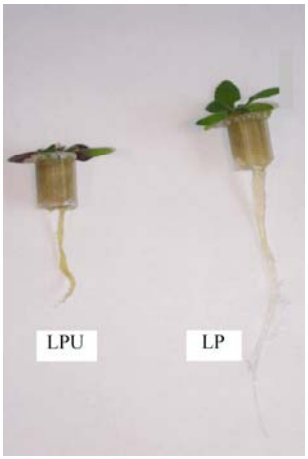

Figure 3.2 - Three-week-old *Arabidopsis thaliana* seedlings exposed for 4 days to 25 µM P + 100 µM U (left) or 25 µM P (control) (right).

3.3.2 Nutrient profile and uranium uptake

Exposure of 3-week-old *Arabidopsis thaliana* seedlings for 4 days to 100 µM U resulted in a decrease of most element concentrations (e.g. Ca, Mn, K, Mg, P, S) in leaves as compared to the low phosphate treatment (table 3.2). Uranium concentrations in the roots (133 mg g^{-1} DW, based on one measurement) were more than 2000 times larger than in the leaves (0.064 ± 0.012 mg g^{-1} DW) indicating a limited root to shoot transfer for uranium. Similar results were obtained in several other experiments (results not shown).

Table 3.2 - Nutrient profile for leaves of 3-week-old *Arabidopsis thaliana* seedlings exposed for 4 days to 100 µM P (HP), 25 µM P (LP) or 25 µM P + 100 µM U (LPU) (data presented are mean ± S.E.).

		HP	LP (control)	LPU
Element concentrations (µg g^{-1} DW) (*** p < 0.01, ** p < 0.05)	***Fe***	65±1	92±19	106±12
	Ca	59634±1179***	35997±819	13590±300***
	Mn	246±2***	144±10	66±1***
	Cu	< 0.05	< 0.05	< 0.05
	Zn	77±20	17±1	15±9
	K	20576±871	18313±95	7743±529***
	Mg	8989±168**	7852±141	3774±110***
	Na	6848±770	8372±1568	3982±214
	P	12600±127***	9292±43	4869±168***
	S	9714±52**	8144±423	3688±75***

Phosphate concentrations also influenced element concentrations in leaves of *Arabidopsis thaliana.* Plants exposed to 100 µM P had generally higher element concentrations (e.g. Ca, Mn, Mg, P, S) than plants exposed to 25 µM P (table 3.2).

3.3.3 Lipid peroxidation

The level of lipid peroxidation in the leaf tissue was based on the thiobarbituric acid reactive compounds (TBA-rc), such as malondialdehyde. In figure 3.3 are the concentrations of the TBA-rc for the different treatments summarized.

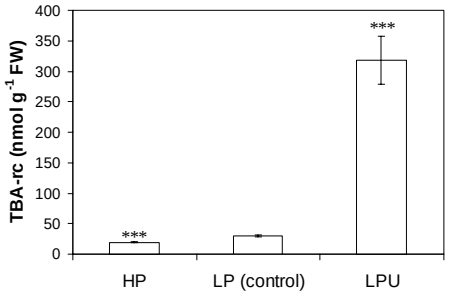

Figure 3.3 - The level of lipid peroxidation, based on the amount of TBA-reactive compounds (nmol TBA-rc g^{-1} FW) in the leaves of 3-week-old *Arabidopsis thaliana* seedlings treated for 4 days with 100 µM P (HP), 25 µM P (LP) or 25 µM P + 100 µM U (LPU). Each point represents the mean ± S.E. of 5 biological replicates for HP and LP and 4 biological replicates for LPU. TBA-rc concentrations with *** are significantly different as compared to LP (p = 0.01).

A significant increase (10-fold) of lipid peroxidation was observed for *Arabidopsis thaliana* leaves treated for four days with 100 µM U compared to the low phosphate treatment.

A significantly lower TBA-rc concentration was observed for the high phosphate treatment (19.42 ± 0.93 nmol g^{-1} FW) compared to the low phosphate treatment (29.45 ± 1.46 nmol g^{-1} FW), but the difference was less pronounced than between the low phosphate and uranium treatment.

3.3.4 Effects on the antioxidative defense system

3.3.4.1 Enzymes

To study the effects of uranium contamination on the antioxidative defense mechanism of plants and to assess the influence of phosphate concentrations on the same mechanism, enzyme capacities for leaves and roots of *Arabidopsis thaliana* were analyzed.

Generally, uranium contamination did not affect enzyme capacities except for CAT and guaiacol peroxidase (GPOD). A decreasing trend in enzyme capacity for CAT in leaves and roots was observed after uranium treatment as compared to the low phosphate treatment (figure 3.4A). Uranium exposure caused a significant increase in GPOD capacity for leaves and roots as compared to their corresponding low phosphate treatment (figure 3.4B).

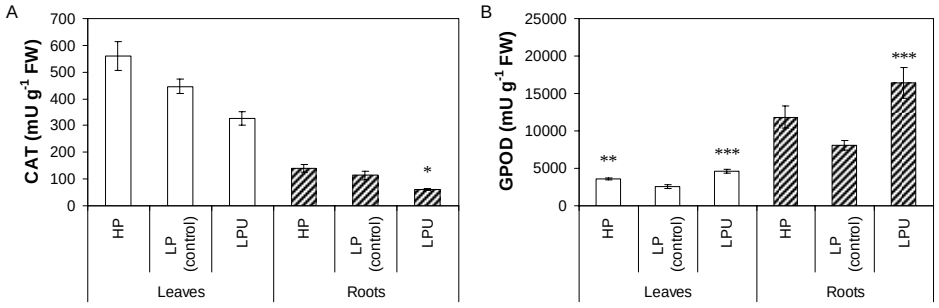

Figure 3.4 - Enzyme capacities (mU g^{-1} FW) of catalase (CAT) and guaiacol peroxidase (GPOD) for leaves and roots of *Arabidopsis thaliana*. Three-week-old *Arabidopsis thaliana* seedlings were treated for 4 days with 100 µM P (HP), 25 µM P (LP) or 25 µM P + 100 µM U (LPU). Values are the mean ± S.E. of at least 3 biological replicates. For statistical analysis, results for leaves and roots are compared with their corresponding LP treatment (significance levels: *** $p < 0.01$, ** $p < 0.05$, * $p < 0.1$).

For most enzymes studied no significant difference was observed between the high and low phosphate treatments (results not shown).

3.3.4.2 Metabolites

Uranium exposure significantly increased the total amount of ascorbate (AsA + DHA) in leaves of *Arabidopsis thaliana* (figure 3.5). This increase was due to a significant increase of reduced ascorbate (AsA). The level of dehydroascorbate (DHA) was not affected by uranium treatment.

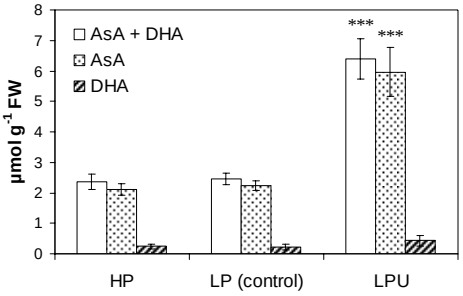

Figure 3.5 - AsA + DHA (total ascorbate), AsA (reduced ascorbate) and DHA (dehydroascorbate) (µmol g^{-1} FW) in the leaves of 3-week-old *Arabidopsis thaliana* seedlings after treatment with 100 µM P (HP), 25µM P (LP) or 25 µM P + 100 µM U (LPU). Each point represents the mean ± S.E. of 4 biological replicates. Ascorbate measurements with *** are significantly different as compared to LP (p = 0.01).

No effect was observed in the AsA and/or DHA content for different phosphate concentrations in the leaves of *Arabidopsis thaliana* (figure 3.5).

3.3.4.3 Gene expression

Gene expression of several ROS-scavenging enzymes, located in different organelles, was analyzed. Exposure of *Arabidopsis thaliana* seedlings to 100 µM U resulted in a significant down-regulated gene expression for *csd1* (cytoplasmic CuZnSOD) in leaves and roots (figure 3.6A). Altering the phosphate concentration from 25 µM P to 100 µM P had no influence on the expression of *csd1*. Although no significant difference was observed for *fsd1* (plastidic FeSOD) expression in the leaves of *Arabidopsis thaliana*, there was a significant increase in expression for the roots (figure 3.6B). While an elevated phosphate concentration resulted in a doubling of the expression, uranium contamination increased transcript levels 20 times compared to expression in the roots with

low phosphate treatment. *Msd1* (mitochondrial MnSOD) expression was not significantly affected by both treatments (figure 3.6C).

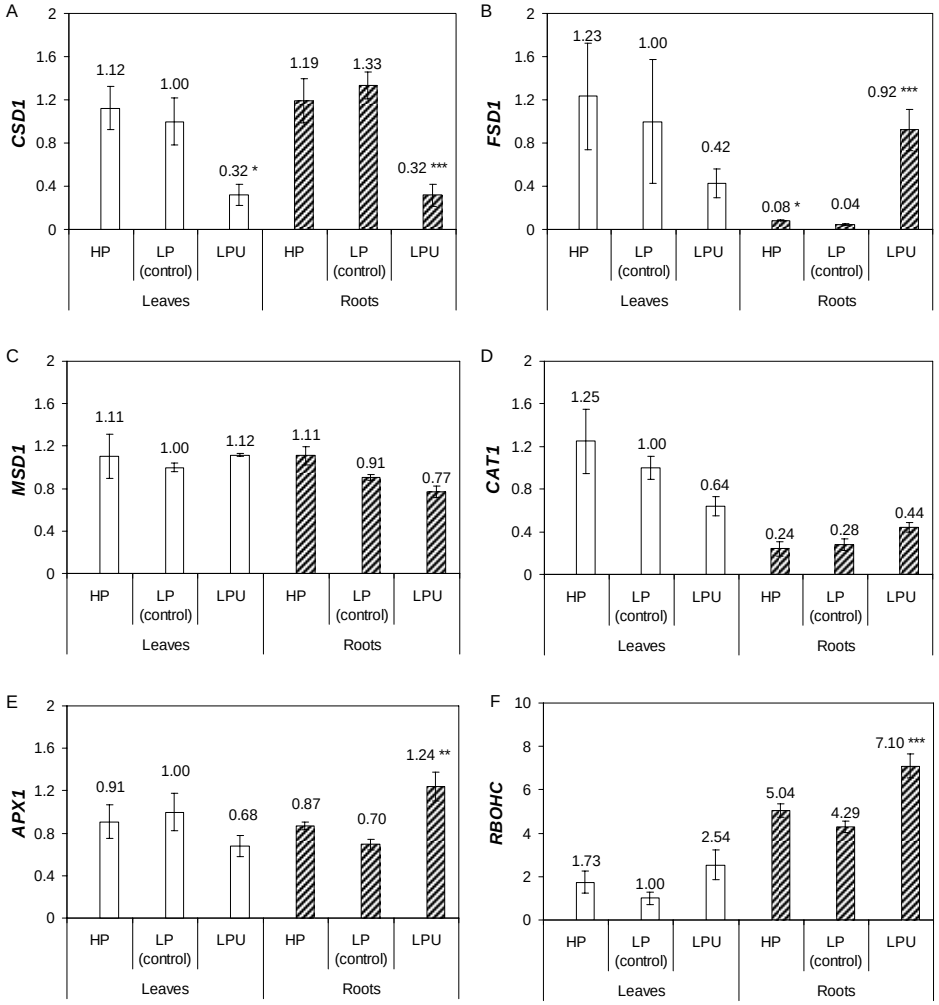

Figure 3.6 - Differences in gene expression of $O_2^{\bullet-}$ and H_2O_2 scavenging enzymes (A-D), an enzyme related to the ascorbate-glutathione cycle (E) and a ROS-producing enzyme (F) after uranium contamination and phosphate treatment. Gene expressions are relative to the control (leaves treated with 25 µM P (LP)) for leaves and roots of *Arabidopsis thaliana*. Three-week-old *Arabidopsis thaliana* seedlings were treated for 4 days with 100 µM P (HP), 25 µM P (LP) or 25 µM P + 100 µM U (LPU). Values are the mean ± S.E. of 3 biological replicates. For statistical analysis, results for leaves and roots are compared with their corresponding LP treatment (significance levels: *** $p < 0.01$, ** $p < 0.05$, * $p < 0.1$).

Transcript levels of *cat1* (peroxisomal CAT) were down-regulated in leaves and up-regulated in roots of *Arabidopsis thaliana* when exposed to 100 µM U,

however differences observed were not significant (figure 3.6D). Phosphorus concentration had no significant effect on the expression of *cat1*.

Additionally, gene expression for APX, an important enzyme of the ascorbate-glutathione cycle, was analyzed. Transcript levels of *apx1* (cytoplasmic APX) were significantly up-regulated in roots of *Arabidopsis thaliana* when exposed to uranium (figure 3.6E).

Finally, expression of *RbohC* (NADPH-oxidase located in the plasma membrane) was investigated. A significant increase for *RbohC* expression was observed in roots treated with uranium (figure 3.6F).

3.4 Discussion

3.4.1 Uranium toxicity

Exposure of plants to environmental stress situations (e.g. heavy metal contamination) disrupts the metabolic balance of cells and enhances the production of ROS as described by several authors (Clijsters et al., 1999; Alscher et al., 2002; Arora et al., 2002; Mittler, 2002). ROS can be generated by several enzymes as NADPH-oxidases, and removed by an array of ROS-scavenging enzymes located in different cellular compartments (Mittler et al., 2004). While oxidative stress situations for plants exposed to other heavy metals are well investigated (Clijsters et al., 1999; Cuypers et al., 2000, 2001, 2002; Ruley et al., 2004; Smeets et al., 2005), induction of the antioxidative defense pathway after exposure of plants to uranium is understudied. As results of a previous study with *Phaseolus vulgaris* showed only effects after exposure to 1000 µM uranium (Vandenhove et al., 2006), this study aimed to investigate if exposure of *Arabidopsis thaliana* to 100 µM uranium induced biological effects before exposing the seedlings to lower uranium concentrations. First, our study showed important oxidative stress effects after uranium exposure. Secondly, the study stated that the use of a lower phosphate concentration had limited influence on growth, cellular damage, gene expression and enzymatic activities of the antioxidative defense pathway.

After uranium exposure a significant reduction in plant growth (figure 3.1) was observed, leaves started to show chlorosis and roots were stunted and turned yellow (figure 3.2). Vandenhove et al. (2006) reported an increasing trend in growth parameters for *Phaseolus vulgaris* after application of 0-10 µM U, but a decrease (not significant) after exposure to 1000 µM U for 7 days. At the latter concentration, leaves also started to show chlorosis and roots turned yellowish. The decrease in growth at a lower concentration in our study can probably be explained by the difference in sensitivity of the two plants used in the studies (*Arabidopsis thaliana* and *Phaseolus vulgaris*). A decrease in growth parameters for plants exposed to heavy metals was shown by different researchers (Smeets et al., 2005; Charles et al., 2006).

Uranium mostly accumulated in the roots and transfer to the leaves was limited. A root to shoot transfer of ± 0.0005 was observed. Vandenhove et al. (2006) found transfer factors ranging from 0.02 at 0.1 µM U to 0.001 at 1000 µM U for *Phaseolus vulgaris*. The low transfer factor for uranium in *Arabidopsis thaliana* suggests that more severe toxicity effects can be expected in the roots as compared to the leaves. Uranium presence affected the nutrient profile of the plants. A decrease in most element concentrations (e.g. Ca, Mn, K, Mg, P, S) in the leaves was observed (table 3.2). In a previous study by Das et al. (1997), cadmium has also been shown to interfere with the uptake, transport and use of several elements (e.g. Ca, K, Mg, P) and water by plants. Theoretical speciation calculations, using the geochemical computer code *The geochemist's Workbench*® database Pro 5.04 (Bethke, 2001) using the NEA thermodynamic data review by Grenthe et al. (1992), indicated rapid formation of uranium-phosphate precipitates suggesting limited bioavailability of phosphate and uranium. Our results show that uranium exposure caused decreased phosphorus contents in the leaves. Speciation calculations revealed that precipitates of uranium with manganese will be formed in a phosphate deficient environment. As an excess of uranium is present, uranium-manganese precipitates are likely to be formed potentially limiting manganese uptake and translocation in the plant. As the uranyl ion (UO_2^{2+}) binds more strongly than Ca^{2+} and Mg^{2+} to their corresponding binding sites (Boileau et al., 1985) competition can occur resulting in a decrease of calcium and magnesium in uranium contaminated plants. Replacement of Ca^{2+} or Mg^{2+} by UO_2^{2+} can inhibit enzyme activity and

cause membrane damage. Because of its affinity for phosphate moieties and sugar alcohol groups of nucleotides and phosphate groups of phospholipids, DNA and membrane damage could also occur via this pathway (Nieboer & Richardson, 1980; Boileau et al., 1985).

A significant increase was observed in lipid peroxidation products after uranium treatment (figure 3.3) affecting membrane integrity and functionality. This is supported by the observed potassium leakage (table 3.2), an indicator of membrane instability. Several studies reported an increase of lipid peroxidation after cadmium treatment (Cho & Seo, 2005; Smeets et al., 2005) or due to other stresses as leaf senescence (Dhindsa et al., 1981). Smeets et al. (2005) reported an increase in the level of lipid peroxidation in the primary leaves of *Phaseolus vulgaris* after treatment with 2 µM $CdSO_4$.

Apart from their role as toxic byproduct of aerobic metabolism, ROS are being used for the control and regulation of biological processes such as growth, programmed cell death, biotic and abiotic stress responses and development (Mittler et al., 2004). ROS-signaling is controlled by production and scavenging. Important enzymes generating ROS are NADPH-oxidases. In the reaction they transform oxygen to a superoxide radical. NADPH-oxidases are located in the membrane as this is the first cellular compartment affected by stressors. Changes in transcript levels were analyzed and used as measure for the importance of NADPH-oxidase in ROS-production after uranium stress. *RbohC* expression was analyzed in roots and shoots of *Arabidopsis thaliana* exposed to 100 µM U and the results showed an increasing trend, although not significant, for the leaves and a significant up-regulated expression for the roots (figure 3.6F). These results suggest an important role for NADPH-oxidases in signaling under uranium stress as was also seen after cadmium stress (Cuypers, pers. comm.). The difference between leaves (increase but not significant) and roots ($p < 0.01$) can be explained by the low root to shoot transfer factor of uranium resulting in about 1500-fold lower uranium concentration in the leaves.

Within a cell, the superoxide dismutases (SODs) constitute the first line of defense against ROS, they transform $O_2^{\bullet-}$ to H_2O_2 (McCord & Fridovich, 1969). SODs are present in different subcellular locations as $O_2^{\bullet-}$ is produced at any location where an electron transport chain is present. Based on the metal co-

factor used by the enzymes, SODs can be classified into three groups: iron SOD (FeSOD) located in the plastids, manganese SOD (MnSOD) located in the mitochondria and peroxisomes, and copper-zinc SOD (CuZnSOD) located in the cytoplasm, chloroplast, peroxisomes and extracellular locations (Alscher et al., 2002; Mittler et al., 2004). To investigate the role of SODs in the defense against uranium stress, transcript levels of 3 genes (*csd1*, *fsd1* and *msd1*) were analyzed. *Csd1* (located in the cytoplasm) expression was significantly down-regulated for leaves and roots under uranium stress (figure 3.6A). Transcript levels of *fsd1* located in the plastids were significantly up-regulated for the roots after uranium treatment (figure 3.6B) suggesting an increased protection against oxidative stress located at the plastids. Gene expression of *msd1* located in the mitochondria was not affected by uranium stress (figure 3.6C). The difference in response between the FeSODs, MnSODs and CuZnSODs, can be correlated with their disparate subcellular locations and the sites of action of the oxidative stress induced by uranium as was also stated by Alscher et al. (2002) after treatment of *Arabidopsis thaliana* with different stresses and observation of changes for SOD activities. In a metal sensitive cultivar of *Phaseolus vulgaris* excess cadmium stimulated the Mn and/or FeSOD but inhibited CuZnSOD probably due to a cadmium-induced zinc-deficiency (Cardinaels et al., 1984; Weckx & Clijsters, 1997). At the protein level no change in total SOD capacity was observed after uranium application as was also reported by Vandenhove et al. (2006) for *Phaseolus vulgaris*. Cho & Seo (2005) reported a decrease in SOD capacity for *Arabidopsis thaliana* after cadmium application.

After conversion of superoxide radicals into hydrogen peroxide, several enzymes regulate the transformation of H_2O_2 into H_2O. A down-regulated trend for CAT located in the peroxisomes was observed at transcriptional (figure 3.6D) and protein (figure 3.4A) level for leaves of *Arabidopsis thaliana* under uranium stress. Also for roots a decrease in CAT capacity was observed (figure 3.4A). These results suggest less H_2O_2 will be detoxified by CAT under uranium stress. Opposite results were reported by Ruley et al. (2004) for CAT activities after lead treatment in *Sesbania drummondii* (an increasing trend was observed). Zhang et al. (2007) reported increasing and decreasing results for CAT capacity depending on the heavy metal concentration used and the plant species used. Peroxidases as GPOD and syringaldazine peroxidase (SPOD) have been reported

as H_2O_2 detoxifying enzymes after heavy metal stress in several studies (Clijsters et al., 1999; Cuypers et al., 2002; Smeets et al., 2005). Uranium induced oxidative stress resulted in a significant enhancement of GPOD capacity for leaves and roots of *Arabidopsis thaliana* (figure 3.4B). For SPOD capacities no significant difference was observed yet an increasing trend was visible. These results indicated an enhanced defense against uranium induced oxidative stress. Similar results were observed in several studies with different heavy metals and model plants. After copper and zinc application generally an increase of GPOD and SPOD capacities was observed for primary leaves and roots of *Phaseolus vulgaris* as reported by Cuypers et al. (2002). For cadmium toxicity the same trends were observed for primary leaves of *Phaseolus vulgaris* as stated by Smeets et al. (2005). Known results for uranium contamination showed comparable results except for an inhibition of enzyme capacity at 1000 µM U for *Phaseolus vulgaris* what is probably due to the severe toxicity of uranium at that concentration (Vandenhove et al., 2006).

The ascorbate-glutathione cycle, comprising several metabolites and enzymes, is an important pathway in detoxifying hydrogen peroxide as described by several authors (Cuypers et al., 2000; Drazkiewicz et al., 2003). In this study two enzymes of the ascorbate-glutathione cycle, APX and glutathione reductase (GR), and the metabolite ascorbate were analyzed. Hydrogen peroxides are detoxified by APX with ascorbate as substrate. The entire ascorbate-glutathione pathway comprises several steps with GR as an important enzyme in one of its steps. After 4 days exposure to 100 µM U, a significant increase in total ascorbate (AsA + DHA) was observed for leaves of *Arabidopsis thaliana* (figure 3.5). This was due to an increase in AsA (reduced form) but a steady-state situation in the amount of DHA (oxidized form). These results suggest an activation of antioxidative defense via the ascorbate-glutathione pathway as an increase in the AsA/DHA ratio is observed. This hypothesis can be confirmed by the increasing trend (not significant) for the APX and GR capacities in the leaves of *Arabidopsis thaliana*. At transcriptional level an increase in *apx1* expression was observed for the roots (figure 3.6E) but no significant increase was found at protein level. An increase of total ascorbate in leaves of *Phaseolus vulgaris* and *Arabidopsis thaliana* after heavy metal treatment (Cu, Cd, Zn) was reported by several authors (Cuypers et al., 2000, 2001; Drazkiewicz et al., 2003; Smeets et

al., 2005). An increase of ascorbate in leaves of *Arabidopsis thaliana* after copper treatment was reported by Drazkiewicz et al. (2003). Ascorbate concentrations increased also in leaves of *Phaseolus vulgaris* as was reported by Cuypers et al. (2000) after copper treatment and by Cuypers et al. (2001) after zinc treatment. Comparable with our results, Cuypers et al. (2000) also reported an increase of APX and GR capacities in leaves of *Phaseolus vulgaris* after copper exposure for 4 days. Capacities of APX and GR also increased for *Phaseolus vulgaris* treated with cadmium as was reported by Smeets et al. (2005). Apart from its role as a primary cellular antioxidant in the ascorbate-glutathione cycle, ascorbate has also a function as a secondary antioxidant because it represents a cellular reservoir to regenerate α-tocopherol, a membrane bound antioxidant that can scavenge lipid peroxide radicals. This latter function of ascorbate might be very important in case of uranium toxicity since membrane stability is strongly affected.

3.4.2 Phosphate influence

As previous results were obtained for *Arabidopsis thaliana* exposed to 100 µM U using 25 µM P, the influence of the low phosphate concentration on oxidative stress responses was analyzed. Plants were therefore exposed to 100 µM P or 25 µM P.

Phosphate fertilization had no effect on growth parameters (figure 3.1). Our results also showed a small decrease of phosphorous concentration in the leaves exposed to 25 µM P compared to 100 µM P. When compared to the nutrient profile of *Arabidopsis thaliana* (Columbia ecotype) shoots reported by Salt (2004), the phosphorous concentration in the leaves of *Arabidopsis thaliana* exposed to 25 µM P was sufficient for normal growth and development. Plants exposed to 100 µM P probably over-consumed phosphorous.

The concentration of TBA-rc was significantly enhanced after low phosphate treatment although compared with uranium application peroxidation of lipids was minimal (figure 3.3). Our results show no evidence of potassium leakage (table 3.2) suggesting the membrane structure is still intact.

For the ROS-signaling system, comprising ROS-producing NADPH-oxidases, ROS-scavenging enzymes as SODs, CAT, GPOD and SPOD, and the ascorbate-

glutathione pathway, minor alterations were observed following low phosphate treatment. No effects on transcriptional level were observed for the genes analyzed (figure 3.6). At protein level some enzymes showed a decrease in capacity after low phosphate treatment for leaves (GR (results not shown), GPOD (figure 3.4B)) and roots (SPOD (results not shown), SOD (results not shown)). No effects were observed for AsA and DHA in the ascorbate-glutathione cycle (figure 3.5).

3.4.3 Conclusions

Limited effects on the oxidative defense pathway are caused by decreased phosphate levels therefore the use of a low phosphate concentration to investigate uranium toxicity is justified.

Exposure of *Arabidopsis thaliana* to 100 µM U resulted in a decreased growth, an unbalanced nutrient profile and membrane damage and affected the antioxidative defense mechanism.

As oxidative stress related responses are triggered in *Arabidopsis thaliana* after exposure to 100 µM U, further investigation is suggested to determine dose-effect relations.

Chapter 4

Uranium induced effects on development and mineral nutrition of *Arabidopsis thaliana*

Vanhoudt N., Vandenhove H., Horemans N., Martinez Bello D., Van Hees M., Wannijn J., Carleer R., Vangronsveld J. & Cuypers A. (2009) Uranium induced effects on development and mineral nutrition of *Arabidopsis thaliana*. *In preparation.*

Abstract

This study aimed to investigate effects on growth and development and alterations in the nutrient profiles for *Arabidopsis thaliana* seedlings following uranium exposure. Seventeen-day-old *Arabidopsis thaliana* seedlings, grown on hydroponics, were exposed to 0, 0.1, 1, 10 and 100 µM uranium for 1, 3 and 7 days. Fresh weight of leaves and roots decreased after exposure to 100 µM uranium for 1 and 3 days and after exposure to 1, 10 and 100 µM uranium for 7 days. Root length decreased after exposure to the highest uranium concentration but an increase in root length was observed for lower uranium concentrations. Anthocyanous-colored leaves and stunted yellow roots were observed after 3 and 7 days exposure to 100 µM uranium. The uranium content of the roots increased with increasing uranium concentration added to the nutrient solution but the root-to-shoot transfer of uranium was limited. Exposure of *Arabidopsis thaliana* seedlings to a uranium concentration range resulted in disturbed nutrient profiles, especially following exposure to 100 µM uranium. For several macronutrients such as sulfur, magnesium and potassium, a decrease in concentration for roots and leaves was observed. The calcium content on the other hand increased in roots and decreased in leaves. The phosphorus content in the roots remained stable while in the leaves, its content decreased. The profiles of several micronutrients such as iron, sodium, copper, manganese and zinc were also altered. This study indicates that elevated uranium concentrations can cause important morphological and physiological effects and disturb the nutrient profiles in *Arabidopsis thaliana* seedlings.

4.1 Introduction

Uranium is a naturally occurring radionuclide and heavy metal present in the continental crust. Industrial activities including uranium mining and milling, metal mining and smelting and the phosphate industry, have caused radioactive contamination of the environment surrounding these installations (Vandenhove, 2002). Considering environmental protection, risk assessment and the derivation of clean-up standards, information on uranium toxicity effects for plants can be of great importance. Unfortunately information on uranium induced biological effects in plants is scant, especially when considering exposure of plants to low uranium concentrations.

Exposure of plants to heavy metals can cause damage at physiological, biochemical and molecular level. Physiological and morphological effects induced by other heavy metals (e.g. cadmium, copper, zinc …) are rather well studied. General symptoms as inhibition of leaf growth and stunted roots can be observed after exposure to heavy metals (Das et al., 1997; Van Belleghem et al., 2007; Gopal & Rizvi, 2008). Cadmium has shown to cause chlorosis of the leaves and at higher concentrations anthocyanous-colored leaves were observed (Van Belleghem et al., 2007). Apart from these visible effects, heavy metals can interfere with the uptake and translocation of nutrients in plants and disrupt the plant metabolism. There can be a competition for specific binding sites between the heavy metals and several nutrients sharing similar chemical properties. Cadmium has been shown to interfere with the uptake, transport and use of several elements (calcium, magnesium, phosphorus and potassium) and water by plants (Das et al., 1997). Hernández et al. (1996) reported a decrease in potassium and manganese concentrations in roots and shoots of pea seedlings exposed to cadmium. Cadmium exposure of *Arabidopsis thaliana* seedlings resulted in a decrease of magnesium, phosphorus, sulfur, potassium, calcium and manganese content in the leaves as shown by Smeets et al. (2008). Results showing an increase of phosphorus in tops and roots of radish following lead exposure were presented by Gopal & Rizvi (2008). In the same study, alterations in sulfur and iron uptake by radish after lead exposure were reported.

Uranium uptake and toxicity effects are dependent on the plant species, uranium speciation and soil characteristics. Uranium is present in the soil primarily in the +6 oxidation state as the uranyl cation (UO_2^{2+}). The results reported by Ebbs et al. (1998) indicated that the free UO_2^{2+}, which predominates at a pH of 5.0-5.5, was the form of uranium most readily accumulated by plants. Differences in uranium uptake by several plant species and the distribution between the roots, stem and leaves were presented by Singh et al. (2005). Sheppard et al. (2005) summarized data that showed toxicity effects in plants exposed to concentrations of 0.5-5 mg uranium kg^{-1} dry soil while other data reported no toxicity effects in plants after exposure to 100-1000 mg uranium kg^{-1} dry soil. Vandenhove et al. (2006) reported that leaves of bean seedlings started to show chlorosis and roots turned yellow after 4 days exposure to 1000 µM uranium. Uranium can react with several plant nutrients, interfere with their uptake and distribution and disturb their function in the plant cell. Cell membranes of plant and animal cells are known to be stabilized by Ca^{2+} (Nieboer et al., 1979). Since UO_2^{2+} binds more strongly than Ca^{2+} to Ca^{2+}-type binding sites, it has the potential to damage cell membranes and increase K^+ permeability (Nieboer & Richardson, 1980).

Previous studies mainly focused on the uptake and distribution of uranium in plants with the accent on soil composition and phytoremediation. But when considering the influence of uranium on the uptake and distribution of nutrients and effects on biochemical and molecular level, information is scant.

The first objective of this study was to analyze uranium toxicity effects on growth and development of the model plant *Arabidopsis thaliana* for a uranium concentration range and several exposure periods. Secondly, the influence of uranium presence on the nutrient profile of *Arabidopsis thaliana* seedlings was studied for different uranium concentrations and harvesting times.

4.2 Materials and methods

4.2.1 Plant culture and uranium exposure

Seeds of *Arabidopsis thaliana* (Columbia ecotype) were placed on moist filter paper at 4 °C for 3 days to synchronize germination. Afterwards, seeds were

sown on plugs from 1.5 ml polyethylene centrifuge tubes filled with 2 % agar (Difco). The plugs were positioned in a PVC cover capable of holding 81 plugs. The PVC cover was then placed on a container filled with 2.9 l of a modified Hoagland solution (macro-elements without phosphate: 1/10 diluted, phosphate solution: 1/20 diluted, micro-elements: 1/10 diluted and iron solution: 1/10 diluted). Plants were grown in a growth chamber (Microclima 1000E, Snijders Scientific B.V.) under a 14 h photoperiod (photosynthetic photon flux density of 200 µmol m^{-2} s^{-1} at the leaf level, supplied by Sylvania BriteGro F36WT8/2084 and F36WT8/2023), with day/night temperatures of 22 °C/18 °C and 65 % relative humidity. Roots were aerated during the entire course of the experiment.

Subsequently, 17-day-old seedlings were exposed to 0, 0.1, 1, 10 and 100 µM uranium for 1, 3 and 7 days. Uranium was added as $UO_2(NO_3)_2.6H_2O$ (Sigma) to the modified Hoagland solution and the pH was adjusted to ± 5.5 with NaOH. As previous experiments recommended the use of 25 µM phosphate in combination with uranium, a 1/80 diluted phosphate solution was used (Vanhoudt et al., 2008).

4.2.2 Plant sampling and biometric measurements

At harvest, fresh weight of leaves and roots was determined and the root length was measured. Samples for nutrient and uranium analyses and for the determination of the dry weight were dried at least for 1 week at 70 °C. For these determinations, leaves were rinsed with distilled water and roots were washed twice for 10 minutes with 10 mM $Pb(NO_3)_2$ at 4 °C to exchange surface-bound uranium.

4.2.3 Uranium and nutrient analyses

After dry-ashing using a muffle furnace, dried plant material was digested in 0.1 M HCl for determination of ^{238}U and several macro- and micronutrients. The ^{238}U concentration was determined by inductively coupled plasma mass spectrometry (ICP-MS, Perkin-Elmer, Elan 5000 utilizing a cross flow nebulizer and a ryton spray chamber). Calibration curves were obtained using uranium standard solutions (0-10 µg l^{-1}) prepared from the elemental standard SPEX solution

(SPEX Industries Inc.). The instrumental uranium detection limit was 10 ng l^{-1}. Typical precision for the samples was below 5 % (relative standard deviation, 10 replicates). A specific activity of 12436 Bg g^{-1} for ^{238}U was considered (Joint Evaluated File (JEF) version 2.2, OECD/NEA Data Bank, Paris, France). Different elements (Ca, Cu, Fe, K, Mg, Mn, Na, P, S and Zn) were analyzed using inductively coupled plasma - atomic emission spectrometry (ICP-AES).

4.2.4 Statistical analyses

The datasets for fresh weight, percentage dry weight, root length, uranium content and nutrient content, were statistically analyzed. Data were analyzed by day, evaluating the effect of uranium treatment, and also by treatment, comparing the means observed at the different sampling times. Statistical analyses were performed using an algorithm ensuring for each dataset a statistical analysis best fitted for the data.

The datasets for percentage dry weight, uranium content and nutrient content were analyzed according to the following algorithm. First, a parametric analysis of variance was performed and the assumptions for normality and constancy of variance were checked (Kutner et al., 2005). If the assumptions were fulfilled, a pair wise comparison was applied with an adjustment of the p-values using Tukey according to Kutner et al. (2005). If the assumptions were not fulfilled, the data was transformed using the Box & Cox method (Box & Cox, 1964). Subsequently, a parametric analysis of variance of the transformed response variables was applied. Again the assumptions for normality and constancy of variance were checked. If the assumptions were fulfilled, again a pair wise comparison, with an adjustment of the p-values using Tukey, was applied. If only the assumption for normality was fulfilled, a parametric analysis of variance for heterocedastic variances was applied according to Westfall et al. (2000). Subsequently, a pair wise comparison was carried out adjusting the p-values using simulated p-values (Westfall et al., 2000). If both assumptions were not fulfilled, a nonparametric analysis of variance was performed (Lehmann & D'Abrera, 1998). Thereupon, a pair wise comparison was applied using Wilcoxon Mann Whitney (Lehmann & D'Abrera, 1998) adjusting the p-values using Benjamini Hochberg (Benjamini & Hochberg, 1995).

The datasets for fresh weight and root length were analyzed according to the same algorithm as described above except for the last step. If after transformation using the Box & Cox method, both assumptions for normality and constancy of variance were not fulfilled, a parametric analysis of variance using a gamma distribution was applied according to McCullagh & Nelder (1989). A pair wise comparison was then applied adjusting the p-values using Benjamini Hochberg (Benjamini & Hochberg, 1995).

4.3 Results and discussion

Exposure of plants to heavy metals can cause an induction of physiological and morphological effects as was described by several authors (Das et al., 1997; Van Belleghem et al., 2007; Gopal & Rizvi, 2008). Heavy metals can also interfere with the uptake and translocation of several nutrients in plants and disrupt the plant metabolism (Hernández et al., 1996; Zhu et al., 2004; Gopal & Rizvi, 2008). While the induction of biological effects on growth and development and alterations of the nutrient profile are well studied for other heavy metals and plant species, the induction of biological effects following bioaccumulation of uranium in *Arabidopsis thaliana* is understudied. First, this study shows that uranium can cause important toxicity effects on growth and development of *Arabidopsis thaliana* seedlings. Secondly, the results indicate that uranium can interfere with the uptake and distribution of several nutrients resulting in disturbed nutrient profiles for leaves and roots.

4.3.1 Biometric parameters

A significant decrease of fresh weight of leaves and roots was observed after exposure to 100 µM uranium for 1 day (figure 4.1A) and 3 days (figure 4.1B) and after exposure to 1, 10 and 100 µM uranium for 7 days (figure 4.1C). On the other hand, the fresh weight of roots exposed to 1 and 10 µM uranium significantly increased after 3 days (figure 4.1B). Dry weight followed a similar trend (results not shown). A decrease of fresh weight of leaves and roots for different plants following exposure to cadmium or other heavy metals was shown by several authors. *Arabidopsis thaliana* seedlings exposed for 21 days to

different cadmium concentrations ranging from 0.1 to 50 µM showed a reduced leaf area starting at 5 µM cadmium and root growth was inhibited for 5 and 50 µM cadmium (Van Belleghem et al., 2007). Hernández et al. (1996) reported a reduction of the fresh weight of shoots and roots of pea seedlings with an increasing accumulation of cadmium in the plant. A decrease in shoot and root growth of *Cucumis sativus* after exposure for 5 days to different concentrations of copper, cadmium and lead was shown by An et al. (2004). Ebbs et al. (1998) reported a decrease in the dry weight of pea roots exposed to 5 µM uranium.

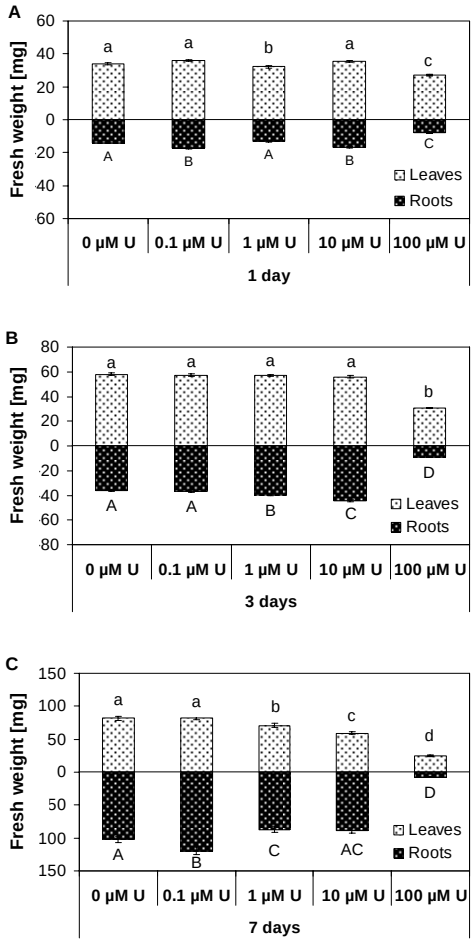

Figure 4.1 - Fresh weight [mg] of leaves and roots of *Arabidopsis thaliana* seedlings exposed to 0, 0.1, 1, 10 and 100 µM uranium for 1 (A), 3 (B) and 7 (C) days. Values represent the mean ± S.E. of at least 52 biological replicates. Data points with different letters are significantly different ($p < 0.05$).

Vandenhove et al. (2006) on the other hand, reported an increasing trend in growth parameters for *Phaseolus vulgaris* seedlings exposed to uranium concentrations ranging from 0.1 to 10 µM. Similar to Vandenhove et al. (2006), our study showed an increase in root fresh weight after exposure for 3 days to lower uranium concentrations. As uranium is added to the plants as uranyl nitrate it is conceivable to attribute this increased root fresh weight to a higher nitrate concentration. However, the extra nitrate added as uranyl nitrate is negligible in comparison to the nitrate present in the Hoagland nutrient solution. The increase in fresh weight for lower uranium concentrations after 3 days exposure seemed like a transient hormesis response as was also shown by Straczek et al. (2009) for hairy roots of carrots exposed to uranium concentrations between 2.5 and 5 mg l^{-1}.

For the fresh weight of leaves and roots, bioassay97 (Onofri, 2005) was used to perform dose-response curve analysis and calculate effective concentration (EC) levels. For leaves exposed during 7 days to a uranium concentration range, EC10, EC30 and EC50 levels for leaf fresh weight reduction were 3.2 ± 1.1, 10.3 ± 2.2 and 24.5 ± 4.4 µM uranium. For 7 days exposed roots, similar values of 6.5 ± 2.7, 10.6 ± 3.0 and 14.6 ± 4.6 µM uranium as EC10, EC30 and EC50 levels were found for root fresh weight reduction. Sheppard et al. (2005) reviewed that uranium concentrations within the normal background values have been reported as toxic for several terrestrial plants while in other studies no toxicity effects were found at concentrations 100 to 1000 times higher. Compared with the uranium benchmark value of 6 µg l^{-1} (~0.025 µM) for freshwater organisms (Jones et al., 2006), our data indicate that uranium toxicity effects on the fresh weight of *Arabidopsis thaliana* leaves and roots are visible at higher uranium concentrations.

The percentage dry weight (expressed as % of fresh weight) of leaves significantly increased after exposure to 100 µM uranium at all harvesting times (table 4.1). For the roots, the percentage dry weight significantly increased following exposure to 10 and 100 µM uranium during 7 days (table 4.1). Thus exposure to the highest uranium concentration caused a disturbed water balance in leaves and roots and generally plants started to wilt. Similar results were reported by Hernández et al. (1996): the relative water content of shoot and

root tissue of pea plants was reduced with increasing cadmium concentration added to the nutrient solution, indicating those plants might be water stressed.

Table 4.1 - Percentage dry weight of leaves and roots of *Arabidopsis thaliana* seedlings exposed for 1, 3 and 7 days to 0, 0.1, 1, 10 and 100 µM uranium. Results present mean ± S.E. of at least 3 biological replicates.

		Percentage dry weight [%]		
		1 day	3 days	7 days
LEAVES	0 µM U	$^{A}10.2 \pm 0.2^{a}$	$^{AB}10.8 \pm 0.4^{a}$	$^{B}11.8 \pm 0.1^{a}$
	0.1 µM U	$^{A}9.8 \pm 0.2^{a}$	$^{A}10.7 \pm 0.3^{a}$	$^{B}12.7 \pm 0.5^{a}$
	1 µM U	$^{A}9.5 \pm 0.3^{a}$	$^{B}10.7 \pm 0.3^{a}$	$^{C}13.5 \pm 0.2^{a}$
	10 µM U	$^{A}9.7 \pm 0.3^{a}$	$^{A}11.4 \pm 0.3^{a}$	$^{A}14.8 \pm 0.1^{a}$
	100 µM U	$^{A}11.4 \pm 0.3^{b}$	$^{B}16.4 \pm 0.4^{b}$	$^{C}21.8 \pm 0.3^{b}$
ROOTS	0 µM U	$^{A}4.8 \pm 0.3^{a}$	$^{A}4.8 \pm 0.6^{ac}$	$^{A}3.4 \pm 0.2^{a}$
	0.1 µM U	$^{A}4.1 \pm 0.3^{a}$	$^{AB}3.5 \pm 0.1^{b}$	$^{B}3.0 \pm 0.2^{a}$
	1 µM U	$^{A}3.8 \pm 0.3^{a}$	$^{A}3.7 \pm 0.1^{ab}$	$^{A}3.5 \pm 0.1^{a}$
	10 µM U	$^{A}4.8 \pm 0.3^{a}$	$^{B}3.5 \pm 0.2^{b}$	$^{A}4.2 \pm 0.1^{b}$
	100 µM U	$^{A}5.0 \pm 0.2^{a}$	$^{A}5.9 \pm 0.5^{c}$	$^{B}9.0 \pm 0.1^{c}$

Statistical analyses were done separately for leaves and roots. Different small letters indicate significant differences between the treatments for day 1, day 3 and day 7 separately ($p < 0.05$). Different capital letters indicate significant differences between the exposure days for the different treatments separately ($p < 0.05$).

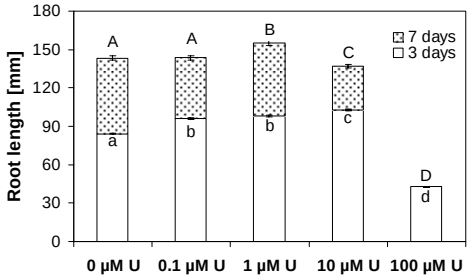

Figure 4.2 - Length [mm] of *Arabidopsis thaliana* roots exposed for 3 and 7 days to 0, 0.1, 1, 10 and 100 µM uranium. Values represent the mean ± S.E. of at least 115 biological replicates. Data points with different small letters are significantly different at 3 days exposure ($p < 0.05$). Different capital letters indicate a significant difference after 7 days exposure ($p < 0.05$).

Root length significantly decreased after exposure to 100 µM uranium for 3 days and from here on roots stopped growing (figure 4.2). For roots exposed to the lower uranium concentrations, a uranium dependent increase was observed for root length at 3 days (figure 4.2).

After 7 days exposure, this increased root length was still visible for 1 µM uranium, but exposure to 10 µM uranium caused a reduction in root length (figure 4.2) suggesting that after 7 days exposure uranium toxicity effects are also present in 10 µM uranium exposed roots.

Exposure of *Arabidopsis thaliana* seedlings to 100 µM uranium for 3 and 7 days resulted in anthocyanous-colored leaves and roots were stunted and turned yellow. Similar effects for the roots were reported by Vandenhove et al. (2006) where yellowish roots of *Phaseolus vulgaris* were observed following exposure to 1000 µM uranium for 4 days. Leaves on the other hand started to show chlorosis at a 1000 µM uranium concentration (Vandenhove et al., 2006). Similar results were found for *Arabidopsis thaliana* leaves exposed to cadmium where, depending on the concentration, chlorosis or anthocyanins production was shown (Van Belleghem et al., 2007). Anthocyanins are water-soluble pigments that can appear at specific developmental stages but may also be induced by a number of environmental factors including light exposure, cold temperatures and water stress as was reviewed by Chalker-Scott (1999). The production and localization of anthocyanins in leaves, roots and stems may allow the plant to develop resistance to a number of environmental stresses. Chalker-Scott (1999) also reviewed the antioxidative ability of anthocyanins under oxidative stress situations. As uranium was shown to induce oxidative stress related responses in *Arabidopsis thaliana* (Vanhoudt et al., 2008), anthocyanins may contribute in the defense against uranium induced oxidative stress.

4.3.2 Uranium uptake and distribution

The uranium concentrations in the roots increased with increasing uranium concentrations added to the nutrient solution (table 4.2). For leaves, the uranium concentrations also increased with the added concentration of uranium but the root-to-shoot transfer of uranium was small (table 4.2). For example, ± 2000 times more uranium was accumulated in the roots than in the leaves after

exposure to 100 µM uranium for 7 days. Uptake and distribution of uranium in plants is dependent on the plant species used and the age of the plant as was presented by Singh et al. (2005). Uranium accumulates mainly in the roots (Ramaswami et al., 2001) but toxicity effects also depend on the plant species as was summarized by Shahandeh et al. (2001). Vandenhove et al. (2006) also reported a limited root-to-shoot transfer of uranium. A 900-fold lower uranium concentration was observed in the leaves as compared to the uranium concentration in the roots of *Phaseolus vulgaris* exposed for 7 days to 1000 µM uranium (Vandenhove et al., 2006).

Table 4.2 - Uranium concentration [µg g^{-1} DW] in leaves and roots of *Arabidopsis thaliana* seedlings after exposure to 0, 0.1, 1, 10 and 100 µM uranium for 1, 3 and 7 days. Results present mean ± S.E. of at least 3 biological replicates.

		Uranium concentration [µg g^{-1} DW]		
		1 day	3 days	7 days
LEAVES	0 µM U	^{A} 0.02 ± 0.01^{a}	^{B} 1.13 ± 0.28^{ab}	^{B} 1.05 ± 0.27^{a}
	0.1 µM U	^{A} 0.07 ± 0.01^{b}	^{B} 0.74 ± 0.12^{ab}	^{B} 1.32 ± 0.22^{a}
	1 µM U	^{A} 0.57 ± 0.25^{c}	^{A} 0.64 ± 0.15^{a}	^{A} 0.87 ± 0.09^{a}
	10 µM U	^{A} 1.73 ± 0.69^{c}	^{A} 2.13 ± 0.71^{b}	^{A} 3.95 ± 0.80^{b}
	100 µM U	^{A} 7.80 ± 0.99^{d}	^{B} 10.24 ± 2.39^{c}	^{AB} 35.30 ± 5.14^{c}
ROOTS	0 µM U	^{A} 1.11 ± 0.32^{a}	^{B} 4.48 ± 0.35^{a}	^{C} 6.84 ± 0.35^{a}
	0.1 µM U	^{A} 243.95 ± 14.22^{b}	^{B} 162.04 ± 7.00^{b}	^{C} 82.98 ± 4.12^{b}
	1 µM U	^{A} 1699.91 ± 51.33^{c}	^{B} 914.72 ± 243.58^{c}	^{B} 778.21 ± 54.08^{c}
	10 µM U	^{A} 8857.47 ± 1354.49^{d}	^{A} 8425.13 ± 1645.68^{d}	^{B} 3728.26 ± 578.47^{d}
	100 µM U	^{A} 67408.50 ± 4202.90^{e}	^{A} 67582.33 ± 3639.51^{e}	^{A} 72531.31 ± 4134.71^{e}

Statistical analyses were done separately for leaves and roots. Different small letters indicate significant differences between the treatments for day 1, day 3 and day 7 separately ($p < 0.05$). Different capital letters indicate significant differences between the exposure days for the different treatments separately ($p < 0.05$).

4.3.3 Nutrient profiles

Mineral nutrients are essential for plant growth and development. They are directly involved in plant metabolism where they have specific and essential functions. Mineral nutrients can for example serve as constituents of important

organic structures as proteins and nucleic acids. They are also required in distinct metabolic steps as enzymatic reactions without being an integral component of an enzymatic structure. Depending on the amount necessary for normal growth and development, nutrients are classified as macro- or micronutrients. In this study, the influence of uranium presence on the uptake and distribution of several macronutrients (phosphorous, sulfur, magnesium, calcium, and potassium) and micronutrients (iron, manganese, copper and zinc) was investigated.

Generally, a decrease in time was observed for most nutrient concentrations (tables 4.3 & 4.4) which could be explained through the fact that the added nutrients in the solution are insufficiently available after 7 days. Because of senescence it could also be possible that the nutrient content of the leaves decreased in time as was demonstrated by Himelblau & Amasino (2001) for 37-day-old leaves of *Arabidopsis thaliana* seedlings. Exposure to 100 µM uranium caused the most severe effects on the nutrient profiles for the roots. At this uranium concentration, roots are dying and cells are damaged, resulting in the leakage of several nutrients.

Phosphorous has important functions in macromolecular structures as it is a component of nucleic acids and phospholipids of biomembranes. As part of the energy-rich ATP (adenosine triphosphate), phosphorous also plays an important role in the process of cellular respiration. Uranium binds to phosphate to form uranylphosphate complexes which are very stable and which may form insoluble precipitates such as autunite (Günther et al., 2003). This may highly influence uranium bioavailability. For the roots, little effects on phosphorous concentrations were observed, also after exposure to 100 µM uranium (table 4.3). Laroche et al. (2005) showed that uranium was precipitated on the root surface as phosphate-rich precipitates. In leaves, a significant decrease in phosphorous concentration was observed after exposure to 100 µM uranium at all harvesting times (table 4.4) possibly leading to membrane effects and damage of nucleic acids. Membrane integrity and stability in *Arabidopsis thaliana* leaves could indeed be affected by uranium presence as was shown by Vanhoudt et al. (2008). The observed decrease in phosphorous concentration for the leaves was in accordance with results reported by Smeets et al. (2008) for leaves of *Arabidopsis thaliana* seedlings exposed to cadmium. Contrastingly,

Gopal & Rizvi (2008) reported an increase in phosphorous content for leaves of radish following lead exposure.

Exposure to 100 µM uranium caused a significant decrease in sulfur concentrations for roots (table 4.3) and leaves (table 4.4). Uranyl is known to react with sulfate ions to form uranyl sulfate complex anions which may decrease sulfate availability. Inconsistent results have been reported for sulfur concentrations following cadmium exposure. Zhang et al. (2000) reported a reduced sulfur concentration in wheat after cadmium addition while Zhu et al. (2004) observed an increase of sulfur concentrations in roots and shoots of Bai Cai following cadmium exposure. Smeets et al. (2008) reported, in accordance with our results, a decrease in sulfur content for *Arabidopsis thaliana* leaves following cadmium exposure. Since sulfur is an important component of amino acids, proteins and coenzymes, deficiency in sulfur can result in damaged biomolecules.

A significant decrease in potassium content was observed for roots (table 4.3) and leaves (table 4.4) of *Arabidopsis thaliana* seedlings exposed to 100 µM uranium at all harvesting times. This potassium leakage can be an indication of membrane instability and damage caused by uranium presence, which was also shown by Vanhoudt et al. (2008). Correspondingly, Hernández et al. (1996) reported a decrease of potassium content in roots and shoots of pea seedlings exposed to cadmium.

As UO_2^{2+} seeks oxygen binding centers, it resembles Ca^{2+} and Mg^{2+}. Because UO_2^{2+} forms complexes of higher stability than the other two ions, a competition between the different ions will appear. Binding of UO_2^{2+} on Ca^{2+} or Mg^{2+} binding sites can result in membrane instability and the inactivation of several enzymes as was described by Boileau et al. (1985). In our study, magnesium concentrations in roots and leaves decreased after exposure to 100 µM uranium for 1 and 3 days and for 7 days exposure, a uranium dependent decrease in magnesium concentrations was observed (tables 4.3 & 4.4). Similar effects for the calcium concentrations were observed for the leaves (table 4.4) but in the roots, calcium concentrations increased following exposure to 100 µM uranium (table 4.3). Similar effects for leaves were reported by Smeets et al. (2008) following cadmium exposure. Straczek et al. (2009) observed similar calcium

concentrations in carrot roots exposed to 10 µM uranium, slightly increased concentration at 40 µM uranium and 3-fold higher calcium levels at 80 µM uranium.

Iron is a micronutrient that plays an important role in several cellular redox systems. In several enzymes, iron can act as a metal component in redox reactions or as a bridging element between enzyme and substrate. Under conditions of iron deficiency, the activity of enzymes such as catalase and peroxidases, enzymes of the antioxidative defense system, can decline and cause changes in metabolic processes. In this study, a decrease in iron content was observed for leaves following exposure to 100 µM uranium for 1 and 3 days, and following exposure to all uranium concentrations for 7 days (table 4.4) suggesting that enzymatic activities may be affected. For roots, iron concentrations decreased for 10 and 100 µM uranium at day 1, for 1, 10 and 100 µM uranium at day 3 but at day 7 iron concentrations increased for 100 µM uranium (table 4.3). Gopal & Rizvi (2008) reported a decrease in tops but an increase of iron content in roots of radish following lead exposure. Cadmium exposure resulted in a decrease of the iron content in leaves but a steady state level of the iron content in roots of pea seedlings as was reported by Hernández et al. (1996).

Manganese has important functions in metalloproteins, where it can act as a structural component, an active binding site or as a redox system. The activity of manganese superoxide dismutase, an isoenzyme of superoxide dismutase for the protection against superoxide radicals, can be decreased in the case of a manganese shortage. Presence of uranium may reduce manganese availability due to the formation of uranium-manganese complexes (Han et al., 2007). Results from geochemical speciation (Bethke, 2001) using the NEA thermodynamic data review by Grenthe et al. (1992) showed that the presence of 25 µM uranium in the hydroponic solution decreased the free manganese concentration more that 10-fold. In our study, the manganese content decreased in roots and leaves following exposure to 100 µM uranium (tables 4.3 and 4.4). These results are in accordance with results reported by Hernández and others (1996): manganese concentrations also decreased in leaves and roots of pea seedlings following cadmium exposure. Manganese is also very important in oxygenic photosynthesis. Photosynthetic water oxidation proceeds

at a tetra-manganese complex bound to a cofactor-protein complex denoted as photosystem II (Dau & others 2005). Decreased manganese content in uranium exposed *Arabidopsis thaliana* seedlings and subsequent reduced photosynthesis capacity may be at the basis of reduced growth. Ohki (1985) found that severe manganese deficiency depressed dry weight, photosynthesis and chlorophyll content of wheat. Studying the lichen *Cladonia rangiferina*, Boileau et al. (1985) found that uranium induced a reduction in the total ^{14}C-fixation rates and decreased photosynthetic activity. Jain & Aery (1997) reported that chlorophyll content of uranium exposed wheat decreased.

Enzymatically bound copper plays a role in redox reactions. The activity of another isoenzyme of superoxide dismutase, copper-zinc superoxide dismutase, can be affected by copper or zinc deficiency. In this study, the copper content increased in the roots after exposure to 10 and 100 µM uranium at all harvesting times (table 4.3). For the leaves on the other hand, copper concentrations decreased after exposure to 10 and 100 µM uranium at 1 and 3 days, and after exposure to all uranium concentrations at day 7 (table 4.4).

Zinc can act as a metal component of enzymes or as a functional, structural or regulatory cofactor of several enzymes. A deficiency in zinc can cause therefore changes in the metabolism. The zinc content decreased in roots and leaves (tables 4.3 & 4.4) following exposure to the highest uranium concentration suggesting possible metabolic disturbances.

Apart from the essential elements as macro- and micronutrients, some beneficial elements can be defined. These elements can compensate for the toxic effects of other elements or simply replace mineral nutrients in some of their less specific functions. In this study, sodium concentrations in roots and leaves were determined. For the roots, a decrease in sodium content was observed following exposure to 100 µM uranium (table 4.3). In leaves, a uranium dependent decrease was observed after 3 days exposure while after 7 days a significant decrease was only visible for 100 µM uranium (table 4.4). As Na^+ can replace K^+ functions in plants, Na^+ leakage can also indicate severe membrane damage and instability.

4.3.4 Conclusions

In conclusion, the highest uranium concentration of 100 µM induced the most severe toxicity effects in *Arabidopsis thaliana* seedlings. Morphological effects on growth and development were already visible at lower uranium concentrations. Uranium presence influenced the uptake and distribution of several nutrients resulting in a disturbed nutrient profile. For most nutrients a decreased concentration was observed following exposure to 100 µM uranium suggesting toxicity effects on enzyme capacity, membrane stability and photosynthetic capacity are possible.

Table 4.3 – Element concentrations [µg g^{-1} DW] in roots of *Arabidopsis thaliana* seedlings after exposure to 0, 0.1, 1, 10 and 100 µM uranium for 1, 3 and 7 days. Results represent mean ± S.E. of at least 3 biological replicates.

		0 µM U	**0.1 µM U**	**1 µM U**	**10 µM U**	**100 µM U**
Ca	*1 day*	$^{AB}1649 \pm 150^{a}$	$^{A}2020 \pm 191^{a}$	$^{AB}2001 \pm 182^{a}$	$^{A}1489 \pm 70^{a}$	$^{A}3734 \pm 300^{b}$
	3 days	$^{A}1619 \pm 105^{ab}$	$^{A}1808 \pm 78^{ab}$	$^{A}1661 \pm 26^{a}$	$^{B}1970 \pm 32^{b}$	$^{A}2945 \pm 153^{c}$
	7 days	$^{B}2186 \pm 131^{ac}$	$^{A}1904 \pm 36^{b}$	$^{B}2329 \pm 40^{a}$	$^{B}2055 \pm 37^{bc}$	$^{A}2881 \pm 77^{d}$
Cu	*1 day*	n.d.	n.d.	n.d.	$^{A}40 \pm 10^{a}$	$^{A}252 \pm 17^{b}$
	3 days	n.d.	n.d.	n.d.	$^{A}29 \pm 7^{a}$	$^{A}259 \pm 15^{b}$
	7 days	n.d.	n.d.	8 ± 0.5^{a}	$^{A}19 \pm 1^{b}$	$^{A}275 \pm 13^{c}$
Fe	*1 day*	$^{A}1942 \pm 165^{a}$	$^{A}1645 \pm 111^{a}$	$^{A}1687 \pm 70^{a}$	$^{A}1112 \pm 81^{b}$	$^{A}520 \pm 119^{c}$
	3 days	$^{B}960 \pm 12^{a}$	$^{B}847 \pm 35^{a}$	$^{B}635 \pm 24^{b}$	$^{B}419 \pm 50^{c}$	$^{A}475 \pm 19^{c}$
	7 days	$^{C}82 \pm 8^{ab}$	$^{C}90 \pm 12^{ab}$	$^{C}103 \pm 9^{a}$	$^{C}63 \pm 6^{b}$	$^{A}356 \pm 16^{c}$
K	*1 day*	$^{A}22651 \pm 5044^{a}$	$^{AB}17117 \pm 4011^{a}$	$^{A}18469 \pm 1941^{a}$	$^{AB}15318 \pm 2399^{ab}$	$^{A}2757 \pm 229^{b}$
	3 days	$^{A}24173 \pm 3547^{a}$	$^{A}25096 \pm 896^{a}$	$^{B}24682 \pm 925^{a}$	$^{A}20641 \pm 1443^{a}$	$^{B}2012 \pm 125^{b}$
	7 days	$^{A}20887 \pm 1881^{a}$	$^{B}16339 \pm 1004^{ab}$	$^{A}16577 \pm 1647^{ab}$	$^{B}12533 \pm 428^{b}$	$^{AB}2582 \pm 74^{c}$
Mg	*1 day*	$^{A}1691 \pm 127^{a}$	$^{A}1844 \pm 139^{a}$	$^{A}1902 \pm 86^{a}$	$^{AB}1547 \pm 83^{a}$	$^{A}935 \pm 83^{b}$
	3 days	$^{AB}1868 \pm 152^{a}$	$^{A}2000 \pm 51^{a}$	$^{AB}1783 \pm 43^{a}$	$^{A}1745 \pm 45^{a}$	$^{AB}831 \pm 46^{b}$
	7 days	$^{B}2464 \pm 194^{a}$	$^{A}1751 \pm 43^{b}$	$^{B}1582 \pm 47^{bc}$	$^{B}1486 \pm 44^{c}$	$^{B}646 \pm 8^{d}$
Mn	*1 day*	$^{A}331 \pm 20^{a}$	$^{A}703 \pm 136^{b}$	$^{A}595 \pm 96^{b}$	$^{A}422 \pm 42^{ab}$	$^{A}392 \pm 24^{ab}$
	3 days	$^{B}1006 \pm 55^{a}$	$^{A}933 \pm 87^{a}$	$^{A}767 \pm 71^{a}$	$^{A}299 \pm 57^{b}$	$^{B}59 \pm 5^{c}$
	7 days	$^{C}91 \pm 12^{a}$	$^{B}88 \pm 10^{a}$	$^{B}75 \pm 6^{a}$	$^{B}63 \pm 5^{ab}$	$^{B}47 \pm 1^{b}$
Na	*1 day*	$^{A}14208 \pm 1208^{a}$	$^{A}18505 \pm 1044^{a}$	$^{A}18078 \pm 752^{a}$	$^{A}14489 \pm 1266^{a}$	$^{A}4622 \pm 548^{b}$
	3 days	$^{A}12445 \pm 375^{abc}$	$^{B}12700 \pm 618^{b}$	$^{B}9305 \pm 536^{a}$	$^{A}13612 \pm 1158^{ab}$	$^{B}3129 \pm 172^{c}$
	7 days	$^{A}15737 \pm 1052^{a}$	$^{B}13128 \pm 316^{a}$	$^{C}13131 \pm 966^{a}$	$^{A}11856 \pm 361^{a}$	$^{B}1662 \pm 38^{b}$
P	*1 day*	$^{A}14163 \pm 1006^{a}$	$^{A}15551 \pm 1104^{a}$	$^{A}16674 \pm 596^{a}$	$^{A}13738 \pm 688^{a}$	$^{A}13222 \pm 955^{a}$
	3 days	$^{A}10976 \pm 846^{a}$	$^{B}11524 \pm 292^{a}$	$^{B}10936 \pm 295^{a}$	$^{B}11257 \pm 550^{a}$	$^{A}12759 \pm 634^{a}$
	7 days	$^{B}5522 \pm 194^{a}$	$^{C}4824 \pm 34^{b}$	$^{C}5109 \pm 94^{ab}$	$^{C}4733 \pm 148^{b}$	$^{A}10467 \pm 477^{c}$
S	*1 day*	$^{A}12516 \pm 912^{a}$	$^{A}13210 \pm 998^{a}$	$^{A}13822 \pm 788^{a}$	$^{A}11403 \pm 634^{a}$	$^{A}5312 \pm 613^{b}$
	3 days	$^{A}14029 \pm 1054^{a}$	$^{A}13281 \pm 420^{a}$	$^{AB}12602 \pm 281^{a}$	$^{B}13286 \pm 304^{a}$	$^{B}2703 \pm 207^{b}$
	7 days	$^{A}13717 \pm 519^{a}$	$^{B}10085 \pm 422^{ab}$	$^{B}10278 \pm 792^{ab}$	$^{C}9118 \pm 305^{b}$	$^{B}2397 \pm 24^{c}$
Zn	*1 day*	$^{A}226 \pm 20^{a}$	$^{A}205 \pm 13^{a}$	$^{A}219 \pm 18^{a}$	$^{A}196 \pm 30^{a}$	$^{A}94 \pm 2^{b}$
	3 days	$^{B}82 \pm 4^{a}$	$^{B}74 \pm 4^{a}$	$^{B}67 \pm 4^{a}$	$^{B}75 \pm 6^{a}$	$^{B}62 \pm 9^{a}$
	7 days	$^{C}22 \pm 5^{ab}$	$^{C}24 \pm 1^{a}$	$^{B}42 \pm 11^{b}$	$^{C}33 \pm 3^{ab}$	$^{C}26 \pm 2^{ab}$

Different small letters indicate significant differences between the treatments for day 1, day 3 and day 7 separately ($p < 0.05$). Different capital letters indicate significant differences between the exposure days for the different treatments separately ($p < 0.05$).

Table 4.4 – Element concentrations [µg g^{-1} DW] in leaves of *Arabidopsis thaliana* seedlings after exposure to 0, 0.1, 1, 10 and 100 µM uranium for 1, 3 and 7 days. Results represent mean ± S.E. of at least 3 biological replicates.

		0 µM U	**0.1 µM U**	**1 µM U**	**10 µM U**	**100 µM U**
Ca	*1 day*	$^{A}38948 \pm 571^{a}$	$^{A}41927 \pm 852^{a}$	$^{A}42300 \pm 880^{a}$	$^{A}42468 \pm 706^{a}$	$^{A}32815 \pm 649^{b}$
	3 days	$^{B}45518 \pm 1317^{a}$	$^{A}43791 \pm 927^{a}$	$^{A}43898 \pm 854^{a}$	$^{A}42147 \pm 396^{a}$	$^{B}21190 \pm 686^{b}$
	7 days	$^{A}41091 \pm 295^{a}$	$^{B}36911 \pm 985^{b}$	$^{B}32487 \pm 491^{c}$	$^{B}29368 \pm 512^{d}$	$^{C}14282 \pm 402^{e}$
Cu	*1 day*	$^{A}13.0 \pm 1.2^{a}$	$^{A}9.0 \pm 0.4^{b}$	$^{A}9.0 \pm 0.5^{b}$	n.d.	n.d.
	3 days	$^{B}7.6 \pm 0.3^{a}$	$^{AB}8.0 \pm 0.2^{a}$	$^{B}7.7 \pm 0.2^{a}$	$^{A}6.3 \pm 0.2^{b}$	$^{A}3.6 \pm 0.1^{c}$
	7 days	$^{B}9.6 \pm 0.1^{a}$	$^{B}7.7 \pm 0.2^{b}$	$^{C}6.6 \pm 0.2^{c}$	$^{B}5.3 \pm 0.1^{d}$	$^{A}3.3 \pm 0.1^{e}$
Fe	*1 day*	$^{A}95 \pm 9^{a}$	$^{A}94 \pm 2^{a}$	$^{A}86 \pm 7^{a}$	$^{A}81 \pm 3^{a}$	$^{A}54 \pm 1^{b}$
	3 days	$^{B}65 \pm 3^{a}$	$^{B}63 \pm 2^{a}$	$^{B}57 \pm 4^{a}$	$^{B}59 \pm 2^{a}$	$^{B}36 \pm 1^{b}$
	7 days	$^{B}63 \pm 1^{a}$	$^{C}52 \pm 1^{b}$	$^{C}47 \pm 1^{bc}$	$^{C}46 \pm 1^{c}$	$^{C}23 \pm 1^{d}$
K	*1 day*	$^{A}20651 \pm 495^{a}$	$^{A}19453 \pm 430^{a}$	$^{A}19224 \pm 505^{a}$	$^{A}19392 \pm 563^{a}$	$^{A}13460 \pm 320^{b}$
	3 days	$^{A}19413 \pm 545^{a}$	$^{AB}21182 \pm 357^{b}$	$^{B}23032 \pm 429^{c}$	$^{B}22215 \pm 293^{bc}$	$^{B}8625 \pm 170^{d}$
	7 days	$^{B}23833 \pm 514^{ab}$	$^{B}23489 \pm 1082^{a}$	$^{B}24520 \pm 1073^{a}$	$^{A}19981 \pm 269^{b}$	$^{C}5259 \pm 112^{c}$
Mg	*1 day*	$^{A}8123 \pm 152^{a}$	$^{AB}8764 \pm 176^{ab}$	$^{A}8939 \pm 199^{b}$	$^{A}9021 \pm 156^{b}$	$^{A}6972 \pm 109^{c}$
	3 days	$^{B}9519 \pm 287^{a}$	$^{A}9337 \pm 198^{a}$	$^{A}9422 \pm 158^{a}$	$^{A}9111 \pm 54^{a}$	$^{B}4624 \pm 132^{b}$
	7 days	$^{AB}9008 \pm 100^{a}$	$^{B}8259 \pm 242^{a}$	$^{B}7389 \pm 114^{b}$	$^{B}6580 \pm 106^{c}$	$^{C}3156 \pm 59^{d}$
Mn	*1 day*	$^{A}156 \pm 2^{a}$	$^{A}181 \pm 4^{b}$	$^{A}185 \pm 4^{b}$	$^{A}172 \pm 5^{ab}$	$^{A}133 \pm 2^{c}$
	3 days	$^{A}166 \pm 6^{a}$	$^{B}137 \pm 6^{b}$	$^{B}138 \pm 5^{b}$	$^{B}138 \pm 5^{b}$	$^{B}78 \pm 1^{c}$
	7 days	$^{B}102 \pm 4^{a}$	$^{C}99 \pm 6^{a}$	$^{C}94 \pm 2^{a}$	$^{C}102 \pm 2^{a}$	$^{C}48 \pm 2^{b}$
Na	*1 day*	$^{A}2782 \pm 117^{a}$	$^{A}3479 \pm 427^{ab}$	$^{A}3806 \pm 241^{b}$	$^{A}4109 \pm 155^{b}$	$^{A}3206 \pm 181^{ab}$
	3 days	$^{A}3499 \pm 145^{a}$	$^{B}2540 \pm 209^{b}$	$^{B}1938 \pm 120^{c}$	$^{B}1478 \pm 120^{c}$	$^{B}1795 \pm 62^{c}$
	7 days	$^{A}2604 \pm 306^{ab}$	$^{C}1998 \pm 25^{a}$	$^{C}2555 \pm 69^{b}$	$^{C}2527 \pm 88^{b}$	$^{C}1157 \pm 96^{c}$
P	*1 day*	$^{A}10429 \pm 151^{a}$	$^{A}10846 \pm 350^{a}$	$^{A}10753 \pm 264^{a}$	$^{A}10768 \pm 206^{a}$	$^{A}8992 \pm 178^{b}$
	3 days	$^{B}9311 \pm 338^{a}$	$^{B}8501 \pm 213^{ab}$	$^{B}8328 \pm 177^{b}$	$^{B}7098 \pm 248^{c}$	$^{B}4895 \pm 36^{d}$
	7 days	$^{C}3996 \pm 42^{a}$	$^{C}3844 \pm 106^{ab}$	$^{C}3802 \pm 38^{ab}$	$^{C}3272 \pm 112^{b}$	$^{C}2524 \pm 7^{c}$
S	*1 day*	$^{A}8641 \pm 87^{a}$	$^{A}9091 \pm 214^{a}$	$^{A}9187 \pm 177^{a}$	$^{A}9262 \pm 157^{a}$	$^{A}7162 \pm 102^{b}$
	3 days	$^{B}9845 \pm 295^{a}$	$^{B}10098 \pm 204^{a}$	$^{B}10275 \pm 324^{a}$	$^{A}9592 \pm 151^{a}$	$^{B}4154 \pm 130^{b}$
	7 days	$^{B}9238 \pm 158^{a}$	$^{A}8552 \pm 302^{a}$	$^{C}8155 \pm 223^{ab}$	$^{B}7225 \pm 133^{b}$	$^{C}2592 \pm 58^{c}$
Zn	*1 day*	$^{A}73 \pm 2^{a}$	$^{A}64 \pm 3^{a}$	$^{A}66 \pm 1^{a}$	$^{A}69 \pm 2^{a}$	$^{A}47 \pm 2^{b}$
	3 days	$^{B}55 \pm 2^{a}$	$^{B}55 \pm 1^{a}$	$^{B}53 \pm 1^{a}$	$^{B}54 \pm 1^{a}$	$^{B}27 \pm 1^{b}$
	7 days	$^{C}33 \pm 1^{a}$	$^{C}25 \pm 1^{b}$	$^{C}26 \pm 1^{b}$	$^{C}25 \pm 1^{b}$	$^{C}18 \pm 0.4^{c}$

Different small letters indicate significant differences between the treatments for day 1, day 3 and day 7 separately ($p < 0.05$). Different capital letters indicate significant differences between the exposure days for the different treatments separately ($p < 0.05$).

Chapter 5

Importance of oxidative stress related responses in *Arabidopsis thaliana* roots following uranium exposure

Vanhoudt N., Vandenhove H., Horemans N., Remans T., Opdenakker K., Smeets K., Martinez Bello D., Wannijn J., Van Hees M., Vangronsveld J. & Cuypers A. (2009) Importance of oxidative stress related responses in *Arabidopsis thaliana* roots following uranium exposure. *In preparation.*

Abstract

Information concerning uranium toxicity effects at molecular and biochemical level in plants is scant. When aiming to evaluate the environmental impact of a uranium contamination, it is important to unravel the mechanisms by which plants respond to uranium stress. As oxidative stress seems an important modulator under other heavy metal stress, this study aimed to investigate oxidative stress related responses in *Arabidopsis thaliana* roots exposed to uranium concentrations ranging from 0.1 to 100 µM for 1, 3 and 7 days. Besides analyzing relevant reactive oxygen species (ROS) producing and scavenging enzymes on protein and transcriptional level, the importance of the ascorbate-glutathione cycle under uranium stress was investigated. Results indicated that oxidative stress related responses were only triggered following exposure to the highest uranium concentration of 100 µM. A fast oxidative burst was suggested based on the observed enhancement of *LOX1* and *RBOHD* transcript levels already after 1 day. For the antioxidative defense system, the first line of defense was attributed to SOD, also triggered from the first day. An enhanced SOD capacity was observed on protein level which corresponded with an enhanced expression of *FSD1* located in the plastids. Gene expressions of other SOD isoforms on the other hand were down-regulated (*CSD1*, *CSD2*) or remained stable (*MSD1*). For the detoxification of hydrogen peroxide, an early increase in *CAT1* transcript levels was observed while SPX and GPX capacities were enhanced at the later stage of 3 days. Although the APX capacity and *APX1* gene expression increased, the AsA/DHA redox balance was completely disrupted and shifted towards the oxidized form. This disrupted balance could not be inverted by the glutathione part of the cycle although the glutathione redox balance could be maintained and GR capacity and *GR1* transcript levels increased.

5.1 Introduction

Environmental uranium contamination due to anthropogenic activities as uranium mining and milling, metal mining and smelting and the phosphate industry has occurred in many countries (Vandenhove, 2002). Uranium is a naturally occurring radionuclide and heavy metal with a greater risk of chemical toxicity than radiological toxicity because of its low specific activity (Sheppard et al., 2005). When evaluating the environmental impact of uranium contaminations, mechanisms by which plants respond to uranium stress should be unraveled. But information concerning uranium induced stress response mechanisms at molecular and biochemical level in plants is scant.

Induction of oxidative stress related responses in plants seems an important stress response mechanism for other heavy metals as was reported by several authors (Cuypers et al., 2001; Cuypers et al., 2002; Smeets et al., 2008). The oxidative burst is one of the earliest responses of plant cells under various stress conditions, possibly acting as an alarm signal to alert metabolism and gene expression for possible modifications (Foyer et al., 1994). Plasma membrane NADPH oxidases can be a source of reactive oxygen species (ROS) during the oxidative burst and the transcriptional activation of certain NADPH oxidases is an essential intermediate step in the activation or amplification of defense responses (Dat et al., 2000; Mittler et al., 2004). Lipid peroxidation can be due to an increase in lipoxygenase (LOX) activity, which initiates the formation of oxylipins (Porta & Rocha-Sosa, 2002). LOXs are shown to play a role in cadmium induced oxidative stress in *Arabidopsis thaliana* roots (Smeets et al., 2008).

ROS are also produced under normal circumstances and have a dual role as both toxic byproducts of aerobic metabolism and key regulators of biological processes as growth, cell cycle, biotic and abiotic stress responses (Mittler et al., 2004). These ROS can cause cellular damage by oxidizing biological molecules as DNA, proteins and lipids. To regulate the amount of ROS and thus to allow signal transduction processes but limit oxidative damage under normal circumstances and in stress situations, plants dispose of an antioxidative defense system comprising ROS scavenging enzymes and metabolites located in different plant cell compartments. Superoxide dismutase (SOD) constitutes the

first line of defense against ROS as $O_2^{\bullet-}$ detoxifying enzyme while enzymes such as catalase (CAT) and peroxidases (PX) have a role in the scavenging of hydrogen peroxide, which can act as a signaling molecule. Alterations in enzyme capacities of relevant enzymes of the antioxidative defense system in plant roots following heavy metal stress have been reported by several authors (Cuypers et al., 2001; Cuypers et al., 2002; Smeets et al., 2008). The ascorbate-glutathione pathway also plays an important role in the antioxidative defense mechanism against heavy metal stress as was reported by Cuypers et al. (2001) for *Phaseolus vulgaris* roots exposed to zinc.

Previous studies already suggested a role for the cellular redox balance as a modulator in uranium stress for *Arabidopsis thaliana* (Vanhoudt et al., 2008) and *Phaseolus vulgaris* (Vandenhove et al., 2006) but information remains limited. Vanhoudt et al. (2008) reported an induction of oxidative stress related responses in *Arabidopsis thaliana* leaves and roots exposed to 100 µM uranium. As in the latter study a single uranium concentration of 100 µM already disrupted the cellular redox balance, a more profound research was suggested to further unravel uranium stress response mechanisms.

The objective of this study was to further unravel uranium induced oxidative stress related responses in *Arabidopsis thaliana* roots and achieve a better understanding of the importance of the cellular redox balance as a modulator in uranium stress. For this purpose, *Arabidopsis thaliana* seedlings were exposed to uranium concentrations ranging from 0.1 to 100 µM for 1, 3 and 7 days. We investigated which NADPH oxidases and LOXs contribute to an enhanced ROS production while several ROS scavenging enzymes (SOD, CAT, PX) were analyzed to unravel their role in the protection from and regulation of ROS under uranium stress. In addition, different enzymes and metabolites contributing to the ascorbate-glutathione cycle were analyzed to evaluate their importance under uranium stress.

5.2 Materials and methods

5.2.1 Plant culture and uranium exposure

Seeds of *Arabidopsis thaliana* (Columbia ecotype) were spread on moist filter paper at 4 °C for 3 days in order to synchronize germination. Afterwards, the seeds were sown on polyethylene plugs filled with 2 % agar (Difco). The plugs were placed in a PVC cover capable of holding 81 plugs. Next, the PVC cover was placed on a container filled with 2.9 l of a modified Hoagland solution (macro-elements without phosphate: 1/10 diluted, phosphate solution: 1/20 diluted, micro-elements: 1/10 diluted and iron solution: 1/10 diluted). Plants were grown in a growth chamber (Microclima 1000E, Snijders Scientific B.V.) under a 14 h photoperiod (photosynthetic photon flux density of 200 µmol m^{-2} s^{-1} at the leaf level, supplied by Sylvania BriteGro F36WT8/2084 and F36WT8/2023 lamps), with day/night temperatures of 22 °C/18 °C and 65 % relative humidity. Roots were aerated during the entire experiment.

Subsequently, 17-day-old seedlings were exposed to 0, 0.1, 1, 10 and 100 µM uranium. Uranium was added as $UO_2(NO_3)_2.6H_2O$ (Sigma) to the modified Hoagland solution and the pH was adjusted to ± 5.5 with NaOH. As previous experiments recommended the use of 25 µM phosphate in combination with uranium, a 1/80 diluted phosphate solution was used (Vanhoudt et al., 2008).

Following 1, 3 and 7 days exposure, roots were harvested as ± 100 mg samples, snap frozen in liquid nitrogen and stored at -80 °C.

5.2.2 Analysis of enzyme capacities

Frozen root tissue (approximately 100 mg) was homogenized in ice-cold 0.1 M Tris-HCl buffer (pH 7.8) containing 1 mM EDTA, 1 mM dithiotreitol and 4 % insoluble polyvinylpyrrolidone (2 ml buffer for 100 mg FW), using a mortar and pestle. The homogenate was squeezed through a nylon mesh and centrifuged at 20000 × g and 4 °C for 10 minutes. The enzyme capacities, i.e. potential activity measured in vitro under non-limiting reaction conditions, were measured spectrophotometrically in the supernatant at 25 °C.

Guaiacol peroxidase and syringaldazine peroxidase capacities (GPX, SPX, EC 1.11.1.7) were measured at 436 nm and 530 nm according to Bergmeyer et al. (1974) and Imberty et al. (1984), respectively. Ascorbate peroxidase capacity (APX, EC 1.11.1.11) was measured at 298 nm following the method of Gerbling et al. (1984). Analysis of superoxide dismutase capacity (SOD, EC 1.15.1.1) was based on the inhibition of cytochrome c at 550 nm according to McCord & Fridovich (1969). Analyses of the capacities of glutathione reductase (GR, EC 1.6.4.2) and catalase (CAT, EC 1.11.1.6) were performed as described by Bergmeyer et al. (1974).

5.2.3 Gene expression analysis

Frozen root tissue (approximately 100 mg) was ground thoroughly in liquid nitrogen using a mortar and pestle. RNA was extracted using the RNeasy Plant Mini Kit (Qiagen). The RNA quantity was determined spectrophotometrically at 260 nm (Nanodrop, Isogen Life Science). The RNA quality was checked electrophoretically using the Bioanalyzer (Agilent Technologies). Before cDNA synthesis, the RNA sample was incubated during 2 minutes in gDNA wipeout buffer at 42°C in order to effectively eliminate genomic DNA. First strand cDNA synthesis was primed with a combination of oligo(dT)-primers and random hexamers according to the manufacturer's instructions using the QuantiTect Reverse Transcription Kit (Qiagen) and equal amounts of starting material were used (1 µg). Quantitative Real-Time PCR was performed with the 7500 Fast Real-Time PCR System (Applied Biosystems), using Sybr Green chemistry. Primers used for gene expression analyses are given in table 5.1. PCR amplifications were performed in a total volume of 10 µl containing 2.5 µl cDNA sample, 5 µl Fast Sybr Green Master Mix (Applied Biosystems), 0.3 µl forward primer, 0.3 µl reverse primer and 1.9 µl RNase-free H_2O.

Gene expression data were normalized against multiple housekeeping genes (*At2g28390*, *At5g08290*, *At5g15710*, *UBQ10*) according to Vandesompele et al. (2002) and presented relative to the control treatment (untreated roots after 1 day).

Table 5.1 - Sequences of forward and reverse primers used in gene expression analysis

Gene	Forward primer	Reverse primer
At2g28390	AACTCTATGCAGCATTTGATCCACT	TGATTGCATATCTTTATCGCCATC
At5g08290	TTACTGTTTCGGTTGTTCTCCATTT	CACTGAATCATGTTCGAAGCAAGT
At5g15710	TTTCGGCTGAGAGGTTCGAGT	GATTCCAAGACGTAAAGCAGATCAA
APX1	TGCCACAAGGATAGGTCTGG	CCTTCCTTCTCTCCGCTCAA
CAT1	AAGTGCTTCATCGGGAAGGA	CTTCAACAAAACGCTTCACGA
CSD1	TCCATGCAGACCCTGATGAC	CCTGGAGACCAATGATGCC
CSD2	GAGCCTTTGTGGTTCACGAG	CACACCACATGCCAATCTCC
FSD1	CTCCCAATGCTGTGAATCCC	TGGTCTTCGGTTCTGGAAGTC
GR1	CTCAAGTGTGGAGCAACCAAAG	ATGCGTCTGGTCACACTGC
MSD1	ATGTTTGGGAGCACGCCTAC	AACCTCGCTTGCATATTTCCA
LOX1	TTGGCTAAGGCTTTTGTCGG	GTGGCAATCACAAACGGTTC
LOX2	TTTGCTCGCCAGACACTTG	GGGATCACCATAAACGGCC
RBOHC	TCACCAGAGACTGGCACAATAAA	GATGCTCGACCTGAATGCTC
RBOHD	TATGCATCGGAGAGGCTGCT	TAGAGACAACACGTTCCCGGG
RBOHF	GGTGTCATGAACGAAGTTGCA	AATGAGAGCAGAACGAGCATCA
UBQ10	GGCCTTGTATAATCCCTGATGAATAAG	AAAGAGATAACAGGAACGGAAACATAGT

5.2.4 Metabolite analysis

Ascorbate and glutathione concentrations in *Arabidopsis thaliana* roots were determined by HPLC analysis. Therefore approximately 100 mg tissue was ground thoroughly in liquid nitrogen using a pre-cooled mortar and pestle. When a homogenous powder was obtained, 1 ml of ice cold 6 % (w/v) meta-phosphoric acid was added and the mixture was clarified by centrifugation at 20000 × g and 4 °C for 10 minutes. The resulting supernatant was kept frozen until HPLC analysis. Antioxidants were separated on a 100 mm × 4.6 mm Polaris C18-A reversed phase HPLC column (3 µm particle size, 30 °C, Varian, CA USA) with an isocratic flow of 1 ml min^{-1} of the elution buffer (25 mM K/PO_4-buffer, pH 3.0). The components were quantified using a home-made electrochemical detector with glassy carbon electrode and a Scott pt 62 reference electrode (Mainz, Germany). The purity and identity of the peaks were confirmed using a diode array detector (SPD-M10AVP, Shimadzu, Hertogenbosch, Netherlands) which was placed on line with the electrochemical detector. The concentrations of oxidized DHA (dehydroascorbate) or GSSG (glutathione disulphide) were measured indirectly as the difference between the total concentration of antioxidants in a DTT (dithiothreitol) reduced fraction and the concentration in a

sample prior to reduction. Reduction of the sample was obtained by incubation of an aliquot of the extract in 400 mM Tris and 200 mM DTT for 15 minutes in the dark. The pH of this mixture was checked to be between 6.0 and 7.0. After 15 minutes, the pH was lowered again by 4-fold dilution in elution buffer prior to HPLC analysis.

5.2.5 Statistical analysis

The datasets for enzyme capacities and metabolites were analyzed by day, evaluating the effect of uranium treatment. Statistical analyses were done following the algorithm described below, ensuring for each dataset a statistical analysis best fitted for the data.

First, a parametric analysis of variance was performed and the assumptions for normality and constancy of variance were checked (Kutner et al., 2005). If the assumptions were fulfilled, a pair wise comparison was applied with an adjustment of the p-values using Tukey multiple comparisons procedure according to Kutner et al. (2005). If the assumptions were not fulfilled, the data was transformed using the Box and Cox method (Box & Cox, 1964). Subsequently, a parametric analysis of variance of the transformed response variables was applied. Again the assumptions for normality and constancy of variance were checked. If both assumptions were fulfilled, again a pair wise comparison, with an adjustment of the p-values using Tukey multiple comparisons procedure, was applied. If only the assumption for normality was fulfilled, a parametric analysis of variance for heterocedastic variances was applied according to Westfall et al. (2000). A pair wise comparison was then carried out adjusting the p-values using simulated p-values (Westfall et al., 2000). If neither assumption was fulfilled, a nonparametric analysis of variance was applied (Lehmann & D'Abrera, 1998) adjusting the p-values using Benjamini Hochberg False Discovery Rate (BH-FDR) adjustment (Benjamini & Hochberg, 1995).

The gene expression dataset was analyzed using global permutations with p-value adjustment as it was presented by Lin et al. (2008), using the Benjamini and Hochberg False Discovery Rate (BH-FDR) adjustment (Benjamini & Hochberg, 1995).

5.3 Results

5.3.1 Enzyme capacities

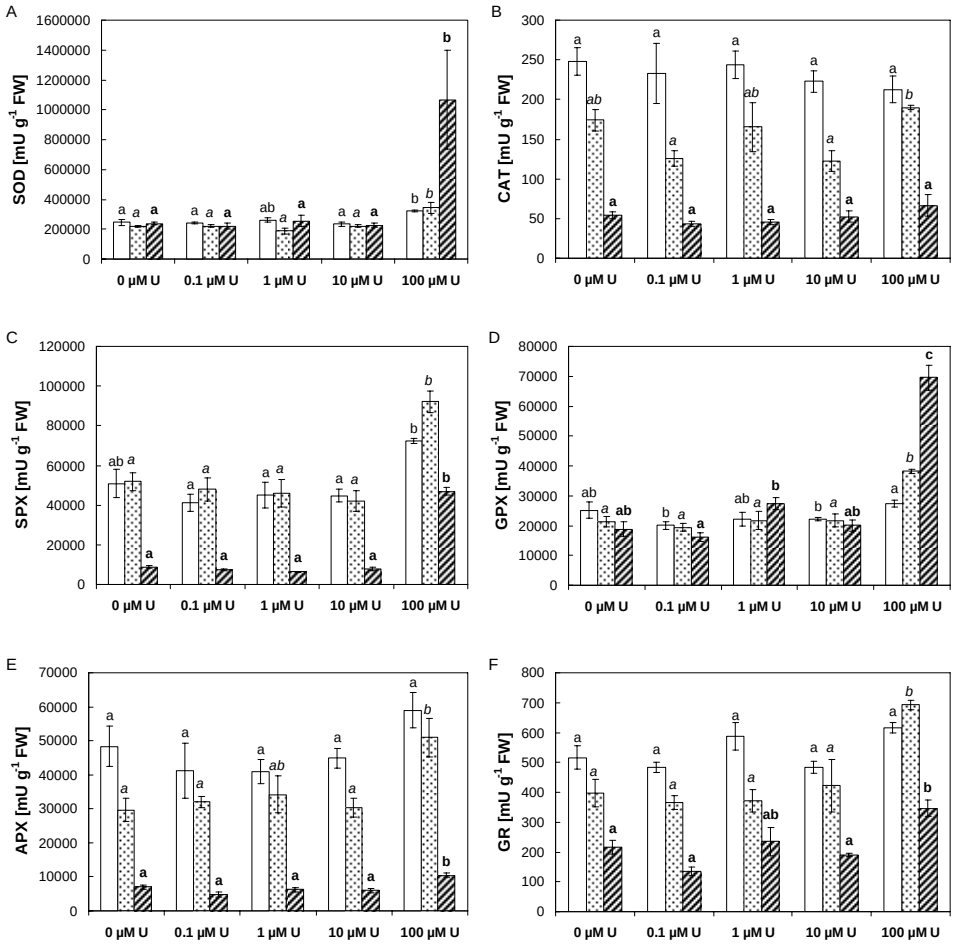

Figure 5.1 - Capacities [mU g^{-1} FW] of ROS scavenging enzymes and enzymes related to the ascorbate-glutathione pathway. Capacities of SOD (superoxide dismutase), CAT (catalase), SPX (syringaldazine peroxidase), GPX (guaiacol peroxidase), APX (ascorbate peroxidase) and GR (glutathione reductase) were measured in *Arabidopsis thaliana* roots exposed to 0, 0.1, 1, 10 and 100 µM uranium for 1 (white bars), 3 (dotted bars) and 7 days (striped bars). Data represent the mean ± S.E. of at least 3 biological replicates. Different letters above the bars indicate significant differences in enzyme capacity between the different uranium treatments for day 1 (normal), 3 (*italic*) and 7 (**bold**) ($p < 0.05$).

To evaluate the importance of the cellular redox balance in uranium stress responses, relevant enzymes of the antioxidative defense system were analyzed on protein level for roots of *Arabidopsis thaliana* seedlings (figure 5.1).

For all enzymes studied, except CAT where uranium had hardly any effect on its capacity, capacities increased significantly after exposure to the highest uranium concentration. For SOD this increase was already observed 1 day after exposure while for SPX, GPX, APX and GR this increase just started 3 days after exposure.

5.3.2 Gene expression

To evaluate the importance of oxidative stress related responses in roots of *Arabidopsis thaliana* during uranium stress, transcript levels of relevant ROS producing and scavenging enzymes were analyzed using quantitative Real-Time PCR.

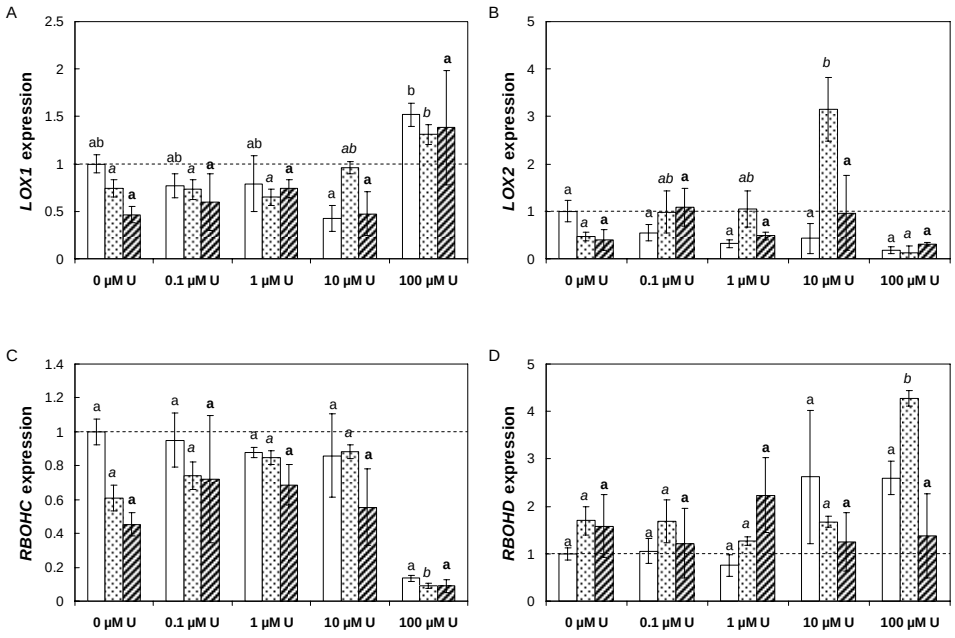

Figure 5.2 - Gene expression of ROS producing enzymes following uranium exposure. *Arabidopsis thaliana* seedlings were exposed for 1 (white bars), 3 (dotted bars) and 7 days (striped bars) to a uranium concentration range. Transcript levels of *LOX1* (lipoxygenase), *LOX2*, *RBOHC* (NADPH oxidase) and *RBOHD* in roots were expressed relative to the control treatment of day 1 (dashed line). Data represent the mean ± S.E. of 3 biological replicates. Different letters above the bars indicate significant differences in gene expression between the uranium treatments for day 1 (normal), 3 (*italic*) and 7 (**bold**) ($p < 0.05$).

First, transcript levels of several ROS producing enzymes were investigated. *LOX1* (lipoxygenase 1) transcript levels increased following exposure to 100 µM uranium for 1 and 3 days (figure 5.2A). Expression levels of *LOX2* (lipoxygenase

2) remained stable following uranium exposure except for a significant increase following exposure to 10 µM uranium for 3 days (figure 5.2B). Gene expression of different isoforms of NADPH oxidases (*RBOH*), located in the plasma membrane, was analyzed. A decreasing trend was observed for transcript levels of *RBOHC* following exposure to 100 µM uranium, but this was only significant for 3 days exposure (figure 5.2C). *RBOHD* expression levels on the other hand significantly increased after exposure to 100 µM uranium for 3 days (figure 5.2D) while *RBOHF* transcript levels remained stable for all treatments (results not shown).

Secondly, transcript levels of different isoforms of SOD, $O_2^{\bullet-}$ scavenging enzymes, were analyzed.

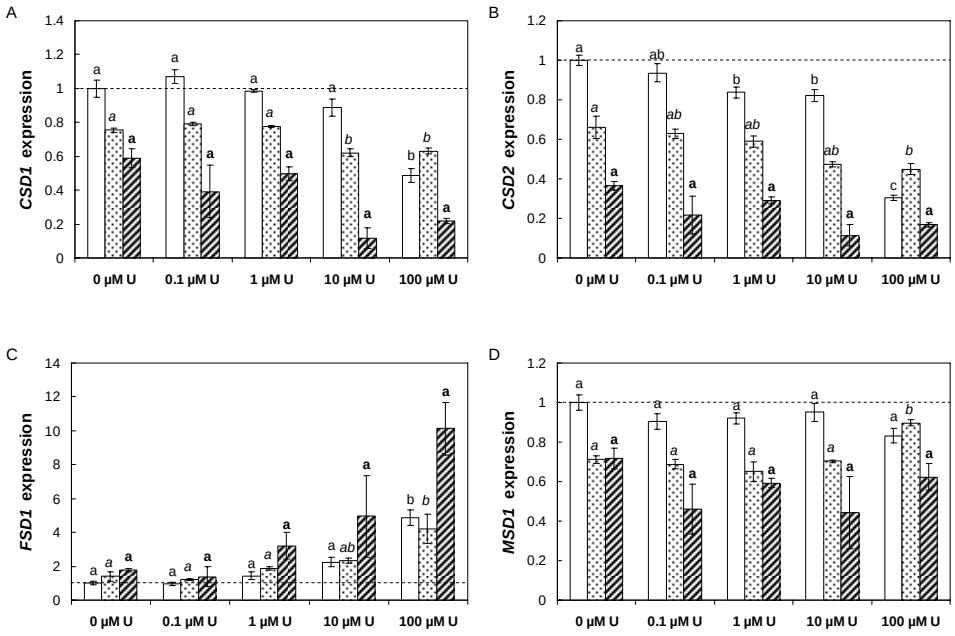

Figure 5.3 - Gene expression of $O_2^{\bullet-}$ scavenging enzymes following uranium exposure. Transcript levels of different isozymes of SOD (superoxide dismutase) were measured for *Arabidopsis thaliana* roots exposed for 1 (white bars), 3 (dotted bars) and 7 days (striped bars) to a uranium concentration range, and expressed relative to the control treatment of day 1 (dashed line). Values give the mean ± S.E. of 3 biological replicates. Different letters above the bars indicate significant differences in gene expression between the uranium concentrations for day 1 (normal), 3 (*italic*) and 7 (**bold**) ($p < 0.05$).

Following 1 day of exposure, *CSD1* (cytoplasmic copper/zinc SOD) and *CSD2* (plastidic copper/zinc SOD) significantly decreased after exposure to 100 µM uranium and 1, 10 and 100 µM uranium respectively (figure 5.3A-B). A

significant increase in gene expression for *FSD1* (plastidic iron SOD) was observed following exposure to 100 µM uranium (figure 5.3C) while *MSD1* (mitochondrial manganese SOD) transcript levels remained stable (figure 5.3D). Similar effects were observed following 3 days of exposure. Transcript levels of *CSD1* and *CSD2* were significantly decreased after exposure to 10 and 100 µM uranium and 100 µM uranium respectively (figure 5.3A-B) while *FSD1* transcript levels showed a significant increase following exposure to 100 µM uranium (figure 5.3C). A small increase in *MSD1* expression was observed after exposure to 100 µM uranium (figure 5.3D). Gene expression levels remained stable for all SOD isoforms studied after 7 days of exposure to the uranium concentration range (figure 5.3A-D).

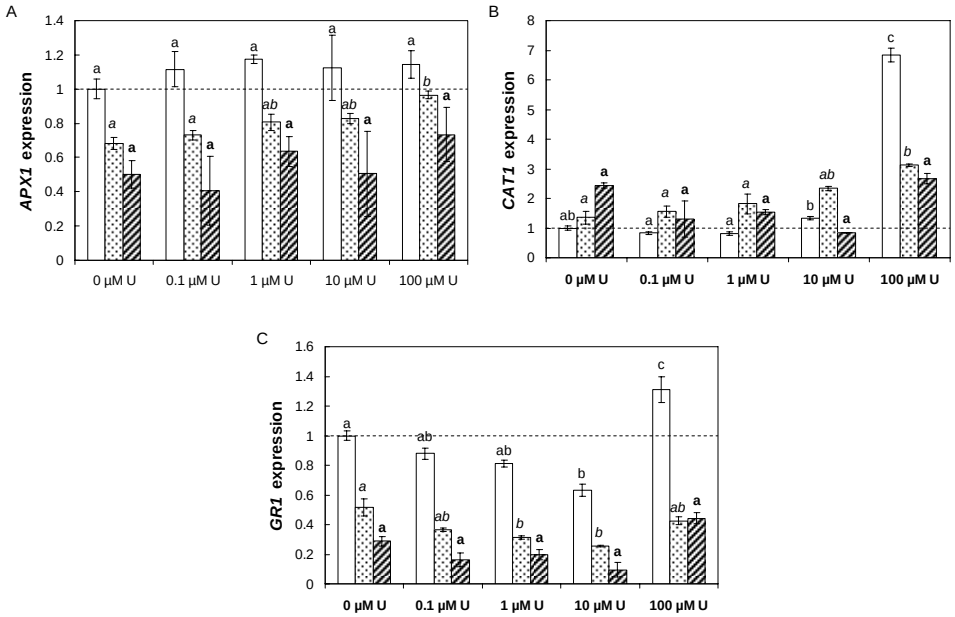

Figure 5.4 - Gene expression of H_2O_2 scavenging enzymes and enzymes related to the ascorbate-glutathione pathway after uranium exposure. Gene expression of *CAT1* (catalase), *APX1* (ascorbate peroxidase) and *GR1* (glutathione reductase) were measured in *Arabidopsis thaliana* roots exposed to a uranium concentration range for 1 (white bars), 3 (dotted bars) and 7 days (striped bars). Transcript levels were expressed relative to the control treatment of day 1 (dashed line). Values represent the mean ± S.E. of 3 biological replicates. Different letters above the bars indicate significant differences in gene expression between the uranium treatments for day 1 (normal), 3 (*italic*) and 7 (**bold**) ($p < 0.05$).

Finally, gene expression of H_2O_2-scavenging enzymes and enzymes related to the ascorbate-glutathione pathway was analyzed. In general, *APX1* (cytoplasmic APX) expression levels remained stable following uranium exposure except for a

significant increase after exposure to 100 µM uranium for 3 days (figure 5.4A). Transcript levels of *CAT1* (peroxisomal CAT) and *GR1* (cytosolic GR) significantly increased after 1 day for roots exposed to 100 µM uranium (figure 5.4B-C).

5.3.3 Metabolites

To investigate the importance of the ascorbate-glutathione pathway in the defense against uranium stress, ascorbate (table 5.2) and glutathione (table 5.3) concentrations were also determined.

Alterations in the ascorbate pool were visible following exposure to 100 µM uranium for 3 and 7 days. While the total ascorbate concentration (AsA + DHA) in roots exposed to 100 µM uranium remained stable, a decrease of ascorbate (AsA) combined with an increase of dehydroascorbate (DHA) was observed for 3 and 7 days.

Table 5.2 - Ascorbate concentrations [nmol g^{-1} FW] in *Arabidopsis thaliana* roots following uranium exposure.

		0 µM U	**0.1 µM U**	**1 µM U**	**10 µM U**	**100 µM U**
AsA + DHA	*1 day*	791±74^{a}	1025±107^{a}	944±115^{a}	922±54^{a}	1173±54^{a}
	3 days	839±83^{a}	974±83^{a}	1029±48^{a}	917±44^{a}	924±98^{a}
	7 days	723±18^{ab}	571±35^{a}	665±75^{a}	918±79^{bc}	1199±77^{c}
AsA	*1 day*	412±113^{a}	614±176^{a}	419±167^{a}	429±114^{a}	525±53^{a}
	3 days	728±79^{a}	809±50^{a}	898±42^{a}	798±43^{a}	153±8^{b}
	7 days	583±15^{ab}	426±31^{ac}	490±51^{a}	719±69^{b}	228±31^{c}
DHA	*1 day*	378±92$^{\mathbf{a}}$	411±74$^{\mathbf{a}}$	526±78$^{\mathbf{a}}$	493±76$^{\mathbf{a}}$	648±10$^{\mathbf{a}}$
	3 days	112±9$^{\mathbf{a}}$	165±44$^{\mathbf{a}}$	132±10$^{\mathbf{a}}$	119±11$^{\mathbf{a}}$	771±92$^{\mathbf{b}}$
	7 days	139±10$^{\mathbf{a}}$	145±7$^{\mathbf{a}}$	174±27$^{\mathbf{a}}$	199±19$^{\mathbf{a}}$	971±49$^{\mathbf{b}}$

Ascorbate concentrations [nmol g^{-1} FW] were determined in roots exposed for 1, 3 and 7 days to uranium concentrations ranging from 0.1 to 100 µM. The total ascorbate concentration represents the reduced and oxidized form (AsA: ascorbic acid = reduced form; DHA: dehydroascorbate = oxidized form). Data represent the mean ± S.E. of 6 biological replicates. Different small letters indicate significant differences between the different treatments for day 1, 3 and 7 separately ($p < 0.05$). Statistical analyses were done separately for AsA + DHA (normal), AsA (*italic*) and DHA (**bold**).

Glutathione concentrations (glutathione (GSH), glutathione disulphide (GSSG) and GSH + GSSG) generally decreased after 3 days exposure to 100 µM uranium.

Table 5.3 - Glutathione concentrations [nmol g^{-1} FW] in *Arabidopsis thaliana* roots following uranium exposure.

		0 µM U	**0.1 µM U**	**1 µM U**	**10 µM U**	**100 µM U**
GSH+GSSG	*1 day*	110±13^{a}	136±11^{ab}	171±14^{b}	133±16^{ab}	137±2^{ab}
	3 days	193±35^{ab}	198±19^{ab}	312±36^{a}	302±27^{a}	74±17^{b}
	7 days	46±2^{a}	41±7^{a}	52±6^{a}	51±7^{a}	67±5^{a}
GSH	*1 day*	77±10^{a}	91±11^{a}	107±10^{a}	83±11^{a}	76±3^{a}
	3 days	99±14^{a}	112±8^{ab}	144±10^{b}	142±10^{ab}	37±6^{c}
	7 days	44±3^{a}	37±5^{a}	42±6^{a}	52±7^{a}	41±2^{a}
GSSG	*1 day*	33±6$^{\mathbf{a}}$	45±4$^{\mathbf{ab}}$	64±8$^{\mathbf{b}}$	50±6$^{\mathbf{ab}}$	60±3$^{\mathbf{ab}}$
	3 days	94±22$^{\mathbf{ab}}$	86±21$^{\mathbf{ab}}$	168±27$^{\mathbf{a}}$	160±19$^{\mathbf{a}}$	37±11$^{\mathbf{b}}$
	7 days	2±2$^{\mathbf{a}}$	4±2$^{\mathbf{a}}$	9±3$^{\mathbf{a}}$	n.d.	26±5$^{\mathbf{b}}$

Glutathione concentrations [nmol g^{-1} FW] were determined in roots exposed for 1, 3 and 7 days to uranium concentrations ranging from 0.1 to 100 µM. The total glutathione concentration represents the reduced and oxidized forms (GSH: glutathione = reduced form; GSSG: glutathione disulphide = oxidized form). Values are the mean ± S.E. of 6 biological replicates. Different small letters indicate significant differences between the treatments for day 1, day 3 and day 7 separately ($p < 0.05$). Statistical analyses were done separately for GSH + GSSG (normal), GSH (*italic*) and GSSG (**bold**).

5.4 Discussion

Unraveling the mechanisms by which plants respond to uranium stress can be of great importance when aiming to evaluate its environmental impact. As Vanhoudt et al. (2008) indicated that oxidative stress related responses are triggered in *Arabidopsis thaliana* after exposure to 100 µM uranium, this study aimed to perform a more profound investigation of the ROS signature in roots following uranium exposure. Seventeen-day-old *Arabidopsis thaliana* roots were exposed to uranium concentrations ranging from 0.1 to 100 µM. Responses on molecular and biochemical level were analyzed following 1, 3 and 7 days exposure to the uranium concentration range.

In general, toxicity effects in roots were only induced by 100 µM uranium, therefore this discussion will mainly focus on these results. While results for the lower uranium concentrations (0.1-10 µM) remained mostly unaltered, toxicity effects will probably be manifested at a later stage.

The oxidative burst, during which ROS are generated, is one of the earliest responses of plant cells under biotic and abiotic stress situations (Bhattacharjee, 2005). The oxidative burst can be due to elevated NADPH oxidases dependent $O_2^{\bullet-}$ production and an increased activity of lipoxygenases or cell wall peroxidases. Following 100 µM uranium exposure, the increase in transcript levels of *RBOHD* (figure 5.2D) and *LOX1* (figure 5.2A) is a fast uranium stress response triggered already after 1 day. Diverse roles for NADPH oxidase generated ROS in plant cells have been described including defense responses, development and cellular signal transduction (Sagi & Fluhr, 2006). Lipoxygenases are known to initiate the synthesis of oxylipins being signaling molecules in stress situations (Porta & Rocha-Sosa, 2002). To determine the signaling or damaging role of oxidative burst generated ROS under high uranium stress, a more in depth determination of membrane damage, hydrogen peroxide and other ROS concentrations is needed. As root growth was severely inhibited under 100 µM uranium in combination with a measured potassium leakage, roots are undoubtedly severely damaged and 100 µM uranium is highly toxic for *Arabidopsis thaliana* seedlings (chapter 4).

During the oxidative burst, the production of $O_2^{\bullet-}$ and its transformation to H_2O_2 are of great importance (Low & Merida, 1996). Besides inducing oxidative damage to plant cells, ROS such as H_2O_2 can also act as signaling molecules, triggering various cellular responses (Bhattacharjee, 2005) including enzyme activation, gene expression and programmed cell death (Neill et al., 2002). The ROS presence in plant cells needs therefore be regulated by a highly efficient antioxidative defense system (Halliwell, 2006).

As $O_2^{\bullet-}$ detoxifying system, SODs constitute the first line of defense against ROS produced during the oxidative burst. The significant increase in SOD capacity at 100 µM uranium (figure 5.1A), was again a fast response to high uranium stress already triggered after 1 day, indicating an enhanced detoxification of $O_2^{\bullet-}$ resulting in an elevated production of H_2O_2. Correspondingly, gene expression

analyses showed a significant increase in *FSD1* transcript levels following exposure to 100 µM uranium (figure 5.3C) which was similar to the SOD response on protein level (figure 5.1A). The increase in *FSD1* transcript levels probably compensates the reduction in gene expression levels observed for *CSD1* and *CSD2* (figure 5.3A-B). *FSD1* and *CSD1* transcript levels were confirmed by results obtained by Vanhoudt et al. (2008) for *Arabidopsis thaliana* roots under high uranium stress. The increase in *FSD1* and decrease in *CSD2* expression levels has also been reported by Smeets et al. (2008) for *Arabidopsis thaliana* roots under cadmium stress. The difference in response between the different isoforms could be explained by their disparate subcellular locations and the site of action of uranium stress as was also suggested by Alscher et al. (2002).

For the detoxification of hydrogen peroxide, a significant increase in *CAT1* transcript levels was again a fast response under high uranium stress, already triggered after 1 day (figure 5.4B). Although transcript levels were highly increased, no alterations on protein level were observed (figure 5.1B) which could probably be attributed to the presence of multiple allo- or isozymes. The results could also indicate that uranium could promote posttranslational modifications of the protein as was suggested by Romero-Puertas et al. (2007) for pea leaves under cadmium stress.

Together with CAT, PXs are also responsible for the enzymatic removal of hydrogen peroxide in plants and our results suggest again that hydrogen peroxide is a key ROS present during high uranium stress. Peroxidases such as SPX and GPX are found throughout the cell (Asada, 1992; Arora et al., 2002). In addition to the early CAT responses, SPX and GPX responses start at the later stage of 3 days. Our results show a significant increase in enzyme capacities of SPX and GPX following exposure to 100 µM uranium (figure 5.1C-E) indicating again an enhanced defense against hydrogen peroxide. These results could also point to an increased cell wall lignification, possibly giving rise to enhanced extracellular uranium complexation. An increase in SPX and GPX capacities was also reported by Cuypers et al. (2002) under copper stress for roots of *Phaseolus vulgaris*, where it was shown that SPX are mainly located extracellular and therefore are implicated in lignification processes.

For the detoxification of hydrogen peroxide in plant cells, the ascorbate-glutathione cycle is also an important pathway. Since ascorbate and glutathione are involved in the regulation of gene expression, adjustment of the ratios of their reduced and oxidized forms may be of regulatory significance (Noctor & Foyer, 1998). Similar with SPX and GPX, this cycle was also triggered at the later stage of 3 days. The APX capacity was enhanced after 3 and 7 days exposure to the highest uranium concentration (figure 5.1E) indicating an increased functioning of this enzyme in hydrogen peroxide detoxification. The pattern observed on protein level partly corresponded with *APX1* transcript levels (figure 5.4A). As reduced ascorbate is the electron donor in this conversion of hydrogen peroxide, the AsA/DHA redox balance completely shifted towards the oxidized form under high uranium stress (table 5.2). The disruption of the ascorbate redox balance could not be inverted by action of the glutathione part of the cycle although the glutathione redox balance could be maintained (table 5.3) and GR capacity (figure 5.1F) and *GR1* transcript levels (figure 5.4C) increased. In line with our results, Cuypers et al. (2001) reported that the cellular redox balance of *Phaseolus vulgaris* roots was very sensitive to zinc treatment as here also an overall increase of the ratio DHA/AsA was found after heavy metal exposure. In general, heavy metal stress induced disturbances of the ascorbate-glutathione cycle were reported by several authors (Cuypers et al., 2001; Drazkiewicz et al., 2003; Smeets et al., 2005).

In conclusion, this study aimed to further unravel mechanisms by which *Arabidopsis thaliana* roots respond to uranium stress. Results have shown that oxidative stress related responses were only triggered in roots after exposure to the highest uranium concentration (100 µM). Plasma membrane damage of the root cells and an immediate ROS producing oxidative burst are the first responses to high uranium stress. The first line of defense can be attributed to SOD, detoxifying $O_2^{\bullet-}$ as a fast response. Hydrogen peroxide can be postulated as a signaling molecule under uranium stress, triggering further responses. Controlling hydrogen peroxide levels by APX seems to be important, but regeneration of oxidized ascorbate by glutathione is hampered at this high uranium concentration. Therefore further research on the importance and role of ascorbate under uranium stress is necessary at intermediate concentrations between 10 and 100 µM.

Chapter 6

Importance of oxidative stress related responses in *Arabidopsis thaliana* leaves following uranium exposure

Vanhoudt N., Vandenhove H., Horemans N., Remans T., Opdenakker K., Smeets K., Martinez Bello D., Havaux M., Wannijn J., Van Hees M., Vangronsveld J. & Cuypers A. (2009) Importance of oxidative stress related responses in *Arabidopsis thaliana* leaves following uranium exposure. *In preparation*.

Abstract

The cellular redox balance seems an important modulator under heavy metal stress. While for other heavy metals these processes are well studied, oxidative stress related responses are also known to be triggered under uranium stress but information remains limited. This study aimed to further unravel the mechanisms by which plant leaves respond to uranium stress. Seventeen-day-old *Arabidopsis thaliana* seedlings, grown on a modified Hoagland solution under controlled conditions, were exposed to 0, 0.1, 1, 10 and 100 µM uranium for 1, 3 and 7 days. As several responses were already visible following 1 day exposure, when uranium concentrations in the leaves were negligible, a root-to-shoot signaling system was suggested in which plastids could be important sensing sites. While lipid peroxidation, based on the amount of TBA reactive compounds, was observed after exposure to 100 µM uranium, affecting membrane structure and function, a transient concentration dependent response pattern was visible for lipoxygenase initiated lipid peroxidation. This transient character of uranium stress responses in leaves was emphasized by results of *LOX2* and antioxidative enzyme transcript levels, enzyme capacities and glutathione concentrations both in time as with concentration. The ascorbate redox balance seemed an important modulator of uranium stress responses in the leaves as in addition to the previous transient responses, the ascorbate concentration and AsA/DHA redox balance increased in a concentration and time dependent manner. This could represent either a slow transient response or a stable increase with regard to plant acclimation to uranium stress.

6.1 Introduction

Industrial activities as uranium mining and milling, metal mining and smelting and the phosphate industry have caused radioactive contamination of the environment in many countries (Vandenhove, 2002). While uranium toxicity effects are predominantly studied on man and animal species, information on plant toxicity effects is scant (Ribera et al., 1996). When evaluating the uranium contamination impact on the environment, mechanisms by which plants respond to uranium stress should be unraveled. Uranium can induce physiological and metabolic effects and alter the nutrient profile of plants (chapter 4; Vandenhove et al., 2006; Vanhoudt et al., 2008). Apart from these effects on growth and development, uranium is known to induce oxidative stress related responses in *Arabidopsis thaliana* (Vanhoudt et al., 2008) and *Phaseolus vulgaris* (Vandenhove et al., 2006).

Reactive oxygen species (ROS) are produced under normal circumstances and have a dual role as both toxic byproducts of aerobic metabolism and key regulators of biological processes as growth, cell cycle, biotic and abiotic stress responses (Mittler et al., 2004). ROS can be extremely reactive and have the potential to oxidize biological molecules as DNA, proteins and lipids. To allow signal transduction processes but limit oxidative damage, cellular levels of ROS must be tightly controlled. Therefore, plants dispose of a well-equipped antioxidative defense system comprising ROS-scavenging enzymes (e.g. superoxide dismutase (SOD), catalase (CAT) peroxidases (PX)) and metabolites (e.g. ascorbate, glutathione) located in different plant cell compartments.

Exposure of plants to stress situations (e.g. heavy metals, drought, radiation) can disrupt the metabolic balance of cells, causing an enhanced production of ROS (Mittler et al., 2004). Depending on the amount produced, ROS can exacerbate the caused damage or act as signaling molecules, activating defense responses (Dat et al., 2000).

ROS can be generated in plants at plasma membrane level or extracellulary in the apoplast. A rise in H_2O_2 (a signaling molecule) production can be related to the plasma membrane associated NADPH-oxidase ($O_2^{\bullet -}$-producing enzyme) together with apoplastic SOD ($O_2^{\bullet -}$-scavenging and H_2O_2-producing enzyme).

Besides direct induction by ROS, lipid peroxidation can also be due to an increase in lipoxygenase (LOX) activity. Lipoxygenases initiate the formation of oxylipins, which are products of fatty acid oxidation and can function as precursors for signaling molecules such as jasmonates (Porta & Rocha-Sosa, 2002).

Regulatory mechanisms function both at gene and protein level to coordinate antioxidant responses (Bhattacharjee, 2005). Previous studies indicate the importance of ROS-scavenging enzymes (SOD, CAT, PX) and the ascorbate-glutathione pathway in the plant's defense against heavy metal stress (Cuypers et al., 2000; Smeets et al., 2005; Semane et al., 2007). Only recent studies also include analyses of ROS producing and scavenging enzymes at transcriptional level (Smeets et al., 2008). For uranium stress, Vandenhove et al. (2006) reported toxicity effects in *Phaseolus vulgaris* following exposure to 1000 µM uranium. In roots and leaves of *Arabidopsis thaliana* seedlings, oxidative stress related responses were already induced following exposure to 100 µM uranium as was reported by Vanhoudt et al. (2008). In the latter study, a single uranium concentration (100 µM) was applied and a more profound research was suggested to further unravel the uranium stress response mechanisms.

Therefore, this study will investigate the importance of the cellular redox balance as a modulator in uranium stress. Relevant ROS producing and scavenging enzymes will be analyzed on protein and transcriptional level and antioxidant metabolite concentrations will be determined. Stress responses in *Arabidopsis thaliana* leaves will be investigated following exposure to a uranium concentration range and harvest after 1, 3 and 7 days.

6.2 Materials and methods

6.2.1 Plant culture and uranium exposure

Arabidopsis thaliana seeds (Columbia ecotype) were spread on moist filter paper for 3 days at 4 °C in order to synchronize germination. Subsequently, seeds were sown on polyethylene plugs filled with 2 % agar (Difco). These plugs were positioned in a PVC cover capable of holding 81 plugs. The PVC cover was then placed on a black container filled with 2.9 l of a modified Hoagland solution

(macro-elements without phosphate: 1/10 diluted, phosphate solution: 1/20 diluted, micro-elements: 1/10 diluted and iron solution: 1/10 diluted). Plants were grown in a growth chamber (Microclima 1000E, Snijders Scientific B.V.) under a 14 h photoperiod (photosynthetic photon flux density: 200 µmol m^{-2} s^{-1} at the leaf level, supplied by Sylvania BriteGro F36WT8/2084 and F36WT8/2023), with day/night temperatures of 22 °C/18 °C and 65 % relative humidity. Roots were aerated during the entire experiment.

Subsequently, 17-day-old seedlings were contaminated with 0, 0.1, 1, 10 and 100 µM uranium. Uranium was added as $UO_2(NO_3)_2.6H_2O$ (Sigma) to the modified Hoagland solution and the pH was adjusted to ± 5.5 with NaOH. As previous experiments recommended the use of 25 µM phosphate in combination with uranium, a 1/80 diluted phosphate solution was used (Vanhoudt et al., 2008).

Following 1, 3 and 7 days exposure, leaves were harvested as ± 100 mg samples, flash frozen in liquid nitrogen and stored at -80 °C.

6.2.2 Determination of lipid peroxidation

The level of lipid peroxidation was determined using two techniques. First, the amount of TBA (thiobarbituric acid) reactive compounds (mainly malondialdehyde) was used as a measure of lipid peroxidation in *Arabidopsis thaliana* leaves. Plant tissue (approximately 100 mg) was homogenized with 2 ml 0.1 % TCA (trichloroacetic acid) using a mortar and pestle. After centrifugation at 20000 × g for 10 minutes, 0.5 ml of the supernatant was added to 2 ml 0.5 % TBA. This mixture was then heated at 95 °C for 30 minutes and quickly cooled in an ice bath. After centrifugation at 20000 × g for 10 minutes, the absorbance of the supernatant was measured spectrophotometrically at 532 nm corrected for unspecific absorbance at 600 nm according to Dhindsa et al. (1981).

Secondly, lipids were extracted from 500 mg frozen leaf tissue by grinding with 2 × 1 ml $CHCl_3$ containing 1 mg ml^{-1} triphenyl phosphine and 0.05 % (w/v) butylated hydroxytoluene, with 15-hydroxy-11,13(Z,E)-eicosadienoic acid as internal standard. The organic phase was evaporated under a steam of N_2. The residue was recovered in 1.25 ml ethanol and 1.25 ml 3.5 M NaOH and

hydrolyzed at 80 °C for 15 min. After addition of 2.2 ml 1 M citric acid, hydroxyl fatty acids were extracted with 2 × 1 ml hexane/ether (50/50). An aliquot of the organic phase (50 µl) was submitted to straight phase HPLC (Waters, Millipore, St Quentin-Yvelines, France) using a Zorbax rx-SIL column (4.6 · 250 mm, 5 µm particle size, Hewlett Packard, Les Ullis, France), isocratic elution with 70/30/0.25 (v/v/v) hexane/diethyl ether/acetic acid at a flow rate of 1.5 ml min^{-1}, and UV detection at 234 nm. ROS-induced lipid peroxidation was evaluated from the levels of the different hydroxyoctadecatrienoic acid (HOTE) isomers as previously described using 15-hydroxy-11,13(Z,E)-eicosadienoic acid as internal standard (Montillet et al., 2004). LOX-induced lipid peroxidation was estimated from the level of 13-HOTE after subtraction of racemic 13-HOTE (attributable to ROS-mediated lipid peroxidation), as explained by Montillet et al. (2004).

6.2.3 Analysis of enzyme capacities

Frozen leaf tissue (approximately 100 mg) was homogenized in ice-cold 0.1 M Tris-HCl buffer (pH 7.8) containing 1 mM EDTA, 1 mM dithiotreitol and 4 % insoluble polyvinylpyrrolidone (2 ml buffer for 100 mg FW), using a mortar and pestle. The homogenate was squeezed through a nylon mesh and centrifuged at 20000 × g and 4 °C for 10 minutes. The enzyme capacities, i.e. potential activity measured in vitro under non-limiting reaction conditions, were measured spectrophotometrically in the supernatant at 25 °C.

Guaiacol peroxidase and syringaldazine peroxidase capacities (GPX, SPX, EC 1.11.1.7) were measured at 436 nm and 530 nm according to Bergmeyer et al. (1974) and Imberty et al. (1984), respectively. Ascorbate peroxidase capacity (APX, EC 1.11.1.11) was measured at 298 nm following the method of Gerbling et al. (1984). Analysis of superoxide dismutase capacity (SOD, EC 1.15.1.1) was based on the inhibition of cytochrome c at 550 nm according to McCord & Fridovich (1969). Analyses of the capacities of glutathione reductase (GR, EC 1.6.4.2) and catalase (CAT, EC 1.11.1.6) were performed as described by Bergmeyer et al. (1974).

6.2.4 Gene expression analysis

Frozen leaf tissue (approximately 100 mg) was ground thoroughly in liquid nitrogen using a mortar and pestle. RNA was extracted using the RNeasy Plant Mini Kit (Qiagen). The RNA quantity was determined spectrophotometrically at 260 nm (Nanodrop, Isogen Life Science). The RNA quality was checked electrophoretically using the Bioanalyzer (Agilent Technologies). Before cDNA synthesis, the RNA sample was incubated during 2 minutes in gDNA wipeout buffer at 42 °C in order to effectively eliminate genomic DNA. First strand cDNA synthesis was primed with a combination of oligo(dT)-primers and random hexamers according to the manufacturer's instructions using the QuantiTect Reverse Transcription Kit (Qiagen) and equal amounts of starting material were used (1 µg). Quantitative real time PCR was performed with the 7500 Fast Real-Time PCR System (Applied Biosystems), using Sybr Green chemistry. Primers used for gene expression analyses are given in table 6.1. PCR amplifications were performed in a total volume of 10 µl containing 2.5 µl cDNA sample, 5 µl Fast Sybr Green Master Mix (Applied Biosystems), 0.3 µl forward primer, 0.3 µl reverse primer and 1.9 µl RNase-free H_2O.

Table 6.1 - Sequences of forward and reverse primers used in gene expression analysis

Gene	Forward primer	Reverse primer
At2g28390	AACTCTATGCAGCATTTGATCCACT	TGATTGCATATCTTTATCGCCATC
At5g08290	TTACTGTTTCGGTTGTTCTCCATTT	CACTGAATCATGTTCGAAGCAAGT
At5g15710	TTTCGGCTGAGAGGTTCGAGT	GATTCCAAGACGTAAAGCAGATCAA
APX1	TGCCACAAGGATAGGTCTGG	CCTTCCTTCTCTCCGCTCAA
CAT1	AAGTGCTTCATCGGGAAGGA	CTTCAACAAAACGCTTCACGA
CAT2	AACTCCTCCATGACCGTTGGA	TCCGTTCCCTGTCGAAATTG
CSD1	TCCATGCAGACCCTGATGAC	CCTGGAGACCAATGATGCC
CSD2	GAGCCTTTGTGGTTCACGAG	CACACCACATGCCAATCTCC
CSD3	GTTGTTGTGCATGCGGATCC	CACATCCAACTCTCGAGCCTG
FSD1	CTCCCAATGCTGTGAATCCC	TGGTCTTCGGTTCTGGAAGTC
GR1	CTCAAGTGTGGAGCAACCAAAG	ATGCGTCTGGTCACACTGC
MSD1	ATGTTTGGGAGCACGCCTAC	AACCTCGCTTGCATATTTCCA
LOX1	TTGGCTAAGGCTTTTGTCGG	GTGGCAATCACAAACGGTTC
LOX2	TTTGCTCGCCAGACACTTG	GGGATCACCATAAACGGCC
RBOHC	TCACCAGAGACTGGCACAATAAA	GATGCTCGACCTGAATGCTC
RBOHD	TATGCATCGGAGAGGCTGCT	TAGAGACAACACGTTCCCGGG
RBOHF	GGTGTCATGAACGAAGTTGCA	AATGAGAGCAGAACGAGCATCA
UBQ10	GGCCTTGTATAATCCCTGATGAATAAG	AAAGAGATAACAGGAACGGAAACATAGT

Gene expression data were normalized against multiple housekeeping genes (At2g28390, At5g08290, At5g15710, UBQ10) according to Vandesompele et al. (2002) and Remans et al. (2008) and represented relative to the control treatment (untreated leaves after 1 day).

6.2.5 Metabolite analysis

Ascorbate and glutathione concentrations in *Arabidopsis thaliana* leaves were determined by HPLC analysis. Therefore approximately 100 mg tissue was ground thoroughly in liquid nitrogen using a pre-cooled mortar and pestle. When a homogenous powder was obtained, 1 ml of ice cold 6 % (w/v) meta-phosphoric acid was added and the mixture was clarified by centrifugation at 20000 $\times$ g and 4 °C for 10 minutes. The resulting supernatant was kept frozen until HPLC analysis. Antioxidants were separated on a 100 mm $\times$ 4.6 mm Polaris C18-A reversed phase HPLC column (3 µm particle size, 30 °C, Varian, CA USA) with an isocratic flow of 1 ml min^{-1} of the elution buffer (25 mM K/PO_4-buffer, pH 3.0). The components were quantified using a home-made electrochemical detector with glassy carbon electrode and a Scott pt 62 reference electrode (Mainz, Germany). The purity and identity of the peaks were confirmed using a diode array detector (SPD-M10AVP, Shimadzu, Hertogenbosch, Netherlands) which was placed on line with the electrochemical detector. The concentrations of oxidized DHA (dehydroascorbate) or GSSG (glutathione disulphide) were measured indirectly as the difference between the total concentration of antioxidants in a DTT (dithiothreitol) reduced fraction and the concentration in a sample prior to reduction. Reduction of the sample was obtained by incubation of an aliquot of the extract in 400 mM Tris and 200 mM DTT for 15 minutes in the dark. The pH of this mixture was checked to be between 6.0 and 7.0. After 15 minutes, the pH was lowered again by 4-fold dilution in elution buffer prior to HPLC analysis.

6.2.6 Statistical analysis

The datasets for lipid peroxidation, enzyme capacities and metabolites were analyzed by day, evaluating the effect of uranium treatment. Statistical analyses were done following the algorithm described below, ensuring for each dataset a statistical analysis best fitted for the data.

A parametric analysis of variance was performed and the assumptions for normality and constancy of variance were checked (Kutner et al., 2005). This was done on original data or after transformation of the data (Box & Cox, 1964). Then, a pair wise comparison was applied with an adjustment of the p-values using Tukey according to Kutner et al. (2005). If only the assumption for normality was fulfilled, a parametric analysis of variance for heterocedastic variances was applied according to Westfall et al. (2000). A pair wise comparison was then carried out adjusting the p-values using simulated p-values (Westfall et al., 2000). If neither assumption was fulfilled, a nonparametric analysis of variance was applied (Lehmann & D'Abrera, 1998) adjusting the p-values using Benjamini Hochberg (Benjamini & Hochberg, 1995).

The gene expression dataset was analyzed by day, evaluating the effect of uranium treatment, using global permutations with p-value adjustment as it was presented by Lin et al. (2008), using the Benjamini and Hochberg False Discovery Rate (BH-FDR) adjustment (Benjamini et al., 1995).

6.3 Results

6.3.1 Lipid peroxidation

As a measure for the level of lipid peroxidation in *Arabidopsis thaliana* leaves following uranium exposure, first the amount of TBA reactive compounds was determined (figure 6.1). For all the harvesting times, a significant increase in the amount of TBA reactive compounds was observed in leaves following exposure to 100 µM uranium as compared to the other treatments and the control. The amount of TBA reactive compounds also increased with increasing exposure time for leaves exposed to 100 µM uranium.

Secondly, a distinction was made between ROS induced lipid peroxidation (figure 6.2A) and LOX induced lipid peroxidation (figure 6.2B). Only leaves exposed for 7 days to the uranium concentration range were analyzed. For both types of lipid peroxidation a bell-shaped curve was observed, meaning hydroxyl-octadecatrienoic acid levels significantly increased following exposure to 1 µM uranium but did not change significantly for the other uranium concentrations applied.

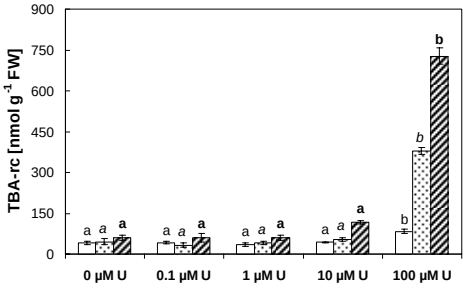

Figure 6.1 – Amount of TBA (thiobarbituric acid) reactive compounds in leaves following uranium exposure. Lipid peroxidation measurement was based on the amount of TBA reactive compounds [nmol g^{-1} FW]. *Arabidopsis thaliana* seedlings were exposed to a uranium concentration range for 1 (white bars), 3 (dotted bars) and 7 days (striped bars). Data represent the mean ± S.E. of 3 biological replicates. Different letters above the bars indicate significant differences in lipid peroxidation between the different treatments for day 1 (normal), 3 (*italic*) and 7 (**bold**) ($p < 0.05$).

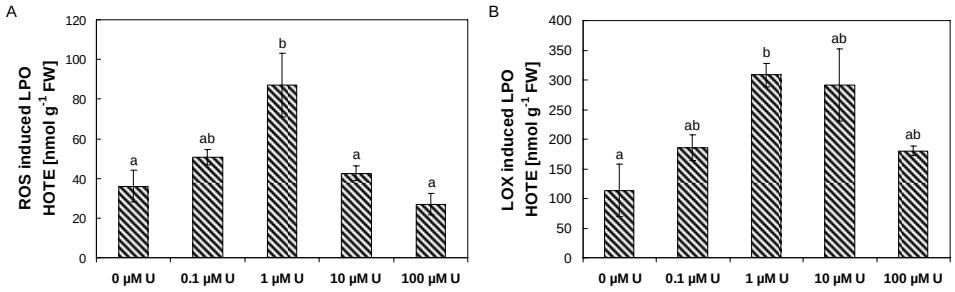

Figure 6.2 – Lipid peroxidation analysis in *Arabidopsis thaliana* leaves following uranium exposure during 7 days. A difference was made between ROS induced (A) and LOX induced (B) lipid peroxidation by analyzing the levels of the corresponding HOTE (hydroxyoctadecatrienoic acid) isomers [nmol g^{-1} FW]. Data represent the mean ± S.E. of 3 biological replicates. Different letters above the bars indicate significant difference in lipid peroxidation levels between the different treatments.

6.3.2 Enzyme capacities

To investigate the influence of uranium contamination on oxidative stress responses at protein level, enzyme capacities of relevant enzymes of the antioxidative defense system were determined in *Arabidopsis thaliana* leaves.

Generally, following 1 day of exposure, no alterations in enzyme capacities were observed for the enzymes studied, only a slight significant increase was observed in GR capacity for leaves exposed to 100 µM uranium as compared to the control treatment (figure 6.3F).

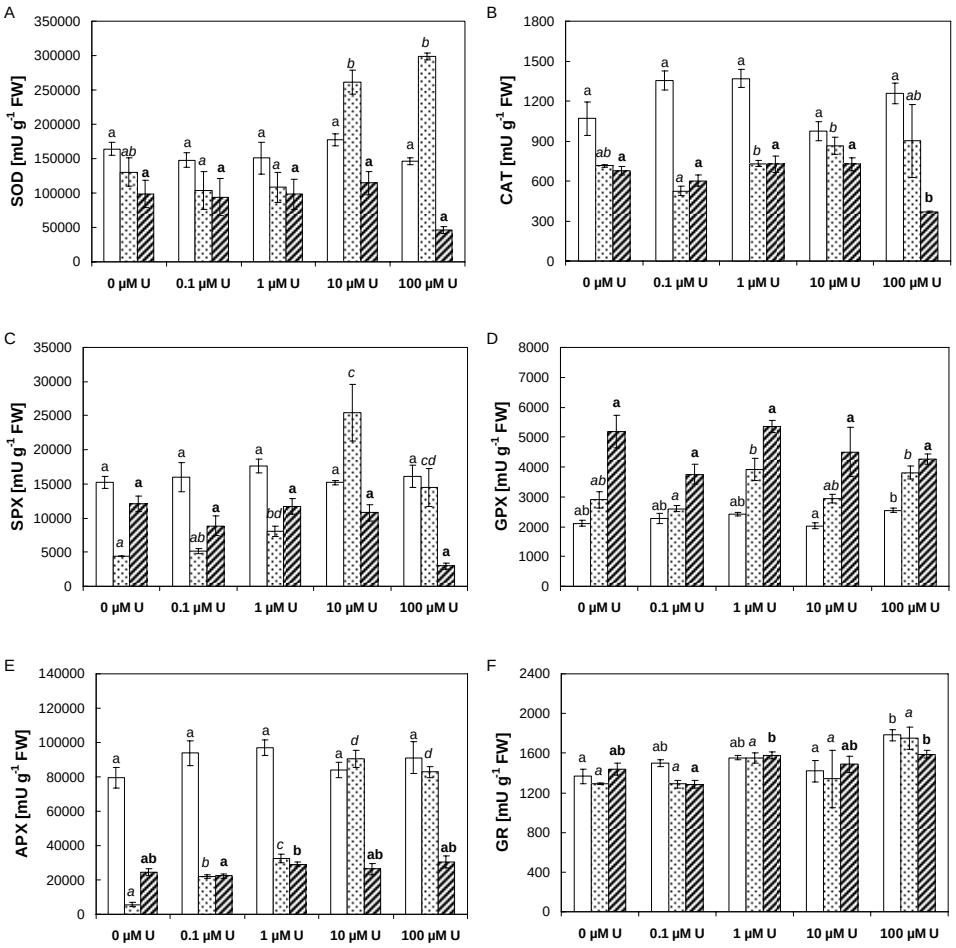

Figure 6.3 – Capacities [mU g^{-1} FW] of ROS (reactive oxygen species)-scavenging enzymes and enzymes related to the ascorbate-glutathione pathway. Enzyme capacities were determined in leaves of *Arabidopsis thaliana* seedlings exposed to a uranium concentration range for 1 (white bars), 3 (dotted bars) and 7 days (striped bars). Values are the mean ± S.E. of at least 3 biological replicates. Different letters above the bars indicate significant differences in enzyme capacity between the different treatments for day 1 (normal), 3 (*italic*) and 7 (**bold**) ($p < 0.05$).

After 3 days of exposure, significant alterations were visible for the capacities of several enzymes. Capacities of SOD and SPX increased significantly after exposure to 10 and 100 µM uranium (figure 6.3A & C). APX capacities significantly increased with increasing uranium concentration added to the nutrient solution (figure 6.3E). Fluctuations in capacities of CAT and GPX were observed but no clear pattern was visible (figures 6.3B & D). GR capacities remained stable for all uranium concentrations (figure 6.3F).

Following 7 days of exposure, all enzyme capacities remained stable, except the CAT capacity significantly decreased following exposure to the highest uranium concentration (figure 6.3B).

6.3.3 Gene expression

To evaluate the importance of the ROS signature during uranium stress, important ROS producing and scavenging enzymes were analyzed at transcriptional level using quantitative real time PCR.

First, gene expression of several ROS producing enzymes was analyzed. Important alterations in transcript levels were observed for *LOX2* (lipoxygenase 2 located in the chloroplasts) as they already increased significantly after 1 day exposure to 100 µM uranium (figure 6.4B) with an increasing trend for 10 µM uranium after 3 days and 1 µM uranium after 7 days. *LOX1* (lipoxygenase 1 located in the cytoplasm) gene expression was significantly decreased after 3 days exposure to 100 µM uranium (figure 6.4A). Transcript levels for different isoforms of NADPH oxidase (*RBOHC*, *RBOHD* and *RBOHF*) were also analyzed on transcriptional level but no alterations were observed (results not shown).

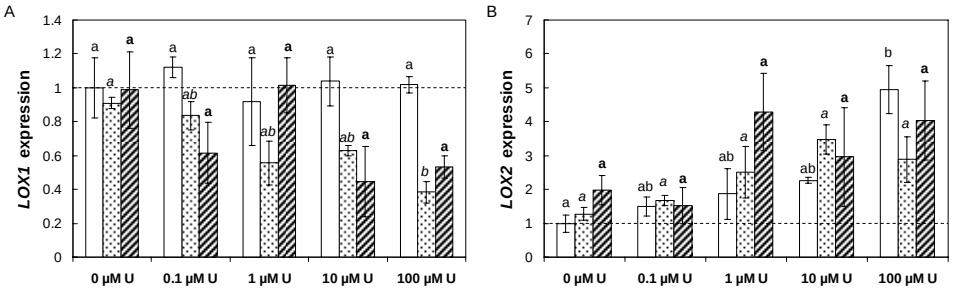

Figure 6.4 – Alterations in gene expression of lipoxygenases following uranium exposure. *Arabidopsis thaliana* seedlings were exposed for 1 (white bars), 3 (dotted bars) and 7 days (striped bars) to uranium concentrations ranging from 0.1 to 100 µM. Gene expression of *lox1* and *lox2* in leaves was expressed relative to the control treatment of day 1 (dashed line). Values represent the mean ± S.E. of 3 biological replicates. Different letters above the bars indicate significant differences in gene expression between the uranium concentrations for day 1 (normal), 3 (*italic*) and 7 (**bold**) ($p < 0.05$).

Secondly, to investigate gene expression of $O_2^{\bullet-}$ scavenging enzymes, different isoenzymes of SOD were analyzed. No alterations in transcript levels were observed for *CSD3* (peroxisomal copper/zinc SOD) and *MSD1* (mitochondrial manganese SOD) between the uranium concentrations for the 3 harvesting

times (results not shown). Following 1 day exposure, a significant down regulation in gene expression was observed for *CSD1* (cytoplasmic copper/zinc SOD) and *CSD2* (chloroplastic copper/zinc SOD) after exposure to 100 µM uranium (figure 6.5A-B). Transcript levels of *FSD1* (plastidic iron SOD) remained stable (results not shown). Three days exposure resulted in a significant down regulated gene expression of *CSD1* when exposed to 10 and 100 µM uranium (figure 6.5A), of *CSD2* when exposed to 1, 10 and 100 µM uranium (figure 6.5B) and of *FSD1* when exposed to 100 µM uranium as compared to the control (results not shown). An exposure time of 7 days resulted in a decreased expression of *CSD2* (figure 6.5B) and *FSD1* when exposed to 100 µM uranium (results not shown). Transcript levels of *CSD1* remained stable for all uranium concentrations (figure 6.5A).

Finally, gene expression of several H_2O_2 scavenging enzymes was analyzed. Following 1 day exposure, transcript levels of *CAT1* (peroxisomal CAT), *CAT2* (peroxisomal CAT) and *APX1* (cytoplasmic APX) remained stable for all treatments (figure 6.5C-E). A significant down regulated gene expression of *GR1* (cytosolic GR) was observed after exposure to 10 and 100 µM uranium (figure 6.5F). After 3 days of exposure, a significant up regulation in *CAT1* expression was observed following exposure to 1 and 10 µM uranium (figure 6.5C). *CAT2* transcript levels on the other hand were almost completely absent in leaves exposed to 10 and 100 µM uranium (figure 6.5D). For *APX1* expression, a significant down regulation was observed in leaves exposed to 100 µM uranium (figure 6.5E) while *GR1* transcript levels significantly decreased with increasing uranium concentration added to the nutrient solution (figure 6.5F). Following 7 days exposure, the significant increase in gene expression for *CAT1*, observed after 3 days, was still visible for 1 µM uranium (figure 6.5C) while *CAT2* gene expression decreased even further in leaves exposed to 10 and 100 µM uranium (figure 6.5D). *APX1* transcript levels remained stable (figure 6.5E) and a significant decrease in gene expression for *GR1* was observed for 1, 10 and 100 µM uranium (figure 6.5F).

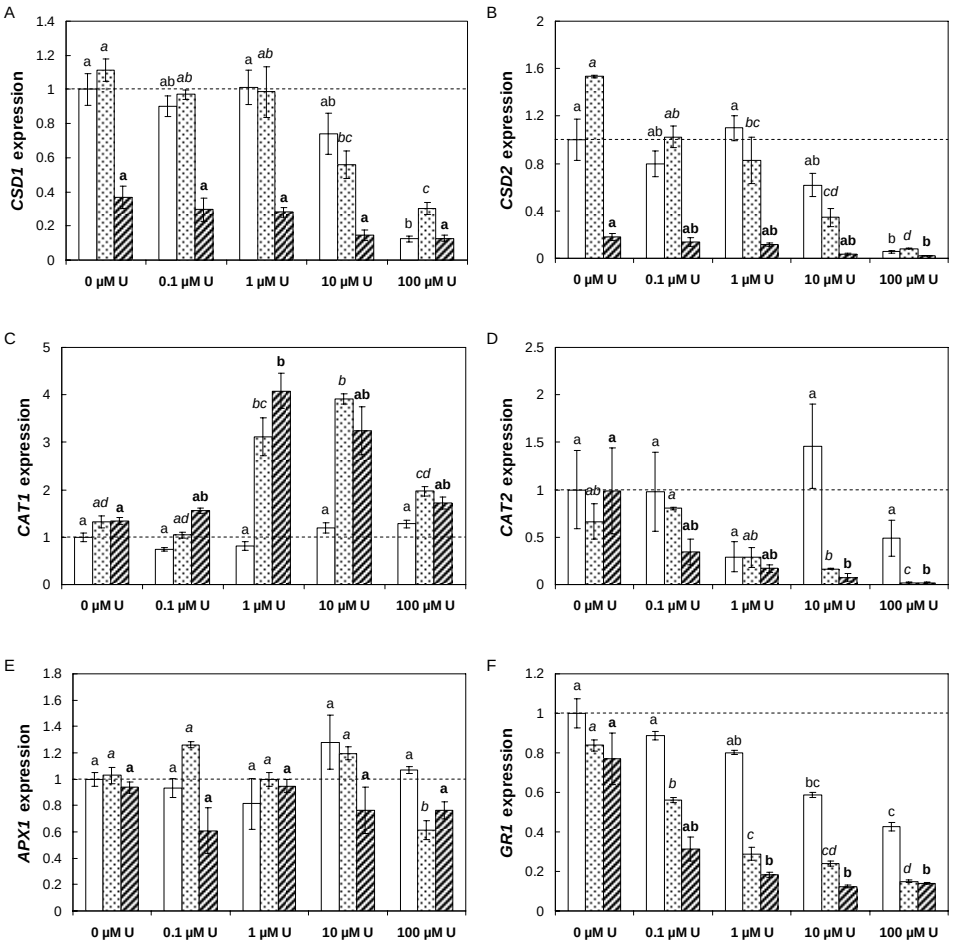

Figure 6.5 - Gene expression of several $O_2^{\bullet-}$ and H_2O_2 scavenging enzymes following uranium exposure. Gene expression of *csd1*, *csd2*, *cat1*, *cat2*, *apx1* and *gr1* in leaves of *Arabidopsis thaliana* seedlings exposed to a uranium concentration range for 1 (white bars), 3 (dotted bars) and 7 days (striped bars), was expressed relative to the control treatment of day 1 (dashed line). Data represent the mean ± S.E. of 3 biological replicates. Different letters above the bars indicate significant differences in gene expression between the uranium concentrations for day 1 (normal), 3 (*italic*) and 7 (**bold**) ($p < 0.05$).

6.3.4 Metabolites

To evaluate the importance of the ascorbate-glutathione pathway in H_2O_2 detoxification in response to uranium stress, the concentrations of the antioxidants ascorbate (table 6.2) and glutathione (table 6.3) were determined.

Table 6.2 – Ascorbate concentrations [nmol g^{-1} FW] in *Arabidopsis thaliana* leaves following uranium exposure.

		0 µM U	**0.1 µM U**	**1 µM U**	**10 µM U**	**100 µM U**
AsA + DHA	*1 day*	3066±116^{a}	3186±155^{a}	3501±199^{a}	3248±188^{a}	4749±228^{b}
	3 days	4847±167^{a}	4929±138^{a}	5556±601^{ab}	6511±269^{b}	9938±198^{c}
	7 days	6400±82^{a}	5512±325^{a}	7707±174^{b}	8477±186^{c}	12866±1034^{d}
AsA	*1 day*	2162±131^{a}	2122±178^{a}	2232±295^{a}	2362±219^{a}	3503±247^{b}
	3 days	4511±149^{a}	4636±115^{a}	4826±216^{a}	6143±296^{b}	9605±171^{c}
	7 days	5694±225^{a}	4534±408^{a}	6778±213^{b}	7716±150^{c}	12228±1037^{d}
DHA	*1 day*	904±24$^{\mathbf{a}}$	1064±207$^{\mathbf{a}}$	1270±186$^{\mathbf{a}}$	886±56$^{\mathbf{a}}$	1246±63$^{\mathbf{a}}$
	3 days	336±60$^{\mathbf{a}}$	294±51$^{\mathbf{a}}$	730±450$^{\mathbf{a}}$	368±71$^{\mathbf{a}}$	333±74$^{\mathbf{a}}$
	7 days	706±82$^{\mathbf{a}}$	978±177$^{\mathbf{a}}$	929±159$^{\mathbf{a}}$	761±111$^{\mathbf{a}}$	638±83$^{\mathbf{a}}$

Seventeen-day-old *Arabidopsis thaliana* seedlings were exposed to uranium concentrations ranging from 0.1 to 100 µM for 1, 3 and 7 days. The total ascorbate concentration represents the reduced and oxidized forms (AsA: ascorbic acid = reduced form; DHA: dehydroascorbate = oxidized form). Values represent the mean ± S.E. of 6 biological replicates. Different small letters indicate significant differences between the treatments for day 1, day 3 and day 7 separately ($p < 0.05$). Statistical analyses were done separately for AsA + DHA (normal), AsA (*italic*) and DHA (**bold**).

Table 6.3 – Glutathione concentrations [nmol g^{-1} FW] in *Arabidopsis thaliana* leaves following uranium exposure.

		0 µM U	**0.1 µM U**	**1 µM U**	**10 µM U**	**100 µM U**
GSH + GSSG	*1 day*	227±8^{a}	267±6^{ac}	313±9^{b}	331±14^{b}	297±12^{bc}
	3 days	284±12^{a}	408±21^{bc}	517±51^{b}	529±25^{b}	357±20^{ac}
	7 days	268±25^{ab}	213±27^{a}	387±28^{b}	334±23^{ab}	262±43^{a}
GSH	*1 day*	152±5^{a}	166±7^{a}	184±16^{ab}	222±11^{b}	184±10^{b}
	3 days	263±7^{a}	371±14^{b}	407±25^{b}	500±20^{c}	365±19^{b}
	7 days	271±19^{ac}	219±27^{a}	403±35^{b}	368±19^{bc}	223±36^{a}
GSSG	*1 day*	75±5$^{\mathbf{a}}$	101±10$^{\mathbf{ab}}$	129±11$^{\mathbf{b}}$	109±9$^{\mathbf{ab}}$	112±6$^{\mathbf{b}}$
	3 days	21±8$^{\mathbf{a}}$	37±14$^{\mathbf{ab}}$	110±44$^{\mathbf{b}}$	29±24$^{\mathbf{ab}}$	n.d.*
	7 days	n.d.*	n.d.*	n.d.*	n.d.*	38±13$^{\mathbf{a}}$

Seventeen-day-old *Arabidopsis thaliana* seedlings were exposed to uranium concentrations ranging from 0.1 µM to 100 µM for 1, 3 and 7 days. The total glutathione concentration represents the reduced and oxidized forms (GSH: glutathione = reduced form; GSSG: glutathione disulphide = oxidized form). Data represent the mean ± S.E. of 6 biological replicates. Different small letters indicate significant differences between the treatments for day 1, day 3 and day 7 separately ($p < 0.05$). Statistical analyses were done separately for GSH + GSSG (normal), GSH (*italic*) and GSSG (**bold**). *n.d. = not detectable.

After 1, 3 and 7 days exposure, the total ascorbate concentration (AsA + DHA) significantly increased after exposure to 100 µM uranium, 10 and 100 µM uranium and 1, 10 and 100 µM uranium respectively. This increase was due to a significant increase of ascorbic acid (AsA) while the level of dehydroascorbate (DHA) remained unaffected.

Following 1 day exposure, the total glutathione concentration (GSH + GSSG) significantly increased after exposure to 1, 10 and 100 µM uranium. Correspondingly, a significant increase in glutathione (GSH) and glutathione disulphide (GSSG) concentrations was observed following exposure to 10 and 100 µM uranium and 1 and 100 µM uranium respectively. After 3 days exposure, the GSH + GSSG concentration significantly increased after exposure to 0.1, 1 and 10 µM uranium with correspondingly a significant increase in the GSH concentration after exposure to 0.1, 1, 10 and 100 µM uranium. The GSSG concentration significantly increased after exposure to 1 µM uranium. Seven days exposure did not affect the total glutathione concentration but did cause a significant increase in GSH concentration after exposure to 1 and 10 µM uranium and in GSSG concentration after exposure to 100 µM uranium.

6.4 Discussion

When considering evaluating the environmental impact of uranium, which can be present in elevated levels due to several anthropogenic activities, or when intending to establish crops or vegetation on uranium contaminated land, an investigation of the cellular mechanisms triggered in response to uranium stress in plants should be performed. Previous studies have indicated an important role for the ROS signature as a modulator in heavy metal stress (Smeets et al., 2005; Semane et al., 2007; Smeets et al., 2008). Uranium exposure can also disrupt the cellular redox balance and induce oxidative stress related responses in leaves of *Arabidopsis thaliana* plants (Vanhoudt et al., 2008) but information remains limited. This study aimed to further unravel the mechanisms by which plant cells respond to uranium induced oxidative stress. Therefore, seventeen-day-old *Arabidopsis thaliana* seedlings were exposed for 1, 3 and 7 days to uranium concentrations ranging from 0.1 to 100 µM.

Generally, the oxidative burst, during which ROS are rapidly generated and accumulated, is one of the earliest responses of plant cells under various biotic and abiotic stresses (Low & Merida, 1996). An important source of ROS production, such as $O_2^{\bullet-}$, is at the plasma membrane level by NADPH oxidase (Bhattacharjee, 2005). Our data indicate that a NADPH oxidase mediated oxidative burst is not an important ROS generating pathway in the leaves under uranium stress as gene expression levels of several isoforms of NADPH oxidase (*RBOHC*/*D*/*F*) remained unchanged for all uranium treatments. Oxidative stress in the leaves is probably generated via other mechanisms such as root-to-shoot signaling, as almost no uranium translocation to the leaves is observed (chapter 4). The heavy metal induced ROS production can cause lipid peroxidation in plant cells resulting in membrane damage. Exposure of *Arabidopsis thaliana* plants to 100 µM uranium resulted in a significant increase in the amount of TBA reactive compounds in the leaves for all the harvesting times (figure 6.1) affecting membrane integrity and functionality. This corresponds with previous results obtained by Vanhoudt et al. (2008) in *Arabidopsis thaliana* leaves exposed to 100 µM uranium for 4 days. An increased level of TBA reactive compounds in plant leaves under cadmium toxicity was reported by Smeets et al. (2005) for *Phaseolus vulgaris* and by Razinger et al. (2008) for *Lemna minor*. In our study, the seriousness of the membrane damage seems to increase with increasing exposure time (figure 6.1) which corresponds with an increased amount of uranium in the leaves (chapter 4). The enhanced membrane damage can also be linked with the increase in potassium leakage at 100 µM uranium as was shown in chapter 4. Besides being initiated by a number of ROS, lipid peroxidation in plant cells can also be initiated by the enzyme lipoxygenase, inducing damage but also increasing precursors for signaling molecules such as jasmonates and other oxylipins (Porta & Rocha-Sosa, 2002). While in the roots an important role was attributed to *LOX1* (cytoplasmic lipoxygenase) under uranium stress (chapter 5), the LOX enzyme located in the cytoplasm seems less important in response to uranium stress in leaves based on its gene expression levels (figure 6.4A). Smeets et al. (2008) reported that *LOX1* transcript levels in *Arabidopsis thaliana* leaves were not significantly affected under cadmium stress. On the other hand, our results suggest that chloroplasts could be an important sensing site in the leaves in response to uranium stress

as a pattern for *LOX2* (plastidic lipoxygenase) transcript levels could be distinguished which could also be partly extended to the antioxidative defense system. While after 1 day transcript levels were significantly induced for 100 µM uranium, 3 days exposure resulted in an increasing trend for 10 µM uranium which shifted to 1 µM uranium after 7 days of exposure (figure 6.4B). The latter observation is in agreement with the significant increase of LOX induced lipid peroxidation for 1 µM uranium after 7 days of exposure (figure 6.2B).

ROS produced under environmental stress conditions can play a dual role in plant cells: they can exacerbate damage or can act as signaling molecules activating stress-response and defense pathways (Dat et al., 2000; Foyer & Noctor, 2005). In order to regulate different ROS in various cellular compartments, plants possess an antioxidative defense system comprising ROS scavenging enzymes and metabolites (Dat et al., 2000). Within a cell, the SODs constitute the first line of defense against stress induced $O_2^{\bullet-}$ production. These enzymes are likely to be central in the defense mechanism as their capacities determine the concentrations of $O_2^{\bullet-}$ and H_2O_2 (Bowler et al., 1992). As $O_2^{\bullet-}$ can be generated at various cellular locations such as the chloroplasts, mitochondria and peroxisomes, different isoforms of SOD can be distinguished depending on their site of action and metal cofactor used (Bowler et al., 1992; Alscher et al., 2002). An increased defense against $O_2^{\bullet-}$ produced under uranium stress was suggested as on protein level the total SOD capacity was significantly increased in leaves exposed to 10 and 100 µM uranium for 3 days (figure 6.3A). To further regulate the cellular redox balance in response to uranium stress, peroxidases and catalases are present in plant cells in order to detoxify H_2O_2 and regulate its function as signaling molecule. Similar with SOD capacities, a significant increase in SPX capacities was observed following exposure to 1, 10 and 100 µM uranium for 3 days (figures 6.3C) while for APX this increase already started with 0.1 µM uranium but was most pronounced at 10 and 100 µM uranium for 3 days (figure 6.3E). These results indicate an enhanced detoxification of H_2O_2 in response to uranium stress. Elevated SPX and APX capacities in plant leaves under heavy metal stress were also reported by several authors (Cuypers et al., 2002; Cho & Seo, 2005; Smeets et al., 2008). In general, results on protein level for enzymes of the antioxidative defense system indicate that responses were mostly triggered after 3 days exposure to 10 and 100 µM uranium. This

can probably be explained by the very low root-to-shoot transfer factor of uranium. In time, the uranium concentration increased in the leaves and an elevated root-to-shoot signaling system lead up to activation of the antioxidative defense system at the protein level after 3 days. This induction of the capacities of ROS scavenging enzymes seemed transient as after 7 days exposure, a new balance was obtained and ROS scavenging enzyme capacities were again comparable with the corresponding control values. This transient induction of the antioxidative defense system was also reported by Jansen et al. (2008) under UV-B stress.

In contrast to the increased or stable antioxidative capacities observed at protein level, transcriptional levels of the corresponding genes generally decreased following uranium exposure. For SOD, clear transient effects were observed for *CSD1* and *CSD2* gene expression. Transcript levels for both genes were already significantly decreased after 1 day exposure to 100 µM uranium and after 3 days this down-regulation was significant for 10 and 100 µM uranium for *CSD1* (figure 6.5A) and 1, 10 and 100 µM uranium for *CSD2* (figure 6.5B). After 7 days exposure, expression levels were again more or less balanced for both genes. A decrease in CuZnSOD transcript levels was also observed for pea leaves under cadmium toxicity by Romero-Puertas et al. (2007). A decrease in transcript levels for *CSD2* was also observed in *Arabidopsis thaliana* leaves under cadmium stress (Smeets et al., 2008).

Whereas CAT capacities showed no clear pattern, gene expression results depended on the isoform studied. *CAT1* expression levels significantly increased after exposure to 1 and 10 µM uranium for 3 days and 1 µM uranium for 7 days (figure 6.5C). These results are in correspondence with results reported by Smeets et al. (2008) who also observed an increase in *CAT1* transcription, but no change in CAT activity in *Arabidopsis thaliana* leaves under cadmium stress. As Smeets et al. (2008) suggested that these discrepancies could be due to the presence of multiple allo- or isozymes, we also analyzed *CAT2* expression levels. In contrast to *CAT1* expression, *CAT2* transcript levels significantly decreased after exposure to 10 and 100 µM uranium for 3 and 7 days (figure 6.5D). Zimmermann et al. (2006) showed that the *CAT2* down regulation was an initial step in producing an elevated hydrogen peroxide level in the regulatory

mechanism during senescence, indicating cadmium can induce early senescence as was suggested by Cuypers et al. (submitted).

As CAT is mostly present in the peroxisomes and not in the mitochondria and chloroplasts and CAT has a rather low affinity for H_2O_2, thereby only removing the bulk of H_2O_2, the ascorbate-glutathione cycle is another pathway present in plant cells for the further detoxification of H_2O_2 (Halliwell, 2006; Noctor & Foyer, 1998). Ascorbate and glutathione are also involved in the regulation of gene expression in plant cells. The ratios of the reduced and oxidized forms of these metabolites can be of regulatory significance (Noctor et al., 1998). Our results indicate that ascorbate and glutathione respond immediately and more sensitive to uranium induced oxidative stress than enzyme capacities and gene expression. The ascorbate redox balance seems an important modulator under early uranium stress responses in the leaves. A concentration and time dependent increase in the total amount of ascorbate (AsA + DHA) and its reduced form (AsA) were observed in our study, while the concentrations of the oxidized form (DHA) remained stable (table 6.2). These results indicate that by increasing the amount of ascorbate in their leaves, *Arabidopsis thaliana* plants increase the capacity to detoxify H_2O_2 in response to uranium stress. These results can also be linked with the increase in APX capacity with increasing uranium concentration added to the nutrient solution for 3 days (figure 6.3E). Furthermore, by maintaining ascorbate in its reduced form, the cell maintains its redox balance, which is also important in signaling.

To evaluate the importance of glutathione in response to uranium stress, concentrations of GSH and GSSG indicate that glutathione seems more sensitive under uranium stress than ascorbate as alterations were already observed following 1 day exposure to lower uranium concentrations (table 6.3), but it should be highlighted that this increase is showing a transient course.

In conclusion, as several responses were already visible after 1 day, when uranium concentrations in the leaves were negligible, a root-to-shoot signaling system is suggested. Under these circumstances, plastids seem important sensing sites in the leaves. A transient concentration dependent response pattern was visible for lipoxygenase initiated lipid peroxidation. Results of *LOX2* and antioxidative enzyme transcript levels, enzyme capacities and glutathione

concentrations emphasized this transient character of the leaf response to uranium stress both in time as in concentration. Within the time frame of this study, ascorbate concentrations continuously increased in a concentration and time dependent way. As no change in DHA concentrations was visible, this suggests an increased ascorbate biosynthesis. In addition to the previous transient responses, the ascorbate related responses point towards a stable stress response. In plants acclimating to UV-B irradiation, fast and slow transient responses or stable increases were shown depending on the effects studied (Jansen et al., 2008). In our plants exposed to uranium stress we also observed different phases in response. While several fast transient effects were visible, the increase in ascorbate could represent either a slow transient response or a stable increase with regard to plant acclimation to uranium. However this can only be assumed for the lower uranium concentrations as 100 µM uranium toxicity effects in the roots are too severe to allow plant survival.

Chapter 7

Induction of DNA damage in *Arabidopsis thaliana* plants following uranium exposure

Abstract

DNA damage can be induced when plants are exposed to environmental stress situations but also during normal metabolic actions. Several DNA repair mechanisms work together to repair double strand breaks and hereby protecting cells against the induction of chromosomal aberrations or incorrect genetic information. To better evaluate the uranium impact on the environment, it is important to further unravel uranium induced biological effects in plants on the level of DNA damage and repair. Here fore, *Arabidopsis thaliana* seedlings, grown on hydroponics under controlled conditions, were exposed for 1, 3 and 7 days to uranium concentrations ranging from 0.1 to 100 µM. While DNA damage and transcript levels of DNA repair related genes were analyzed for leaves and roots, effects were mostly visible for roots. By usage of the neutral comet assay and analysis of the % tail DNA, it was shown that DNA damage in roots generally increased in time and root DNA seemed completely dispersed following exposure to 100 µM uranium. Besides some alterations in expression levels after exposure to 100 µM uranium, genes important for DNA repair and the cell cycle remained mostly unaffected by lower uranium concentrations. It can therefore be concluded that 100 µM uranium can induce DNA damage and alterations in the repair machinery in *Arabidopsis thaliana* roots but further research is necessary to unravel how the different pathways collaborate in the defense against uranium stress. Complementary, a more in depth study of the time dependence of the DNA repair system should be performed.

7.1 Introduction

Exposure of plants to stress conditions can induce DNA damage and trigger the DNA repair machinery. When aiming to evaluate the uranium impact on the environment, it is important to further unravel uranium induced biological effects in plants on the level of DNA damage and repair.

The single cell gel electrophoresis (SCGE) assay or comet assay is a suitable technique to measure DNA strand breaks. When isolated nuclei, embedded in a thin agarose layer, are subjected to electrophoresis, DNA fragments will migrate out of the nuclei toward the anode, resulting in a comet-like shape. DNA damage can be qualified by the percentage DNA that migrates out of the nuclei and forms the tail of the comet. Different types of DNA damage can be visualized depending on the protocol used. While exposure of DNA to high alkali prior to electrophoresis allows for the preferential detection of single strand breaks, the neutral comet assay is used primarily for the detection of double strand breaks (Fairbairn et al., 1995). This technique has been used for several plant species to study DNA damage and repair in normal plant developmental situations (Koppen et al., 1999; Koppen & Verschaeve, 2001) but also under various stress conditions (Koppen et al., 1998; Menke et al., 2001; Ptacek et al., 2002; Mancini et al., 2006; Vandenhove et al., 2006).

While DNA damage can be generated by environmental stressors such as heat, chemicals and ionizing radiation, it can also suffer spontaneous and metabolically induced damage. To protect plants against genomic deficiencies, various cellular DNA repair mechanisms work together. To investigate the importance of the DNA repair machinery under uranium stress, several genes, essential during DNA repair, were studied on transcriptional level. *AtKU80* and *AtLIG4* for example, are required for the initiation and completion of the non-homologous end joining pathway for the repair of double strand breaks and are sensitive to ionizing radiation as was reported by Friesner & Britt (2003). For the homologous recombination pathway to repair double strand breaks, *AtRAD51* and *AtDMC1* are important genes of which *AtRAD51* was shown to be sensitive to ionizing radiation as reported by Doutriaux et al. (1998). Beside genes directly related to double strand break repair, several genes are important in the

regulation of the cell cycle and the induction of signaling pathways under normal metabolic conditions and stress situations (De Veylder et al., 2001a, 2001b; Pierrugues et al., 2001; Mori et al., 2005).

This study aimed to investigate the induction of DNA damage and the importance of DNA damage and repair related gene expression following exposure of *Arabidopsis thaliana* seedlings to 0, 0.1, 1, 10 and 100 µM uranium for 1, 3 and 7 days.

7.2 Materials and methods

7.2.1 Plant culture and uranium exposure

Seeds of *Arabidopsis thaliana* (Columbia ecotype) were placed on moist filter paper at 4 °C for 3 days to synchronize germination. Afterwards, seeds were sown on plugs from 1.5 ml polyethylene centrifuge tubes filled with 2 % agar (Difco). The plugs were positioned in a PVC cover capable of holding 81 plugs. The PVC cover was then placed on a container filled with 2.9 l of a modified Hoagland solution (macro-elements without phosphate: 1/10 diluted, phosphate solution: 1/20 diluted, micro-elements: 1/10 diluted and iron solution: 1/10 diluted). Plants were grown in a growth chamber (Microclima 1000E, Snijders Scientific B.V.) under a 14 h photoperiod (photosynthetic photon flux density of 200 µmol m^{-2} s^{-1} at the leaf level, supplied by Sylvania BriteGro F36WT8/2084 and F36WT8/2023), with day/night temperatures of 22 °C/18 °C and 65 % relative humidity. Roots were aerated during the entire course of the experiment.

Subsequently, 17-day-old seedlings were exposed to 0, 0.1, 1, 10 and 100 µM uranium for 1, 3 and 7 days. Uranium was added as $UO_2(NO_3)_2.6H_2O$ (Sigma) to the modified Hoagland solution and the pH was adjusted to ± 5.5 with NaOH. As previous experiments recommended the use of 25 µM phosphate in combination with uranium, a 1/80 diluted phosphate solution was used (Vanhoudt et al., 2008).

At harvest, ± 100 mg samples of leaves and roots were snap frozen in liquid nitrogen and stored at -80 °C.

7.2.2 Neutral comet assay

The neutral comet assay was carried out on the isolated nuclei of *Arabidopsis thaliana* leaves and roots. Therefore, each sample of ± 100 mg was chopped in 300 µl of ice cold PBS extraction buffer, containing 10 ml PBS10x (Dulbecco's Phosphate Buffered Saline 10x solution Sigma), 0.5 ml 200 mM Na_2EDTA and 89.5 ml water, using a razor blade and a small petri dish on ice. After filtration through an 80 µm nylon sieve, 20 µl of the filtrate was mixed with 300 µl 0.8 % low-melting-point (LMP) agarose (Sigma) in phosphate buffered saline at 40 °C. The mixture was layered on a microscope slide, pre-coated with 100 µl of 0.5 % LMP agarose in phosphate buffered saline, by using a cover slip, and put on ice for 20 min to allow solidification. After removing the cover slips, the slides were put for at least 30 min in a lysis solution containing 100 ml of the TBE working solution and 2.5 g sodium dodecyl sulfate (SDS) (Sigma). The TBE working solution contains 5.40 g TRIS, 2.75 g boric acid and 1,85 g Na_2EDTA for 1 l. Subsequently, the slides were rinsed in ice cold TBE solution for at least 5 min for the removal of soap. Then the slides were placed in a horizontal electrophoresis chamber filled with the TBE solution followed by electrophoresis for 2 min at 1 V/cm. After electrophoresis, the slides were rinsed in cold distilled water for at least 10 min an allowed to air dry. All steps were performed under yellow light. The slides were then stained for 5 min with 100 µl of 10 µg/ml propidium iodide using a cover slide to spread the solution evenly. The slides were then washed again by adding 100 µl water and spreading with a cover slide. The comets were viewed with a Leitz BM-RBE fluorescence microscope (200x or 400x) using an excitation filter of 515-560 nm. Measurements of the comets were done with equipped image analysis system Komet 3.1 (Kinetic Imaging, Liverpool, England). Fifty comets per biological replicate were analyzed and for each treatment 3 biological replicates were used. The percentage of migrated DNA in the tail was used as an indicator for DNA damage.

7.2.3 Gene expression analysis

Frozen plant tissue (± 100 mg) was ground thoroughly in liquid nitrogen using a mortar and pestle. RNA was extracted using the RNeasy Plant Mini Kit (Qiagen). The RNA quantity was determined spectrophotometrically at 260 nm (Nanodrop, Isogen Life Science). The RNA quality was checked electrophoretically using the

Bioanalyzer (Agilent Technologies). Before cDNA synthesis, the RNA sample was incubated during 2 minutes in gDNA wipeout buffer at 42 °C in order to effectively eliminate genomic DNA. First strand cDNA synthesis was primed with a combination of oligo(dT)-primers and random hexamers according to the manufacturer's instructions using the QuantiTect Reverse Transcription Kit (Qiagen) and equal amounts of starting material were used (1 µg). Quantitative real time PCR was performed with the 7500 Fast Real-Time PCR System (Applied Biosystems), using Sybr Green® chemistry. Primers used for gene expression analyses were designed using Primer Express® (Applied Biosystems) and are given in table 7.1. PCR amplifications were performed in a total volume of 10 µl containing 2.5 µl cDNA sample, 5 µl Fast Sybr Green® Master Mix (Applied Biosystems), 0.3 µl forward primer, 0.3 µl reverse primer and 1.9 µl RNase-free H_2O.

Table 7.1 - Forward and reverse primers used in gene expression analysis

Gene	Forward primer	Reverse primer
At2g28390	AACTCTATGCAGCATTTGATCCACT	TGATTGCATATCTTTATCGCCATC
At5g08290	TTACTGTTTCGGTTGTTCTCCATTT	CACTGAATCATGTTCGAAGCAAGT
At5g15710	TTTCGGCTGAGAGGTTCGAGT	GATTCCAAGACGTAAAGCAGATCAA
CKS1	CACGTCGTTCTTCCTCCTGAAG	TCCTATCGCTCGCCATTCG
DMC1	ATGAAGACGAAGATCTATTTGAGATGATT	CTTGTAGCTTTTTCACATCTCCTGC
GAR1	CTAAGATGGTTGGTGATGCAAGAGA	CGCTAAGCTCATCCAAACCCTT
KRP2	GGAATAAGTTGTTGGAATGTTCTATGAAGT	AACCCACTCGTATCTTCCTCCAC
KU80	CTTCTTCCAGCACAACTCCTCAA	CTACGCATCGCAGGACCTACAT
LIG4	TGATGTATCGG ATATCAAGGGCA	GAATGGGACCGAGGCACG
LPP1	TCACTTTCTGATGACAATAGGGTCG	CCTCTCTGCGCCTCCTGG
MND1	GAACGAGATGGTACAATTTGCTGA	CCGACTGGTGAGCAACTTCAAT
PARP1	TGCATTGGGAGAAATACATGAGC	CCGAGCCCTTTGGTCGAG
PARP2	ATCGGAGGTGATTGATCGGTATG	AAATCATGAGGTATCACTGTGTAGAACTCT
POLG1	GAAACTGGACGCTTATCGGCTAG	CTGACGGATTTTGTACCGATCTTT
RAD51	GTCCAACAACAAGACGATGAAGAA	AACAGAAGCAATACCTGCTGCC
UBQ10	GGCCTTGTATAATCCCTGATGAATAAG	AAAGAGATAACAGGAACGGAAACATAGT

Gene expression data were normalized against multiple housekeeping genes (*At2g28390*, *At5g08290*, *At5g15710*, *UBQ10*) according to Vandesompele et al. (2002) and represented relative to the control treatment (untreated leaves or roots after 1 day).

7.2.4 Statistical analysis

Statistical analyses on the data obtained by the comet test were performed using a linear mixed model with pair wise comparisons adjusted by the Tukey procedure.

For gene expression, statistical analyses were performed using an ANOVA test in SAS 9.1 (Neter et al., 1996). The ANOVA test was carried out separately for leaves and roots. Mean values of treatments were compared using Tukey's multiple comparison test and transformations were applied when necessary to approximate the assumptions of normality and same error variance.

7.3 Results and discussion

7.3.1 Neutral single cell gel electrophoresis assay or comet assay

The neutral comet assay was used to visualize and determine uranium induced DNA double strand breaks in *Arabidopsis thaliana* leaves and roots. Here fore, the percentage DNA that migrated out of the nuclei, forming the comets tail, was used to quantify DNA damage. For leaves no significant differences were observed in the % tail DNA (figure 7.1A), indicating uranium, or ROS produced under uranium stress, did not cause an increase in DNA double strand breaks in the leaves. This could probably be explained by the low root-to-shoot transfer factor for uranium, resulting in only a small amount of uranium in the leaves as was reported in chapter 4. For the roots on the other hand, the % tail DNA was significantly lower at day 1 than at day 3 and day 7 for all the uranium concentrations combined (figure 7.1B), indicating an increase in double strand breaks with increasing time. The % tail DNA was also significantly lower after exposure to 100 µM uranium for all the harvesting times combined in comparison with the other uranium concentrations (figure 7.1B). After exposure to the highest uranium concentration, DNA was completely dispersed, explaining the decrease in % tail DNA. The DNA damage in the roots could be induced directly by uranium presence, but also indirectly by ROS produced as response mechanism under uranium stress.

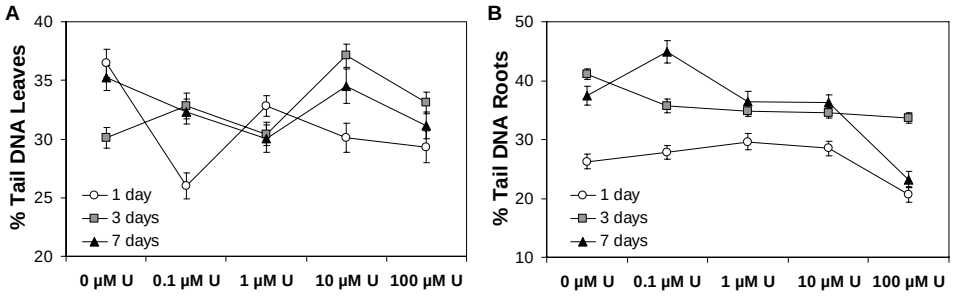

Figure 7.1 - DNA integrity (% tail DNA) of leaves (A) and roots (B) of *Arabidopsis thaliana* seedlings exposed for 1, 3 and 7 days to a uranium concentration range was analyzed with the neutral comet assay. Each data point represents the mean of 3 biological replicates ± S.E. and for each biological replicate 50 comets were analyzed, giving an average of 150 comets per data point.

These results are in accordance with Vandenhove et al. (2006), who also reported no effects on *Phaseolus vulgaris* shoots after exposure to 0.1-1000 µM uranium and for roots no increased DNA migration was observed up to 100 µM uranium while after exposure to 1000 µM uranium, DNA was also completely dispersed.

7.3.2 Gene expression of DNA damage and repair related genes

To study uranium induced DNA damage and the induction of the DNA repair cycle, expression levels of several genes related to DNA damage and repair were investigated.

While damage of the cellular genetic material can arise from exposure to DNA damaging agents such as ROS, ionizing radiation or chemicals, it can also be induced from normal cell metabolism during DNA replication and repair. One or both strands of the DNA double helix can be damaged but while a single strand break can be repaired using the complementary strand, no template is available for the repair of a double strand break. The failure to repair a double strand break can cause chromosomal aberrations. Therefore all organisms possess multiple pathways to repair DNA breaks.

Double strand breaks can be repaired by 2 distinct pathways being non-homologous recombination and homologous recombination. Non-homologous recombination is a straightforward and simple pathway that rejoins the ends of the break. Consequently it is an inaccurate process in which a DNA sequence is often deleted or inserted resulting in a loss of genetic information. Within double

strand repair by non-homologous recombination, the non-homologous end joining is the most dominant pathway in plants in contrast to the micro-homology mediated end joining. This process generally involves rejoining of blunt end or ends with short overhangs and begins with recognition of the juxtaposition of the broken ends. In mammalian cells, this step is promoted by the DNA dependent protein kinase (DNA-PK), a complex composed of the KU heterodimer, which in turn is composed of 70-86 kDa subunits (Ku70 and Ku80), and the DNA-PK catalytic subunit. It is suggested that KU is involved in the recognition and protection of double strand break ends and that it can form a bridge between the two ends of a break contributing to their juxtaposition. Subsequently the Artemis protein is involved in the maturation of the double strand break ends and the Xrcc4/DNA ligase IV complex catalyses the ligation of the broken ends (Bleuyard et al., 2006). Bleuyard et al. (2006) reviewed that inactivation of *AtKU70*, *AtKU80* or *AtLIG4* in *Arabidopsis thaliana* plants results in hypersensitivity to double strand breaks inducing reagents, furthermore the absence of the AtKu80 protein strongly reduces the efficiency of non-homologous end joining in an *in vivo* plasmid based end joining assay. As also Friesner & Britt (2003) reported an important role for *AtKU80* and *AtLIG4* required for the initiation and completion of the non-homologous end joining pathway in the repair of double strand breaks under ionizing radiation stress, *AtKU80* and *AtLIG4* gene expression was analyzed in this study to evaluate their importance under uranium stress (tables 7.2 & 7.3). For *KU80*, no alterations were observed in leaves or roots following uranium exposure. *LIG4* on the other hand was significantly down regulated in roots after exposure for 3 days to 100 µM uranium but no alterations were observed in leaves.

Homologous recombination involves extensive DNA sequence homology between the interacting molecules and due to this homologous template, homologous recombination is generally a more accurate pathway that ensures the repair of double strand breaks without any loss of genetic information in most cases. After double strand breaks are formed, single strand DNA is generated by nucleases near the breaks. Recombinases such as *RAD51* then form a Rad51/ssDNA nucleofilament which can invade a homologous DNA double strand molecule to serve as template to repair double strand breaks making it a conservative pathway. While *AtRAD51* can be induced both by ionizing radiation

and in meiosis, *DMC1* is a meiotic-specific protein related to *RAD51*. Although expression of the *AtDMC1* gene is specific to tissues undergoing meiosis, it is also expressed in *Arabidopsis* cell culture in a cell cycle related manner as was reviewed by Bleuyard et al. (2006). Doutriaux et al. (1998) reported an expression of *AtRAD51* and *AtDMC1* in *Arabidopsis thaliana* flower buds and mitotically active cells from a suspension culture but only transcript levels of *AtRAD51* were increased after gamma irradiation of the cells. While only minor effects were observed for *AtRAD51* expression levels following uranium exposure in our study (tables 7.2 & 7.3), *AtDMC1* expression was significantly up-regulated in roots following 3 days exposure to 100 µM uranium (table 7.3).

To further unravel the mechanisms of double strand break repair in plants, Domenichini et al. (2006) characterized the function of the *Arabidopsis Mnd1* homologue (*AtMnd1*) which is required for meiotic DNA repair and it may also function in double strand break repair in somatic cells as its expression levels are strongly induced by gamma radiation. Only minor alterations were observed in *AtMND1* gene expression in *Arabidopsis thaliana* leaves (table 7.2) and roots (table 7.3) following uranium exposure except for a significant up-regulation in the leaves following 7 days exposure to 100 µM uranium.

Mori et al. (2005) reported that *AtPolI-like B* expression, a DNA polymerase located in the plastids and mitochondria, could be induced by exposure to hydrogen peroxide. This suggested that *AtPolI-like B* has a role in the repair of oxidation induced DNA damage in the plastids. We identified this gene as the *AtPOLG1* (polymerase gamma 1) in the *Arabidopsis thaliana* database but no alterations were observed in expression levels in uranium exposed leaves or roots (tables 7.2 & 7.3).

Doucet-Chabeaud et al. (2001) isolated AtPARP1, a protein that is highly homologous to the vertebrate poly(ADP-ribose) polymerase (PARP1). PARP1 has an important function in cell recovery from DNA damage induced by ionizing radiation due to its role in base excision repair (BER). PARP1 is a nuclear protein which, when bound to DNA strand breaks, catalyses the formation of branched polymers of poly(ADP-ribose) using NAD^+ as substrate which are transferred to a limited number of protein acceptors involved in modulating chromatin architecture or in DNA metabolism. Besides the AtPARP1 protein, Doucet-

Chabeaud et al. (2001) also identified the *AtPARP2* gene. They reported that ionizing radiation induced DNA strand breaks caused an accumulation of *AtPARP1* and *AtPARP2* transcript levels, whereas dehydration and cadmium exposure induced the accumulation of *AtPARP2* transcript levels indicating a general role for plant *PARP2* in the response to oxidative stress, while the *AtPARP1* gene is more specifically activated by DNA strand breaks. This also suggests that the quality of damage is important for specific *PARP* gene induction in *Arabidopsis thaliana* and that *AtPARP2* rather than *AtPARP1* may be implicated in additional signaling processes that are independent of DNA damage. Analyses of gene expression levels of *AtPARP1* and *AtPARP2* in *Arabidopsis thaliana* following uranium exposure showed only minor alterations in *AtPARP1* expression in roots (table 7.3) and no differences in leaves (table 7.2). While *AtPARP2* fluctuated for leaves (table 7.2), a significant increased was observed in roots (table 7.3) exposed for 3 days to 0.1, 1 and 10 µM uranium.

Pierrugues et al. (2001) isolated an *Arabidopsis thaliana* gene *AtLPP1*, encoding for a lipid phosphate phosphatase enzyme, that was transiently induced by ionizing radiation and other stress responses. Phospholipids are major structural components of cell membranes and can serve as reservoir for several lipid-signaling molecules. Molecules such as phosphatidate, diacylglycerol and diacylglycerol pyrophosphate are products of lipid metabolism that serve roles as second messengers in several signal transduction pathways. These signaling pathways may be partly regulated by lipid phosphate phosphatase enzymes under stress situations. While in our study no alterations were observed in *AtLPP1* expression levels in leaves (table 7.2), *AtLPP1* transcript levels were significantly up-regulated in roots after exposure to 100 µM uranium for 1 day (table 7.3) indicating an early signaling pathway could have been triggered.

Besides genes directly related to double strand break repair, this study also investigated different genes related to the cell cycle which could be affected in order to allow DNA repair. De Veylder et al. (2001a) reported that over-expression of *AtCKS1* in *Arabidopsis thaliana* is shown to reduce leaf size and root growth rates. The reduction in root growth was due to an increase in the cell-cycle duration that was associated by extension of both G1 and G2 phases. Deveaux et al. (2000) isolated the *AtGAR1* (*Arabidopsis thaliana* gamma response 1) gene that is expressed in mitotically active tissues and

endoreduplicating tissues from unstressed plants and that is similar in some respects to the expression profile of *AtCKS1*. They also indicated a potential role for *AtGAR1* in the response to genotoxic stress by blocking mitotic cell division in irradiated cells and thus preventing premature entry into mitosis before completion of DNA repair. De Veylder et al. (2001b) reported that KRP2, a cyclin dependent kinase inhibitor, exerts a plant growth inhibitory activity by reducing cell proliferation in leaves but it may not control the timing of cell cycle exit and differentiation. In our study, *AtCKS1* expression levels were significantly up-regulated in *Arabidopsis thaliana* leaves after exposure for 7 days to 100 µM uranium (table 7.2) while for the roots transcript levels were already significantly increased after 3 and 7 days exposure to 100 µM uranium (table 7.3). Only minor alterations were observed in *AtGAR1* gene expression in *Arabidopsis thaliana* leaves and roots after uranium exposure (tables 7.2 & 7.3). *AtKRP2* expression levels decreased significantly for leaves and roots exposed for 3 days to 10 and 100 µM uranium (tables 7.2 & 7.3).

7.3.3 Conclusions

As uranium was applied to the roots and due to the very small root-to-shoot transfer factor, effects were mostly visible in the roots. By usage of the neutral comet assay and analysis of the % tail DNA, it was shown that DNA damage generally increased in time. After exposure to 100 µM uranium DNA seemed completely dispersed in roots. Besides some alterations in expression levels after 100 µM uranium, genes important for DNA repair and the cell cycle remained mostly unaffected by lower uranium concentrations. It can therefore be concluded that 100 µM uranium can induce DNA damage and alterations in the repair machinery but further research is necessary to unravel how the different pathways collaborate in the defense against uranium stress.

Table 7.2 – Gene expression of DNA damage and repair related genes in leaves of *Arabidopsis thaliana* seedlings exposed for 1, 3 and 7 days to 0.1, 1, 10 and 100 µM U.

			0 µM U	0.1 µM U	1 µM U	10 µM U	100 µM U
Non-homologous recombination	*KU80*	*1 d*	1.00±0.34^{a}	1.05±0.50^{a}	0.42±0.26^{a}	2.90±0.83^{a}	1.54±0.63^{a}
		3 d	0.76±0.23^{a}	1.63±0.16^{a}	1.28±0.42^{a}	1.07±0.10^{a}	0.80±0.26^{a}
		7 d	0.82±0.50^{a}	0.62±0.28^{a}	0.80±0.18^{a}	0.82±0.40^{a}	1.39±0.28^{a}
	LIG4	*1 d*	1.00±0.33^{a}	1.17±0.27^{a}	1.06±0.43^{a}	1.66±0.07^{a}	1.51±0.31^{a}
		3 d	1.66±0.29^{a}	2.07±0.06^{a}	1.52±0.41^{a}	2.23±0.11^{a}	1.57±0.22^{a}
		7 d	1.64±0.46^{a}	1.28±0.50^{a}	2.42±0.08^{a}	1.26±0.61^{a}	1.73±0.26^{a}
Homologous recombination	*RAD51*	*1 d*	1.00±0.36^{ab}	0.98±0.42^{ab}	0.36±0.19^{a}	2.24±0.59^{b}	0.56±0.25^{ab}
		3 d	0.65±0.17^{a}	0.97±0.05^{a}	0.76±0.28^{a}	0.65±0.10^{a}	0.41±0.11^{a}
		7 d	0.28±0.13^{a}	0.21±0.08^{a}	0.37±0.08^{a}	0.37±0.18^{a}	0.34±0.09^{a}
	DMC1	*1 d*	1.00±0.25^{a}	0.77±0.20^{a}	0.41±0.21^{a}	1.97±0.64^{a}	0.81±0.35^{a}
		3 d	0.50±0.07^{a}	0.73±0.07^{a}	0.77±0.21^{a}	0.63±0.05^{a}	0.47±0.10^{a}
		7 d	0.31±0.13^{a}	0.28±0.07^{a}	0.39±0.09^{a}	0.38±0.18^{a}	0.39±0.03^{a}
DSB repair	*MND1*	*1 d*	1.00±0.07^{ab}	0.57±0.07^{ab}	0.36±0.10^{a}	1.30±0.37^{b}	0.58±0.18^{ab}
		3 d	0.47±0.08^{a}	0.42±0.03^{a}	0.51±0.03^{a}	0.47±0.06^{a}	0.62±0.12^{a}
		7 d	0.36±0.09^{ab}	0.23±0.03^{a}	0.32±0.07^{ab}	0.60±0.07^{b}	1.05±0.08^{c}
Poly-merase	*POLG1*	*1 d*	1.00±0.20^{a}	1.19±0.20^{a}	0.83±0.26^{a}	1.26±0.06^{a}	0.75±0.16^{a}
		3 d	1.25±0.05^{a}	1.53±0.21^{a}	0.85±0.18^{a}	1.21±0.04^{a}	1.04±0.19^{a}
		7 d	1.27±0.08^{a}	0.60±0.19^{a}	1.07±0.01^{a}	0.79±0.37^{a}	1.31±0.24^{a}
BER	*PARP1*	*1 d*	1.00±0.03^{a}	0.80±0.16^{a}	0.38±0.06^{a}	1.29±0.34^{a}	0.68±0.19^{a}
		3 d	0.42±0.05^{a}	0.59±0.06^{a}	0.43±0.10^{a}	0.33±0.04^{a}	0.26±0.09^{a}
		7 d	0.30±0.06^{a}	0.33±0.03^{a}	0.24±0.05^{a}	0.35±0.06^{a}	0.37±0.09^{a}
Signaling	*PARP2*	*1 d*	1.00±0.11^{ab}	0.76±0.14^{ab}	0.41±0.14^{a}	1.86±0.44^{b}	0.62±0.22^{a}
		3 d	0.37±0.05^{a}	0.72±0.07^{a}	0.70±0.17^{a}	0.52±0.05^{a}	0.36±0.10^{a}
		7 d	0.24±0.08^{a}	0.21±0.05^{a}	0.31±0.10^{a}	0.37±0.14^{a}	0.31±0.01^{a}
	LPP1	*1 d*	1.00±0.29^{a}	1.43±0.34^{a}	1.52±0.70^{a}	2.34±0.31^{a}	2.00±0.37^{a}
		3 d	3.46±1.01^{a}	3.29±0.39^{a}	3.07±1.21^{a}	1.92±0.09^{a}	1.16±0.32^{a}
		7 d	12.10±4.82^{a}	1.83±0.52^{a}	21.12±9.41^{a}	1.83±0.82^{a}	3.90±2.69^{a}
Cell cycle regulation	*CKS1*	*1 d*	1.00±0.09^{a}	0.92±0.14^{a}	0.85±0.19^{a}	1.14±0.07^{a}	0.94±0.06^{a}
		3 d	1.31±0.02^{a}	1.05±0.10^{a}	1.35±0.27^{a}	1.57±0.07^{a}	1.69±0.08^{a}
		7 d	1.01±0.16^{a}	0.69±0.23^{a}	1.21±0.07^{a}	0.91±0.29^{a}	2.39±0.19^{b}
	GAR1	*1 d*	1.00±0.25^{ab}	0.75±0.21^{ab}	0.37±0.16^{a}	1.82±0.52^{b}	0.47±0.20^{ab}
		3 d	0.57±0.12^{ab}	0.62±0.02^{ab}	0.70±0.14^{a}	0.55±0.09^{ab}	0.18±0.06^{b}
		7 d	0.39±0.21^{a}	0.19±0.06^{a}	0.24±0.06^{a}	0.26±0.12^{a}	0.24±0.06^{a}
	KRP2	*1 d*	1.00±0.09^{a}	0.71±0.15^{a}	0.32±0.07^{a}	1.18±0.31^{a}	0.69±0.24^{a}
		3 d	0.67±0.06^{a}	0.59±0.04^{ab}	0.48±0.10^{ab}	0.35±0.05^{b}	0.34±0.06^{b}
		7 d	0.57±0.20^{a}	0.54±0.05^{a}	0.31±0.10^{a}	0.49±0.11^{a}	0.59±0.08^{a}

Data are expressed relative to the control treatment and represent the mean of 3 biological replicates ± S.E. Different small letters indicate significant differences between the treatments for day 1, day 3 and day 7 separately ($p < 0.05$).

Table 7.3 – Gene expression of DNA damage and repair related genes in roots of *Arabidopsis thaliana* seedlings exposed for 1, 3 and 7 days to 0.1, 1, 10 and 100 µM U.

			0 µM U	0.1 µM U	1 µM U	10 µM U	100 µM U
Non-homologous recombination	*KU80*	*1 d*	1.00±0.11^{A}	0.92±0.23^{A}	0.57±0.18^{A}	2.64±1.80^{A}	1.23±0.39^{A}
		3 d	1.33±0.18^{AB}	2.05±0.23^{A}	1.34±0.22^{AB}	1.50±0.04^{AB}	1.15±0.07^{B}
		7 d	0.43±0.03^{A}	1.00±0.35^{A}	0.90±0.08^{A}	0.39±0.15^{A}	0.71*
	LIG4	*1 d*	1.00±0.04^{A}	0.92±0.16^{A}	0.72±0.03^{A}	0.68±0.30^{A}	0.68±0.13^{A}
		3 d	1.08±0.04^{A}	1.15±0.08^{A}	1.13±0.11^{A}	1.21±0.03^{A}	0.53±0.07^{B}
		7 d	0.60±0.01^{A}	0.66±0.34^{A}	0.64±0.07^{A}	0.47±0.20^{A}	0.27±0.12^{A}
Homologous recombination	*RAD51*	*1 d*	1.00±0.08^{A}	0.93±0.19^{A}	0.70±0.21^{A}	2.80±1.79^{A}	0.62±0.17^{A}
		3 d	1.67±0.14^{A}	1.90±0.18^{A}	1.43±0.16^{A}	2.14±0.11^{A}	1.82±0.15^{A}
		7 d	0.40±0.04^{A}	0.92±0.29^{A}	1.27±0.27^{A}	0.50±0.06^{A}	0.89*
	DMC1	*1 d*	1.00±0.12^{A}	0.76±0.10^{A}	0.63±0.20^{A}	1.70±1.01^{A}	0.41±0.14^{A}
		3 d	1.26±0.14^{AB}	1.20±0.13^{AB}	0.96±0.12^{AB}	1.10±0.06^{AB}	1.66±0.08^{AB}
		7 d	0.50±0.06^{A}	0.63±0.12^{A}	0.93±0.21^{A}	0.36±0.15^{A}	0.64*
DSB repair	*MND1*	*1 d*	1.00±0.10^{A}	0.83±0.07^{A}	0.65±0.21^{A}	1.96±0.88^{A}	0.63±0.12^{A}
		3 d	1.03±0.10^{AB}	1.12±0.07^{AB}	0.95±0.03^{A}	1.27±0.17^{AB}	1.67±0.23^{B}
		7 d	0.79±0.06^{AB}	0.56±0.20^{A}	1.37±0.18^{B}	0.92±0.14^{AB}	1.21*
Poly-merase	*POLG1*	*1 d*	1.00±0.11^{A}	1.07±0.14^{A}	0.92±0.03^{A}	0.86±0.26^{A}	0.66±0.03^{A}
		3 d	0.97±0.08^{A}	1.03±0.11^{A}	0.96±0.06^{A}	0.97±0.05^{A}	1.27±0.06^{A}
		7 d	0.47±0.09^{A}	0.62±0.09^{A}	0.62±0.09^{A}	0.43±0.20^{A}	0.88±0.40^{A}
BER	*PARP1*	*1 d*	1.00±0.15^{A}	0.86±0.08^{A}	0.63±0.20^{A}	1.81±0.72^{A}	0.47±0.06^{A}
		3 d	0.94±0.03^{A}	1.20±0.08^{B}	0.90±0.05^{A}	1.06±0.06^{AB}	1.01±0.03^{AB}
		7 d	0.49±0.05^{A}	0.44±0.20^{A}	0.92±0.10^{A}	0.40±0.10^{A}	0.73*
Signaling	*PARP2*	*1 d*	1.00±0.14^{A}	0.80±0.14^{A}	0.83±0.23^{A}	2.47±1.30^{A}	0.14±0.03^{A}
		3 d	0.85±0.09^{A}	1.34±0.07^{B}	1.33±0.09^{B}	1.70±0.03^{C}	0.59±0.04^{A}
		7 d	0.71±0.05^{A}	0.61±0.30^{A}	1.43±0.12^{A}	0.63±0.22^{A}	0.46*
	LPP1	*1 d*	1.00±0.13^{A}	1.20±0.28^{A}	0.95±0.03^{A}	1.00±0.37^{A}	2.24±0.04^{B}
		3 d	1.19±0.14^{A}	1.10±0.24^{A}	1.55±0.23^{A}	1.59±0.10^{A}	1.55±0.20^{A}
		7 d	0.91±0.18^{A}	1.86±0.65^{A}	1.04±0.19^{A}	0.78±0.25^{A}	0.87±0.44^{A}
Cell cycle regulation	*CKS1*	*1 d*	1.00±0.05^{A}	0.99±0.13^{A}	1.01±0.10^{AB}	1.06±0.24^{AB}	1.75±0.21^{B}
		3 d	1.01±0.03^{A}	1.16±0.04^{AB}	1.22±0.09^{AB}	1.22±0.08^{AB}	1.36±0.02^{B}
		7 d	0.76±0.06^{A}	0.76±0.35^{A}	0.90±0.14^{A}	0.64±0.30^{A}	0.74±0.20^{A}
	GAR1	*1 d*	1.00±0.11^{A}	0.93±0.15^{A}	0.73±0.20^{A}	2.59±1.68^{A}	0.54±0.18^{A}
		3 d	1.34±0.10^{A}	1.44±0.08^{A}	1.04±0.04^{A}	1.29±0.06^{A}	1.30±0.14^{A}
		7 d	0.42±0.05^{A}	0.39±0.18^{A}	0.89±0.14^{A}	1.00±0.52^{A}	0.74*
	KRP2	*1 d*	1.00±0.14^{A}	0.68±0.04^{A}	0.65±0.19^{A}	1.43±0.56^{A}	0.22±0.02^{A}
		3 d	0.82±0.03^{A}	0.85±0.08^{A}	0.62±0.09^{AB}	0.49±0.03^{B}	0.36±0.01^{B}
		7 d	0.40±0.07^{A}	0.32±0.02^{A}	0.56±0.07^{A}	0.27±0.12^{A}	0.26*

Data are expressed relative to the control treatment and represent the mean of 3 biological replicates ± S.E. Different capital letters indicate significant differences between the treatments for day 1, day 3 and day 7 separately ($p < 0.05$). * One biological replicate.

Chapter 8

Biological effects and oxidative stress related responses induced in *Arabidopsis thaliana* following exposure to uranium and cadmium

Vanhoudt N., Vandenhove H., Horemans N., Wannijn J., Bujanic A., Vangronsveld J. & Cuypers A. (2009) Biological effects and oxidative stress related responses induced in *Arabidopsis thaliana* following exposure to uranium and cadmium. *In preparation*.

Abstract

At contaminated sites, uranium always occurs in combination with other stressors such as heavy metals or radionuclides. Previous studies have already indicated that toxicity effects in a multiple stressor situation can differ from the individually induced effects. When aiming to better evaluate the environmental uranium impact, this multiple stressor context should not be neglected. In this study, toxicity effects in plants of uranium in a binary pollution condition were investigated by studying biological responses and unraveling oxidative stress related mechanisms in *Arabidopsis thaliana* seedlings, grown on hydroponics and exposed for 3 days to 10 µM uranium in combination with 5 µM cadmium. While uranium mostly accumulated in the roots with very low root-to-shoot transport, cadmium was less taken up by the roots but with higher translocation to the shoots. Under mixed exposure, cadmium highly influenced uranium uptake but not the other way round resulting in a doubled uranium concentration in the roots. Under our mixed exposure conditions, it is clear that micronutrient concentrations in the roots are strongly influenced by addition of cadmium as a second stressor, while leaf macronutrient concentrations are mostly influenced by uranium. Oxidative stress related responses on the other hand are highly affected by cadmium while uranium influence is more limited. Hereby, an important role was attributed to the ascorbate redox balance together with glutathione as both metabolites, but more explicitly for ascorbate, increased their reduced form, indicating an important defense and regulatory function. While for roots, based on an increase in *FSD1* gene expression, oxidative stress was suggested to be superoxide induced, in leaves on the other hand, hydrogen peroxide related genes were mostly altered.

8.1 Introduction

As primordial radionuclide and heavy metal, uranium can be found naturally in all environmental matrices with soil concentrations of 0.3-11.7 mg kg^{-1} and ground and surface water concentrations of 3×10^{-3}-2 µg l^{-1} (Bleise et al., 2003). Uranium can be redistributed due to various anthropogenic activities such as the mining, processing and waste storage of uranium containing ores and minerals and as an important waste product in the phosphate industry, causing uranium contamination at several industrial sites throughout the world (Vandenhove, 2002). At these polluted areas uranium always occurs in combination with other radioactive elements such as ^{232}Th and ^{226}Ra and non-radioactive contaminants such as cadmium, zinc and copper. Information on uranium toxicity effects in plants is rather scant but previous studies already described important uranium toxicity effects on growth, development and plant nutrition and suggested an important role for the cellular redox balance as a modulator under uranium stress (Charles et al., 2006; Vandenhove et al., 2006; Vanhoudt et al., 2008). But as previous studies already indicated that effects induced in a multiple stressor situation can markedly deviate from the individually induced effects (Chaoui et al., 1997; Charles et al., 2006; Mittler, 2006) and when aiming to evaluate uranium toxicity effects in an environmentally more relevant situation, this multiple pollution context should not be neglected and uranium induced effects also need to be studied in a multiple stressor situation.

Cadmium is a heavy metal omnipresent in the environment with an average concentration of 0.2 mg kg^{-1} in the earth's crust and < 0.1 µg l^{-1} in river water. It is an element associated with several ores and it can occur as an impurity in phosphate minerals. Cadmium induced effects in plants are well documented and besides studies reporting cadmium induced morphological and physiological alterations, oxidative stress is also suggested as an important modulator under cadmium stress (Semane et al., 2007; Van Belleghem et al., 2007; Smeets et al., 2008; Hasan et al., 2009).

An early oxidative burst, characterized by an elevated ROS production, can be one of the first stress response mechanisms in plant cells, potentially being an alarm signal to alert plant metabolism and gene expression for possible

modifications (Foyer et al., 1994). Herewith, plasma membrane related NADPH oxidases, together with apoplastic superoxide dismutase (SOD), are an important source of oxidative burst related superoxide and hydrogen peroxide production (Dat et al., 2000; Bhattacharjee, 2005). Reactive oxygen species (ROS) can interact with various macromolecules causing important cellular damage such as lipid peroxidation and interfere with normal cell metabolism. Besides being directly induced by ROS, lipid peroxidation can also be initiated by lipoxygenases (LOX) which are known to initiate the formation of oxylipins that can function as signaling molecules under stress situations (Porta & Rocha-Sosa, 2002). In addition, although ROS are toxic byproducts of aerobic metabolism and hence produced under normal circumstances, a role as signaling molecules has been ascribed to ROS. They are involved in the regulation of biological processes such as development and defense pathways and multiple studies demonstrate their enhanced production under stress conditions (Dat et al., 2000; Mittler et al., 2004).

To protect plant cells against ROS induced damage but to allow signaling functions, plants dispose of several enzymes and metabolites making up the antioxidative defense system. SOD's, catalyzing the conversion of superoxide into hydrogen peroxide, together with hydrogen peroxide scavenging enzymes such as catalases (CAT) and peroxidases (PX) and the ascorbate-glutathione pathway with its specific enzymes and metabolites, are known to hold important functions under uranium, cadmium and other heavy metal stress (Weckx & Clijsters, 1996; Cuypers et al., 2001; Smeets et al., 2005; Razinger et al., 2008; Vanhoudt et al., 2008).

This study aimed to further evaluate the impact of uranium on the environment in a binary pollution situation by studying biological responses and unraveling oxidative stress related mechanisms in *Arabidopsis thaliana* plants exposed to uranium in combination with cadmium.

8.2 Materials and methods

8.2.1 Plant culture and uranium-cadmium contamination

Arabidopsis thaliana seeds (Columbia ecotype) were spread on moist filter paper at 4 °C for 3 days to synchronize germination. Subsequently, the seeds were sown on plugs from 1.5 ml polyethylene centrifuge tubes filled with 2 % agar (Difco). The plugs were positioned in a PVC cover capable of holding 36 plugs. Next, the cover was placed on a container filled with 1.35 l of a modified Hoagland solution (macro elements without phosphate: 1/10 diluted, phosphate solution: 1/20 diluted, micro elements: 1/10 diluted and iron solution: 1/10 diluted). Plants were grown in a growth chamber (Microclima 1000E, Snijders Scientific B.V.) under a 14 h photoperiod (photosynthetic photon flux density of 200 µmol m^{-2} s^{-1} at the leaf level, supplied by Sylvania BriteGro F36WT8/2084 and F36WT8/2023), with day/night temperatures of 22 °C/18 °C and 65 % relative humidity.

Subsequently, 17-day-old plants were exposed for 3 days to 10 µM uranium, 5 µM cadmium or a combination of 10 µM uranium with 5 µM cadmium. These concentrations were chosen to induce moderate effects on growth, nutrition and oxidative stress related responses as identified from previous studies (chapter 4-6; Smeets et al., 2008). Uranium was added to the nutrient solution as $UO_2(NO_3)_2.6H_2O$ (Sigma) and cadmium as $3CdSO_4.8H_2O$ (Merck). For all the treatments, a modified Hoagland solution was used with 1/80 phosphate solution as suggested by Vanhoudt et al. (2008).

8.2.2 Plant sampling and biometric measurements

Leaves and roots were harvested separately as ± 100 mg samples, snap frozen in liquid nitrogen and stored at -80 °C. Fresh weight of leaves and roots was determined for at least 20 biological replicates.

Samples for nutrient and heavy metal analyses were dried for 1 week at 70 °C. Leaves were rinsed with distilled water and roots were washed twice for 10 min with 1 mM $Pb(NO_3)_2$ at 4 °C and once for 10 min with distilled water. At least 5 biological replicates were harvested for element determinations.

8.2.3 Nutrient, uranium and cadmium concentrations

After dry-ashing using a muffle furnace, dried plant material was digested in 0.1 M HCl for determination of several nutrients, uranium and cadmium. Copper, iron, manganese, zinc, uranium and cadmium concentrations were determined using inductively coupled plasma mass spectrometry (ICP-MS, Perkin-Elmer, Elan 5000 using a cross flow nebulizer and a ryton spray chamber). Standards for copper, iron, manganese, zinc and cadmium were prepared shortly before analysis from 1000 g l^{-1} elemental standards (Spex Certiprep) by sequential dilution with 18.2 MΩ water from a water purification system (MilliQ water from Millipore) and nitric acid (65 %, pro analyse grade, VWR). Calibration curves for uranium were obtained using uranium standard solutions (0-10 µg l^{-1}) prepared from the elemental standard SPEX solution (SPEX Industries Inc.). A specific activity of 12436 Bg g^{-1} for ^{238}U was considered (Joint Evaluated File (JEF) version 2.2, OECD/NEA Data Bank, Paris, France). The concentrations of calcium, potassium and magnesium were determined using suppressed ion chromatography (HPIC, Dionex, ICS-2500 using a CS12-A cation exchange column with guard column, a CSRS-UltraII self-regenerating suppressor and an ED50A electrochemical detector). Standards for the elements were prepared shortly before analysis from 1000 g l^{-1} ion chromatography standards (Fluka) by sequential dilution with 18.2 MΩ water (MilliQ water from Millipore).

8.2.4 Lipid peroxidation

Thiobarbituric acid (TBA) reactive compounds (mainly malondialdehyde) were used as measure of lipid peroxidation in *Arabidopsis thaliana* leaves. Leaf tissue (± 100 mg) was homogenized with 2 ml 0.1 % TCA (trichloroacetic acid) using a mortar and pestle. After centrifugation for 10 min at 20000 × g, 0.5 ml of the supernatant was added to 2 ml 0.5 % TBA. This mixture was heated for 30 min at 95 °C and quickly cooled in an ice bath. After centrifugation for 10 min at 20000 × g, the absorbance of the supernatant was measured spectro-photometrically at 532 nm and corrected for unspecific absorbance at 600 nm according to Dhindsa et al. (1981).

8.2.5 Enzyme capacities

Frozen leaf or root tissue (± 100 mg) was homogenized in ice cold 0.1 M Tris-HCl buffer (pH 7.8) containing 1 mM EDTA, 1 mM dithiotreitol and 4 % insoluble polyvinylpyrrolidone (2 ml buffer 100 mg^{-1} FW) using a mortar and pestle. The homogenate was squeezed through a nylon mesh and centrifuged at 20000 × g and 4 °C for 10 min. The enzyme capacities, *i.e.* potential activity measured in vitro under non-limiting reaction conditions, were measured spectrophotometrically in the supernatant at 25 °C.

Guaiacol peroxidase (GPX) and syringaldazine peroxidase (SPX) capacities were measured at 436 nm and 530 nm according to Bergmeyer et al. (1974) and Imberty et al. (1984) respectively. Ascorbate peroxidase (APX) capacity was measured at 298 nm following the method of Gerbling et al. (1984). Analysis of superoxide dismutase (SOD) capacity was based on the inhibition of cytochrome c at 550 nm according to McCord & Fridovich (1969). Analysis of the capacities of glutathione reductase (GR) and catalase (CAT) were performed as described by Bergmeyer et al. (1974).

8.2.6 Gene expression analyses

Frozen leaf or root tissue (± 100 mg) was ground thoroughly in liquid nitrogen using a mortar and pestle. RNA was extracted using the RNeasy Plant Mini Kit (Qiagen). The RNA quantity was determined spectrophotometrically at 260 nm (Nanodrop, Isogen Life Science). The RNA quality was checked electrophoretically using the Bioanalyzer (Agilent Technologies). Before cDNA synthesis, the RNA sample was incubated during 2 minutes in gDNA wipeout buffer at 42 °C in order to effectively eliminate genomic DNA. First strand cDNA synthesis was primed with a combination of oligo(dT)-primers and random hexamers according to the manufacturer's instructions using the QuantiTect Reverse Transcription Kit (Qiagen) and equal amounts of starting material were used (1 µg). Quantitative Real-Time PCR was performed with the 7500 Fast Real-Time PCR System (Applied Biosystems), using Sybr Green® chemistry. Primers used for gene expression analyses are given in table 8.1. PCR amplifications were performed in a total volume of 10 µl containing 2.5 µl cDNA

sample, 5 µl Fast Sybr Green® Master Mix (Applied Biosystems), 0.3 µl forward primer, 0.3 µl reverse primer and 1.9 µl RNase-free H_2O.

Gene expression data were normalized against multiple housekeeping genes (*At2g28390*, *At5g08290*, *At5g15710*, *UBQ10*) according to Vandesompele et al. (2002) and presented relative to the control treatment.

Table 8.1 - Forward and reverse primers used in gene expression analysis

Gene	Forward primer	Reverse primer
At2g28390	AACTCTATGCAGCATTTGATCCACT	TGATTGCATATCTTTATCGCCATC
At5g08290	TTACTGTTTCGGTTGTTCTCCATTT	CACTGAATCATGTTCGAAGCAAGT
At5g15710	TTTCGGCTGAGAGGTTCGAGT	GATTCCAAGACGTAAAGCAGATCAA
APX1	TGCCACAAGGATAGGTCTGG	CCTTCCTTCTCTCCGCTCAA
CAT1	AAGTGCTTCATCGGGAAGGA	CTTCAACAAAACGCTTCACGA
CAT2	AACTCCTCCATGACCGTTGGA	TCCGTTCCCTGTCGAAATTG
CAT3	TCTCCAACAACATCTCTTCCCTCA	GTGAAATTAGCAACCTTCTCGATCA
CSD1	TCCATGCAGACCCTGATGAC	CCTGGAGACCAATGATGCC
CSD2	GAGCCTTTGTGGTTCACGAG	CACACCACATGCCAATCTCC
CSD3	GTTGTTGTGCATGCGGATCC	CACATCCAACTCTCGAGCCTG
FSD1	CTCCCAATGCTGTGAATCCC	TGGTCTTCGGTTCTGGAAGTC
FSD2	TTGGAAAGGTTCAAGTCGGCT	CATTTGCAACGTCAAGTCTATTCG
FSD3	AACGGGAATCCTTTACCCGA	TGTCTCCACCACCAGGTTGC
GR1	CTCAAGTGTGGAGCAACCAAAG	ATGCGTCTGGTCACACTGC
MSD1	ATGTTTGGGAGCACGCCTAC	AACCTCGCTTGCATATTTCCA
LOX1	TTGGCTAAGGCTTTTGTCGG	GTGGCAATCACAAACGGTTC
LOX2	TTTGCTCGCCAGACACTTG	GGGATCACCATAAACGGCC
RBOHC	TCACCAGAGACTGGCACAATAAA	GATGCTCGACCTGAATGCTC
RBOHD	TATGCATCGGAGAGGCTGCT	TAGAGACAACACGTTCCCGGG
RBOHF	GGTGTCATGAACGAAGTTGCA	AATGAGAGCAGAACGAGCATCA
UBQ10	GGCCTTGTATAATCCCTGATGAATAAG	AAAGAGATAACAGGAACGGAAACATAGT

8.2.7 Metabolite concentrations

Ascorbate and glutathione concentrations in *Arabidopsis thaliana* roots were determined by HPLC analysis. Therefore approximately 100 mg tissue was ground thoroughly in liquid nitrogen using a pre-cooled mortar and pestle. When a homogenous powder was obtained, 1 ml of ice cold 6 % (w/v) meta-phosphoric acid was added and the mixture was clarified by centrifugation at 20000 × g and 4 °C for 10 minutes. The resulting supernatant was kept frozen until HPLC analysis. Antioxidants were separated on a 100 mm × 4.6 mm Polaris

C18-A reversed phase HPLC column (3 µm particle size, 30 °C, Varian, CA USA) with an isocratic flow of 1 ml min^{-1} of the elution buffer (25 mM K/PO_4-buffer, pH 3.0). The components were quantified using a home-made electrochemical detector with glassy carbon electrode and a Scott pt 62 reference electrode (Mainz, Germany). The purity and identity of the peaks were confirmed using a diode array detector (SPD-M10AVP, Shimadzu, Hertogenbosch, Netherlands) which was placed on line with the electrochemical detector. The concentrations of oxidized DHA (dehydroascorbate) or GSSG (glutathione disulphide) were measured indirectly as the difference between the total concentration of antioxidants in a DTT (dithiothreitol) reduced fraction and the concentration in a sample prior to reduction. Reduction of the sample was obtained by incubation of an aliquot of the extract in 400 mM Tris and 200 mM DTT for 15 minutes in the dark. The pH of this mixture was checked to be between 6.0 and 7.0. After 15 minutes, the pH was lowered again by 4-fold dilution in elution buffer prior to HPLC analysis.

8.2.8 Statistical analyses

Statistical analyses were performed using an ANOVA test in SAS 9.1 (Neter et al., 1996). The ANOVA test was performed separately for leaves and roots. Mean values for the different treatments were compared using Tukey's multiple comparison tests. Transformations were applied when necessary to approximate the assumptions of normality and same error variance. Data presented are mean values ± standard error (S.E.).

8.3 Results and discussion

As previous studies indicated that effects induced by single stressors can differ markedly with those induced under mixed exposure conditions (Charles et al., 2006; Mittler, 2006), the influence of a second contaminant on uranium induced toxicity effects and response mechanisms in plants was investigated in this study. Therefore, 17-day-old *Arabidopsis thaliana* seedlings were exposed for 3 days to 10 µM uranium, 5 µM cadmium or simultaneously to both stressors. While in general toxicity effects were visible under both heavy metals applied, a

distinction can be made between nutrient composition induced effects and oxidative stress related responses for the metal inducing the effects.

8.3.1 Growth responses and nutrient profile

At the concentrations applied and exposure time studied, leaf growth remained unaffected by heavy metal exposure while in roots very small alterations were already visible. While the single stressors did not reduce root growth, root fresh weight was significantly decreased for plants exposed to both stressors in comparison with the uranium exposed plants (figure 8.1).

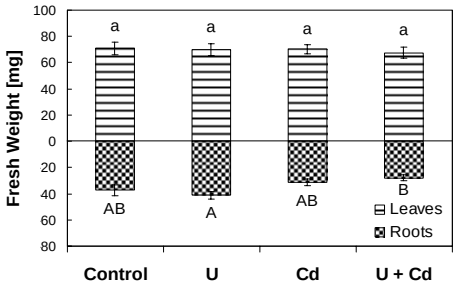

Figure 8.1 - Fresh weight of leaves and roots of *Arabidopsis thaliana* seedlings exposed for 3 days to 10 µM uranium, 5 µM cadmium or a combination of both. Data represent the mean ± S.E. of 20 biological replicates. Different letters indicate significant differences in fresh weight between the treatments for leaves and roots separate ($p < 0.05$).

As a measure for membrane damage induced directly by heavy metal presence or indirectly by ROS, the amount of TBA reactive compounds was determined in *Arabidopsis thaliana* leaves but no alterations were observed between the different treatments (results not shown). Previously described results indicate that heavy metal exposed *Arabidopsis thaliana* leaves remain unaffected at morphological level and seem to cope well these first 3 days following exposure to the applied heavy metal concentrations. Roots are directly exposed to high concentrations of the heavy metals applied and hence toxicity effects are already seen in roots after 3 days of exposure to a combination of uranium and cadmium. Although we assumed to see already minor root growth reduction effects for the applied single stressor concentrations (chapter 4-6; Van Belleghem et al., 2007; Smeets et al., 2008), 10 µM uranium and 5 µM cadmium were probably borderline to induce any macroscopic effects after 3

days. Three days exposure to both stressors simultaneously on the other hand showed a discrete start of growth reduction (figure 8.1).

When applied as a single stressor, uranium was readily taken up from the nutrient solution but mostly retained in the roots as the root-to-shoot transfer factor was very low (table 8.2 & 8.3). This was in general agreement with previous studies which reported that uranium mainly accumulates in the roots with limited transfer to the shoots even though differences in uranium uptake and distribution are plant species and age dependent (Shahandeh & Hossner, 2002; Singh et al., 2005; Vandenhove et al., 2006; Vanhoudt et al., 2008). Ebbs et al. (1998) reported that the uranyl ion, generally among the most abundant uranium species around pH 5.5, is the form most readily taken up and transferred to the shoots by plants and can compete with Ca^{2+} and Mg^{2+} for their binding sites (Nieboer & Richardson, 1980). Cadmium as a single stressor on the other hand was less taken up by the roots than uranium, but was, due to a higher root-to-shoot transfer factor, more present in the shoots than uranium (table 8.2 & 8.3). Cadmium also accumulated more in the roots as compared to the shoots which is in general agreement with other studies (Hernández et al., 1996; Zhu et al., 2004; Smeets et al., 2008). Cadmium is known to be easily transported within plants in the form of metallo-organic complexes but the mechanisms are complex as was reviewed by Hasan et al. (2009). When uranium exposed plants were simultaneously exposed to cadmium, a boost in uranium uptake by the roots was observed as its concentration almost doubled which was also observed in the leaves (table 8.2 & 8.3). Cadmium concentrations in the mixed exposed plants remained unchanged as compared to the single stressor exposed plants (table 8.2 & 8.3). An et al. (2004) reported that the bioaccumulation of a single metal (cadmium, copper or lead) in *Cucumus sativus* was influenced by the presence of other metals resulting in inhibited or enhanced bioaccumulation of one metal in the mixture, but the bioaccumulation pattern in mixtures was not always consistent with plant growth responses. In our study it is shown that cadmium influences uranium uptake but not the other way round. Although the mechanism by which these heavy metals interfere is unknown, we hypothesized that this interesting observation could be due to an alteration in uranium speciation, following application of cadmium. It was found that addition of cadmiumsulfate may induce subtle increases in the

pH of the nutrient medium (Horemans & Raeymaekers, personal communication). We hypothesize that a subtle increase in cadmium induced pH can enhance the uranium concentration in the roots as previously shown by Ebbs et al. (1998).

Table 8.2 – Nutrient, uranium and cadmium concentrations in roots of 17-day-old *Arabidopsis thaliana* seedlings exposed for 3 days to 10 µM uranium, 5 µM cadmium or a combination of both (U + Cd).

		ROOTS			
		Control	**Uranium**	**Cadmium**	**U + Cd**
[mg g^{-1} DW]	*Ca*	0.65±0.22^{A}	1.64±0.29^{B}	1.32±0.14^{B}	1.79±0.27^{B}
	K	6.48±0.58^{A}	6.24±0.51^{A}	5.52±0.83^{A}	8.29±1.10^{A}
	Mg	1.48±0.17^{A}	1.35±0.05^{A}	1.41±0.06^{A}	1.21±0.04^{A}
[µg g^{-1} DW]	*Cu*	7.05±0.47^{A}	9.46±0.24^{B}	20.22±1.17^{C}	14.55±0.33^{D}
	Fe	1368.0±66.0^{A}	1480.7±46.3^{A}	1937.1±86.9^{B}	1823.6±26.2^{B}
	Mn	289.16±13.10^{A}	315.74±18.86^{A}	15.47±1.07^{B}	32.09±1.41^{C}
	Zn	97.63±4.34^{A}	109.67±4.99^{AB}	125.13±6.51^{B}	91.80±3.24^{A}
	U	n.d.	5950.0±136.8^{A}	1.00±0.05^{B}	10679.1±705.9^{C}
	Cd	19.05±9.30^{A}	n.d.	937.8±41.2^{B}	855.4±19.7^{B}

Data represent the mean ± S.E. of 5 biological replicates. Different letters indicate significant differences between the treatments ($p < 0.05$).

Table 8.3 – Nutrient, uranium and cadmium concentrations in leaves of 17-day-old *Arabidopsis thaliana* seedlings exposed for 3 days to 10 µM uranium, 5 µM cadmium or a combination of both (U + Cd).

		LEAVES			
		Control	**Uranium**	**Cadmium**	**U + Cd**
[mg g^{-1} DW]	*Ca*	25.01±1.10^{a}	29.24±1.05^{b}	25.29±0.77^{a}	31.01±1.09^{b}
	K	27.17±1.04^{a}	30.99±0.61^{b}	31.32±0.85^{b}	33.58±0.24^{b}
	Mg	6.36±0.24^{a}	7.25±0.21^{bc}	6.66±0.27^{ab}	8.07±0.26^{c}
[µg g^{-1} DW]	*Cu*	6.10±0.15^{a}	5.26±0.27^{a}	6.12±0.27^{a}	6.08±0.46^{a}
	Mn	56.94±2.92^{a}	50.61±1.37^{ab}	47.07±0.78^{b}	49.83±1.20^{b}
	Zn	32.74±2.87^{a}	30.32±0.99^{a}	29.13±0.43^{a}	33.53±0.94^{a}
	U	n.d.	1.11±0.18^{a}	n.d.	2.99±0.14^{b}
	Cd	n.d.	n.d.	138.2±17.9^{a}	253.7±47.2^{a}

Data represent the mean ± S.E. of 5 biological replicates. Different letters indicate significant differences between the treatments ($p < 0.05$).

Uranium, cadmium and other heavy metals are known to compete with the uptake via transmembrane carriers and transport of essential nutrients in plants thereby disturbing their mineral nutrition (Hernández et al. 1996; Das et al., 1997; di Toppi & Gabbrielli, 1999). Therefore concentrations of several macro- and micronutrients were determined for all treatments. Although no alterations

in potassium and magnesium concentrations in *Arabidopsis thaliana* roots were noticed, calcium uptake seemed to be stimulated by single heavy metal presence as all treatments caused a significant enhancement in calcium concentrations (table 8.2). The latter observation was in agreement with a previous study for uranium by Sela et al. (1988), showing an increased calcium concentration in uranium exposed *Azolla* roots and a cadmium study by Smeets et al. (2008) reporting a cadmium induced calcium increase in *Arabidopsis thaliana* roots. When uranium exposed roots were simultaneously exposed to cadmium, the enhanced calcium concentration was similar with the one observed for uranium or cadmium as single stressors (table 8.2). Minor alterations in the root micronutrients were observed for zinc- and iron concentrations that increased following cadmium exposure, which was found again for iron in the mixed stressor exposed roots (table 8.2). Copper was already significantly increased after uranium exposure but was much more elevated following cadmium exposure. The rise in uranium induced copper content was further stimulated by simultaneous exposure to cadmium, although the level of increase caused by the latter contaminant applied as a single stressor could not be reached (table 8.2). While no alterations were observed in manganese concentrations following uranium exposure, cadmium presence caused a large fall back in manganese content which could be found again under the mixed exposure condition (table 8.2). The latter observation was in agreement with Hernández et al. (1996) who observed a cadmium induced manganese decrease in *Pisum sativum* roots exposed for 15 days to 1.5-6.0 mg l^{-1} cadmium. In general in the roots, at the level of macronutrients, the mixed exposure used in this study did not influence their contents in comparison with exposure to the single stressors. Concerning the micronutrient concentrations, they are strongly influenced by the addition of cadmium as a second stressor, especially manganese or even uranium itself.

The alterations observed in nutrient concentrations in the leaves are only minor and although uranium is less represented than cadmium in the leaves, responses are mostly influenced by uranium. This can be illustrated by an observed increase in calcium and magnesium concentrations following uranium exposure that was again found under mixed exposure conditions (table 8.3). The increase in calcium concentrations can be correlated with the observed increase

in the roots. Despite the large decrease observed in manganese concentrations in the roots following cadmium and mixed exposure, only a minor decrease in manganese content was observed for the leaves (table 8.3). While Smeets et al. (2008) reported significant decreases in nutrient concentrations in *Arabidopsis thaliana* leaves following exposure to 20 µM cadmium for 1 day, possibly indicating that cadmium affects xylem loading and 20 µM cadmium is highly toxic, exposure to lower cadmium concentrations did not affect the nutrient profile in *Arabidopsis thaliana* leaves as is in correspondence with our results.

8.3.2 Oxidative stress related responses

Capacities of several enzymes related to the antioxidative defense system in plant cells were analyzed to investigate their importance under binary heavy metal stress. In general, almost no alterations were observed in enzyme capacities for SOD, CAT, SPX, GPX and GR in uranium and cadmium exposed *Arabidopsis thaliana* leaves and roots (table 8.4). Therefore, it can be concluded that at the metal concentrations applied and exposure time used, plants cope well under heavy metal presence and do not show signs of oxidative stress on the protein level of the enzymatic antioxidative defense mechanism.

Table 8.4 - Antioxidative enzyme capacities [U g^{-1} FW] in leaves and roots of 17-day-old *Arabidopsis thaliana* seedlings exposed for 3 days to 10 µM uranium, 5 µM cadmium or a combination of both stressors (U + Cd)

		Enzyme capacity [U g^{-1} FW]					
		APX	*CAT*	*GPX*	*GR*	*SOD*	*SPX*
LEAVES	**Control**	23.0±2.1^{a}	0.70±0.04^{ab}	1.85±0.16^{a}	1.99±0.08^{a}	66.5±5.9^{a}	2.90±0.49^{a}
	Uranium	28.7±1.2^{a}	0.77±0.04^{b}	1.55±0.13^{a}	2.27±0.15^{a}	64.8±6.5^{a}	2.02±0.30^{a}
	Cadmium	26.4±1.5^{a}	0.58±0.04^{a}	1.94±0.35^{a}	1.68±0.23^{a}	92.1±5.4^{a}	3.46±0.60^{a}
	U + Cd	23.8±1.3^{a}	0.58±0.02^{a}	1.54±0.15^{a}	2.03±0.13^{a}	76.7±9.3^{a}	2.86±0.52^{a}
ROOTS	**Control**	3.4±0.4^{A}	0.14±0.02^{A}	22.6±2.6^{A}	0.48±0.07^{A}	66.8±4.1^{A}	12.2±1.2^{A}
	Uranium	3.9±0.6^{A}	0.16±0.01^{A}	26.2±2.1^{A}	0.55±0.08^{A}	73.5±7.4^{A}	12.9±2.8^{A}
	Cadmium	14.7±2.0^{B}	0.17±0.01^{A}	30.0±3.5^{A}	0.64±0.10^{A}	69.2±9.7^{A}	11.6±3.2^{A}
	U + Cd	7.5±2.4^{AB}	0.18±0.01^{A}	32.6±3.5^{A}	0.72±0.07^{A}	74.9±9.3^{A}	14.2±2.7^{A}

Data represent the mean ± S.E. of 5 biological replicates. Different letters indicate significant differences between the treatments for leaves (small letters) and roots (capital letters) ($p < 0.05$).

The only indication to assume a moderate distress is the observed significant enhancement in APX capacity in the roots following cadmium exposure that also

causes a small, yet not significant, increase in APX capacity in the roots after mixed exposure (table 8.4). In addition, ascorbate and glutathione concentrations were determined to further unravel the role of the ascorbate-glutathione pathway under mixed contamination. These results are in accordance with the APX capacities as in roots the total ascorbate concentration significantly increased after cadmium and mixed exposure conditions. This increase was due to a significant increase of reduced ascorbate and a steady state level of the oxidized form (table 8.5). These results show that the ascorbate redox balance can be maintained and increased in roots under cadmium stress indicating that roots are fully able to react and defend themselves against cadmium induced oxidative stress. Cadmium, applied in a single or mixed exposure context, caused also in the leaves a significant increase in reduced ascorbate, together with a significant decrease in the oxidized form, but with no alterations in the total ascorbate pool (table 8.5). As also here the ascorbate redox balance can be maintained or increased, these results also support a positive situation in which leaves are able to activate the antioxidative defense system in response to cadmium stress.

Table 8.5 - Ascorbate and glutathione concentrations [nmol g^{-1} FW] in leaves and roots of *Arabidopsis thaliana* seedlings exposed for 3 days to 10 µM uranium, 5 µM cadmium or a combination of both

		Control	**Uranium**	**Cadmium**	**U + Cd**
LEAVES	*AsA + DHA*	4211±317^{a}	4819±407^{a}	4109±187^{a}	4925±169^{a}
	AsA	1210±115^{a}	1636±107^{a}	2951±75^{b}	3760±141^{c}
	DHA	3001±260^{a}	3068±470^{a}	1158±199^{b}	1164±70^{b}
	GSH + GSSG	431±16^{a}	615±60^{b}	396±16^{a}	497±15^{ab}
	GSH	318±9^{ab}	385±25^{a}	272±11^{b}	365±20^{a}
	GSSG	113±23^{a}	230±72^{a}	123±24^{a}	133±14^{a}
ROOTS	*AsA + DHA*	638±44^{A}	558±67^{A}	1018±37^{B}	983±66^{B}
	AsA	539±36^{A}	398±54^{A}	885±45^{B}	815±62^{B}
	DHA	99±23^{A}	160±16^{A}	132±23^{A}	168±10^{A}
	GSH + GSSG	85±10^{A}	65±9^{A}	62±5^{A}	73±6^{A}
	GSH	24±6^{AB}	14±3^{A}	29±4^{AB}	37±1^{B}
	GSSG	61±10^{A}	51±8^{A}	33±3^{A}	37±6^{A}

The total ascorbate concentration represents the reduced and oxidized forms (AsA: ascorbic acid = reduced form; DHA: dehydroascorbate = oxidized form). The total glutathione concentration also represents the reduced and oxidized forms (GSH: glutathione = reduced form; GSSG: glutathione disulphide = oxidized form). Data represent the mean ± S.E. of 5 biological replicates and different letters indicate significant differences between the treatments for each metabolite separately ($p < 0.05$).

While for glutathione concentrations no alterations were observed in the roots, a decrease in GSH concentration was observed in cadmium exposed leaves probably used for the complexation of cadmium (table 8.5) as was also suggested by Semane et al. (2007). As uranium exposure caused an enhancement in the total glutathione concentration, the glutathione pool was probably sufficient for cadmium complexation under mixed conditions, explaining GSH concentrations under mixed exposure remained unaltered (table 8.5). Results for the metabolite concentrations are in accordance with various previous studies that also attribute an important role for the ascorbate-glutathione pathway under cadmium and other heavy metal stress. Cuypers et al. (2000) for instance also reported an increase of the ascorbate pool and maintenance in its reduced form in *Phaseolus vulgaris* leaves at the beginning of the 50 µM copper treatment. For *Phaseolus vulgaris* seedlings exposed to 50 µM zinc, Cuypers et al. (2001) reported an increase in the total ascorbate pool in leaves while in roots an overall oxidation of ascorbate occurred immediately after zinc treatment. Although previous studies already indicated an important role for the ascorbate redox balance in *Arabidopsis thaliana* leaves under uranium exposure (chapter 6), results indicate that during mixed exposure conditions used in our study, cadmium is the most important activator of the ascorbate-glutathione pathway as cellular regulatory and defense mechanism.

Besides analyzing the importance of the antioxidative defense system on protein level, we were interested in unraveling alterations occurring at transcriptional level. Therefore, gene expression levels of some ROS producing enzymes (lipoxygenases *LOX1/2* and NADPH oxidases *RBOHC/D/F*), together with several SOD and CAT isoforms (copper zinc SODs *CSD1/2/3*, iron SODs *FSD1/2/3*, manganese SOD *MSD1* and catalases *CAT1/2/3*) and enzymes of the ascorbate-glutathione cycle (ascorbate peroxidase *APX1* and glutathione reductase *GR1*), were analyzed in roots (figure 8.2) and leaves (figure 8.3). In general, on transcriptional level, and in accordance with protein and metabolite levels, toxicity effects under mixed exposure conditions used in our study were again mostly influenced by cadmium.

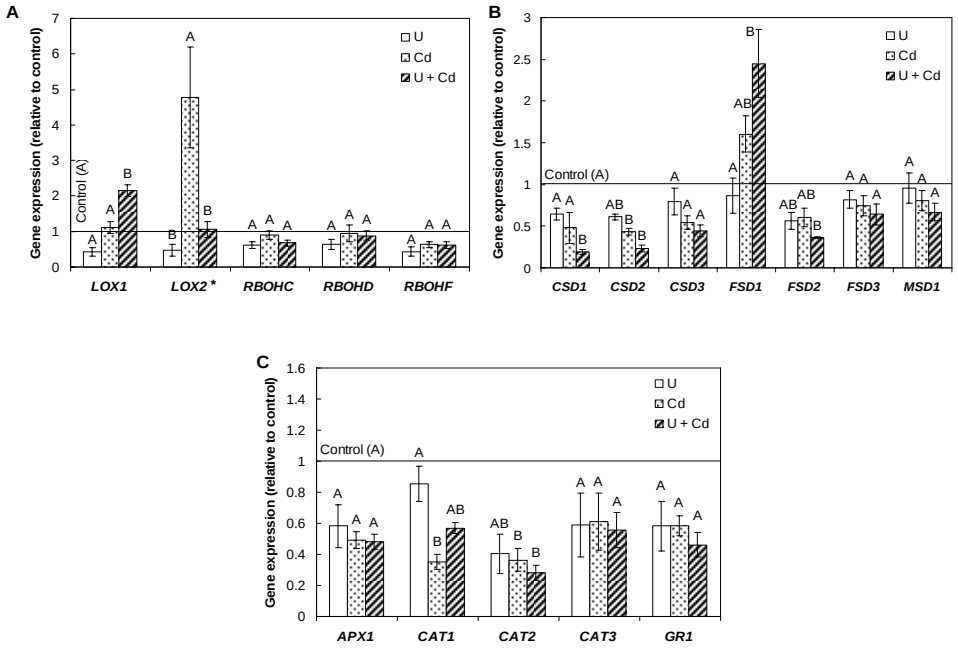

Figure 8.2 - Gene expression levels for *Arabidopsis thaliana* roots exposed for 3 days to 10 µM uranium, 5 µM cadmium or a combination of both. Transcript levels were determined for ROS-producing enzymes (A), $O_2^{\bullet-}$ scavenging enzymes (SOD isoforms) (B) and H_2O_2 scavenging enzymes and enzymes related to the ascorbate-glutathione pathway (C). Transcript levels are expressed relative to the control treatment and represent the mean ± S.E. of 4 biological replicates. Different letters indicate significant differences between the treatments for each gene separately ($p < 0.05$). *The statistical identification letter for the control treatment of *LOX2* is AB.

In *Arabidopsis thaliana* roots, *LOX1* transcript levels were significantly up-regulated under uranium and cadmium mixed exposure (figure 8.2A). This could indicate that an increase in lipid peroxidation can be expected, resulting in membrane damage but also resulting in more precursors for signaling molecules such as jasmonates. A strong increase in *LOX1* transcript levels in 1 day cadmium exposed *Arabidopsis thaliana* roots was reported by Smeets et al. (2008). When investigating gene expression of several SOD isoforms, located at various cellular compartments, a decrease in *CSD2* transcript levels in the roots was present under cadmium and mixed exposure which was again in accordance with Smeets et al. (2008) and other previous cadmium experiments (Cuypers, personal communication). For SOD isoforms in general, a significant decrease was observed for *CSD1*, *CSD2* and *FSD2* transcript levels after mixed exposure while a significant increase for *FSD1* transcript levels was present following

mixed exposure (figure 8.2B). The latter observation was also in accordance with Smeets et al. (2008) who reported a significant up regulation of *FSD1* transcript levels in cadmium exposed *Arabidopsis thaliana* roots. The increase in *FSD1* expression can, as superoxide scavenger, indicate an enhanced superoxide induced oxidative stress level in the roots. As in enzyme activity no change in total SOD capacity was observed, the increase in *FSD1* could compensate for the decrease in *CSD1*, *CSD2* and *FSD2* transcript levels. While a significant decrease in *CAT1* following cadmium exposure and *CAT2* following cadmium and mixed exposure was observed, gene expression of *CAT3*, *APX1* and *GR1* remained unaltered in heavy metal exposed roots (figure 8.2C). The *CAT2* down regulation was shown to be an initial step in producing an elevated hydrogen peroxide level in the regulatory mechanism during senescence (Zimmermann et al., 2006) indicating cadmium can induce early senescence as was suggested by Cuypers et al. (submitted).

For *Arabidopsis thaliana* leaves in general, transcript levels for all genes studied and most treatments were down regulated (figure 8.3). When considering the ROS producing enzymes, lipoxygenases (*LOX1/2*), initiating lipid peroxidation and forming precursors of signaling molecules, were down regulated for all treatments and for different NADPH oxidase isoforms (*RBOHC/D/F*), related to an early oxidative burst, transcript levels of *RBOHD* were significantly decreased following all treatments (figure 8.3A). In contrast to the present results, an early oxidative burst was seen in *Arabidopsis thaliana* seedlings exposed to cadmium for 24 hours (Smeets et al., 2008). The significantly down-regulation of *CSD1* and *CSD2* transcript levels in leaves after uranium and cadmium exposure (figure 8.3B) was also observed in previous experiments (chapter 6; Smeets et al., 2008). This decrease was even more pronounced after exposure to the combination of uranium and cadmium (figure 8.3B). These results together with the decrease in expression levels for other SOD isoforms suggest oxidative stress caused by cadmium or uranium is probably not due to superoxide in the leaves. Concerning the gene expression of hydrogen peroxide scavenging enzymes (figure 8.3C), the transcript levels were all down-regulated under cadmium and binary exposure. This observation is in accordance with the decrease in the DHA/AsA ratio under cadmium and binary exposure (table 8.5).

Under these circumstances, the antioxidative capacity of the leaves is sufficient to cope with the induced stress.

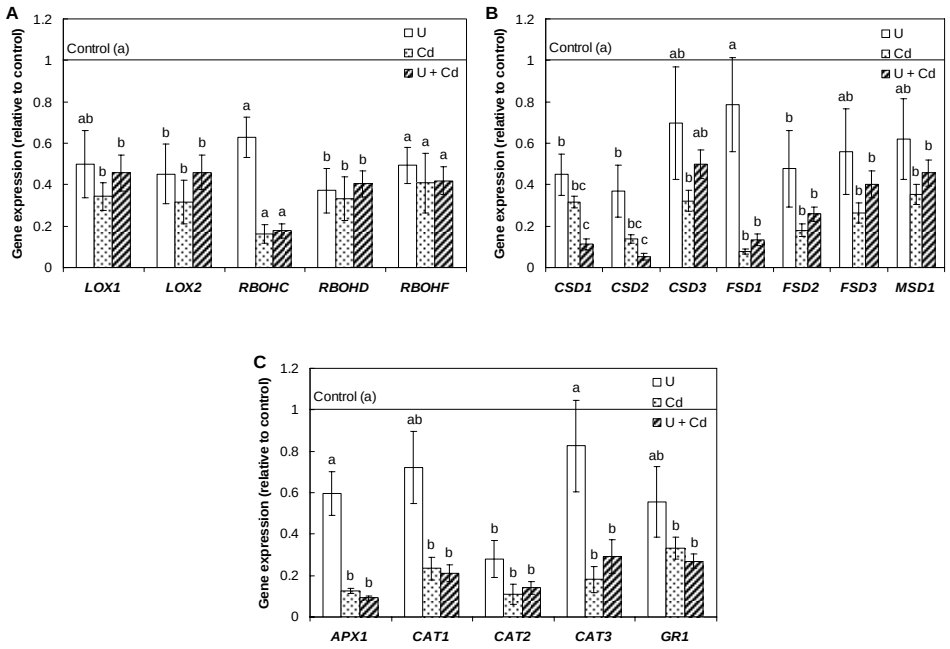

Figure 8.3 - Transcript levels for *Arabidopsis thaliana* leaves exposed for 3 days to 10 µM uranium, 5 µM cadmium or a combination of both. Gene expression levels were determined for ROS-producing enzymes (A), $O_2^{\bullet-}$ scavenging enzymes (SOD isoforms) (B) and H_2O_2 scavenging enzymes and enzymes related to the ascorbate-glutathione pathway (C) and expressed relative to the control treatment. Values represent the mean ± S.E. of 4 biological replicates. Different letters indicate significant differences between the treatments for each gene separately ($p < 0.05$).

8.3.3 Conclusions

When both stressors, uranium and cadmium, are simultaneously applied, cadmium highly influences uranium uptake but not the other way round. Under the mixed exposure conditions used in this study, it is clear that micronutrient concentrations in the roots are strongly influenced by addition of cadmium as a second stressor, while leaf macronutrient concentrations are mostly influenced by uranium.

Oxidative stress related responses under our mixed exposure conditions, are highly affected by cadmium while uranium influence is more limited. The decrease in the DHA/AsA ratio, similar as under cadmium presence, indicated that *Arabidopsis thaliana* seedlings were able to maintain their cellular redox

balance and defend themselves against the induced stress. While for roots, oxidative stress was suggested to be superoxide induced, in leaves on the other hand, hydrogen peroxide related genes were mostly altered.

The observed effects suggest that heavy metals influence each other on an additive, antagonistic or synergetic manner, but further research is needed to identify these responses.

Chapter 9

The combined effect of uranium and gamma radiation on biological responses and oxidative stress induced in *Arabidopsis thaliana*

Vanhoudt N., Vandenhove H., Horemans N., Wannijn J., Van Hees M., Vangronsveld J. & Cuypers A. (2009) The combined effect of uranium and gamma radiation on biological responses and oxidative stress induced in *Arabidopsis thaliana*. *In preparation.*

Abstract

To evaluate the combined effect of uranium and gamma radiation on growth, nutrient uptake and oxidative stress, 18-day-old *Arabidopsis thaliana* seedlings were exposed for 3 days to 10 µM uranium and ~3.5 Gy gamma radiation as single stressors and in combination. Gamma radiation interfered with uranium uptake and translocation, resulting in a decreased uranium concentration in the roots, but with higher transport to the leaves. This decreased uranium root concentration resulted in a better root growth while the increased leaf lipid peroxidation under mixed exposure could be correlated with the higher uranium concentration in the shoots. For the roots, uranium and gamma radiation worked together to cause nutrient decreases under mixed exposure. Nutrient alterations in the leaves on the other hand were mostly induced by uranium under mixed exposure. For the oxidative stress related responses in the roots, alterations on gene expression level under uranium stress were mostly reinforced by gamma radiation. For leaves, gene expression effects under uranium stress were either reinforced or counteracted by simultaneous gamma irradiation. Furthermore, an important role is suggested for *CAT1/2/3* gene expression under uranium and mixed stress conditions in the leaves.

9.1 Introduction

Uranium is a naturally occurring radionuclide and heavy metal present in minerals and sedimentary rocks but due to anthropogenic activities such as uranium and metal mining and the phosphate industry, elevated uranium levels can be found at various environmental sites (Vandenhove, 2002). Previous studies have shown that uranium causes important alterations on plant growth and development and oxidative stress seems an important response mechanism under uranium stress (Vandenhove et al., 2006; Vanhoudt et al., 2008). However uranium never occurs as a single pollutant in the environment, but always in combination with other stressors such as ionizing radiation. As previous studies already indicated that mixed contaminant effects can markedly differ from the effects induced by the stressors individually (An et al., 2004; Geras'kin et al., 2005; Mittler et al., 2006), this multiple pollution context should not be neglected when evaluating the impact of uranium on the environment.

Besides the natural presence of ionizing radiation in the environment due to cosmic radiation or naturally occurring radionuclides, previously described anthropogenic activities can also enhance the environmental level of ionizing radiation (Van der Stricht & Kirchmann, 2001). Gamma radiation, composed of high energy photons, is an important type of ionizing radiation capable of penetrating and interacting with plant or animal tissue. Although gamma radiation can cause a decreased growth rate and reproduction capacity and induce DNA damage and morphological changes in plants as reported by several authors (Daly & Thompson, 1975; Kovalchuk et al., 1999; Zaka et al., 2004; Kovalchuk et al., 2007; Wi et al., 2007), irradiation with low doses on the other hand can stimulate growth as was reviewed by Sax (1954). These studies have also indicated that the radiosensitivity of plants is dependent on the plant species used and growth stage in which they are irradiated as younger plants seem to be more sensitive due to their high proliferation rate. It has also been assumed that the radiosensitivity is proportional with the size of the genome indicating that plants with a very small genome are more radioresistant than plants with a larger genome (Sparrow & Miksche, 1961).

By energy transfer from the radiation field to plant tissue, ionizing radiation can directly induce DNA strand breaks, lipid oxidation or enzyme denaturation. Besides directly damaging macromolecules, reactive oxygen species (ROS) can be generated during radiolysis of water, indirectly inducing cellular damage. As ROS are also produced under natural metabolism, being toxic molecules, but also functioning as signaling molecules regulating normal growth, development and stress responses, plants possess an antioxidative defense system comprising enzymes (e.g. superoxide dismutase (SOD) and catalase (CAT)) and metabolites (e.g. ascorbate and glutathione) to regulate the amount of ROS in cells (Mittler et al., 2004).

Previous studies already indicated an important role for the antioxidative defense system under uranium and other heavy metal stress (Cuypers et al., 2002; Vandenhove et al., 2006; Smeets et al., 2008; Vanhoudt et al., 2008) and it could also be an important pathway under gamma radiation stress as was suggested by several other authors (Wada et al., 1998; Zaka et al., 2002; Kim et al., 2005; Nagata et al., 2005). Also for other types of non-ionizing radiation (e.g. UV radiation, radiofrequency radiation), oxidative stress seems an important modulator under radiation stress (Tkalec et al., 2007; Agrawal & Mishra, 2009).

This study first aimed to investigate the combined effect of uranium and gamma radiation on biological effects such as growth, development and the nutrient profile in *Arabidopsis thaliana* leaves and roots. As previous studies indicated an important role for oxidative stress as a response mechanism under both stressors separately, secondly this study aimed to unravel oxidative stress related responses under a combination of uranium and gamma radiation stress in *Arabidopsis thaliana* leaves and roots. Whereas uranium is present in the nutrient solution, readily taken up by plant roots and transported to the leaves, complete *Arabidopsis thaliana* plants are exposed to a homogenous distributed external gamma radiation field. Uranium and gamma radiation will consequently differ in their site of action and probably also in their induced biological effects. To investigate combined effects, 18-day-old *Arabidopsis thaliana* seedlings were exposed for 3 days to 10 µM uranium, ~3.5 Gy gamma radiation or a combination of both stressors and several endpoints such as growth, nutrient profile, lipid peroxidation, antioxidative metabolite concentrations and protein

and transcriptional levels of ROS producing and scavenging enzymes were analyzed.

9.2 Materials and methods

9.2.1 Plant culture, uranium contamination and gamma irradiation

Arabidopsis thaliana seeds (Columbia ecotype) were spread on moist filter paper at 4 °C for 3 days to synchronize germination. Subsequently, the seeds were sown on plugs from 1.5 ml polyethylene centrifuge tubes filled with 2 % agar (Difco). The plugs were positioned in a PVC cover capable of holding 36 plugs. Next, the cover was placed on a container filled with 1.35 l of a modified Hoagland solution (macro elements without phosphate: 1/10 diluted, phosphate solution: 1/20 diluted, micro elements: 1/10 diluted and iron solution: 1/10 diluted). Plants were grown in a growth chamber (Microclima 1000E, Snijders Scientific B.V.) under a 14 h photoperiod (photosynthetic photon flux density of 200 µmol m^{-2} s^{-1} at the leaf level, supplied by Sylvania BriteGro F36WT8/2084 and F36WT8/2023), with day/night temperatures of 22 °C/18 °C and 65 % relative humidity.

Subsequently, 18-day-old plants were transferred to the irradiation unit of SCK•CEN where they were divided into 4 groups, each receiving a different treatment but all within environmental conditions similar as during the pre-culture. The first group was exposed for 3 days to 10 µM uranium added to the nutrient solution as $UO_2(NO_3)_2.6H_2O$ (Sigma). This uranium concentration was based on a previous experiment inducing 30 % root growth reduction for *Arabidopsis thaliana* for 7 days (chapter 5). The second group of plants was irradiated with gamma radiation from a ^{137}Cs source (1.25×10^{12} Bq) during 3 days, receiving a total dose of ~3.5 Gy with an average dose rate of ~50 mGy h^{-1}. The selection of this dose was based on a previous experiment where 3 Gy induced 30 % growth reduction for *Arabidopsis thaliana* when applied over a 7 week period (Vandenhove et al., in preparation). The third group was exposed to 10 µM uranium while irradiated with gamma radiation, also receiving a total dose of ~3.5 Gy over a 3 days period. The fourth group was the unexposed control group. For all groups, a modified Hoagland nutrient solution with a 1/80

diluted phosphate solution was used during the 3 days exposure as recommended by Vanhoudt et al. (2008) to minimize uranium precipitation.

9.2.2 Plant sampling and biometric measurements

Leaves and roots were harvested separately as ± 100 mg samples, snap frozen in liquid nitrogen and stored at -80 °C. Fresh weight of leaves and roots was determined for at least 20 biological replicates.

Samples for nutrient analyses were dried for 1 week at 70 °C. Leaves were rinsed with distilled water and roots were washed twice for 10 min with 1 mM $Pb(NO_3)_2$ at 4 °C and once for 10 min with distilled water. At least 5 biological replicates were harvested for element determinations.

9.2.3 Uranium and nutrient concentrations

After dry-ashing using a muffle furnace, dried plant material was digested in 0.1 M HCl for determination of several nutrients and uranium. Copper, iron, manganese, zinc and uranium concentrations were determined using inductively coupled plasma mass spectrometry (ICP-MS, Perkin-Elmer, Elan 5000 using a cross flow nebulizer and a ryton spray chamber). Standards for the nutrients were prepared shortly before analysis from 1000 g l^{-1} elemental standards (Spex Certiprep) by sequential dilution with 18.2 MΩ water from a water purification system (MilliQ water from Millipore) and nitric acid (65 %, pro analyse grade, VWR). Calibration curves for uranium were obtained using uranium standard solutions (0-10 µg l^{-1}) prepared from the elemental standard SPEX solution (SPEX Industries Inc.). A specific activity of 12436 Bg g^{-1} for ^{238}U was considered (Joint Evaluated File (JEF) version 2.2, OECD/NEA Data Bank, Paris, France). The concentrations of calcium, potassium and magnesium were determined using suppressed ion chromatography (HPIC, Dionex, ICS-2500 using a CS12-A cation exchange column with guard column, a CSRS-UltraII self-regenerating suppressor and an ED50A electrochemical detector). Standards for the elements were prepared shortly before analysis from 1000 g l^{-1} ion chromatography standards (Fluka) by sequential dilution with 18.2 MΩ water (MilliQ water from Millipore).

9.2.4 Lipid peroxidation

Thiobarbituric acid (TBA) reactive compounds (mainly malondialdehyde) were used as measure of lipid peroxidation in *Arabidopsis thaliana* leaves. Leaf tissue (± 100 mg) was homogenized with 2 ml 0.1 % TCA (trichloroacetic acid) using a mortar and pestle. After centrifugation for 10 min at 20000 × g, 0.5 ml of the supernatant was added to 2 ml 0.5 % TBA. This mixture was heated for 30 min at 95 °C and quickly cooled in an ice bath. After centrifugation for 10 min at 20000 × g, the absorbance of the supernatant was measured spectrophotometrically at 532 nm corrected for unspecific absorbance at 600 nm according to Dhindsa et al. (1981).

9.2.5 Enzyme capacities

Frozen leaf or root tissue (± 100 mg) was homogenized in ice cold 0.1 M Tris-HCl buffer (pH 7.8) containing 1 mM EDTA, 1 mM dithiotreitol and 4 % insoluble polyvinylpyrrolidone (2 ml buffer 100 mg^{-1} FW) using a mortar and pestle. The homogenate was squeezed through a nylon mesh and centrifuged at 20 000 × g and 4 °C for 10 min. The enzyme capacities, i.e. potential activity measured in vitro under non-limiting reaction conditions, were measured spectrophotometrically in the supernatant at 25 °C.

Guaiacol peroxidase (GPX) and syringaldazine peroxidase (SPX) capacities were measured at 436 nm and 530 nm according to Bergmeyer et al. (1974) and Imberty et al. (1984) respectively. Ascorbate peroxidase (APX) capacity was measured at 298 nm following the method of Gerbling et al. (1984). Analysis of superoxide dismutase (SOD) capacity was based on the inhibition of cytochrome *c* at 550 nm according to McCord and Fridovich (1969). Analysis of the capacities of glutathione reductase (GR) and catalase (CAT) were performed as described by Bergmeyer et al. (1974).

9.2.6 Gene expression analyses

Frozen leaf or root tissue (± 100 mg) was ground thoroughly in liquid nitrogen using a mortar and pestle. RNA was extracted using the RNeasy Plant Mini Kit (Qiagen). The RNA quantity was determined spectrophotometrically at 260 nm (Nanodrop, Isogen Life Science). The RNA quality was checked

electrophoretically using the Bioanalyzer (Agilent Technologies). Before cDNA synthesis, the RNA sample was incubated during 2 minutes in gDNA wipeout buffer at 42 °C in order to effectively eliminate genomic DNA. First strand cDNA synthesis was primed with a combination of oligo(dT)-primers and random hexamers according to the manufacturer's instructions using the QuantiTect Reverse Transcription Kit (Qiagen) and equal amounts of starting material were used (1 µg). Quantitative Real-Time PCR was performed with the 7500 Fast Real-Time PCR System (Applied Biosystems), using Sybr Green® chemistry. Primers used for gene expression analyses are given in table 9.1. PCR amplifications were performed in a total volume of 10 µl containing 2.5 µl cDNA sample, 5 µl Fast Sybr Green® Master Mix (Applied Biosystems), 0.3 µl forward primer, 0.3 µl reverse primer and 1.9 µl RNase-free H_2O.

Gene expression data were normalized against multiple housekeeping genes (*At2g28390*, *At5g08290*, *At5g15710*, *UBQ10*) according to Vandesompele et al. (2002) and presented relative to the control treatment.

Table 9.1 - Forward and reverse primers used in gene expression analysis

Gene	Forward primer	Reverse primer
At2g28390	AACTCTATGCAGCATTTGATCCACT	TGATTGCATATCTTTATCGCCATC
At5g08290	TTACTGTTTCGGTTGTTCTCCATTT	CACTGAATCATGTTCGAAGCAAGT
At5g15710	TTTCGGCTGAGAGGTTCGAGT	GATTCCAAGACGTAAAGCAGATCAA
CAT1	AAGTGCTTCATCGGGAAGGA	CTTCAACAAAACGCTTCACGA
CAT2	AACTCCTCCATGACCGTTGGA	TCCGTTCCCTGTCGAAATTG
CAT3	TCTCCAACAACATCTCTTCCCTCA	GTGAAATTAGCAACCTTCTCGATCA
CSD1	TCCATGCAGACCCTGATGAC	CCTGGAGACCAATGATGCC
CSD2	GAGCCTTTGTGGTTCACGAG	CACACCACATGCCAATCTCC
CSD3	GTTGTTGTGCATGCGGATCC	CACATCCAACTCTCGAGCCTG
FSD1	CTCCCAATGCTGTGAATCCC	TGGTCTTCGGTTCTGGAAGTC
FSD2	TTGGAAAGGTTCAAGTCGGCT	CATTTGCAACGTCAAGTCTATTCG
FSD3	AACGGGAATCCTTTACCCGA	TGTCTCCACCACCAGGTTGC
MSD1	ATGTTTGGGAGCACGCCTAC	AACCTCGCTTGCATATTTCCA
LOX1	TTGGCTAAGGCTTTTGTCGG	GTGGCAATCACAAACGGTTC
LOX2	TTTGCTCGCCAGACACTTG	GGGATCACCATAAACGGCC
RBOHC	TCACCAGAGACTGGCACAATAAA	GATGCTCGACCTGAATGCTC
RBOHD	TATGCATCGGAGAGGCTGCT	TAGAGACAACACGTTCCCGGG
RBOHF	GGTGTCATGAACGAAGTTGCA	AATGAGAGCAGAACGAGCATCA
UBQ10	GGCCTTGTATAATCCCTGATGAATAAG	AAAGAGATAACAGGAACGGAAACATAGT

9.2.7 Metabolite concentrations

Ascorbate and glutathione concentrations in *Arabidopsis thaliana* roots were determined by HPLC analysis. Therefore approximately 100 mg tissue was ground thoroughly in liquid nitrogen using a pre-cooled mortar and pestle. When a homogenous powder was obtained, 1 ml of ice cold 6 % (w/v) meta-phosphoric acid was added and the mixture was clarified by centrifugation at 20000 × g and 4 °C for 10 minutes. The resulting supernatant was kept frozen until HPLC analysis. Antioxidants were separated on a 100 mm × 4.6 mm Polaris C18-A reversed phase HPLC column (3 µm particle size, 30 °C, Varian, CA USA) with an isocratic flow of 1 ml min^{-1} of the elution buffer (25 mM K/PO_4-buffer, pH 3.0). The components were quantified using a home-made electrochemical detector with glassy carbon electrode and a Scott pt 62 reference electrode (Mainz, Germany). The purity and identity of the peaks were confirmed using a diode array detector (SPD-M10AVP, Shimadzu, Hertogenbosch, Netherlands) which was placed on line with the electrochemical detector. The concentrations of oxidized DHA (dehydroascorbate) or GSSG (glutathione disulphide) were measured indirectly as the difference between the total concentration of antioxidants in a DTT (dithiothreitol) reduced fraction and the concentration in a sample prior to reduction. Reduction of the sample was obtained by incubation of an aliquot of the extract in 400 mM Tris and 200 mM DTT for 15 minutes in the dark. The pH of this mixture was checked to be between 6.0 and 7.0. After 15 minutes, the pH was lowered again by 4-fold dilution in elution buffer prior to HPLC analysis.

9.2.8 Statistical analyses

Statistical analyses were performed using an ANOVA test in SAS 9.1 (Neter et al., 1996). The ANOVA test was performed separately for leaves and roots. Mean values for the different treatments were compared using Tukey's multiple comparison tests. Transformations were applied when necessary to approximate the assumptions of normality and same error variance. Data presented are mean values ± standard error (S.E.).

9.3 Results

9.3.1 Growth responses

A significant reduction in root fresh weight was observed following exposure of *Arabidopsis thaliana* seedlings to 10 µM uranium while exposure to external gamma radiation did not affect root growth (figure 9.1). Although exposure of *Arabidopsis thaliana* seedlings to a combination of both stressors showed an unaltered root biomass production as compared to the control treatment, the root fresh weight was significantly increased as compared to the uranium treatment but the fresh weight was still significantly lower in comparison with roots exposed to gamma radiation (figure 9.1).

The fresh weight of *Arabidopsis thaliana* leaves remained unaltered for all the different treatments (figure 9.1).

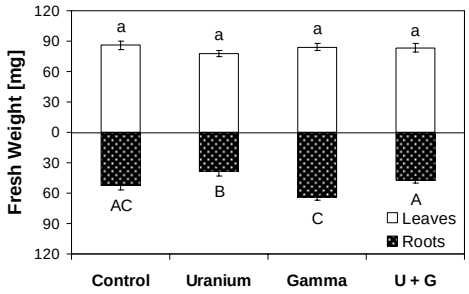

Figure 9.1 – Fresh weight of leaves and roots of 18-day-old *Arabidopsis thaliana* seedlings exposed for 3 days to 10 µM uranium, ~3.5 Gy gamma radiation or a combination of both stressors (U + G). Values represent the mean ± S.E. of 20 biological replicates and data points with different letters are significantly different ($p < 0.05$).

9.3.2 Uranium content and nutrient profile

The uranium concentrations measured in the control and gamma irradiated roots were very small. Nevertheless, the uranium uptake in plant roots under irradiation was significantly lower than for non irradiated plants (table 9.2). The root-to-shoot transfer of uranium is always very limited, but seemed to be increased under gamma irradiation as the uranium concentration in *Arabidopsis thaliana* leaves was significantly higher for uranium treated plants under gamma radiation than for non irradiated plants (table 9.3).

Table 9.2 – Nutrient and uranium concentrations in roots of 18-day-old *Arabidopsis thaliana* seedlings exposed for 3 days to 10 µM uranium, ~3.5 Gy gamma radiation or a combination of both (U + G).

		ROOTS			
		Control	**Uranium**	**Gamma**	**U + G**
[mg g^{-1} DW]	*Ca*	7.0±1.5^{A}	8.1±0.7^{A}	5.1±0.2^{A}	7.2±0.5^{A}
	K	12.9±4.6^{A}	4.6±0.6^{A}	15.4±1.8^{A}	18.8±4.4^{A}
	Mg	2.2±0.2^{A}	2.0±0.03^{A}	1.8±0.1^{A}	2.9±0.6^{A}
[µg g^{-1} DW]	*Cu*	14.5±3.6^{A}	9.6±0.3^{A}	15.9±3.5^{A}	10.5±3.2^{A}
	Fe	1127.4±54.4^{A}	1092.6±57.3^{A}	997.0±30.6^{A}	682.2±79.9^{B}
	Mn	217.2±8.4^{A}	177.6±4.0^{AB}	223.6±24.0^{A}	109.6±10.1^{B}
	Zn	77.4±4.4^{A}	93.0±1.3^{A}	80.9±1.5^{A}	137.2±36.1^{A}
	U	10.7±1.9^{A}	7270.4±543.0^{B}	12.2±1.1^{A}	4509.4±270.5^{C}

Data represent the mean ± S.E. of 5 biological replicates. Different letters indicate significant differences between the treatments ($p < 0.05$).

Table 9.3 – Nutrient and uranium concentrations in leaves of 18-day-old *Arabidopsis thaliana* seedlings exposed for 3 days to 10 µM uranium, ~3.5 Gy gamma radiation or a combination of both (U + G).

		LEAVES			
		Control	**Uranium**	**Gamma**	**U + G**
[mg g^{-1} DW]	*Ca*	41.6±1.5^{a}	37.4±0.3^{b}	40.2±0.3^{ab}	37.9±0.4^{b}
	K	30.7±2.0^{a}	31.9±0.2^{a}	33.1±0.4^{a}	31.0±1.3^{a}
	Mg	9.1±0.3^{a}	8.5±0.1^{ab}	8.8±0.1^{ab}	8.4±0.1^{b}
[µg g^{-1} DW]	*Cu*	10.0±1.0^{a}	4.8±0.2^{b}	7.7±0.8^{ac}	6.5±0.2^{bc}
	Mn	135.2±3.0^{a}	114.3±1.3^{b}	118.0±2.7^{b}	116.4±3.5^{b}
	Zn	31.1±1.7^{a}	25.6±0.6^{b}	28.5±1.2^{ab}	25.1±0.4^{b}
	U	n.d.	2.0±0.3^{a}	n.d.	3.4±0.4^{b}

Data represent the mean ± S.E. of 5 biological replicates. Different letters indicate significant differences between the treatments ($p < 0.05$).

To investigate stress induced effects on the uptake and root-to-shoot distribution of nutrients, concentrations of several important macronutrients (calcium, potassium and magnesium) and micronutrients (copper, iron, manganese and zinc) were determined under uranium and gamma stress and a combination of both. While for the roots no alterations were observed in macronutrient concentrations for all treatments, a significant decrease was observed in iron and manganese concentrations after exposure to a combination of uranium and gamma radiation compared to the control treatment and the single stressor treatments (table 9.2).

For *Arabidopsis thaliana* leaves (table 9.3), a significant decrease in calcium concentration was observed after uranium exposure and exposure to a

combination of uranium and gamma radiation. While no alterations were observed for the potassium content in the leaves, a significant decrease was observed in the magnesium content for the combination treatment, but only in comparison with the control treatment. For the micronutrients, copper concentrations decreased for the uranium and combination treatment as compared to the control with also a decrease for the uranium treatment in comparison with gamma radiation exposure. Manganese concentrations significantly decreased for all treatments as compared to the control with no differences between the treatments. Zinc concentrations on the other hand only decreased for the uranium and combination treatment as compared to the control but no differences were observed in comparison with gamma irradiated leaves.

9.3.3 Lipid peroxidation

The amount of TBA reactive compounds, such as malondialdehyde, was used as a measure for the level of lipid peroxidation in leaf tissue and a significant increase was observed for all treatments as compared to the control (figure 9.2).

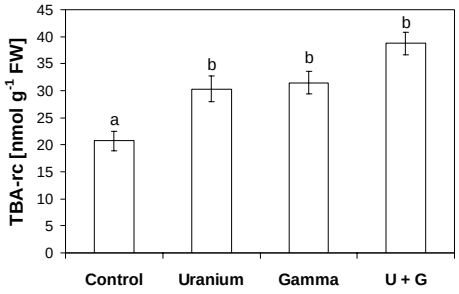

Figure 9.2 - Lipid peroxidation measurement, based on the amount of TBA reactive compounds in leaves of 18-day-old *Arabidopsis thaliana* leaves exposed for 3 days to 10 µM uranium, ~3.5 Gy gamma radiation or a combination of both stressors (U + G). Data represent the mean ± S.E. of 5 biological replicates and different letters indicate significant differences between the treatments ($p < 0.05$).

9.3.4 Oxidative stress related responses

To study the effects of uranium, gamma radiation and a combination of both on the antioxidative defense system and to achieve a better understanding of the importance of the cellular redox balance as a regulator in a multiple stressor

situation, several ROS producing and scavenging enzymes were studied on protein and transcriptional level and metabolite concentrations were determined.

9.3.4.1 Enzyme capacities and antioxidant metabolites

Capacities for CAT, APX, SPX, GPX, SOD and GR were analyzed for leaves and roots exposed to uranium, gamma radiation or a combination of both stressors, but no alterations were observed (results not shown).

The oxidized and reduced forms of ascorbate and glutathione were determined but concentrations remained unaltered under single and mixed exposure conditions (results not shown).

9.3.4.2 Gene expression

First, gene expression of several ROS producing enzymes was analyzed in roots and leaves of *Arabidopsis thaliana* seedlings exposed to the different conditions during 3 days. In the roots, no alterations were observed for *LOX2*, *RBOHC*, *RBOHD* and *RBOHF* gene expression (results not shown). Only a down regulation for *LOX1* transcript levels was observed for the combined treatment in comparison with uranium exposed roots (figure 9.3A). In the leaves on the other hand, *LOX1* and *RBOHD* transcript levels remained unchanged (results not shown). *LOX2* transcript levels were significantly decreased after uranium exposure as compared to the gamma irradiated leaves and the combination treatment (figure 9.4A). *RBOHC* expression levels significantly decreased after the combined treatment as compared to the gamma irradiated leaves (figure 9.4B) and *RBOHF* expression was down regulated after uranium exposure and the combined exposure as compared to the control treatment, but expression levels were also different in comparison with each other with the combined exposure causing the lowest expression (figure 9.4C).

Secondly, expression levels of different isoforms of the superoxide scavenging enzyme SOD were analyzed in leaves and roots for the different treatments. In the roots, no alterations in *CSD1*, *FSD1* and *MSD1* expression levels were observed (results not shown). *CSD2* transcript levels were down regulated following uranium exposure and exposure to the combined stressors as compared to the control treatment (figure 9.3B). *CSD3* and *FSD2* transcript

levels followed a similar pattern as they were both down regulated for the combined treatment as compared to the control roots (figures 9.3C-D). In the leaves, while *CSD1* transcript levels were only significantly down regulated after uranium exposure compared to the control treatment (figure 9.4D), *CSD2* transcript levels decreased after uranium treatment and the combined treatment as compared to the control and the gamma irradiated leaves (figure 9.4E). The other SOD isoforms remained unaltered (results not shown).

Finally, gene expression of some hydrogen peroxide scavenging enzymes was analyzed and for roots no alterations in gene expression were observed for *CAT1*, *CAT2* and *CAT3* (results not shown). For leaves on the other hand, *CAT1* and *CAT3* transcript levels follow a similar pattern as they are both significantly down regulated after uranium exposure in comparison with the gamma irradiated leaves and the combined stressor treatment (figures 9.4F, H). *CAT2* expression levels were only down regulated after exposure to the combination of stressors as compared to the control leaves (figure 9.4G).

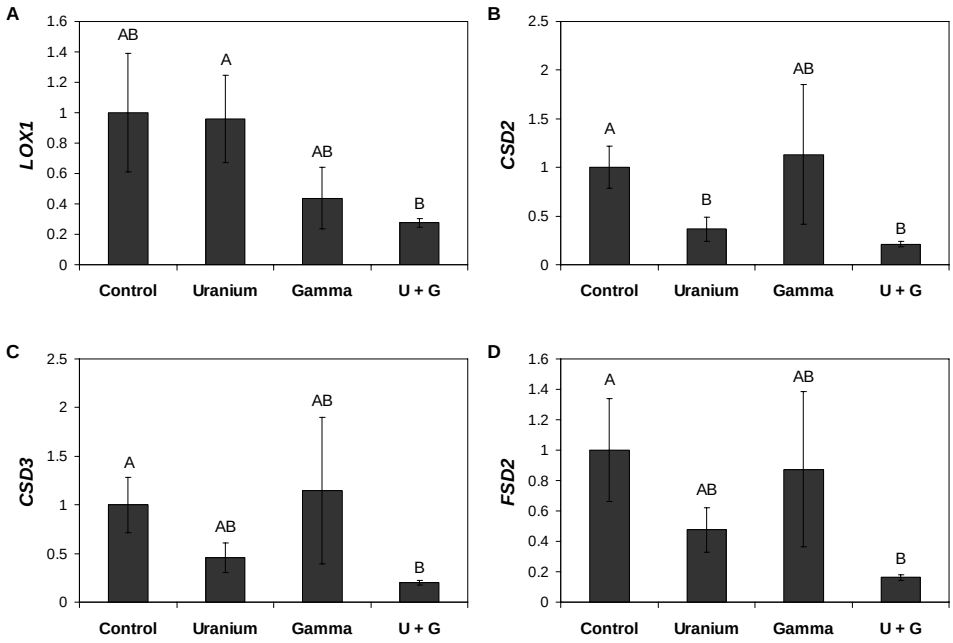

Figure 9.3 - Gene expression of ROS producing and superoxide scavenging enzymes altered in *Arabidopsis thaliana* roots following exposure to 10 µM uranium, ~3.5 Gy gamma radiation or a combination of both. Gene expression was calculated relatively to the control treatment and values represent the mean ± S.E. of 4 biological replicates and different letters indicate significant differences between the treatments ($p < 0.05$).

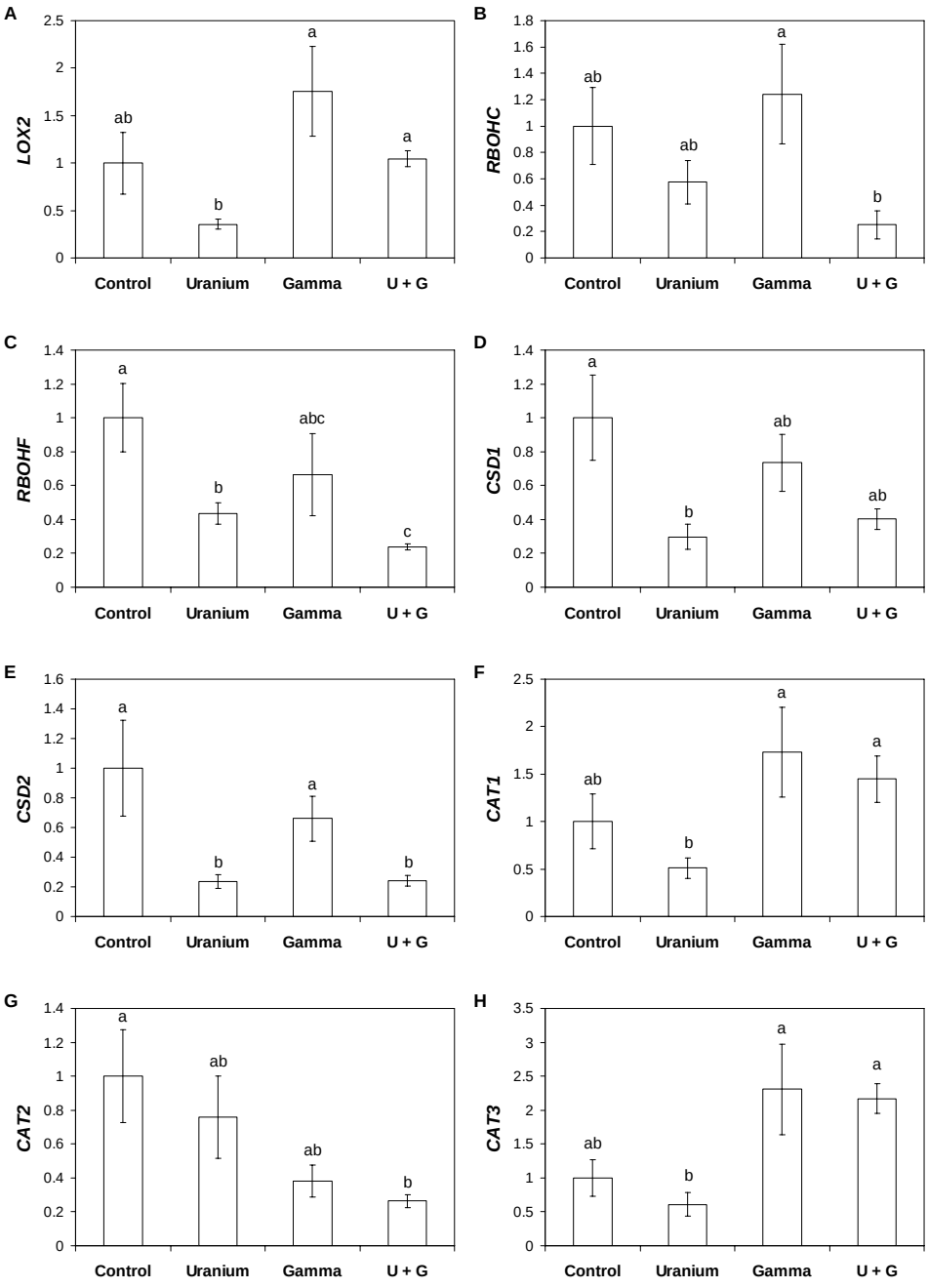

Figure 9.4 - Gene expression of several ROS producing and scavenging enzymes altered in *Arabidopsis thaliana* leaves following exposure to 10 µM uranium, ~3.5 Gy gamma radiation or a combination of both stressors (U + G). Transcript levels are expressed relative to the control treatment and represent the mean ± S.E. of 4 biological replicates. Data points with different letters are significantly different ($p < 0.05$).

9.4 Discussion

Effects induced under mixed exposure conditions can markedly differ from the individually induced effects. Therefore, this study aimed to investigate the induction of biological and oxidative stress related responses in *Arabidopsis thaliana* leaves and roots following uranium and gamma radiation exposure separately, but mainly to evaluate the combined effect of uranium and gamma irradiation on biological responses and to unravel the importance of the cellular redox balance as modulator in a multiple stressor situation.

Heavy metal stress (e.g. cadmium and uranium) can induce physiological and morphological alterations with plant growth reduction, leaf chlorosis and stunted roots as general symptoms (Vandenhove et al., 2006; Van Belleghem et al., 2007; Vanhoudt et al., 2008). Our results are in accordance with previous results as exposure of *Arabidopsis thaliana* plants to 10 µM uranium resulted in a significant decrease of root fresh weight (figure 9.1). Irradiation with ~3.5 Gy of gamma radiation on the other hand did not induce any alterations in roots fresh weight which could probably be explained by the relatively low dose applied and the radioresistance of *Arabidopsis thaliana* plants as was also suggested by Daly & Thompson (1975). Although a 30 % growth reduction was observed after applying a total dose of 3.5 Gy over 7 weeks, the lack in our study could probably be attributed to the difference between chronic and acute exposure. Kovalchuk et al. (2007) for example reported fundamental differences in plant responses between chronic and acute irradiation. Also for screening purposes a difference is made between chronic and acute exposure as a lower dose chronically applied can induce more effects than the same dose acute (ERICA, 2006). Previous studies also reported different results depending on the plant species used and radiation dose applied (Witherspoon & Corney, 1970; Zaka et al., 2004; Wi et al., 2005). While exposure to low doses of 0.1-1 Gy already caused low injuries in pine trees (Arkhipov et al., 1994), Kim et al. (2005) reported growth stimulating effects for red pepper plants after irradiation with 2 and 4 Gy and growth inhibition following exposure to 8 and 16 Gy. Irradiation of *Arabidopsis thaliana* plants which are simultaneously exposed to 10 µM uranium resulted in an increase in root fresh weight as compared to the uranium exposed roots resulting in fresh weight levels similar as the control treatment (figure

9.1). In such a way, gamma irradiation counterbalanced the negative effect of uranium but the root fresh weight after the combined treatment was still significantly lower than only irradiated plants (figure 9.1). This increase in fresh weight under mixed exposure as compared to uranium exposure can be explained by the decreased uranium uptake under simultaneous gamma irradiation (table 9.2) although interaction mechanisms still need to be revealed.

Uranium uptake and transfer to the leaves is dependent on the plant species used but uranium mainly accumulates in plant roots (Ramaswami et al., 2001; Singh et al., 2005). Vandenhove et al. (2006) also reported limited root-to-shoot transfer of uranium as 900 times less uranium was found in the leaves as compared to the roots of *Phaseolus vulgaris* exposed to 1000 µM uranium for 7 days. In our study, uranium also predominantly accumulated in the roots (table 9.2) and a very small amount (3600 times less uranium) was transported to the shoots (table 9.3). Root-to-shoot transfer on the other hand seemed to be enhanced as, even with decreased root uptake, significant higher uranium concentrations were measured in simultaneous irradiated and uranium exposed leaves (table 9.3).

The uptake and distribution of several macronutrients (calcium, potassium and magnesium) and micronutrients (copper, iron, manganese and zinc), essential for normal plant growth and development, was determined. For the roots, a significant decrease was observed in iron and manganese concentrations following simultaneously irradiation and uranium exposure (table 9.2). These results indicate that while exposure to the single stressors does not cause any effect on the roots nutrient profile, both stressors work together to induce a negative effect on the uptake of several micronutrients. For the leaves (table 9.3), uranium exposure caused a significant decrease in most element concentrations and gamma irradiation mostly did not interfere with element uptake and distribution. When leaves were exposed to both stressors, the effects were similar as for the uranium exposed leaves so gamma irradiation did mostly not interfere with uranium induced effects. This is obviously in contrast with uranium transport to the leaves which gamma radiation did influence. Previous studies have shown that heavy metals such as cadmium can interfere with the uptake and translocation of certain nutrients in plants (Hernández et al., 1996; Das et al., 1997; Smeets et al., 2008). Uranium can also disturb the nutrient

profile in plant cells as was shown by Vanhoudt et al. (2008) for *Arabidopsis thaliana* leaves exposed to 100 µM uranium. There can be a competition for specific binding sites between heavy metals and several nutrients having similar chemical properties. Since UO_2^{2+}, the form of uranium most readily taken up by plant species, binds more strongly than Ca^{2+} to Ca^{2+}-type binding sites, it has the potential to damage cell membranes and increase K^+ permeability (Nieboer et al., 1979; Nieboer & Richardson 1980).

Under various stress conditions, an early oxidative burst is one of the first stress responses during which ROS are rapidly produced. Enhanced levels of superoxide can be generated through plasma membrane related NADPH oxidases which in turn can be transformed to hydrogen peroxide via membrane related SODs (Bhattacharjee, 2005). Various roles such as signal transduction and defense responses are described for these ROS (Sagi & Fluhr, 2006). Although our data present no evidence for an NADPH mediated oxidative burst under uranium and gamma mixed exposure conditions, further results however indicate that oxidative stress is induced. If ROS production is present during irradiation, it is probably mostly produced via a water radiolytic reaction.

Lipid peroxidation is a process that can be initiated via interaction with ROS, affecting plant cell membrane function and stability. Exposure of *Arabidopsis thaliana* plants to uranium or gamma radiation as single stressors caused a similar significant increase in lipid peroxidation in leaves (figure 9.2). Our results are in accordance with previous studies that have also shown an increase in lipid peroxidation for heavy metal exposure (Smeets et al., 2005; Vanhoudt et al., 2008) or UV-B exposure (Agrawal & Mishra, 2009). When uranium exposed leaves were simultaneous irradiated with gamma radiation, the level of lipid peroxidation did again significantly increase as compared to the control treatment with the tendency to be higher as for the single stressors (figure 9.2) corresponding with the increased uranium concentration in the leaves under mixed exposure (table 9.3). Agrawal & Mishra (2009) reported that exposure of *Pisum sativum* to a combination of UV-B radiation and cadmium stress also caused an increase in lipid peroxidation. They also reported that the interactions produced by UV-B and cadmium were mostly antagonistic but individually they exert less effect than their joint stress.

To limit oxidative damage but allowing signaling pathways to function, cells comprise a good antioxidative defense system composed of ROS scavenging enzymes and metabolites present in various cellular compartments (Dat et al., 2000). As superoxide scavenging enzymes, SODs constitute the first line of defense against ROS (Alscher et al., 2002). While gamma radiation did not induce any alterations in SOD responses (figure 9.3B-D & 9.4D-E), uranium exposure did cause fluctuations on gene expression level. In general, uranium exposure caused a decrease in gene expression for SOD isoforms and this decrease remained stable following simultaneous exposure to gamma radiation (figure 9.3B-D & 9.4D-E). Under heavy metal stress, Smeets et al. (2008) reported no alterations in SOD capacity in *Arabidopsis thaliana* leaves after cadmium exposure although a decrease in *CSD2* gene expression was observed. Fluctuations in SOD capacity were also observed by Lin et al. (2007) and Zhang et al. (2007) in plants after heavy metal stress. For gamma radiation stress, Kim et al. (2005) reported an increase in SOD capacities after gamma irradiation of red pepper plants while Zaka et al. (2002) reported no alterations in SOD capacity in gamma irradiated leaves of *Stipa capillata*. From these studies it is clear that responses differ depending on the stressor, dose and plant species used and to further elucidate the importance and effects of the different SOD isoforms in our study, further research on protein level is necessary.

CAT is an important hydrogen peroxide scavenging enzyme present in plant cell peroxisomes (Willekens et al., 1995). CAT seems to play an important role in the response against uranium induced oxidative stress in plant leaves. Whereas *CAT1* and *CAT3* transcript levels were only down regulated under uranium stress, *CAT2* expression was only decreased under mixed exposure (figure 9.4F-H). This balance between the different CAT isoforms is also important during senescence as reported by Zimmermann et al. (2006). During senescence a down-regulation of *CAT2* expression levels appeared to be an initial step in producing elevated hydrogen peroxide levels, followed by an induction of *CAT3* expression. Our results also indicate an important role for the different CAT isoforms under uranium and mixed stress situations, possibly related with senescence processes, but further research to hydrogen peroxide levels is necessary.

9.5 Conclusions

Gamma radiation interfered importantly with uranium uptake and translocation, resulting in a decreased uranium root concentration with higher transport to the shoots. This interesting observation also resulted in a better root growth but increased leaf lipid peroxidation when simultaneously irradiated and uranium exposed. While for the roots, uranium and gamma radiation worked together to cause only nutrient decreases under mixed exposure, nutrient alterations in the leaves under mixed exposure were uranium induced. For the oxidative stress related responses in the roots, alterations on gene expression level under uranium stress were mostly reinforced by gamma radiation under mixed exposure. For leaves on the other hand, gene expression effects under uranium stress were either reinforced or counteracted by simultaneous gamma irradiation. In addition, an important role has been ascribed to *CAT1/2/3* gene expression under uranium and mixed stress conditions in the leaves that might be related with senescence processes, but a further in depth research is needed.

Chapter 10

General discussion, conclusions and perspectives

10.1 General discussion

10.1.1 Introduction

Anthropogenic activities such as uranium mining and milling, metal mining and smelting and the phosphate industry, have caused environmental uranium contamination in many countries. To evaluate the impact of uranium on the environment, it is important to enlarge the scant information available on uranium toxicity effects in plants and unravel by which mechanisms plants respond to uranium stress. The main objective of this research concerns studying uranium toxicity effects on morphological and metabolic level in *Arabidopsis thaliana* plants and investigating the role of oxidative stress as a modulator during uranium stress. Therefore, oxidative stress related responses, together with general developmental alterations, were studied for *Arabidopsis thaliana* plants exposed during several time periods to soil solution uranium concentrations ranging from 0.1 µM found at contaminated Belgian sites to 100 µM found at uranium mining sites. Figure 10.1 gives an overview of the general toxicity effects and oxidative stress related responses induced in *Arabidopsis thaliana* leaves and roots following uranium exposure.

At these polluted sites, uranium never occurs as a single stressor, but always in combination with other stressors such as radionuclides with their concomitant radiation and heavy metals. Uranium behavior and toxicity effects can therefore be influenced by the presence of other pollutants. The second objective was to investigate the influence of a secondary stressor on previously described uranium toxicity effects in *Arabidopsis thaliana* seedlings. As they are very distinct stressors, cadmium and ionizing radiation were chosen for experiments under binary stressor conditions with uranium.

10.1.2 Uranium toxicity effects in Arabidopsis thaliana roots

As roots were directly exposed to uranium via the nutrient solution, and by using a low phosphate concentration to limit the formation of uranium-phosphate precipitates (chapter 3), uranium was readily taken up by *Arabidopsis thaliana* roots (table 4.2). Toxicity effects were immediately visible as exposure to the highest uranium concentration (100 µM) caused stunted roots (figure 3.2 and

figure 4.2), a decrease in fresh weight (figure 4.1), a disrupted nutrient profile and a disturbed water balance indicating plants started to wilt (table 4.1). Exposure to the lower uranium concentrations (0.1-10 µM) on the other hand, resulted in a transient hormesis effect based on the transient increase of fresh weight (figure 4.1). While effects at morphological and physiological level were visible at all uranium concentrations applied, oxidative stress related responses were only present at the highest uranium concentration (100 µM).

Plasma membranes of root cells are the first targets of oxidative damage and a possible fast role for NADPH oxidases as ROS producers during a uranium-induced early oxidative burst has been suggested based on the increase in *RBOHD* transcript levels (figure 5.2D). While potassium leakage can be an indication for membrane damage (table 4.3), the increased *LOX1* expression, already observed after the first day, can also point to fast lipoxygenase mediated lipid peroxidation resulting in an enhancement of precursors for signaling molecules such as jasmonates (figure 5.2A). Indications for increased signaling functions under uranium stress were also presented by increased *LPP1* and *PARP2* expression levels that are enzymes implicated in signaling processes during stress response (table 7.3). As ROS can both cause cellular damage and function as signaling molecules during stress response, their presence needs to be tightly regulated. SOD is an important $O_2^{\bullet-}$ scavenging enzyme during the early oxidative burst as its capacity immediately increased (figure 5.1A) which was accompanied by a simultaneous increase in *FSD1* transcript levels but a down-regulation for *CSD1* and *CSD2* expression (figure 5.3A-C). For the detoxification of hydrogen peroxide, the increase in *CAT1* transcript levels (figure 5.4B) was again a fast response while increased peroxidase capacities were observed at a later stage (figure 5.1C-D). Although the APX capacity increased (figure 5.1E), the ascorbate redox balance completely shifted towards its oxidized form (table 5.2) and this could not be inverted by action of glutathione (table 5.3). The cellular redox balance of the roots was, also based on growth and morphological effects, completely disturbed by the highly toxic uranium concentration of 100 µM.

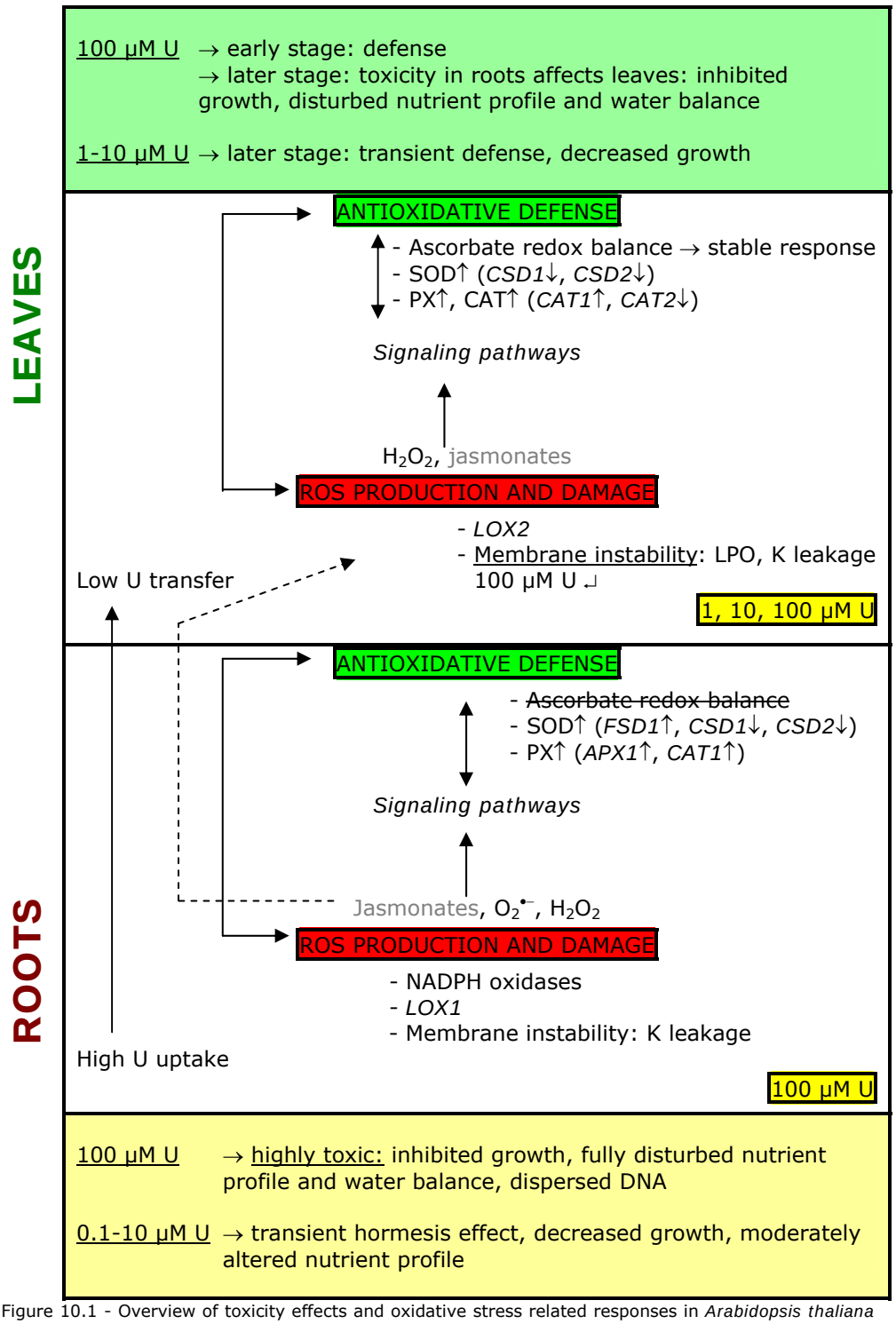

Figure 10.1 - Overview of toxicity effects and oxidative stress related responses in *Arabidopsis thaliana* leaves and roots following uranium exposure.

This conclusion could also be strengthened by the completely dispersed DNA present after exposure to 100 µM uranium as indicated by the comet assay (figure 7.1). Following gene expression observations, mechanisms for homologous and non-homologous recombination were not triggered at the levels studied, but an adaption of the cell cycle was suggested to allow DNA repair (table 7.3).

10.1.3 Uranium toxicity effects in Arabidopsis thaliana leaves

Due to a very low root-to-shoot transfer factor, only low uranium concentrations were present in the leaves. Nevertheless, toxicity effects were visible after exposure to uranium concentrations ranging from 1 to 100 µM. On growth and development level, leaf fresh weight decreased after exposure to 100 µM uranium for 1 and 3 days and this decrease was after 7 days also visible for 1 and 10 µM uranium (figure 4.1). In accordance with the roots, wilting of the plants was also demonstrated by the disturbed water balance of the leaves (table 4.1). Uranium uptake also disturbed the nutrient profile with an important decrease in calcium and magnesium due to the competition with the uranyl ion for their binding sites (table 4.4).

As in leaves several responses were already visible after 1 day when uranium concentrations were negligible in the leaves and no proof was found for an early oxidative burst, oxidative stress was probably generated via other mechanisms such as root-to-shoot signaling. While an increase of membrane damage was indicated by the increase in TBA-reactive compounds (figure 6.1) and potassium leakage (table 4.4) after 100 µM uranium, also an enhancement in signaling molecules was proposed by LOX induced lipid peroxidation for which a transient concentration dependent response pattern was visible (figure 6.2B). This transient character, both in time as with concentration, of leaf responses to uranium stress was emphasized by *LOX2* transcript levels (figure 6.4B), antioxidative enzyme capacities (figure 6.3) and gene expression (figure 6.5) and glutathione concentrations (table 6.3). The ascorbate pool on the other hand continuously increased in a concentration and time dependent way characterized by an increase of the AsA/DHA balance towards its reduced form (table 6.2). The increase and maintenance of the ascorbate redox balance is an important response for hydrogen peroxide detoxification or a response in

signaling functions. In addition to the several fast transient effects, the increase in ascorbate could represent either a slow transient response or a stable increase with regard to plant acclimation to uranium. However this can only be assumed for the lower uranium concentrations as 100 µM uranium toxicity effects in the roots are too severe to allow plant survival.

In contrast to the roots, no DNA damage was observed in the leaves but effects on alterations of the cell cycle were similar as for roots but at a later time point.

10.1.4 Influence of binary exposure conditions on uranium toxicity effects

Two distinct secondary stressors, cadmium and gamma radiation, were used to investigate their influence on uranium (10 µM) induced toxicity effects. Cadmium, also a heavy metal applied to the roots in an environmental realistic concentration of 5 µM, was readily taken up by plant roots and in comparison with uranium, accumulated less in the roots. With a higher cadmium translocation to the shoots, this resulted in a much higher cadmium than uranium concentration in the leaves (table 8.2 & 8.3). Although not yet visible at the concentration applied and exposure time considered, cadmium is known to reduce plant growth. In contrast to heavy metals, gamma radiation, known for its ionizing characteristics, was applied by full plant irradiation at a relatively high total dose of 3.5 Gy, but was shown to cause an increasing trend for root fresh weight (figure 9.1). Uranium uptake and distribution was highly influenced by the presence of other stressors but effects were greatly dependent on the stressor applied and the site of action. Cadmium presence resulted in an enhanced (doubled) uranium uptake and consequently an enhanced uranium concentration in the leaves (table 8.2 & 8.3). Simultaneous exposure to uranium and radiation, however, obstructed uranium uptake but stimulated root-to-shoot uranium translocation (table 9.2 & 9.3). This was also reflected in the corresponding root fresh weight. Due to the presence of both uranium and cadmium heavy metals with on top an increase in uranium root concentration, root fresh weight decreased after exposure to the mixed heavy metals (figure 8.1). By simultaneous irradiation of uranium exposed roots, obstructing uranium uptake, the observed decrease in root fresh weight after uranium exposure as single stressor was counteracted by gamma irradiation (figure 9.1).

In roots under mixed exposure, oxidative stress related responses were mostly influenced by cadmium with less uranium contribution. Based on the increased AsA/DHA redox balance, similar as under cadmium stress, it was shown that roots were able to defend themselves against the induced stress (table 8.5). Oxidative stress was shown to be mainly due to superoxide as expression of related genes (SODs) was mostly altered (figure 8.3). When uranium exposed roots were simultaneously irradiated, the little observed effects due to uranium were sometimes reinforced by gamma radiation (figure 9.3).

When oxidative stress related responses were studied in leaves simultaneously exposed to uranium and cadmium, gene expression effects were again mostly influenced by cadmium possibly due to the higher cadmium concentration in the leaves (figure 8.2). The ascorbate redox balance was an important first response to heavy metal stress in the leaves, mostly altered by cadmium (table 8.5). In contrast to superoxide in the roots, hydrogen peroxide related genes were mostly altered in the leaves (figure 8.3). When simultaneously irradiated, effects were mostly due to uranium but although not consequently, gamma radiation sometimes interfered with uranium, enhancing or opposing uranium induced effects (figure 9.4).

10.2 Conclusions

The aim of this study was first to investigate uranium toxicity effects and to unravel mechanisms by which plants respond to uranium stress. In a next phase, the influence of secondary stressors on uranium induced effects was investigated.

The highest uranium concentration of 100 µM uranium is extremely toxic for *Arabidopsis thaliana* plants with a completely inhibited growth, a fully disturbed nutrient profile, wilting and although making an effort to increase antioxidative defense, suffering from severe oxidative stress with a completely disturbed metabolic balance. While at lower uranium concentrations no oxidative stress related responses are visible in roots, leaves show an increased defense against uranium stress with an important regulatory role for the ascorbate pool as an early and stable stress response mechanism. *Arabidopsis thaliana* plants are

therefore able to defend themselves under moderate environmental uranium contamination conditions although responses differ for leaves and roots.

Toxicity effects during mixed exposure were mostly due to cadmium, indicating its higher toxicity in comparison to uranium for the concentrations applied. Nevertheless, uranium induced similar effects and worked at similar sites of action. Therefore, when uranium is present in combination with cadmium or probably also other heavy metals, uranium induced effects will be influenced. As gamma radiation was already applied in a relatively high dose and only minor effects could be ascribed to it, gamma radiation induced effects can be considered negligible when during environmental realistic situations uranium exposed plants are simultaneously irradiated.

10.3 Future perspectives

To get more insight in uranium and heavy metal stress response mechanisms and to identify possible biomarkers to better evaluate its environmental impact, underlying stress response mechanisms should be further unraveled such as the specific role for the ascorbate redox balance in signaling and regulating defense pathways. In addition, research should be extended to the role and induction of specific signal transduction pathways under uranium stress and enhanced knowledge on uranium uptake mechanisms could further elucidate toxicity effects in plants. Further techniques to investigate stress response mechanisms include the application of a full microarray study or the usage of specific knock-out mutants.

When aiming to evaluate the environmental uranium impact, also more realistic situations should be studied by further evaluating the influence of binary stressors such as pH, variable soil characteristics and other contaminants on uranium induced toxicity effects. To get more insight in the additive, antagonistic or synergistic character of multiple stressors, research should be extended by determining individual dose-effect relationships and extending it to multiple combination studies which can in turn be used in multiple pollution modeling.

References

AGRAWAL S.B. & Mishra S. (2009) Effects of supplemental ultraviolet-B and cadmium on growth, antioxidants and yield of *Pisum sativum* L. *Ecotoxicology and Environmental Safety* 72, 610-618.

ALSCHER R.G., Erturk N. & Heath L.S. (2002) Role of superoxide dismutases (SODs) in controlling oxidative stress in plants. *Journal of Experimental Botany* 53, 1331-1341.

ALTENBURGER R., Backhaus T., Boedeker W., Faust M., Scholze M. & Grimme L.H. (2000) Predictability of the toxicity of multiple chemical mixtures to *Vibrio fischeri*: mixtures composed of similarly acting chemicals. *Environmental Toxicology and Chemistry* 19, 2341-2347.

AN Y.J., Kim Y.M., Kwon T.I. & Jeong S.W. (2004) Combined effect of copper, cadmium and lead upon *Cucumis sativus* growth and bioaccumulation. *Science of the Total Environment* 326, 85-93.

ARKHIPOV N.P., Kuchma N.D., Askbrant S., Pasternak P.S. & Musica V.V. (1994) Acute and long-term effects of irradiation on pine (*Pinus silvestris*) stands post-Chernobyl. *The Science of the Total Environment* 157, 383-386.

ARORA A., Sairam R.K. & Srivastava G.C. (2002) Oxidative stress and antioxidative system in plants. *Current Science* 82, 1227-1238.

ASADA K. (1992) Ascorbate peroxidase – a hydrogen peroxide-scavenging enzyme in plants. *Physiologia Plantarum* 85, 235-241.

ASADA K. (2006) Production and scavenging of reactive oxygen species in chloroplasts and their functions. *Plant Physiology* 141, 391-396.

ATSDR (1999) Toxicological profile for uranium. U.S. Department of Health and Human Services. Public Health Service. Agency for Public Substances and Disease Registry, Atlanta.

BACKHAUS T., Altenburger R., Boedeker W., Faust M., Scholze M. & Grimme L.H. (2000) Predictability of the toxicity of a multiple mixture of dissimilarly acting chemicals to *Vibrio fischeri*. *Environmental Toxicology and Chemistry* 19, 2348-2356.

BENAVIDES M.P., Gallego M. & Tomaro M.L. (2005) Cadmium toxicity in plants. *Brazilian Journal of Plant Physiology* 17, 21-34.

BENJAMINI Y. & Hochberg Y. (1995) Controlling the false discovery rate: a practical and powerful approach to multiple testing. *Journal of the Royal Statistical Society Series B – Statistical Methodology* 57, 289-300.

BERGMEYER H.U., Gawehn K. & Grassl M. (1974) Enzymes as biochemical reagents. In: Bergmeyer H.U. (Ed.) Methods of enzymatic analysis, Academic Press, New York, pp 425-522.

BETHKE C.M. (2001) The Geochemist's Workbench®, release 3.2, a User's Guide to Rxn, Act2, Tact, React and Gtplot, Hydrogeology Program, University of Illinois, Urbana, USA.

BHATTACHARJEE S. (2005) Reactive oxygen species and oxidative burst: roles in stress, senescence and signal transduction in plants. *Current Science* 89, 1113-1121.

BLEISE A., Danesi P.R. & Burkart W. (2003) Properties, use and health effects of depleted uranium (DU): a general overview. *Journal of Environmental Radioactivity* 64, 93-112.

BLEUYARD J.Y., Gallego M.E. & White C.I. (2006) Recent advances in understanding of the DNA double-strand break repair machinery of plants. *DNA Repair* 5, 1-12.

BOILEAU L.J.R., Nieboer E. & Richardson D.H.S. (1985) Uranium accumulation in the lichen *Cladonia rangiferina*. Part II. Toxic effects of cationic, neutral, and anionic forms of the uranyl ion. *Candian Journal of Botany* 63, 390-397.

BOWLER C., Van Montagu M. & Inzé D. (1992) Superoxide dismutase and stress tolerance. *Annual Review of Plant Physiology and Plant Molecular Biology* 43, 83-116.

BOWLER C., Van Camp W., Van Montagu M. & Inzé D. (1994) Superoxide dismutase in plants. *Critical Reviews in Plant Sciences* 13, 199-218.

BOX G.E.P. & Cox D.R. (1964) An analysis of transformations. *Journal of the Royal Statistical Society Series B – Statistical Methodology* 26, 211-246.

BURKART W., Danesi P.R. & Hendry J.H. (2005) Properties, use and health effects of depleted uranium. *International Congress Series* 1276, 133-136.

CARDINAELS C., Put C., Van Assche F. & Clijsters H. (1984) The superoxide dismutase as a biochemical indicator, discriminating between zinc and cadmium toxicity. *Archives Internationales de Physiologie de Biochimie et de Biophysique* 92, 2-3.

CHALKER-SCOTT L. (1999) Environmental significance of anthocyanins in plant stress responses. *Photochemistry and Photobiology* 70, 1-9.

CHAOUI A., Ghorbal M.H. & El Ferjani E. (1997) Effects of cadmium-zinc interactions on hydroponically grown bean (*Phaseolus vulgaris* L.). *Plant Science* 126, 21-28.

CHARLES A.L., Markich S.J. & Ralph P. (2006) Toxicity of uranium and copper individually, and in combination, to a tropical freshwater macrophyte (*Lemna aequinoctialis*). *Chemosphere* 62, 1224-1233.

CHO U.H. & Seo N.H. (2005) Oxidative stress in Arabidopsis thaliana exposed to cadmium is due to hydrogen peroxide accumulation. *Plant Science* 168, 113-120.

CLEMENS S. (2006) Toxic metal accumulation, responses to exposure and mechanisms of tolerance in plants. *Biochimie* 88, 1707-1719.

CLIJSTERS H., Cuypers A. & Vangronsveld J. (1999) Physiological responses to heavy metals in higher plants; defence against oxidative stress. *Zeitschrift fur Naturforschung* 54c, 730-734.

CUYPERS A., Vangronsveld J. & Clijsters H. (2000) Biphasic effect of copper on the ascorbate-glutathione pathway in primary leaves of *Phaseolus vulgaris* seedlings during the early stages of metal assimilation. *Physiologia Plantarum* 110, 512-517.

CUYPERS A., Vangronsveld J. & Clijsters H. (2001) The redox status of plant cells (AsA and GSH) is sensitive to zinc imposed oxidative stress in roots and primary leaves of *Phaseolus vulgaris*, *Plant Physiology and Biochemistry* 39, 657-664.

CUYPERS A., Vangronsveld J. & Clijsters H. (2002) Peroxidases in roots and primary leaves of *Phaseolus vulgaris* copper and zinc phytotoxicity: a comparison. *Journal of Plant Physiology* 159, 869-876.

COWART J.B. & Burnett W.C. (1994) The distribution of uranium and thorium decay-series radionuclides in the environment – a review. *Journal of Environmental Quality* 23, 651-662.

DALY K. & Thompson K.H. (1975) Quantitative dose-response of growth and development in *Arabidopsis thaliana* exposed to chronic gamma-radiation. *International Journal of Radiation Biology* 28, 61-66.

DAS P., Samantaray S. & Rout G.R. (1997) Studies on cadmium toxicity in plants: a review. *Environmental Pollution* 98, 29-36.

DAT J., Vandenabeele S., Vranová E., Van Montagu M., Inzé D. & Van Breusegem F. (2000) Dual action of the active oxygen species during plant stress responses. *Cellular and Molecular Life Sciences* 57, 779-795.

DAVIES C., Howard D., Tam G. & Wong N. (1994) Isolation of Arabidopsis thaliana mutants hypersensitive to gamma radiation. *Molecular & General Genetics* 243, 660-665.

DAU H., Liebisch P. & Haumann M. (2005) The manganese complex of oxygenic photosynthesis: conversion of five-coordinated Mn(III) to six-coordinated Mn(IV) in the S_2-S_3 transition is implied by XANES simulations. *Physica Scripta* T115, 844-846.

DEVEAUX Y., Alonso B., Pierrugues O., Godon C. & Kazmaier M. (2000) Molecular cloning and developmental expression of *AtGR1*, a new growth-related Arabidopsis gene strongly induced by ionizing radiation. *Radiation Research* 154, 355-364.

DE VEYLDER L., Beemster G., Beeckman T. & Inzé D. (2001a) *CKS1At* overexpression in *Arabidopsis thaliana* inhibits growth by reducing meristem size and inhibiting cell-cycle progression.

DE VEYLDER L., Beeckman T., Beemster G., Krois L., Terras F., Landrieu I., Van Der Schueren E., Maes S., Naudts M. & Inzé D. (2001b) Functional analysis of cyclin-dependent kinase inhibitors of Arabidopsis. *The Plant Cell* 13, 1653-1667.

DHINDSA R.S., Plumb-Dhindsa P. & Thorpe T.A. (1981) Leaf senescence: correlated with increased levels of membrane permeability and lipid peroxidation, and decreased levels of superoxide dismutase and catalase. *Journal of Experimental Botany* 32, 93-101.

DI TOPPI L.S. & Gabbrielli R. (1999) Response to cadmium in higher plants. *Environmental and Experimental Botany* 41, 105-130.

DOMENICHINI S., Raynaud C., Ni D.A., Henry Y. & Bergounioux C. (2006) Atmnd1-Δ1 is sensitive to gamma-irradiation and defective in meiotic DNA repair. *DNA Repair* 5, 455-464.

DOUCET-CHABEAUD G., Godon C., Brutesco C., de Murcia G. & Kazmaier M. (2001) Ionizing radiation induces the expression of *PARP-1* and *PARP-2* genes in *Arabidopsis*. *Molecular Genetics and Genomics* 265, 954-963.

DOUTRIAUX M.P., Couteau F., Bergounioux C. & White C. (1998) Isolation and characterization of the *RAD51* and *DMC1* homologs from *Arabidopsis thaliana*. *Molecular and General Genetics* 257, 283-291.

DRAZKIEWICZ M., Skorzynska-Polit E. & Krupa Z. (2003) Response of the ascorbate-glutathione cycle to excess copper in *Arabidopsis thaliana* (L.). *Plant Science* 164, 195-202.

EBBS S.D., Brady D.J. & Kochian L.V. (1998) Role of uranium speciation in the uptake and translocation of uranium by plants. *Journal of Experimental Botany* 49, 1183-1190.

ERICA (2006) Deliverable 5: Derivation of predicted-no-effect-dose-rate values for ecosystems (and their sub-organizational levels) exposed to radioactive substances.

FAIRBAIRN D.W., Olive P.L. & O'Neill K.L. (1995) The comet assay: a comprehensive review. *Mutation Research* 339, 37-59.

FOYER C.H. & Noctor G. (2003) Redox sensing and signaling associated with reactive oxygen in chloroplasts, peroxisomes and mitochondria. *Physiologia Plantarum* 119, 355-364.

FOYER C.H. & Noctor G. (2005a) Redox homeostasis and antioxidant signaling: a metabolic interface between stress perception and physiological responses. *The Plant Cell* 17, 1866-1875.

FOYER C.H. & Noctor G. (2005b) Oxidant and antioxidant signaling in plants: a re-evaluation of the concept of oxidative stress in a physiological context. *Plant, Cell and Environment* 28, 1056-1071.

FOYER C.H., Descouvrières P. & Kunert K.J. (1994) Protection against oxygen radicals: an important defence mechanism studied in transgenic plants. *Plant, Cell and Environment* 17, 507-523.

FOYER C.H., Groten K. & Kunert K. (2003) Oxidative stress. In: Thomas B., Murphy D.J. & Murray B.G. (Eds.) Encyclopedia of applied plant sciences, Elsevier Science & Technology Books, pp 419-430.

FRIESNER J. & Britt A.B. (2003) *Ku80*- and *DNA ligase IV*-deficient plants are sensitive to ionizing radiation and defective in T-DNA integration. *The Plant Journal* 34, 427-440.

GERAS'KIN S.A., Kim J.K., Dikarev V.G., Oudalova A.A., Dikareva N.S. & Spirin Y.V. (2005) Cytogenetic effects of combined radioactive (^{137}Cs) and chemical (Cd, Pb, and 2,4-D herbicide) contamination on spring barley intercalar meristem cells. *Mutation Research* 586, 147-159.

GERBLING K.P., Kelly G.J., Fischer K.H. & Latzko E. (1984) Partial purification and properties of soluble ascorbate peroxidases from pea leaves. *Journal of Plant Physiology* 115, 59-67.

GOPAL R. & Rizvi A.H. (2008) Excess lead alters growth, metabolism and translocation of certain nutrients in radish. *Chemosphere* 70, 1539-1544.

GRENTE I., Furger J., Konings R.J.M, Lemire R.J., Muller A.B., Nguy-en-Trung C. & Wanner H. (1992) Chemical thermodynamics of uranium, Elsevier, Amsterdam, The Netherlands.

GÜNTHER A., Bernhard G., Geipel G., Reich T., Rossberg A. & Nitsche H. (2003) Uranium speciation in plants. *Radiochimica Acta* 91, 319-328.

HALLIWELL B. (2006) Reactive species and antioxidants. Redox biology is a fundamental theme of aerobic life. *Plant Physiology* 141, 312-322.

HAN R., Zou W., Wang Y. & Zhu L. (2007) Removal of uranium(VI) from aqueous solutions by manganese oxide coated zeolite: discussion of adsorption isotherms and pH effect. *Journal of Environmental Radioactivity* 93, 127-143.

HASAN S.A., Fariduddin Q., Ali B., Hayat S. & Ahmad A. (2009) Cadmium: toxicity and tolerante in plants. *Journal of Environmental Biology* 30, 165-174.

HERNÁNDEZ L.E., Carpena-Ruiz R. & Gárate A. (1996) Alterations in the mineral nutrition of pea seedlings exposed to cadmium. *Jounal of Plant Nutrition* 19, 1581-1598.

HIGGY R.H. & Pimpl M. (1998) Natural and man-made radioactivity in soils and plants around the research reactor of Inshass. *Applied Radiation and Isotopes* 49, 1709-1712.

HIMELBLAU E. & Amasino R.M. (2001) Nutrients mobilized from leaves of *Arabidopsis thaliana* during leaf senescence. *Journal of Plant Physiology* 158, 1317-1323.

IMBERTY A., Goldberg R. & Catesson A.M. (1984) Tetramethylbenzidine and *p*-phenylenediamine-pyrocatechol for peroxidase histochemistry and biochemistry: two new, non-carcinogenic chromogens for investigating lignification process. *Plant Science Letters* 35, 103-108.

JAIN G.S. & Aery N.C. (1997) Effects of uranium addition on certain biochemical constituents and uranium accumulation in wheat. *Biologia Bratislava* 52, 599-604.

Jansen M.A.K., Hectors K., O'Brien M.N., Guisez Y. & Potters G. (2008) Plant stress and human health: Do human consumers benefit from UV-B acclimated crops? *Plant Science* 175, 449-458.

JÄRUP L., Berglund M., Elinder C.G., Nordberg G. & Vahter M. (1998) Health effects of cadmium exposure – a review of the literature and a risk estimate. *Scandinavian Journal of Work Environment & Health* 24, Suppl. 1.

JONES D., Humphrey C., Iles M. & vanDam R. (2006) An approach to deriving surface water quality criteria with implications for closure – Ranger mine case study. In: Fourie A. & Tibbert M. (Eds.) Proceedings of the First Int Seminar on Mine Closure, Mine Closure 2006, September 13-15, Perth, pp 635-646.

JONKER M.J., Svendsen C., Bedaux J.J.M., Bongers M. & Kammenga J.E. (2005) Significance testing of synergetic/antagonistic, dose level-dependent, or dose ratio-dependent effects in mixture dose-response analysis. *Environmental Toxicology and Chemistry* 24, 2701-2713.

KIM J.H., Chung B.Y., Kim J.S. & Wi S.G. (2005) Effects of *in planta* gamma-irradiation on growth, photosynthesis, and antioxidative capacity of red pepper (*Capsicum annuum* L.) plants. *Journal of Plant Biology* 48, 47-56.

KOPPEN G. & Angelis K.J. (1998) Repair of X-ray induced DNA damage measured by the comet assay in roots of *Vicia faba*. *Environmental and Molecular Mutagenesis* 32, 281-285.

KOPPEN G. & Verschaeve L. (2001) The alkaline single-cell gel electrophoresis/comet assay: a way to study DNA repair in radicle cells of germinating *Vicia faba*. *Folia Biologica* 47, 50-54.

KOPPEN G., Toncelli L.M., Triest L. & Verschaeve L. (1999) The comet assay: a tool to study alterations of DNA integrity in developing plant leaves. *Mechanisms of Ageing and Development* 110, 13-24.

KOVALCHUK O., Kovalchuk I., Titov V., Arkhipov A. & Hohn B. (1999) Radiation hazard caused by the Chernobyl accident in inhabited areas of Ukraine can be monitored by transgenic plants. *Mutation Research* 446, 49-55.

KOVALCHUK I., Molinier J., Yao Y., Arkhipov A. & Kovalchuk O. (2007) Transcriptome analysis reveals fundamental differences in plant response to acute and chronic exposure to ionizing radiation. *Mutation Research* 624, 101-113.

KUTNER M.H., Nachtsheim C.J., Neter J. & Li W. (2005) Applied linear statistical models. 5th ed. Mac Graw Hill, Boston.

LANGMUIR D. (1978) Uranium solution-mineral equilibria at low temperature with applications to sedimentary ore deposits. *Geochimica et Cosmochimica Acta* 42, 547-569.

LAROCHE L., Henner P., Camilleri V. & Morello M. (2005) Garnier-Laplace J., Root uptake of uranium by a higher plant model (*Phaseolus vulgaris*) – bioavailability from soil solution. *Radioprotection* 40, S33-S39.

LAUWERYS R., Amery A., Bernard A., Bruaux P., Buchet J.P., Claeys F., De Plaen P., Ducoffre G., Fagard R., Lijnen P., Nick L., Roels H., Rondia D., Saint-Remy A., Sartor F. & Staessen J. (1990) Health effects of environmental exposure to cadmium: objectives, design and organization of the Cadmibel study: a cross-sectional morbidity study carried out in Belgium from 1985 to 1989. *Environmental Health Perspectives* 87, 283-289.

LEHMANN E.L. & D'Abrera H.J.M. (1998) Nonparametrics, statistical methods based on ranks. Prentice Hall, Upper Saddle River, New Jersey.

LIN R., Wang X., Luo Y., Du W., Guo H. & Yin D. (2007) Effects of soil cadmium on growth, oxidative stress and antioxidant system in wheat seedlings (*Triticum aestivum* L.). *Chemosphere* 69, 89-98.

LIN D., Shkedy Z., Burzykowski T., Ion R., Göhlmann H.W.H., De Bondt A., Perera T., Geerts T., Van den Wyngaert I. & Bijnens L. (2008) An investigation on performance of Significance Analysis of Microarray (SAM) for the comparisons of several treatments with one control in the presence of small-variance genes. *Biometrical Journal* 50, 801-823.

LIVAK K.J. & Schmittgen T.D. (2001) Analysis of relative gene expression data using real-time quantitative PCR and the $2^{-\Delta\Delta Ct}$ method. *Methods* 25, 402-408.

LOW P.S. & Merida J.R. (1996) The oxidative burst in plant defense: function and signal transduction. *Physiologia Plantarum* 96, 533-542.

MAGDER S. (2006) Reactive oxygen species: toxic molecules or spark of life? *Critical Care* 10:208 (doi: 10.1186/cc3992)

MANCINI A., Buschini A., Restivo F.M., Rossi C. & Poli P. (2006) Oxidative stress as DNA damage in different transgenic tobacco plants. *Plant Science* 170, 845-852.

MARCIULIONIENE D., Kiponas D., Luksiene B. & Gaina V. (2005) Effects of ^{137}Cs low level exposure (internal and external) doses on plants. *Nukleonika* 50, 161-166.

MCCORD J.M. & Fridovich I. (1969) Superoxide dismutase: an enzymic function for erythrocuprein (hemocuprein). *The Journal of Biological Chemistry* 244, 6049-6055.

MCCULLAGH P. & Nelder J.A. (1989) Generalized linear models. 2nd ed. Chapman and Hall, London.

MENKE M., Chen I.P., Angelis K.J. & Schubert I. (2001) DNA damage and repair in *Arabidopsis thaliana* as measured by the comet assay after treatment with different classes of genotoxins. *Mutation Research* 493, 87-93.

MITTLER R. (2002) Oxidative stress, antioxidants and stress tolerance. *Trends in Plant Science* 7, 405-410.

MITTLER R. (2006) Abiotic stress, the field environment and stress combination. *Trends in Plant Science* 11, 15-19.

MITTLER R., Vanderauwera S., Gollery M. & Van Breusegem F. (2004) Reactive oxygen gene network of plants. *Trends in Plant Science* 9, 490-498.

MOLLER A.P. & Mousseau T.A. (2006) Biological consequences of Chernobyl: 20 years on. *Trends in Ecology and Evolution* 21, 200-207.

MONTILLET J.L., Cacas J.L., Garnier L., Montané M.H., Douki T., Bessoule J.J., Polkowska-Kowalczyk L., Maciejewska U., Agnel J.P., Vial A. & Triantaphylidès C. (2004) The upstream oxylipin profile of *Arabidopsis thaliana*: a tool to scan for oxidative stresses. *The Plant Journal* 40, 439-451.

MORI Y., Kimura S., Saotome A., Kasai N., Sakaguchi N., Uchiyama Y., Ishibashi T., Yamamoto T., Chiku H. & Sakaguchi K. (2005) Plastid DNA polymerases from higher plants, *Arabidopsis thaliana*. *Biochemical and Biophysical Research Communications* 334, 43-50.

NAGATA T., Yamada H., Du Z., Todoriki S. & Kikuchi S. (2005) Microarray analysis of genes that respond to γ-irradiation in *Arabidopsis*. *Journal of Agricultural and Food Chemistry* 53, 1022-1030.

NAWROT T., Plusquin M., Hogervorst J., Roels H.A., Celis H., Thijs L., Vangronsveld J., Van Hecke E. & Staessen J.A. (2006) Environmental exposure to cadmium and risk of cancer: a prospective population-based study. *Lancet Oncology* 7, 119-126.

NEILL S., Desikan R. & Hancock J. (2002) Hydrogen peroxide signaling. *Current Opinion in Plant Biology* 5, 388-395.

NETER J., Kutner M.H., Nachtsheim C.J. & Wasserman W. (1996) Applied linear statistical models, The McGraw-Hill Companies.

NIEBOER E. & Richardson D.H.S. (1980) The replacement of the nondescript term 'heavy metals' by a biologically and chemically significant classification of metal ions. *Environmental Pollution* 1, 3-26.

NIEBOER E., Richardson D.H.S., Lavoie P. & Padovan D. (1979) The role of metal-ion binding in modifying the toxic effects of sulphur dioxide on the lichen *Umbilicaria muhlenbergii*. *New Phytologist* 82, 621-632.

NOCTOR G. & Foyer C.H. (1998) Ascorbate and glutathione: Keeping active oxygen under control. *Annual Review of Plant Physiology and Plant Molecular Biology* 49, 249-279.

OHKI K. (1985) Manganese deficiency and toxicity effects on photosynthesis, chlorophyll, and transpiration in wheat. *Crop Science* 25, 187-191.

OKAMOTO H. & Tatara A. (1995) Effects of low-dose γ-irradiation on the cell cycle duration of barley roots. *Environmental and Experimental Botany* 35, 379-388.

ONOFRI A. (2005) BIOASSAY97: a new EXCEL VBA macro to perform statistical analyses on herbicide dose-response data. *Rivista Italiana Agrometeorologia* 3, 40-45.

PASCHOA A.S. & Godoy J.M. (2002) The areas of high natural radioactivity and TENORM wastes. *International Congress Series* 1225, 3-8.

PIERRUGUES O., Brutesco C., Oshiro J., Gouy M., Deveaux Y., Carman G.M., Thuriaux P. & Kazmaier M. (2001) Lipid phosphate phosphatases in *Arabidopsis*. *The journal of Biological Chemistry* 276, 20300-20308.

PORTA H. & Rocha-Sosa M. (2002) Plant lipoxygenases. Physiological and molecular features. *Plant Physiology* 130, 15-21.

PRASAD M.N.V. (1995) Cadmium toxicity and tolerance in vascular plants. *Environmental and Experimental Botany* 35, 525-545.

PROTECT (2008) Numerical benchmarks for protecting biota against radiation in the environment: proposed levels and underlying reasoning. Protection of the Environment from Ionising Radiation in a Regulatory Context.

PTÁCEK O., Mühlfeldová Z., Dostálek J., Cechák T. & Gichner T. (2002) Monitoring DNA damage in wood small-reed (*Calamagrostis epigejos*) plants growing in a sediment reservoir with substrates from uranium mining. *Journal of Environmental Monitoring* 4, 592-595.

RAMASWAMI A., Carr P. & Burkhardt M. (2001) Plant-uptake of uranium: hydroponic and soil system studies. *International Journal of Phytoremediation* 3, 189-201.

RAZINGER J., Dermastia M., Dolenc Koce J. & Zrimec A. (2008) Oxidative stress in duckweed (*Lemna minor* L.) caused by short-term cadmium exposure. *Environmental Pollution* 153, 687-694.

REMANS T., Smeets K., Opdenakker K., Mathijsen D., Vangronsveld J. & Cuypers A. (2008) Normalization of real-time RT-PCR gene expression measurements in *Arabidopsis thaliana* exposed to increased metal concentrations. *Planta* 227, 1343-1349.

RIBERA D., Labrot F., Tisnerat G. & Narbonne J.F. (1996) Uranium in the environment: occurrence, transfer and biological effects. *Reviews of Environmental Contamination and Toxicology* 146, 53-89.

ROMERO-PUERTAS M.C., Corpas F.J., Rodriguez-Serrano M., Gomez M., del Rio L.A. & Sandalio L.M. (2007) Differential expresión and regulation of antioxidative enzymes by cadmium in pea plants. *Journal of Plant Physiology* 164, 1346-1357.

RUFYIKIRI G., Wannijn J., Wang L. & Thiry Y. (2006) Effects of phosphorus fertilization on the availability and uptake of uranium and nutrients by plants grown on soil derived from uranium mining debris. *Environmental Pollution* 141, 420-427.

RULEY A.T., Sharma N.C. & Sahi S.V. (2004) Antioxidant defense in a lead accumulating plant, *Sesbania drummondii*. *Plant Physiology and Biochemistry* 42, 899-906.

SAGI M. & Fluhr R. (2006) Production of reactive oxygen species by plant NADPH oxidases. *Plant Physiology* 141, 336-340.

SALT D.E. (2004) Update on plant ionomics. Plant Physiology 136, 2451-2456.

SAX K. (1954) The effect of ionizing radiation on plant growth. *American Journal of Botany* 42, 360-364.

SELA M., Tel-Or E., Fritz E. & Huttermann A. (1988) Localization and toxic effects of cadmium, copper and uranium in *Azolla*. *Plant Physiology* 88, 30-36.

SEMANE B., Cuypers A., Smeets K., Van Belleghem F., Horemans N., Schat H. & Vangronsveld J. (2007) Cadmium responses in *Arabidopsis thaliana*: glutathione metabolism and antioxidative defence system. *Physiologia Plantarum* 129, 519-528.

SHAHANDEH H. & HOSSNER L.R. (2002) Role of soil properties in phytoaccumulation of uranium. *Water, Air and Soil Pollution* 141, 165-180.

SHAHANDEH H., Lee J.H., Hossner L.R. & Loeppert R.H. (2001) Bioavailability of uranium and plutonium to plants in soil-water systems and the potential of phytoremediation. In: Gobran G., Wenzel W. & Lombi E. (Eds.) Trace elements in the rhizosphere, CRC Press, Boca Raton, Florida, USA, pp 93-124.

SHEPPARD S.C., Sheppard M.I., Gallerand M.O. & Sanipelli B. (2005) Derivation of ecotoxicity thresholds for uranium. *Journal of Environmental Radioactivity* 79, 55-83.

SINGH S., Malhotra R. & Bajwa B.S. (2005) Uranium uptake studies in some plants. *Radiation Measurements* 40, 666-669.

SMEETS K., Cuypers A., Lambrechts A., Semane B., Hoet P., Van Laere A. & Vangronsveld J. (2005) Induction of oxidative stress and antioxidative mechanisms in *Phaseolus vulgaris* after Cd application. *Plant Physiology and Biochemistry* 43, 437-444.

SMEETS K., Ruytinx J., Semane B., Van Belleghem F., Remans T., Van Sanden S., Vangronsveld J. & Cuypers A. (2008) Cadmium-induced transcriptional and enzymatic alterations related to oxidative stress. *Environmental and Experimental Botany* 63, 1-8.

SPARROW A.H. & Miksche J.P. (1961) Correlation of nuclear volume and DNA content with higher plant tolerance to chronic radiation. *Science* 134, 282-283.

STAESSEN J.A., Roels H.A., Emelianov D., Kuznetsova T., Thijs L., Vangronsveld J. & Fagard R. (1999) Environmental exposure to cadmium, forearm bone density, and risk of fractures: prospective population study. *The Lancet* 353, 1140-1144.

STRACZEK A., Wannijn J., Van Hees M., Thijs H. & Thiry Y (2009) Tolerance of hairy roots of carrots to U chronic exposure in a standardized in vitro device. *Environmental and Experimental Botany* 65, 82-89.

TAMÁS L., Dudiková J., Durceková K., Halusková L., Huttová J., Mistrik I. & Ollé M. (2008) Alterations of the gene expression, lipid peroxidation, proline and thiol content along the barley root exposed to cadmium. *Journal of Plant Physiology* 165, 1193-1203.

TKALEC M., Malaric K. & Pevalek-Kozlina B. (2007) Exposure to radiofrequency radiation induces oxidative stress in duckweed *Lemna minor* L. *Science of the Total Environment* 388, 78-89.

UNSCEAR (2000) Report to the general assembly: sources and effects of ionizing radiation. United Nations Scientific Committee on the Effects of Atomic Radiation, Vienna.

UPTON A.C. (2001) Radiation hormesis: data and interpretations. *Critical Reviews in Toxicology* 31, 681-695.

VAN BELLEGHEM F., Cuypers A., Semane B., Smeets K., Vangronsveld J., d'Haen J. & Valcke R. (2007) Subcellular localization of cadmium in roots and leaves of *Arabidopsis thaliana*. *New Phytologist* 173, 495-508.

VANDENHOVE H. (2002) European sites contaminated by residues from the ore-extracting and -processing industries. *International Congress Series* 1225, 307-315.

VANDENHOVE H. (2005) Effect of soil physicochemistry on uranium speciation and availability to plants. In: Bréchignac F. & Howard B. (Eds.) Scientific trends in radiological protection of the environment ECORAD 2004, pp 59-83.

VANDENHOVE H., Cuypers A., Van Hees M., Koppen G. & Wannijn J. (2006) Oxidative stress reactions induced in beans (*Phaseolus vulgaris*) following exposure to uranium. *Plant Physiology and Biochemistry* 44, 795-805.

VAN DER STRICHT E. & Kirchmann (Eds.) (2001) Radioecology: radioactivity & ecosystems, International Union of Radioecology, Liège, Belgium.

VANDESOMPELE J., De Preter K., Pattyn F., Poppe B., Van Roy N., De Paepe A. & Speleman F. (2002) Accurate normalization of real-time quantitative RT-PCR data by geometric averaging of multiple internal control genes. Genome Biology 3: research 0034.

VANHOUDT N., Vandenhove H., Smeets K., Remans T., Van Hees M., Wannijn J., Vangronsveld J. & Cuypers A. (2008) Effects of uranium and phosphate concentrations on oxidative stress related responses induced in *Arabidopsis thaliana*. *Plant Physiology and Biochemistry* 46, 987-996.

WADA H., Koshiba T., Matsui T. & Satô M. (1998) Involvement of peroxidase in differential sensitivity to γ-radiation in seedlings of two *Nicotiana* species. *Plant Science* 132, 109-119.

WARD J.F. (1988) DNA damage produced by ionizing radiation in mammalian cells: identities, mechanisms of formation, and reparability. *Progress in Nucleic Acid Research and Molecular Biology* 35, 95-125.

WECKX J.E.J. & Clijsters H.M.M. (1996) Oxidative damage and defense mechanisms in primary leaves of *Phaseolus vulgaris* as a result of root assimilation of toxic amounts of copper. *Physiologia Plantarum* 96, 506-512.

WECKX J.E.J. & Clijsters H.M.M. (1997) Zn phytotoxicity induces oxidative stress in primary leaves of *Phaseolus vulgaris*. *Plant Physiology and Biochemistry* 35, 405-410.

WEDEPOHL K.H. (1995) The composition of the continental crust. *Geochimica et Cosmochimica Acta* 59, 1217-1232.

WESTFALL P.H., Tobias R.D., Rom D., Wolfinger R.D. & Hochberg Y. (2000) Multiple comparisons and multiple tests. Using the SAS system. SAS Institute, Cary, North Carolina.

WHO (2000) Chapter 6.3 Cadmium: Air Quality Guidelines - Second edition. World Health Organization, Regional Office for Europe, Copenhagen, Denmark.

WHO (2004) Cadmium in drinking water. Background document for development of WHO Guidelines for drinking-water Quality. World Health Organization.

WI S.G., Chung B.Y., Kim J.H., Baek M.H., Yang D.H., Lee J.W. & Kim J.S. (2005) Ultrastructural changes of cell organelles in *Arabidopsis* stems after gamma irradiation. *Journal of Plant Biology* 48, 195-200.

WI S.G., Chung B.Y., Kim J.S., Kim J.H., Baek M.H., Lee J.W. & Kim Y.S. (2007) Effects of gamma irradiation on morphological changes and biological responses in plants. *Micron* 38, 553-564.

WILLEKENS H., Inzé D., Van Montagu M. & van Camp W. (1995) Catalases in plants. *Molecular Breeding* 1, 207-228.

WITHERSPOON J.P. & Corney A.K. (1970) Differential and combined effects of beta, gamma and fast neutron irradiation of soybeen seedlings. *Radiation Botany* 10, 429-435.

ZAKA R., Vandecasteele C.M. & Misset M.T. (2002) Effects of low chronic doses of ionizing radiation on antioxidant enzymes and G_6PDH activities in *Stipa capillata* (Poaceae). *Journal of Experimental Botany* 376, 1979-1987.

ZAKA R., Chenal C. & Misset M.T. (2004) Effects of low doses of short-term gamma irradiation on growth and development through two generations of *Pisum sativum*. *Science of the Total Environment* 320, 121-129.

ZHANG G.P., Fukami M. & Sekimoto H. (2000) Genotypic differences in effects of cadmium on growth and nutrient compositions in wheat. *Journal of Plant Nutrition* 23, 1337-1350.

ZHANG F.Q., Wang Y.S., Lou Z.P. & Dong J.D. (2007) Effect of heavy metal stress on antioxidative enzymes and lipid peroxidation in leaves and roots of two mangrove plant seedlings (*Kandelia candel* and *Bruguiera gymnorrhiza*). *Chemosphere* 67, 44-50.

ZHU Z.J., Sun G.W., Fang X.Z., Qian Q.Q. & Yang X.E. (2004) Genotypic differences in effects of cadmium exposure on plant growth and contents of cadmium and elements in 14 cultivars of Bai Cai. *Journal of Environmental Science and Health part B - Pesticides Food Contaminants and Agricultural Wastes* B39, 675-687.

ZIMMERMANN P., Heinlein C., Orendi G. & Zentgraf U. (2006) Senescence-specific regulation of catalases in *Arabidopsis thaliana* (L.) Heynh. *Plant Cell and Environment* 29, 1049-1060.